ASTR 595: Astrophysical Flows

a consice treatment of fluid dynamics,
collisionless dynamics & plasma physics,
with an application to astrophysics


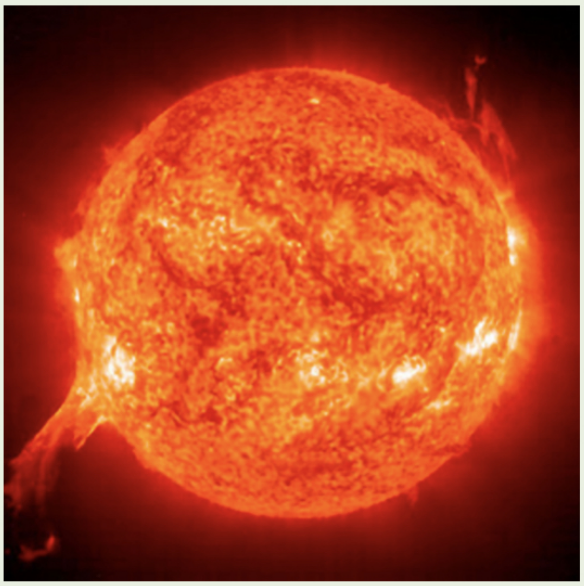

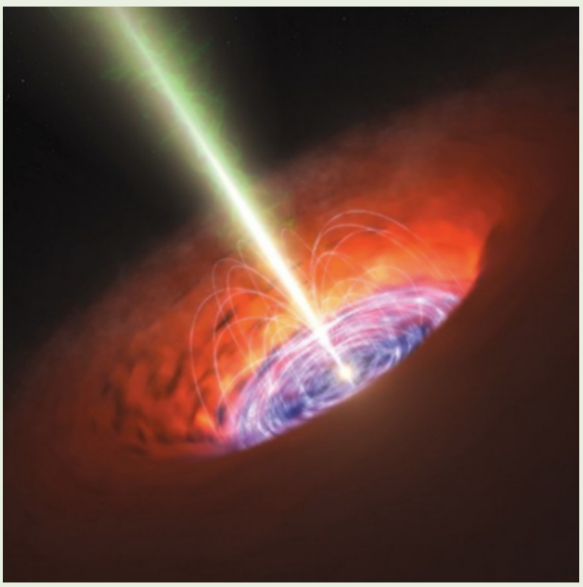

Frank C. van den Bosch

These lecture notes describe the material covered during the Spring 2020 semester of the course Astrophysical Flows at Yale University

One goes deep into the flow
Becomes busy flowing to it
Lost in the flow
What happens
Is that the one forgets
What he is flowing for

from "The River Flows" by *Sachin Subedi*

CONTENTS

APPENDICES

LITERATURE

The material covered and presented in these lecture notes has relied heavily on a number of excellent textbooks listed below.

- **The Physics of Fluids and Plasmas**
  by A. Choudhuri (ISBN-0-521-55543)
- **The Physics of Astrophysics–II. Gas Dynamics**
  by F. Shu (ISBN-0-935702-65-2)
- **Introduction to Plasma Theory**
  by D. Nicholson (ISBN-978-0-894-6467705)
- **The Physics of Plasmas**
  by T. Boyd & J. Sanderson (ISBN-978-0-521-45912-9)
- **Modern Fluid Dynamics for Physics and Astrophysics**
  by O. Regev, O. Umurhan & P. Yecko (ISBN-978-1-4939-3163-7)
- **Theoretical Astrophysics**
  by M. Bartelmann (ISBN-978-3-527-41004-0)
- **Principles of Astrophysical Fluid Dynamics**
  by C. Clarke & B.Carswell (ISBN-978-0-470-01306-9)
- **Introduction to Modern Magnetohydrodynamics**
  by S. Galtier (ISBN-978-1-316-69247-9)
- **Modern Classical Physics**
  by K. Thorne & R. Blandford (ISBN-978-0-691-15902-7)
- **Galactic Dynamics**
  by J. Binney & S. Tremaine (ISBN-978-0-691-13027-9)
- **Galaxy Formation & Evolution**
  by H. Mo, F. van den Bosch & S. White (ISBN-978-0-521-85793-2)

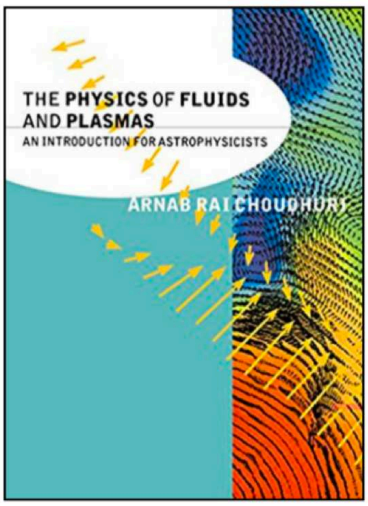
THE PHYSICS OF FLUIDS AND PLASMAS
AN INTRODUCTION FOR ASTROPHYSICISTS
ARNAB RAI CHOUDHURY

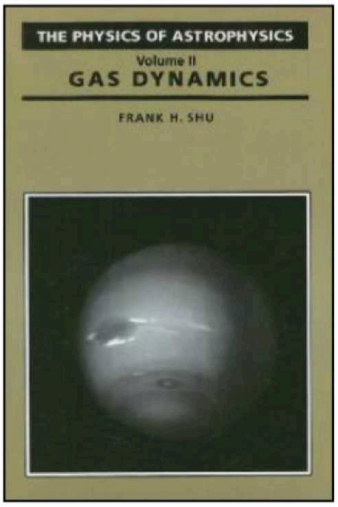
THE PHYSICS OF ASTROPHYSICS
Volume II
GAS DYNAMICS
FRANK H. SHU

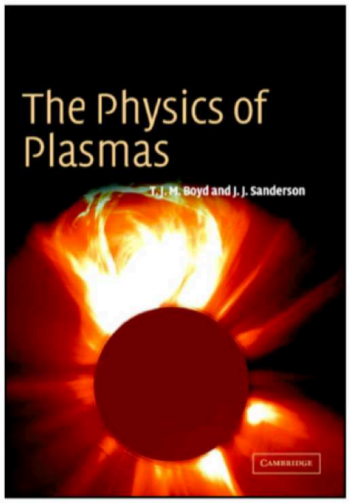
The Physics of Plasmas
T. J. M. Boyd and J. J. Sanderson
CAMBRIDGE

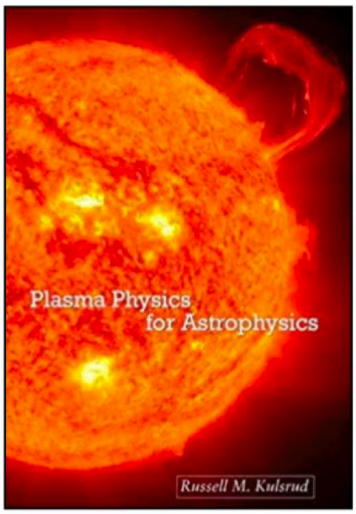
Plasma Physics for Astrophysics
Russell M. Kulsrud

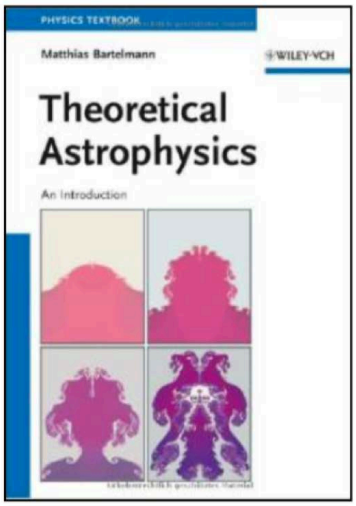
PHYSICS TEXTBOOK
Matthias Bartelmann
WILEY-VCH
Theoretical Astrophysics
An Introduction

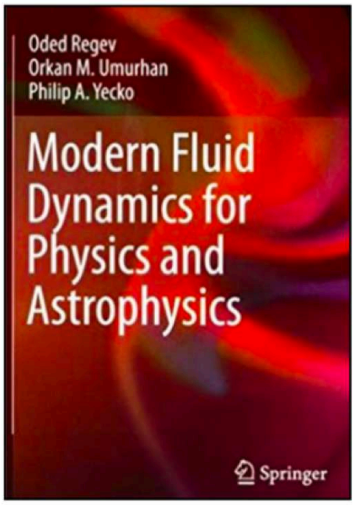
Oded Regev
Orkan M. Umurhan
Philip A. Yecko
Modern Fluid Dynamics for Physics and Astrophysics
Springer

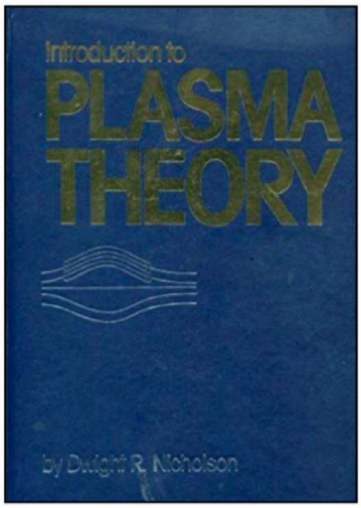
Introduction to
PLASMA THEORY
by Dwight R. Nicholson

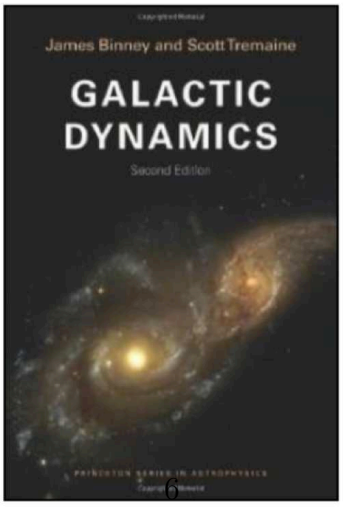
James Binney and Scott Tremaine
GALACTIC DYNAMICS
Second Edition

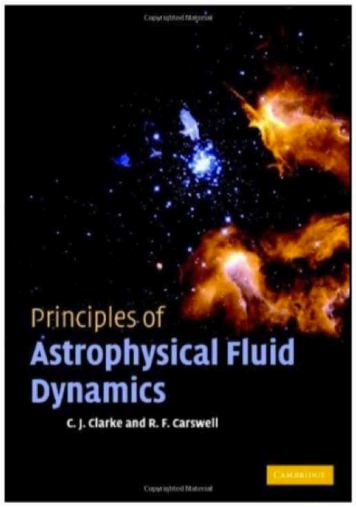
Principles of
Astrophysical Fluid Dynamics
C. J. Clarke and R. F. Carswell
CAMBRIDGE

CHAPTER 1

Introduction to Fluids & Plasmas

What is a fluid?

A fluid is a substance that can flow, has no fixed shape, and offers little resistance to an external stress

- In a fluid the constituent particles (atoms, ions, molecules, stars) can 'freely' move past one another.
- Fluids take on the shape of their container.
- A fluid changes its shape **at a steady rate** when acted upon by a stress force.

What is a plasma?

A plasma is a fluid in which (some of) the consistituent particles are electrically charged, such that the interparticle force (Coulomb force) is long-range in nature.

Fluid Demographics:

All fluids are made up of large numbers of constituent particles, which can be molecules, atoms, ions, dark matter particles or even stars. Different types of fluids mainly differ in the nature of their interparticle forces. Examples of inter-particle forces are the Coulomb force (among charged particles in a plasma), vanderWaals forces (among molecules in a neutral fluid) and gravity (among the stars in a galaxy). Fluids can be both **collisional** or **collisionless**, where we define a collision as *an interaction between constituent particles that causes the trajectory of at least one of these particles to be deflected 'noticeably'.* Collisions among particles drive the system towards **thermodynamic equilibrium** (at least locally) and the velocity distribution towards a **Maxwell-Boltzmann distribution**.

In neutral fluids the particles only interact with each other on very small scales. Typically the inter-particle force is a vanderWaals force, which drops off very rapidly. Put differently, the typical cross section for interactions is the size of the particles (i.e., the Bohr radius for atoms), which is very small. Hence, to good approximation

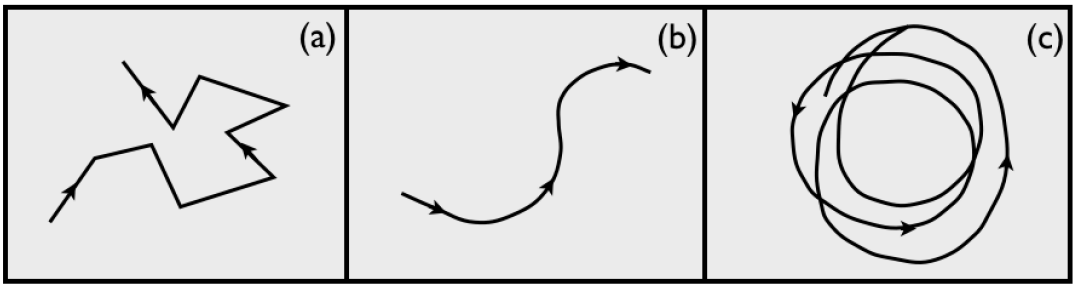

Figure 1: *Examples of particle trajectories in (a) a collisional, neutral fluid, (b) a plasma, and (c) a self-gravitating collisionless, neutral fluid. Note how different the dynamics are.*

particles in a neutral fluid move in straight lines in between highly-localized, large-angle scattering events (**'collisions'**). An example of such a particle trajectory is shown Fig. **1a**. Unless the fluid is extremely dilute, most neutral fluids are collisional, meaning that the mean free path of the particles is short compared to the physical scales of interest. In astrophysics, though, there are cases where this is not necessarily the case. In such cases, the standard equations of fluid dynamics may not be valid!

In a fully ionized plasma the particles exert Coulomb forces ($\vec{F} \propto r^{-2}$) on each other. Because these are long-range forces, the velocity of a charged particle changes more likely due to a succession of many small deflections rather than due to one large one. As a consequence, particles trajectories in a highly ionized plasma (see Fig. **1b**) are very different from those in a neutral fluid.

In a weakly ionized plasma most interactions/collisions are among neutrals or between neutrals and charged particles. These interactions are short range, and a weaky ionized plasma therefore behaves very much like a neutral fluid.

In astrophysics we often encounter fluids in which the mean, dominant interparticle force is gravity. We shall refer to such fluids are N-body systems. Examples are dark matter halos (if dark matter consists of WIMPs or axions) and galaxies (stars act like neutral particles exerting gravitational forces on each other). Since gravity is a long-range force, each particle feels the force from all other particles. Consider the gravitational force $\vec{F}_i$ at a position $\vec{x}_i$ from all particles in a relaxed, equilibrium system. We can then write that

$$\vec{F}_i(t) = \langle \vec{F} \rangle_i + \delta \vec{F}_i(t)$$

Here $\langle \vec{F} \rangle_i$ is the time (or ensemble) averaged force at i and $\delta \vec{F}_i(t)$ is the instantaneous deviation due to the discrete nature of the particles that make up the system. As $N \rightarrow \infty$ then $\delta \vec{F}_i \rightarrow 0$ and the system is said to be **collisionless**; *its dynamics are governed by the collective force from all particles rather than by collisions with individual particles.*

As you learn in Galactic Dynamics, the **relaxation time** of a gravitational N-body system, defined as the time scale on which collisions (i.e., the impact of the $\delta \vec{F}$ above) cause the energies of particles to change considerably, is

$$t_{\rm relax} \simeq \frac{N}{8 \ln N} \, t_{\rm cross}$$

where $t_{\rm cross}$ is the crossing time (comparable to the dynamical time) of the system. Typically $N \sim 10^{10}$ (number of stars in a galaxy) or 10^{50-60} (number of dark matter particles in a halo), and $t_{\rm cross}$ is roughly between 1 and 10 percent of the Hubble time (10^8 to 10^9 yr). Hence, the relaxation time is many times the age of the Universe, and these N-body systems are, for all practical purposes, collisionless. As a consequence, the particle trajectories are (smooth) orbits (see Fig. **1c**), and understanding galactic dynamics requires therefore a solid understanding of orbits. Put differently, 'orbits are the building blocks on galaxies'.

Collisional vs. Collisionless Plasmas: If the collisionality of a gravitational system just depends on N, doesn't that mean that plasmas are also collisionless? After all, the interparticle force in a plasma is the Coulomb force, which has the same long-range $1/r^2$ nature as gravity. And the number of particles N of a typical plasma is huge ($\gg 10^{10}$) while the dynamical time can be large as well (this obviously depends on the length scales considered, but these tend to be large for astrophysical plasmas).
However, an important difference between a gravitational system and a plasma is that the Coulomb force can be either attractive or repulsive, depending on the electrical charges of the particles. On large scales, plasma are neutral. This **charge neutrality** is guaranteed by the fact that any charge imbalance would produce strong electrostatic forces that quickly re-establish neutrality. As we will see when discussing plasmas in detail (Chapter **??**), the effect of electrical charges is screened beyond the **Debye length**:

$$\lambda_{\rm D} = \left(\frac{k_{\rm B} \, T}{8 \pi \, n \, e^2} \right)^{1/2} \simeq 4.9 \, {\rm cm} \; n^{-1/2} \, T^{1/2}$$

Here n is the number density in cm^{-3}, T is the temperature in degrees Kelvin, and e is the electrical charge of an electron in e.s.u. Related to the Debye length is the **Plasma parameter**

$$g \equiv \frac{1}{n\,\lambda_{\rm D}^3} \simeq 8.6 \times 10^{-3}\, n^{1/2}\, T^{-3/2}$$

A plasma is (to good approximation) collisionless if the number of particles within the Debye volume, $N_{\rm D} = n\,\lambda_{\rm D}^3 = g^{-1}$ is sufficiently large. After all, only those particles exert Coulomb forces on each other; particles that outside of each others Debye volume do not exert a long-range Coulomb force on each other.

As an example, let's consider three different astrophysical plasmas: the ISM (interstellar medium), the ICM (intra-cluster medium), and the interior of the Sun. The warm phase of the ISM has a temperature of $T \sim 10^4$K and a number density of $n \sim 1\,\mathrm{cm}^{-3}$. This implies $N_{\rm D} \sim 1.2 \times 10^8$. Hence, the warm phase of the ISM can be treated as a collisionless plasma on sufficiently small time-scales (for example when treating high-frequency plasma waves). The ICM has a much lower average density of $\sim 10^{-4}\ \mathrm{cm}^{-3}$ and a much higher temperature ($\sim 10^7$K). This implies a much larger number of particles per Debye volume of $N_{\rm D} \sim 4 \times 10^{14}$. Hence, the ICM can typically be approximated as a collisionless plasma. The interior of stars, though, has a similar temperature of $\sim 10^7$K but at much higher density ($n \sim 10^{23}\ \mathrm{cm}^{-3}$), implying $N_{\rm D} \sim 10$. Hence, stellar interiors are highly collisional plasmas!

Magnetohydrodynamics: Plasma are excellent conductors, and therefore are quickly shorted by currents; hence in many cases one may ignore the electrical field, and focus exclusively on the magnetic field instead. This is called magneto-hydrodynamics, or **MHD** for short. Many astrophysical plasmas have relatively weak magnetic fields, and we therefore don't make big errors if we ignore them. In this case, when electromagnetic interactions are not important, plasmas behave very much like neutral fluids. Because of this, most of the material covered in this course will focus on neutral fluids, despite the fact that more than 99% of all baryonic matter in the Universe is a plasma.

Compressibility: Fluids and plasmas can be either **gaseous** or **liquid**. A gas is **compressible** and will completely fill the volume available to it. A liquid, on the other hand, is (to good approximation) **incompressible**, which means that a liquid of given mass occupies a given volume.

NOTE: Although a gas is said to be compressible, many gaseous *flows* (and virtually all astrophysical flows) are **incompressible**. When the gas is in a container, you can easily compress it with a piston, but if I move my hand (sub-sonically) through the air, the gas adjust itself to the perturbation in an incompressible fashion (it moves out of the way at the **speed of sound**). The small compression at my hand propagates forward at the speed of sound (**sound wave**) and disperses the gas particles out of the way. In astrophysics we rarely encounter containers, and **subsonic** gas flow is often treated (to good approximation) as being incompressible.

Throughout what follows, we use 'fluid' to mean a **neutral** *fluid, and 'plasma' to refer to a fluid in which the particles are electrically charged.*

Ideal (Perfect) Fluids and Ideal Gases:

As we discuss in more detail in Chapter 4, the resistance of fluids to shear distortions is called **viscosity**, which is a microscopic property of the fluid that depends on the nature of its constituent particles, and on thermodynamic properties such as temperature. Fluids are also **conductive**, in that the microscopic collisions between the constituent particles cause heat conduction through the fluid. In many fluids encountered in astrophysics, the viscosity and conduction are very small. *An ideal fluid, also called a perfect fluid, is a fluid with zero viscosity and zero condution.*

NOTE: An ideal (or perfect) fluid should NOT be confused with an ideal or perfect gas, which is defined as a gas in which the pressure is solely due to the kinetic motions of the constituent particles. As we show in Chapter 11, and as you have probably seen before, this implies that the pressure can be written as $P = n\,k_{\rm B}\,T$, with n the particle number density, $k_{\rm B}$ the Boltzmann constant, and T the temperature.

Examples of Fluids in Astrophysics:

- **Stars:** stars are spheres of gas in **hydrostatic equilibrium** (i.e., gravitational force is balanced by pressure gradients). Densities and temperatures in a given star cover many orders of magnitude. To good approximation, its **equation of state** is that of an **ideal gas**.
- **Giant (gaseous) planets:** Similar to stars, gaseous planets are large spheres of gas, albeit with a rocky core. Contrary to stars, though, the gas is typically

so dense and cold that it can no longer be described with the **equation of state** of an **ideal gas**.

- **Planet atmospheres:** The atmospheres of planets are stratified, gaseous fluids retained by the planet's gravity.

- **White Dwarfs & Neutron stars:** These objects (stellar remnants) can be described as fluids with a **degenerate equation of state**.

- **Proto-planetary disks:** the dense disks of gas and dust surrounding newly formed stars out of which planetary systems form.

- **Inter-Stellar Medium (ISM):** The gas in between the stars in a galaxy. The ISM is typically extremely complicated, and roughly has a **three-phase structure**: it consists of a dense, cold ($\sim$ 10K) molecular phase, a warm ($\sim 10^4$K) phase, and a dilute, hot ($\sim 10^6$K) phase. Stars form out of the dense molecular phase, while the hot phase is (shock) heated by supernova explosions. The reason for this three phase medium is associated with the various cooling mechanisms. At high temperature when all gas is ionized, the main cooling channel is Bremmstrahlung (acceleration of free electrons by positively charged ions). At low temperatures ($< 10^4$K), the main cooling channel is molecular cooling (or cooling through hyperfine transitions in metals).

- **Inter-Galactic Medium (IGM):** The gas in between galaxies. This gas is typically very, very dilute (low density). It is continuously 'exposed' to adiabatic cooling due to the expansion of the Universe, but also is heated by radiation from stars (galaxies) and AGN (active galactic nuclei). The latter, called **'reionization'**, assures that the typical temperature of the IGM is $\sim 10^4$K.

- **Intra-Cluster Medium (ICM):** The hot gas in clusters of galaxies. This is gas that has been shock heated when it fell into the cluster; typically gas passes through an **accretion shock** when it falls into a dark matter halo, converting its infall velocity into thermal motion.

- **Accretion disks:** Accretion disks are gaseous, viscous disks in which the viscosity (enhanced due to turbulence) causes a net rate of radial matter towards the center of the disk, while angular momentum is being transported outwards (accretion)

- **Galaxies (stellar component):** as already mentioned above, the stellar component of galaxies is a collisionless fluid; to very, very good approximation, two stars in a galaxy will never collide with other.
- **Dark matter halos:** Another example of a collisionless fluid (at least, we *assume* that dark matter is collisionless)...

Course Outline:

In this course, we will start with standard hydrodynamics, which applies mainly to neutral, collisional fluids. We derive the fluid equations from kinetic theory: starting with the Liouville theorem we derive the Boltzmann equation, from which in turn we derive the continuity, momentum and energy equations. Next we discuss a variety of different flows; vorticity, incompressible barotropic flow, viscous flow, and turbulent flow, before addressing fluid instabilities and shocks. Next we study numerical fluid dynamics. We discuss methods used to numerically solve the partial differential equations that describe fluids, and we construct a simple 1D hydro-code that we test on an analytical test case (the Sod shock tube problem). After a brief discussion of collisionless fluid dynamics, highlighting the subtle differences between the Jeans equations and the Navier-Stokes equations, we turn our attention to plasmas. We again derive the relevant equations (Vlasov and Lenard-Balescu) from kinetic theory, and then discuss MHD and several applications. The goal is to end with a brief discussion of the Fokker-Planck equation, which describes the impact of long-range collisions in a gravitational N-body system or a plasma.

It is assumed that the reader is familiar with vector calculus, with curvi-linear coordinate systems, and with differential equations. A brief overview of these topics, highlighting the most important essentials, is provided in Appendices A-E.

CHAPTER 2

Dynamical Treatments of Fluids

A **dynamical theory** consists of two characteristic elements:

1. a way to describe the **state** of the system
2. a (set of) equation(s) to describe how the state variables change with time

Consider the following examples:

Example 1: a classical dynamical system

This system is described by the position vectors ($\vec{x}$) and momentum vectors ($\vec{p}$) of all the N particles, i.e., by $(\vec{x}_1, \vec{x}_2, ..., \vec{x}_N, \vec{p}_1, \vec{p}_2, ..., \vec{p}_N)$.
If the particles are trully classical, in that they can't emit or absorb radiation, then one can define a **Hamiltonian**

$$\mathcal{H}(\vec{x}_i, \vec{p}_i, t) \equiv \mathcal{H}(\vec{x}_1, \vec{x}_2, ..., \vec{x}_N, \vec{p}_1, \vec{p}_2, ..., \vec{p}_N, t) = \sum_{i=1}^{N} \vec{p}_i \cdot \dot{\vec{x}}_i - \mathcal{L}(\vec{x}_i, \dot{\vec{x}}_i, t)$$

where $\mathcal{L}(\vec{x}_i, \dot{\vec{x}}_i, t)$ is the system's **Lagrangian**, and $\dot{\vec{x}}_i = \mathrm{d}\vec{x}_i/\mathrm{d}t$.

The equations that describe the time-evolution of these state-variables are the Hamiltonian **equations of motion**:

$$\dot{\vec{x}}_i = \frac{\partial \mathcal{H}}{\partial \vec{p}_i}\,; \qquad \dot{\vec{p}}_i = -\frac{\partial \mathcal{H}}{\partial \vec{x}_i}$$

Example 2: an electromagnetic field

The state of this system is described by the electrical and magnetic fields, $\vec{E}(\vec{x})$ and $\vec{B}(\vec{x})$, respectively, and the equations that describe their evolution with time are the **Maxwell equations**, which contain the terms $\partial\vec{E}/\partial t$ and $\partial\vec{B}/\partial t$.

Example 3: a quantum system

The state of a quantum system is fully described by the (complex) **wavefunction** $\psi(\vec{x})$, the time-evolution of which is described by the **Schrödinger equation**

$$i\hbar\frac{\partial\psi}{\partial t} = \hat{\mathcal{H}}\psi$$

where $\hat{\mathcal{H}}$ is now the Hamiltonian operator.

Level	**Description of state**	**Dynamical equations**
0: N quantum particles	$\psi(\vec{x}_1, \vec{x}_2, ..., \vec{x}_N)$	Schrödinger equation
1: N classical particles	$(\vec{x}_1, \vec{x}_2, ..., \vec{x}_N, \vec{v}_1, \vec{v}_2, ..., \vec{v}_N)$	Hamiltonian equations
2: Distribution function	$f(\vec{x}, \vec{v}, t)$	Boltzmann equation
3: Continuum model	$\rho(\vec{x})$, $\vec{u}(\vec{x})$, $P(\vec{x})$, $T(\vec{x})$	Hydrodynamic equations

Different levels of dynamical theories to describe neutral fluids

The different levels of Fluid Dynamics

There are different 'levels' of dynamical theories to describe fluids. Since all fluids are ultimately made up of constituent particles, and since all particles are ultimately 'quantum' in nature, the most 'basic' level of fluid dynamics describes the state of a fluid in terms of the N-particle wave function $\psi(\vec{x}_1, \vec{x_2}, ..., \vec{x}_N)$, which evolves in time according to the Schrödinger equation. We will call this the **level-0** description of fluid dynamics. Since N is typically extremely large, this level-0 description is extremely complicated and utterly unfeasible. Fortunately, it is also unneccesary.

According to what is known as **Ehrenfest's theorem**, a system of N *quantum* particles can be treated as a system of N *classical* particles if the characteristic separation between the particles is large compared to the 'de Broglie' wavelength

$$\lambda = \frac{h}{p} \simeq \frac{h}{\sqrt{m k_{\rm B} T}}$$

Here h is the Planck constant, p is the particle's momentum, m is the particle mass, $k_{\rm B}$ is the Boltzman constant, and T is the temperature of the fluid. This de Broglie wavelength indicates the 'characteristic' size of the wave-packet that according to quantum mechanics describes the particle, and is typically very small. Except for extremely dense fluids such as white dwarfs and neutron stars, or 'exotic' types of dark matter (i.e., 'fuzzy dark matter'), the de Broglie wavelength is always much smaller than the mean particle separation, and classical, Newtonian mechanics suffices. As we have seen above, a classical, Newtonian system of N particles can be described by a Hamiltonian, and the corresponding equations of motions. We refer to this as the **level-1** description of fluid dynamics (see under 'example 1' above). Clearly, when N is very large is it unfeasible to solve the 2N equations of motion for all the positions and momenta of all particles. We need another approach.

In the **level-2** approach, one introduces the distribution function $f(\vec{x}, \vec{p}, t)$, which describes the number density of particles in 6-dimensional 'phase-space' $(\vec{x}, \vec{p})$ (i.e., how many particles are there with positions in the 3D volume $\vec{x} + {\rm d}\vec{x}$ and momenta in the 3D volume $\vec{p} + {\rm d}\vec{p}$). The equation that describes how $f(\vec{x}, \vec{p}, t)$ evolves with time is called the **Boltzmann equation** for a neutral fluid. If the fluid is collisionless this reduces to the **Collisionless Boltzmann equation** (CBE). If the collisionless fluid is a plasma, the same equation is called the **Vlasov equation**. Often CBE and Vlasov are used without distinction.

At the final **level-3**, the fluid is modelled as a continuum. This means we ignore that fluids are made up of constituent particles, and rather describe the fluid with continuous fields, such as the density and velocity fields $\rho(\vec{x})$ and $\vec{u}(\vec{x})$ which assign to each point in space a scalar quantity ρ and a vector quantity $\vec{u}$, respectively. For an ideal neutral fluid, the state in this level-3 approach is fully described by four fields: the density $\rho(\vec{x})$, the velocity field $\vec{u}(\vec{x})$, the pressure $P(\vec{x})$, and the internal, specific energy $\varepsilon(\vec{x})$ (or, equivalently, the temperature $T(\vec{x})$). In the MHD treatment of plasmas one also needs to specify the magnetic field $\vec{B}(\vec{x})$. The equations that describe the time-evolution of $\rho(\vec{x})$, $\vec{u}(\vec{x})$, and $\varepsilon(\vec{x})$ are called the **continuity equation**, the **Navier-Stokes equations**, and the **energy equation**, respectively. Collectively, we shall refer to these as the **hydrodynamic equations** or **fluid equations**. In MHD you have to slightly modify the Navier-Stokes equations, and add an additional **induction equation** describing the time-evolution of the magnetic

field. For an ideal (or perfect) fluid (i.e., no viscosity and/or conductivity), the Navier-Stokes equations reduce to what are known as the **Euler equations**. For a collisionless gravitational system, the equivalent of the Euler equations are called the **Jeans equations**.

Throughout this course, we mainly focus on the level-3 treatment, to which we refer hereafter as the **macroscopic approach**. However, for completeness we will derive these continuum equations starting from a completely general, **microscopic** level-1 treatment. Along the way we will see how subtle differences in the inter-particle forces gives rise to a rich variety in dynamics (fluid vs. plasma, collisional vs. collisionless).

Fluid Dynamics: The Macroscopic Continuum Approach:

In the macroscopic approach, the fluid is treated as a **continuum**. It is often useful to think of this continuum as 'made up' of **fluid elements** (FE). These are small fluid volumes that nevertheless contain many particles, that are significantly larger than the mean-free path of the particles, and for which one can define local hydrodynamical variables such as density, pressure and temperature. The requirements are:

1. the FE needs to be much smaller than the characteristic scale in the problem, which is the scale over which the hydrodynamical quantities Q change by an order of magnitude, i.e.
$$l_{\rm FE} \ll l_{\rm scale} \sim \frac{Q}{\nabla Q}$$

2. the FE needs to be sufficiently large that fluctuations due to the finite number of particles ('discreteness noise') can be neglected, i.e.,
$$n\, l_{\rm FE}^3 \gg 1$$
where n is the number density of particles.

3. the FE needs to be sufficiently large that it 'knows' about the local conditions through collisions among the constituent particles, i.e.,
$$l_{\rm FE} \gg \lambda$$
where λ is the mean-free path of the fluid particles.

The ratio of the mean-free path, λ, to the characteristic scale, $l_{\rm scale}$ is known as the **Knudsen number:** $\mathrm{Kn} = \lambda/l_{\rm scale}$. Fluids typically have $\mathrm{Kn} \ll 1$; if not, then one is not justified in using the continuum approach (level-3) to fluid dynamics, and one is forced to resort to a more statistical approach (level-2).

Note that fluid elements can NOT be defined for a collisionless fluid (which has an infinite mean-free path). This is one of the reasons why one cannot use the macroscopic approach to derive the equations that govern a collisionless fluid.

Fluid Dynamics: closure:

In general, a fluid element is characterized by the following six hydro-dynamical variables:

mass density	ρ	[g/cm^3]	
fluid velocity	$\vec{u}$	[cm/s]	(3 components)
pressure	P	[erg/cm^3]	
specific internal energy	ε	[erg/g]	

Note that $\vec{u}$ is the velocity of the fluid element, not to be confused with the velocity $\vec{v}$ of individual fluid particles, used in the Boltzmann distribution function. Rather, $\vec{u}$ is (roughly) a vector sum of all particles velocities $\vec{v}$ that make up the fluid element.

In the case of an **ideal (or perfect) fluid** (i.e., with zero viscosity and conductivity), the Navier-Stokes equations (which are the hydrodynamical momentum equations) reduce to what are called the **Euler equations**. In that case, the evolution of fluid elements is describe by the following set of hydrodynamical equations:

1 continuum equation	relating ρ and $\vec{u}$
3 momentum equations	relating ρ, $\vec{u}$ and P
1 energy equation	relating ρ, $\vec{u}$, P and ε

Thus we have a total of 5 equations for 6 unknowns. One can solve the set ('close it') by using a **constitutive relation**. In almost all cases, this is the **equation of state** (EoS) $P = P(\rho, \varepsilon)$.

• Sometimes the EoS is expressed as $P = P(\rho, T)$. In that case another constitution relation is needed, typically $\varepsilon = \varepsilon(\rho, T)$.

• If the EoS is **barotropic**, i.e., if $P = P(\rho)$, then the energy equation is not needed to close the set of equations. There are two barotropic EoS that are encountered frequently in astrophysics: the **isothermal** EoS, which describes a fluid for which cooling and heating always balance each other to maintain a constant temperature, and the **adiabatic** EoS, in which there is no net heating or cooling (other than adiabatic heating or cooling due to the compression or expansion of volume, i.e., the $P\,\mathrm{d}V$ work). We will discuss these cases in more detail later in the course.

• No EoS exists for a **collisionless fluid**. Consequently, for a collisionless fluid one can never close the set of fluid equations, unless one makes a number of simplifying assumptions (i.e., one postulates various symmetries)

• If the fluid is not ideal, then the momentum equations include terms that contain the (kinetic) **viscosity**, ν, and the energy equation includes a term that contains the conductivity, $\mathcal{K}$. Both ν and $\mathcal{K}$ depend on the mean-free path of the constituent particles and therefore depend on the temperature and collisional cross-section of the particles. Closure of the set of hydrodynamic equations then demands additional constitutive equations $\nu(T)$ and $\mathcal{K}(T)$. Often, though, ν and $\mathcal{K}$ are simply assumed to be constant (the T-dependence is ignored).

• In the case the fluid is exposed to an **external force** (i.e., a gravitational or electrical field), the momentum and energy equations contain an extra force term.

• In the case the fluid is **self-gravitating** (i.e., in the case of stars or galaxies) there is an additional unknown, the gravitational potential Φ. However, there is also an additional equation, the **Poisson equation** relating Φ to ρ, so that the set of equations remains closed.

• In the case of a plasma, the charged particles give rise to electric and magnetic fields. Each fluid element now carries 6 additional scalars (E_x, E_y, E_z, B_x, B_y, B_z), and the set of equations has to be complemented with the **Maxwell equations** that describe the time evolution of $\vec{E}$ and $\vec{B}$.

Fluid Dynamics: Eulerian *vs.* Lagrangian Formalism:
One distinguishes two different formalisms for treating fluid dynamics:

- **Eulerian Formalism:** in this formalism one solves the fluid equations 'at fixed positions': the evolution of a quantity Q is described by the local (or partial, or Eulerian) derivative $\partial Q/\partial t$. An Eulerian hydrodynamics code is a 'grid-based code', which solves the hydro equations on a fixed grid, or using an adaptive grid, which refines resolution where needed. The latter is called **Adaptive Mesh Refinement** (AMR).

- **Lagrangian Formalism:** in this formalism one solves the fluid equations 'comoving with the fluid', i.e., either at a fixed particle (collisionless fluid) or at a fixed fluid element (collisional fluid). The evolution of a quantity Q is described by the substantial (or Lagrangian) derivative $\mathrm{d}Q/\mathrm{d}t$ (sometimes written as $\mathrm{D}Q/\mathrm{D}t$). A Lagrangian hydrodynamics code is a 'particle-based code', which solves the hydro equations per simulation particle. Since it needs to smooth over neighboring particles in order to compute quantities such as the fluid density, it is called **Smoothed Particle Hydrodynamics** (SPH).

To derive an expression for the **substantial derivative** $\mathrm{d}Q/\mathrm{d}t$, realize that $Q = Q(t, x, y, z)$. When the fluid element moves, the scalar quantity Q experiences a change

$$\mathrm{d}Q = \frac{\partial Q}{\partial t}\,\mathrm{d}t + \frac{\partial Q}{\partial x}\,\mathrm{d}x + \frac{\partial Q}{\partial y}\,\mathrm{d}y + \frac{\partial Q}{\partial z}\,\mathrm{d}z$$

Dividing by $\mathrm{d}t$ yields

$$\frac{\mathrm{d}Q}{\mathrm{d}t} = \frac{\partial Q}{\partial t} + \frac{\partial Q}{\partial x}\,u_x + \frac{\partial Q}{\partial y}\,u_y + \frac{\partial Q}{\partial z}\,u_z$$

where we have used that $\mathrm{d}x/\mathrm{d}t = u_x$, which is the x-component of the fluid velocity $\vec{u}$, etc. Hence we have that

$$\boxed{\frac{\mathrm{d}Q}{\mathrm{d}t} = \frac{\partial Q}{\partial t} + \vec{u}\cdot\nabla Q}$$

Using a similar derivation, but now for a vector quantity $\vec{A}(\vec{x}, t)$, it is straightforward to show that

$$\boxed{\frac{\mathrm{d}\vec{A}}{\mathrm{d}t} = \frac{\partial \vec{A}}{\partial t} + (\vec{u} \cdot \nabla)\, \vec{A}}$$

which, in index-notation, is written as

$$\frac{\mathrm{d}A_i}{\mathrm{d}t} = \frac{\partial A_i}{\partial t} + u_j \frac{\partial A_i}{\partial x_j}$$

Another way to derive the above relation between the Eulerian and Lagrangian derivatives, is to think of $\mathrm{d}Q/\mathrm{d}t$ as

$$\frac{\mathrm{d}Q}{\mathrm{d}t} = \lim_{\delta t \to 0} \left[\frac{Q(\vec{x} + \delta\vec{x}, t + \delta t) - Q(\vec{x}, t)}{\delta t} \right]$$

Using that

$$\vec{u} = \lim_{\delta t \to 0} \left[\frac{\vec{x}(t + \delta t) - \vec{x}(t)}{\delta t} \right] = \frac{\delta \vec{x}}{\delta t}$$

and

$$\nabla Q = \lim_{\delta \vec{x} \to 0} \left[\frac{Q(\vec{x} + \delta\vec{x}, t) - Q(\vec{x}, t)}{\delta \vec{x}} \right]$$

it is straightforward to show that this results in the same expression for the substantial derivative as above.

Kinematic Concepts: Streamlines, Streaklines and Particle Paths:

In fluid dynamics it is often useful to distinguish the following kinematic constructs:

- **Streamlines:** curves that are instantaneously tangent to the velocity vector of the flow. Streamlines show the direction a massless fluid element will travel in at any point in time.
- **Streaklines:** the locus of points of all the fluid particles that have passed continuously through a particular spatial point in the past. Dye steadily injected into the fluid at a fixed point extends along a streakline.

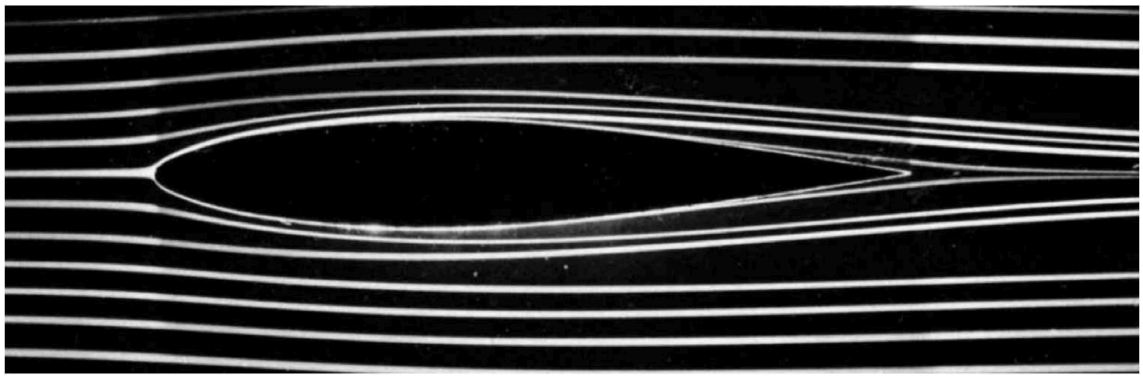

Figure 2: *Streaklines showing laminar flow across an airfoil; made by injecting dye at regular intervals in the flow*

- **Particle paths:** (aka pathlines) are the trajectories that individual fluid elements follow. The direction the path takes is determined by the streamlines of the fluid at each moment in time.

Only if the flow is **steady**, which means that all partial time derivatives (i.e., $\partial\vec{u}/\partial t = \partial\rho/\partial t = \partial P/\partial t$) vanish, will streamlines be identical to streaklines be identical to particle paths. For a non-steady flow, they will differ from each other.

CHAPTER 3

Hydrodynamic Equations for Ideal Fluid

Without any formal derivation (this comes later) we now present the hydrodynamic equations for an ideal, neutral fluid. Note that these equations adopt the level-3 continuum approach discussed in the previous chapter.

	Lagrangian	**Eulerian**
Continuity Eq:	$\dfrac{\mathrm{d}\rho}{\mathrm{d}t} = -\rho\,\nabla\cdot\vec{u}$	$\dfrac{\partial\rho}{\partial t} + \nabla\cdot(\rho\vec{u}) = 0$
Momentum Eqs:	$\dfrac{\mathrm{d}\vec{u}}{\mathrm{d}t} = -\dfrac{\nabla P}{\rho} - \nabla\Phi$	$\dfrac{\partial\vec{u}}{\partial t} + (\vec{u}\cdot\nabla)\,\vec{u} = -\dfrac{\nabla P}{\rho} - \nabla\Phi$
Energy Eq:	$\dfrac{\mathrm{d}\varepsilon}{\mathrm{d}t} = -\dfrac{P}{\rho}\nabla\cdot\vec{u} - \dfrac{\mathcal{L}}{\rho}$	$\dfrac{\partial\varepsilon}{\partial t} + \vec{u}\cdot\nabla\varepsilon = -\dfrac{P}{\rho}\,\nabla\cdot\vec{u} - \dfrac{\mathcal{L}}{\rho}$

Hydrodynamic equations for an ideal, neutral fluid in gravitational field

NOTE: students should become familiar with switching between the **Eulerian** and **Lagrangian** equations, and between the **vector notation** shown above and the **index notation**. The latter is often easier to work with. When writing down the index versions, make sure that each term carries the same index, and make use of the Einstein summation convention. The only somewhat tricky term is the $(\vec{u}\cdot\nabla)\,\vec{u}$-term in the Eulerian momentum equations, which in index form is given by $u_j(\partial u_i/\partial x_j)$, where i is the index carried by each term of the equation.

Continuity Equation: this equation expresses mass conservation. This is clear from the Eulerian form, which shows that changing the density at some fixed point in space requires a converging, or diverging, mass flux at that location.
If a flow is incompressible, then $\nabla\cdot\vec{u} = 0$ everywhere, and we thus have that $\mathrm{d}\rho/\mathrm{d}t = 0$ (i.e., the density of each fluid element is fixed in time as it moves with the flow). If a fluid is incompressible, than $\mathrm{d}\rho/\mathrm{d}t = 0$ and we see that the flow is divergence free

($\nabla \cdot \vec{u} = 0$), which is also called **solenoidal**.

Momentum Equations: these equations simply state than one can accelerate a fluid element with either a gradient in the pressure, P, or a gradient in the gravitational potential, Φ. Basically these momentum equations are nothing by Newton's $\vec{F} = m\vec{a}$ applied to a fluid element. In the above form, valid for an inviscid, ideal fluid, the momentum equations are called the **Euler equations**.

Energy Equation: the energy equation states that the only way that the **specific, internal energy**, ε, of a fluid element can change, in the absence of conduction, is by adiabatic compression or expansion, which requires a non-zero divergence of the velocity field (i.e., $\nabla \cdot \vec{u} \neq 0$), or by radiation (emission or absorption of photons). The latter is expressed via the **net volumetric cooling rate**,

$$\mathcal{L} = \rho \frac{\mathrm{d}Q}{\mathrm{d}t} = \mathcal{C} - \mathcal{H}$$

Here Q is the thermodynamic heat, and $\mathcal{C}$ and $\mathcal{H}$ are the net volumetric cooling and heating rates, respectively.

If the ideal fluid is governed by self-gravity (as opposed to, is placed in an external gravitational field), then one needs to complement the hydrodynamical equations with the **Poisson equation:** $\nabla^2\Phi = 4\pi G\rho$. In addition, closure requires an additional **constitutive relations** in the form of an equation-of-state $P = P(\rho, \varepsilon)$. If the ideal fluid obeys the ideal gas law, then we have the following two constitutive relations:

$$P = \frac{k_\mathrm{B}\,T}{\mu\, m_\mathrm{p}}\,\rho\,, \qquad\qquad \varepsilon = \frac{1}{\gamma - 1}\,\frac{k_\mathrm{B}\,T}{\mu\, m_\mathrm{p}}$$

(see Appendix H for details). Here μ is the mean molecular weight of the fluid in units of the proton mass, m_p, and γ is the adiabatic index, which is often taken to be 5/3 as appropriate for a mono-atomic gas.

Especially for the numerical Eulerian treatment of fluids, it is advantageous to write the hydro equations in **conservative form**. Let $A(\vec{x}, t)$ be some state variable of the fluid (either scalar or vector). The evolution equation for A is said to be in conservative form if

$$\frac{\partial A}{\partial t} + \nabla \cdot \vec{F}(A) = S$$

Here $\vec{F}(A)$ describes the appropriate flux of A and S describes the various sources and/or sinks of A. The continuity, momentum and energy equations for an ideal fluid in conservative form are:

$$\boxed{\begin{aligned} &\frac{\partial \rho}{\partial t} + \nabla \cdot (\rho \vec{u}) = 0 \\ &\frac{\partial \rho \vec{u}}{\partial t} + \nabla \cdot \overline{\overline{\mathbf{\Pi}}} = -\rho \nabla \Phi \\ &\frac{\partial E}{\partial t} + \nabla \cdot \left[(E + P)\, \vec{u} \right] = \rho \frac{\partial \Phi}{\partial t} - \mathcal{L} \end{aligned}}$$

Here

$$\overline{\overline{\mathbf{\Pi}}} = \rho\, \vec{u} \otimes \vec{u} + P$$

is the **momentum flux density tensor** (of rank 2), and

$$E = \rho \left(\frac{1}{2} u^2 + \Phi + \varepsilon \right)$$

is the **energy density**.

NOTE: In the expression for the momentum flux density tensor $\vec{A} \otimes \vec{B}$ is the **tensor product** of $\vec{A}$ and $\vec{B}$ defined such that $(\vec{A} \otimes \vec{B})_{ij} = a_i\, b_j$ (see Appendix A). Hence, the index-form of the momentum flux density tensor is simply $\Pi_{ij} = \rho\, u_i\, u_j + P \delta_{ij}$, with δ_{ij} the Kronecker delta function. Note that this expression is ONLY valid for an ideal fluid; in the next chapter we shall derive a more general expression for the momentum flux density tensor.

Note also that whereas there is no source or sink term for the density, gradients in the gravitational field act as a source of momentum, while its time-variability can cause an increase or decrease in the energy density of the fluid (if the fluid is collisionless, we call this **violent relaxation**). Another source/sink term for the energy density is radiation (emission or absorption of photons).

CHAPTER 4

Viscosity, Conductivity & The Stress Tensor

The hydrodynamic equations presented in the previous chapter are only valid for an **ideal fluid**, i.e., a fluid without viscosity and conduction. We now examine the origin of **conduction** and **viscosity**, and link the latter to the stress tensor, which is an important quantity in all of fluid dynamics.

In an ideal fluid, the particles effectively have a mean-free path of zero, such that they cannot communicate with their neighboring particles. In reality, though, the mean-free path, $\lambda_{\rm mfp} = (n\sigma)^{-1}$ is finite, and particles "communicate" with each other through collisions. These collisions cause an exchange of momentum and energy among the particles involved, acting as a relaxation mechanism. Note that in a collisionless system the mean-free path is effectively infinite, and there is no two-body relaxation, only collective relaxation mechanisms (i.e., violent relaxation or wave-particle interactions).

• When there are gradients in velocity ("**shear**") then the collisions among neighboring fluid elements give rise to a **net transport of momentum**. The collisions drive the system towards equilibrium, i.e., towards no shear. Hence, the collisions act as a resistance to shear, which is called **viscosity**. See Fig. 3 for an illustration.

• When there are gradients in temperature (or, in other words, in specific internal energy), then the collisions give rise to a **net transport of energy**. Again, the collisions drive the system towards equilibrium, in which the gradients vanish, and the rate at which the fluid can erase a non-zero ∇T is called the **(thermal) conductivity**.

The viscosity, μ, and conductivity, $\mathcal{K}$, are called **transport coefficients**. Expressions for μ and $\mathcal{K}$ in terms of the collision cross section, σ, the fluid's temperature T, and the particle mass m, can be derived in a rigorous manner using what is known as the **Chapman-Enskog expansion**. This is a fairly complicated topic, that is outside of the scope of this course. Intertested reader should consult the classical monographs *"Statistical Mechanics"* by K. Huang, or *"The Mathematical Theory of Non-*

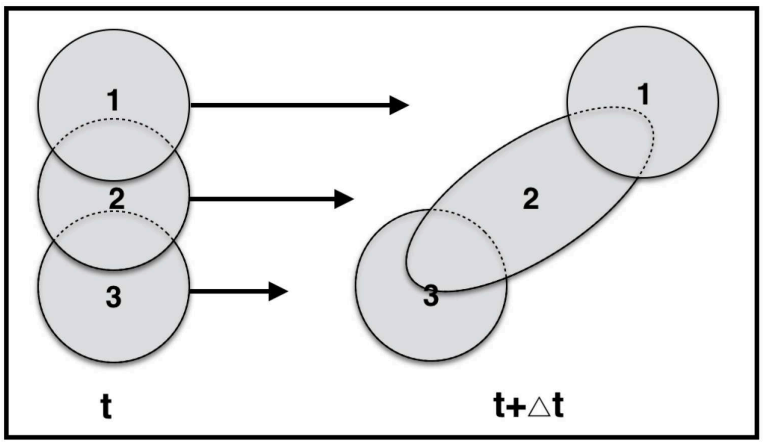

Figure 3: *Illustration of origin of viscosity and shear stress. Three neighboring fluids elements (1, 2 and 3) have different streaming velocities,* $\vec{u}$*. Due to the microscopic motions and collisions (characterized by a non-zero mean free path), there is a net* **transfer of momentum** *from the faster moving fluid elements to the slower moving fluid elements. This net transfer of momentum will tend to erase the shear in* $\vec{u}(\vec{x})$*, and therefore manifests itself as a shear-resistance, known as* **viscosity***. Due to the transfer of momentum, the fluid elements deform; in our figure, 1 transfers linear momentum to the top of 2, while 3 extracts linear momentum from the bottom of 2. Consequently, fluid element 2 is sheared as depicted in the figure at time* $t+\Delta t$*. From the perspective of fluid element 2, some internal force (from within its boundaries) has exerted a* **shear-stress** *on its bounding surface.*

uniform Gases" by S. Chapman and T. Cowling. Briefly, in the Chapman-Enskog expansion one expands the distribution function (DF) as $f = f^{(0)} + \alpha f^{(1)} + \alpha^2 f^{(2)} + ...$ Here $f^{(0)}$ is the equilibrium DF of an ideal fluid, which is the Maxwell-Boltzmann distribution, while α is the **Knudsen number** which is assumed to be small. Substutiting this expansion in the Boltzmann equation, yields, after some tedious algebra, the following expressions for μ and $\mathcal{K}$:

$$\mu = \frac{a}{\sigma} \left(\frac{m\, k_{\rm B}\, T}{\pi} \right)^{1/2} , \qquad \mathcal{K} = \frac{5}{2} c_{\rm V}\, \mu$$

Here a is a numerical factor that depends on the details of the interparticle forces, σ is the collisional cross section, and $c_{\rm V}$ is the specific heat (i.e., per unit mass). Thus, for a given fluid (given σ and m) we basically have that $\mu = \mu(T)$ and $\mathcal{K} = \mathcal{K}(T)$.

Note that $\mu \propto T^{1/2}$; viscosity increases with temperature. This only holds for gases! For liquids we know from experience that viscosity *decreases* with increasing temperature (think of honey). Since in astrophysics we are mainly concerned with gas, $\mu \propto T^{1/2}$ will be a good approximation for most of what follows.

Now that we have a rough idea of what viscosity (resistance to shear) and conductivity (resistance to temperature gradients) are, we have to ask how to incorporate them into our **hydrodynamic equations**.

Both transport mechanisms relate to the microscopic velocities of the individual particles. However, the macroscopic continuum approach of fluid dynamics only deals with the **streaming velocities** $\vec{u}$, which represents the velocities of the fluid elements. In order to link these different velocities we proceed as follows:

Velocity of fluid particles: We split the velocity, $\vec{v}$, of a fluid particle in a streaming velocity, $\vec{u}$, and a 'random' velocity, $\vec{w}$:

$$\vec{v} = \vec{u} + \vec{w}$$

where $\langle \vec{v} \rangle = \vec{u}$, $\langle \vec{w} \rangle = 0$ and $\langle . \rangle$ indicates the average over a fluid *element*. If we define v_i as the velocity in the i-direction, we have that

$$\langle v_i\, v_j \rangle = u_i\, u_j + \langle w_i\, w_j \rangle$$

These different velocities allow us to define a number of different velocity tensors:

Stress Tensor:	$\sigma_{ij} \equiv -\rho\langle w_i\, w_j\rangle$	$\overline{\overline{\sigma}} = -\rho\vec{w}\otimes\vec{w}$
Momentum Flux Density Tensor:	$\Pi_{ij} \equiv +\rho\langle v_i\, v_j\rangle$	$\overline{\overline{\mathbf{\Pi}}} = +\rho\vec{v}\otimes\vec{v}$
Ram Pressure Tensor:	$\Sigma_{ij} \equiv +\rho u_i u_j$	$\overline{\overline{\mathbf{\Sigma}}} = +\rho\vec{u}\otimes\vec{u}$

which are related according to $\overline{\overline{\sigma}} = \overline{\overline{\mathbf{\Sigma}}} - \overline{\overline{\mathbf{\Pi}}}$. Note that each of these tensors is manifest **symmetric** (i.e., $\sigma_{ij} = \sigma_{ji}$, etc.), which implies that they have 6 independent variables.

Note that the **stress tensor** is related to the microscopic random motions. These are the ones that give rise to pressure, viscosity and conductivity! The reason that σ_{ij} is called the stress tensor is that it is related to the **stress** $\vec{\Sigma}(\vec{x},\hat{n})$ acting on a surface with normal vector $\hat{n}$ located at $\vec{x}$ according to

$$\Sigma_i(\hat{n}) = \sigma_{ij}\, n_j$$

Here $\Sigma_i(\hat{n})$ is the i-component of the stress acting on a surface with normal $\hat{n}$, whose j-component is given by n_j. Hence, in general the stress will not necessarily be along the normal to the surface, and it is useful to decompose the stress in a **normal stress**, which is the component of the stress along the normal to the surface, and a **shear stress**, which is the component along the tangent to the surface.

To see that fluid elements in general are subjected to shear stress, consider the following: Consider a flow (i.e., a river) in which we inject a small, spherical blob (a fluid element) of dye. If the only stress to which the blob is subject is normal stress, the only thing that can happen to the blob is an overall compression or expansion. However, from experience we know that the blob of dye will shear into an extended, 'spaghetti'-like feature; hence, the blob is clearly subjected to shear stress, and this shear stress is obvisouly related to another tensor called the **deformation tensor**

$$T_{ij} = \frac{\partial u_i}{\partial x_j}$$

which describes the (local) shear in the fluid flow.

Since $\partial u_i/\partial x_j = 0$ in a **static** fluid ($\vec{u}(\vec{x}) = 0$), we see that in a static fluid the stress tensor can only depend on the normal stress, which we call the **pressure**.

Pascal's law for hydrostatistics: In a **static** fluid, there is no preferred direction, and hence the (normal) stress has to be isotropic:

$$\text{static fluid} \quad \Longleftrightarrow \quad \sigma_{ij} = -P\,\delta_{ij}$$

The minus sign is a consequence of the sign convention of the stress.

Sign Convention: The stress $\vec{\Sigma}(\vec{x},\hat{n})$ acting at location $\vec{x}$ on a surface with normal $\hat{n}$, is exerted *by* the fluid on the side of the surface to which the normal points, *on* the fluid from which the normal points. In other words, *a positive stress results in compression*. Hence, in the case of pure, normal pressure, we have that $\Sigma = -P$.

Viscous Stress Tensor: The expression for the stress tensor in the case of static fluid motivates us to write in general

$$\boxed{\sigma_{ij} = -P\,\delta_{ij} + \tau_{ij}}$$

where we have introduced a new tensor, τ_{ij}, which is known as the viscous stress tensor, or the **deviatoric stress tensor**.

Since the deviatoric stress tensor, τ_{ij}, is only non-zero in the presence of shear in the fluid flow, this suggests that

$$\tau_{ij} = T_{ijkl}\,\frac{\partial u_k}{\partial x_l}$$

where T_{ijkl} is a proportionality tensor of **rank** four. As described in Appendix G (which is NOT part of the curriculum for this course), most (astrophysical) fluids are **Newtonian**, in that they obey a number of conditions. As detailed in that appendix, for a Newtonian fluid, the relation between the stress tensor and the deformation tensor is given by

$$\boxed{\sigma_{ij} = -P\delta_{ij} + \mu\left[\frac{\partial u_i}{\partial x_j} + \frac{\partial u_j}{\partial x_i} - \frac{2}{3}\delta_{ij}\frac{\partial u_k}{\partial x_k}\right] + \eta\,\delta_{ij}\frac{\partial u_k}{\partial x_k}}$$

Here P is the pressure, δ_{ij} is the Kronecker delta function, μ is the **coefficient of shear viscosity**, and η is the **coefficient of bulk viscosity** (aka the 'second viscosity'). We thus see that for a Newtonian fluid, the stress tensor, despite being a symmetric tensor of rank two, only has three independent components: P, μ and η.

Let's take a closer look at these three quantities, starting with the pressure P. To be exact, P is the **thermodynamic equilibrium pressure**, and is normally computed thermodynamically from some equation of state, $P = P(\rho, T)$. It is related to the translational kinetic energy of the particles when the fluid, in equilibrium, has reached **equipartition** of energy among **all** its degrees of freedom, including (in the case of molecules) rotational and vibrations degrees of freedom.

In addition to the thermodynamic equilibrium pressure, P, we can also define a **mechanical pressure**, $P_{\rm m}$, which is purely related to the translational motion of the particles, **independent** of whether the system has reached full equipartition of energy. The mechanical pressure is simply the average normal stress and therefore follows from the stress tensor according to

$$P_{\rm m} = -\frac{1}{3}\,{\rm Tr}(\sigma_{ij}) = -\frac{1}{3}\,(\sigma_{11} + \sigma_{22} + \sigma_{33})$$

Using the above expression for σ_{ij}, and using that $\partial u_k/\partial x_k = \nabla \cdot \vec{u}$ (Einstein summation convention), it is easy to see that

$$P_{\rm m} = P - \eta\,\nabla \cdot \vec{u}$$

From this expression it is clear that the bulk viscosity, η, is only non-zero if $P \neq P_{\rm m}$. This, in turn, can only happen if the constituent particles of the fluid have degrees of freedom beyond position and momentum (i.e., when they are molecules with rotational or vibrational degrees of freedom). Hence, for a fluid of monoatoms (ideal gas), $\eta = 0$. From the fact that $P = P_{\rm m} + \eta\nabla \cdot \vec{u}$ it is clear that for an **incompressible flow** $P = P_{\rm m}$ and the value of η is irrelevant; *bulk viscosity plays no role in incompressible fluids or flows*. The only time when $P_{\rm m} \neq P$ is when a fluid consisting of particles with internal degrees of freedom (e.g., molecules) has just undergone a large volumetric change (i.e., during a shock). In that case there may be a lag between the time the translational motions reach equilibrium and the time when the system reaches full equipartition in energy among all degrees of freedom. In astrophysics, bulk viscosity can generally be ignored, but be aware that it may be important in shocks. This only leaves the shear viscosity μ, which describes the ability of the fluid to resist shear stress via momentum transport resulting from collisions and the non-zero mean free path of the particles.

CHAPTER 5

Hydrodynamic Equations for Non-Ideal Fluid

In the hydrodynamic equations for an ideal fluid presented in Chapter 3 we ignored both viscosity and conductivity. We now examine how our hydrodynamic equations change when allowing for these two transport mechanisms.

As we have seen in the previous chapter, the effect of **viscosity** is captured by the **stress tensor**, which is given by

$$\sigma_{ij} = -P\delta_{ij} + \tau_{ij} = -P\delta_{ij} + \mu\left[\frac{\partial u_i}{\partial x_j} + \frac{\partial u_j}{\partial x_i} - \frac{2}{3}\delta_{ij}\frac{\partial u_k}{\partial x_k}\right] + \eta\,\delta_{ij}\frac{\partial u_k}{\partial x_k}$$

Note that in the limit $\mu \to 0$ and $\eta \to 0$, valid for an ideal fluid, $\sigma_{ij} = -P\delta_{ij}$. This suggests that we can incorporate viscosity in the hydrodynamic equations by simply replacing the pressure P with the stress tensor, i.e., $P\delta_{ij} \to -\sigma_{ij} = P\delta_{ij} - \tau_{ij}$.

Starting from the **Euler equation** in Lagrangian index form;

$$\rho\frac{\mathrm{d}u_i}{\mathrm{d}t} = -\frac{\partial P}{\partial x_i} - \rho\frac{\partial \Phi}{\partial x_i}$$

we use that $\partial P/\partial x_i = \partial(P\delta_{ij})/\partial x_j$, and then make the above substitution to obtain

$$\boxed{\rho\frac{\mathrm{d}u_i}{\mathrm{d}t} = \frac{\partial(-P\delta_{ij})}{\partial x_j} + \frac{\partial \tau_{ij}}{\partial x_j} - \rho\frac{\partial \Phi}{\partial x_i}}$$

These momentum equations are called the **Navier-Stokes equations**.

It is more common, and more useful, to write out the viscous stress tensor, yielding

$$\boxed{\rho\frac{\mathrm{d}u_i}{\mathrm{d}t} = -\frac{\partial P}{\partial x_i} + \frac{\partial}{\partial x_j}\left[\mu\left(\frac{\partial u_i}{\partial x_j} + \frac{\partial u_j}{\partial x_i} - \frac{2}{3}\delta_{ij}\frac{\partial u_k}{\partial x_k}\right)\right] + \frac{\partial}{\partial x_i}\left(\eta\,\frac{\partial u_k}{\partial x_k}\right) - \rho\frac{\partial \Phi}{\partial x_i}}$$

These are the **Navier-Stokes** equations (in Lagragian index form) in all their glory, containing both the **shear viscosity** term and the **bulk viscosity** term (the latter is often ignored).

Note that μ and η are usually functions of density and temperature so that they have spatial variations. However, it is common to assume that these are suficiently small so that μ and η can be treated as constants, in which case they can be taken outside the differentials. In what follows we will make this assumption as well.

The Navier-Stokes equations in **Lagrangian vector form** are

$$\rho\frac{\mathrm{d}\vec{u}}{\mathrm{d}t} = -\nabla P + \mu\nabla^2\vec{u} + \left(\eta + \frac{1}{3}\mu\right)\,\nabla(\nabla\cdot\vec{u}) - \rho\nabla\Phi$$

If we ignore the bulk viscosity ($\eta = 0$) then this reduces to

$$\boxed{\frac{\mathrm{d}\vec{u}}{\mathrm{d}t} = -\frac{\nabla P}{\rho} + \nu\left[\nabla^2\vec{u} + \frac{1}{3}\nabla(\nabla\cdot\vec{u})\right] - \nabla\Phi}$$

where we have introduced the **kinetic viscosity** $\nu \equiv \mu/\rho$. Note that these equations reduce to the **Euler equations** in the limit $\nu \to 0$. Also, note that the $\nabla(\nabla\cdot\vec{u})$ term is only significant in the case of flows with **variable compression** (i.e., viscous dissipation of accoustic waves or shocks), and can often be ignored. This leaves the $\nu\nabla^2\vec{u}$ term as the main addition to the Euler equations. Yet, this simple 'diffuse' term (describing **viscous momentum diffusion**) dramatically changes the character of the equation, as it introduces a higher spatial derivative. Hence, additional boundary conditions are required to solve the equations. When solving problems with solid boundaries (not common in astrophysics), this condition is typically that the *tangential* (or shear) velocity at the boundary vanishes. Although this may sound ad hoc, it is supported by observation; for example, the blades of a fan collect dust.

Recall that when writing the Navier-Stokes equation in **Eulerian** form, we have that $\mathrm{d}\vec{u}/\mathrm{d}t \to \partial\vec{u}/\partial t + \vec{u}\cdot\nabla\vec{u}$. It is often useful to rewrite this extra term using the vector calculus identity

$$\vec{u}\cdot\nabla\vec{u} = \nabla\left(\frac{\vec{u}\cdot\vec{u}}{2}\right) + (\nabla\times\vec{u})\times\vec{u}$$

Hence, for an **irrotational flow** (i.e., a flow for which $\nabla \times \vec{u} = 0$), we have that $\vec{u} \cdot \nabla \vec{u} = \frac{1}{2} \nabla u^2$, where $u \equiv |\vec{u}|$.

Next we move to the **energy equation**, modifying it so as to account for both **viscosity** and **conduction**. We start from

$$\rho \frac{\mathrm{d}\varepsilon}{\mathrm{d}t} = -P \frac{\partial u_i}{\partial x_i} - \mathcal{L}$$

(see Chapter 3, and recall that, with the Einstein summation convention, $\partial u_i / \partial x_i = \nabla \cdot \vec{u}$). As with the momentum equations, we include viscosity by making the transformation $-P\delta_{ij} \rightarrow \sigma_{ij} = -P\delta_{ij} + \tau_{ij}$, which we do as follows:

$$-P \frac{\partial u_i}{\partial x_i} \quad \rightarrow \quad -P\delta_{ij} \frac{\partial u_i}{\partial x_j} \quad \rightarrow \quad -P\delta_{ij} \frac{\partial u_i}{\partial x_j} + \tau_{ij} \frac{\partial u_i}{\partial x_j}$$

This allows us to write the energy equation in vector form as

$$\rho \frac{\mathrm{d}\varepsilon}{\mathrm{d}t} = -P \nabla \cdot \vec{u} + \mathcal{V} - \mathcal{L}$$

where

$$\mathcal{V} \equiv \tau_{ik} \frac{\partial u_i}{\partial x_k}$$

is the **rate of viscous dissipation** which describes the rate at which the work done against viscous forces is irreversibly converted into internal energy.

Now that we have added the effect of viscosity, what remains is to add **conduction**. We can make progress by realizing that, on the microscopic level, conduction arises from collisions among the constituent particles, causing a flux in internal energy. The internal energy density of a fluid element is $\langle \frac{1}{2} \rho w^2 \rangle$, where $\vec{w} = \vec{v} - \vec{u}$ is the random motion of the particle wrt the fluid element (see Chapter 4), and the angle brackets indicate an ensemble average over the particles that make up the fluid element. Based on this we see that the **conductive flux** in the i-direction can be written as

$$F_{\mathrm{cond},i} = \langle \frac{1}{2} \rho w^2 w_i \rangle = \langle \rho \varepsilon w_i \rangle$$

From experience we also know that we can write the conductive flux as

$$\vec{F}_{\mathrm{cond}} = -\mathcal{K} \nabla T$$

with $\mathcal{K}$ the **thermal conductivity**.

Next we realize that conduction only causes a *net* change in the internal energy at some fixed position if the divergence in the conductive flux ($\nabla \cdot \vec{F}_{\rm cond}$) at that position is non-zero. This suggests that the final form of the energy equation, for a non-ideal fluid, and in Lagrangian vector form, has to be

$$\boxed{\rho \frac{{\rm d}\varepsilon}{{\rm d}t} = -P\,\nabla\cdot\vec{u} - \nabla\cdot\vec{F}_{\rm cond} + \mathcal{V} - \mathcal{L}}$$

To summarize, below we list the full set of equations of gravitational, radial hydrodynamics (ignoring bulk viscosity) [1].

Full Set of Equations of Gravitational, Radiative Hydrodynamics

Continuity Eq.	$\dfrac{{\rm d}\rho}{{\rm d}t} = -\rho\,\nabla\cdot\vec{u}$
Momentum Eqs.	$\rho\,\dfrac{{\rm d}\vec{u}}{{\rm d}t} = -\nabla P + \mu\left[\nabla^2\vec{u} + \dfrac{1}{3}\nabla(\nabla\cdot\vec{u})\right] - \rho\,\nabla\Phi$
Energy Eq.	$\rho\,\dfrac{{\rm d}\varepsilon}{{\rm d}t} = -P\,\nabla\cdot\vec{u} - \nabla\cdot\vec{F}_{\rm cond} - \mathcal{L} + \mathcal{V}$
Poisson Eq.	$\nabla^2\Phi = 4\pi G\rho$
Constitutive Eqs.	$P = P(\rho,\varepsilon)\,, \qquad \mu = \mu(T) \propto \dfrac{1}{\sigma}\left(\dfrac{mk_{\rm B}T}{\pi}\right)^{1/2}\,, \qquad \mathcal{K} = \mathcal{K}(T) \simeq \dfrac{5}{2}\,\mu(T)\,c_{\rm V}$
Diss/Cond/Rad	$\mathcal{V} \equiv \tau_{ik}\dfrac{\partial u_i}{\partial x_k}\,, \qquad F_{{\rm cond},k} = \langle\rho\varepsilon w_k\rangle\,, \qquad \mathcal{L} \equiv \mathcal{C} - \mathcal{H}$

[1] Diss/Cond/Rad stands for Dissipation, Conduction, Radiation

CHAPTER 6

Kinetic Theory: From Liouville to Boltzmann

In the previous chapter, we presented the hydrodynamic equations that are valid in the macroscopic, continuum approach to fluid dynamics. We now derive this set of equations rigorously, starting from the microscopic, particle-based view of fluids. We start by reminding ourselves of a few fundamental concepts in dynamics.

Degree of freedom: an independent physical parameter in the formal description of the **state** of the physical system. In what follows we use $n_{\rm dof}$ to indicate the number of degrees of freedom.

Phase-Space: The phase-space of a dynamical system is a space in which all possible states of a system are represented, with each possible state corresponding to one unique point in that phase-space. The dimensionality of phase-space is $n_{\rm dof}$.

`Caution:` I will use 'phase-space' to refer to **both** this $n_{\rm dof}$-dimensional space, in which each state is associated with a point in that space, as well as to the 6-dimensional space $(\vec{x},\vec{v})$ in which each individual particle is associated with a point in that space. In order to avoid confusion, in this chapter I will refer to the former as Γ-space, and the latter as μ-space.

Canonical Coordinates: in classical mechanics, canonical coordinates are coordinates q_i and p_i in phase-space that are used in the Hamiltonian formalism and that satisfy the **canonical commutation relations**:

$$\{q_i,q_j\}=0, \qquad \{p_i,p_j\}=0, \qquad \{q_i,p_j\}=\delta_{ij}$$

Here the curly brackets correspond to **Poisson brackets** (see Appendix I). When q_i is a Cartesian coordinate in configuration space, p_i is the corresponding **linear momentum**. However, when using curvi-linear coordinates and q_i is an angle, then the corresponding p_i is an **angular momentum**. Hence, p_i is therefore not always equal to $m\dot{q}_i$! Note that p_i is called the **conjugate momentum**, to indicate that it belongs to q_i in a canonical sense (meaning, that it obeys the canonical commutation relations).

Let N be the number of constituent particles in our fluid. In all cases of interests, N will be a huge number; $N \gg 10^{20}$. How do you (classically) describe such a system? To completely describe a fluid of N particles, you need to specify **for each particle** the following quantities:

$$\begin{aligned} \textbf{position} \quad & \vec{q} = (q_1, q_2, q_3) \\ \textbf{momentum} \quad & \vec{p} = (p_1, p_2, p_3) \\ \textbf{internal degrees of freedom} \quad & \vec{s} = (s_1, s_2, ..., s_K) \end{aligned}$$

Examples of internal degrees of freedom are electrical charge (in case of a plasma), or the rotation or vibrational modes for molecules, etc. The number of degrees of freedom in the above example is $n_{\rm dof} = N(6 + K)$. In what follows we will only consider particles with zero internal dof (i.e., $K = 0$ so that $n_{\rm dof} = 6N$). Such particles are sometimes called **monoatoms**, and can be treated as point particles. The **microstate** of a system composed of N monoatoms is completely described by

$$\vec{\Gamma} = (\vec{q}_1, \vec{q}_2, ..., \vec{q}_N, \vec{p}_1, \vec{p}_2, ..., \vec{p}_N)$$

which corresponds to a single point in our $6N$-dimensional phase-space (Γ-space).

As already discussed in Chapter 2, the dynamics of our fluid of N monoatoms is described by its **Hamiltonian**

$$\mathcal{H}(\vec{q}_i, \vec{p}_i, t) \equiv \mathcal{H}(\vec{q}_1, \vec{q}_2, ..., \vec{q}_N, \vec{p}_1, \vec{p}_2, ..., \vec{p}_N, t)$$

and the corresponding **equations of motion** are:

$$\boxed{\dot{\vec{q}}_i = \frac{\partial \mathcal{H}}{\partial \vec{p}_i}\,; \qquad \dot{\vec{p}}_i = -\frac{\partial \mathcal{H}}{\partial \vec{q}_i}}$$

In what follows we will often adopt a shorthand notation, which also is more 'symmetric'. We introduce the 6D vector $\vec{w} \equiv (\vec{q}, \vec{p})$, i.e., the 6D array one obtains when combining the 3 components of $\vec{q}$ with the 3 components of $\vec{p}$. Using **Poisson brackets**, we can then write the **Hamiltonian equations of motion** as

$$\boxed{\dot{\vec{w}}_i = \{\vec{w}_i, \mathcal{H}\}}$$

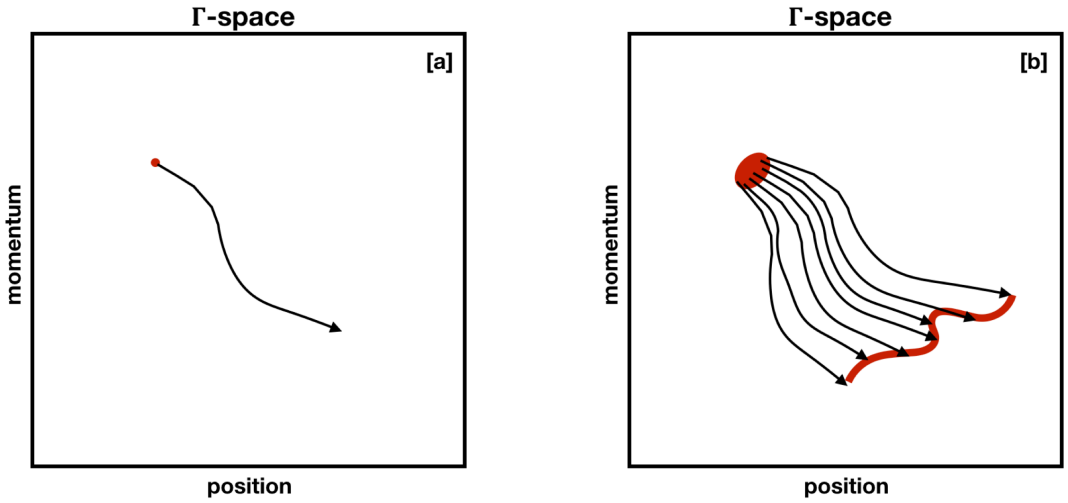

Figure 4: *Illustration of evolution in* Γ*-space. The* x*- and* y*-axes represent the* $3N$*-dimensional position-vector and momentum-vector, respectively. Panel (a) shows the evolution of a state (indicated by the red dot). As time goes on, the potitions and momentum of all the particles change (according to the Hamiltonian equations of motion), and the state moves around in* Γ*-space. Panel (b) shows the evolution of an ensemble of microstates (called a macrostate). As neighboring states evolve slightly differently, the volume in* Γ*-space occupied by the original microstates (the red, oval region) is stretched and sheared into a 'spagetti-like' feature. According to Liouville's theorem, the volume of this spagetti-like feature is identical to that of the original macrostate (i.e., the flow in* Γ*-space is incompressible). Note also, that two trajectories in* Γ*-space can NEVER cross each other.*

Thus, given $\vec{w}_i$ for all $i = 1, 2, ..., N$, at any given time t_0, one can compute the Hamiltonian and solve for the equations of motion to obtain $\vec{w}_i(t)$. This specifies a unique **trajectory** $\vec{\Gamma}(t)$ in this phase-space (see panel [a] of Fig. 4). Note that no two trajectories $\vec{\Gamma}_1(t)$ and $\vec{\Gamma}_2(t)$ are allowed to cross each other. If that were the case, it would mean that the same initial state can evolve differently, which would be a violation of the **deterministic character** of classical physics. The Hamiltonian formalism described above basically is a **complete treatment** of fluid dynamics. In practice, though, it is utterly useless, simply because N is HUGE, making it impossible to specify the complete set of initial conditions. We neither have (nor want) the detailed information that is required to specify a **microstate**. We are only interested in the average behavior of the **macroscopic** properties of the system, such as density, temperature, pressure, etc. With each such **macrostate** corresponds a huge number of microstates, called a **statistical ensemble**.

The ensemble is described statistically by the **N-body distribution function**

$$f^{(N)}(\vec{w}_i) \equiv f^{(N)}(\vec{w}_1, \vec{w}_2, ..., \vec{w}_N) = f^{(N)}(\vec{q}_1, \vec{q}_2, ..., \vec{q}_N, \vec{p}_1, \vec{p}_2, ..., \vec{p}_N)$$

which expresses the ensemble's probability distribution, i.e., $f^{(N)}(\vec{w}_i)\,\mathrm{d}V$ is the probability that the actual microstate is given by $\vec{\Gamma}(\vec{q}_i, \vec{p}_i)$, where $\mathrm{d}V = \prod_{i=1}^{N} \mathrm{d}^6\vec{w}_i = \prod_{i=1}^{N} \mathrm{d}^3\vec{q}_i\,\mathrm{d}^3\vec{p}_i$. This implies the following **normalization condition**

$$\int \mathrm{d}V\, f^{(N)}(\vec{w}_i) = 1$$

In our statistical approach, we seek to describe the evolution of the N-body distribution function, $f^{(N)}(\vec{w}_i, t)$, rather than that of a particular microstate, which instead is given by $\vec{\Gamma}(\vec{w}_i, t)$. Since probability is locally conserved, it must obey a **continuity equation**; any change of probability in one part of phase-space must be compensated by a flow of probability into or out of neighboring regions. As we have seen in Chapter 2, the continuity equation of a (continuum) density field, $\rho(\vec{x})$, is given by

$$\frac{\partial \rho}{\partial t} + \nabla \cdot (\rho\, \vec{v}) = 0$$

which expresses that the local change in the mass enclosed in some volume is balanced by the divergence of the flow out of that volume. In the case of our probability distribution $f^{(N)}$ we have that ∇ is in $6N$-dimensional phase-space, and includes $\partial/\partial\vec{q}_i$ and $\partial/\partial\vec{p}_i$, i.e.,

$$\nabla = \frac{\partial}{\partial \vec{w}_i} = \left(\frac{\partial}{\partial \vec{x}_i}, \frac{\partial}{\partial \vec{p}_i} \right) = \left(\frac{\partial}{\partial \vec{x}_1}, \frac{\partial}{\partial \vec{x}_2}, ..., \frac{\partial}{\partial \vec{x}_N}, \frac{\partial}{\partial \vec{p}_1}, \frac{\partial}{\partial \vec{p}_2}, ..., \frac{\partial}{\partial \vec{p}_N} \right)$$

Similarly, the 'velocity vector' in our $6N$-dimensional Γ-space is given by

$$\dot{\vec{w}} \equiv (\dot{\vec{q}}_i, \dot{\vec{p}}_i) = (\dot{\vec{q}}_1, \dot{\vec{q}}_2, ..., \dot{\vec{q}}_N, \dot{\vec{p}}_1, \dot{\vec{p}}_2, ..., \dot{\vec{p}}_N)$$

Hence, the continuity equation for $f^{(N)}$, which is known as the **Liouville equation**, can be written as

$$\frac{\partial f^{(N)}}{\partial t} + \nabla \cdot (f^{(N)} \, \dot{\vec{w}}) = 0$$

Using the fact that the gradient of the product of a vector and a scalar can be written as the sum of the scalar times the divergence of the vector, plus the dot-product of the vector and the gradient of the scalar (see Appendix A), we have that

$$\nabla \cdot (f^{(N)} \, \vec{w}) = f^{(N)} \, \nabla \cdot \dot{\vec{w}} + \dot{\vec{w}} \cdot \nabla f^{(N)}$$

If we write out the divergence of $\dot{\vec{w}}$ as

$$\nabla \cdot \dot{\vec{w}} = \sum_{i=1}^{N} \left[\frac{\partial \dot{\vec{q}}_i}{\partial \vec{q}_i} + \frac{\partial \dot{\vec{p}}_i}{\partial \vec{p}_i} \right]$$

and use the Hamiltonian equations of motion to write $\dot{\vec{q}}_i$ and $\dot{\vec{p}}_i$ as gradients of the Hamiltonian, we find that

$$\nabla \cdot \dot{\vec{w}} = \sum_{i=1}^{N} \left[\frac{\partial}{\partial \vec{q}_i} \left(\frac{\partial \mathcal{H}}{\partial \vec{p}_i} \right) - \frac{\partial}{\partial \vec{p}_i} \left(\frac{\partial \mathcal{H}}{\partial \vec{q}_i} \right) \right] = \sum_{i=1}^{N} \left[\frac{\partial^2 \mathcal{H}}{\partial \vec{q}_i \, \partial \vec{p}_i} - \frac{\partial^2 \mathcal{H}}{\partial \vec{p}_i \, \partial \vec{q}_i} \right] = 0$$

Thus, we obtain the important result that

In a Hamiltonian system the flow in $\Gamma-$space is incompressible

This is generally known as the **Liouville Theorem**. It implies that the volume in Γ-space occupied by a macrostate does NOT change under Hamiltonian evolution. Although the microstates that make up the macrostate can disperse, the volume they occupy stays connected and constant; it typically will change shape, but its total volume remains fixed (see panel [b] of Fig. 4).

Using this result, we can write the **Liouville equation** in any of the following forms:

$$\boxed{\begin{aligned}
&\frac{\partial f^{(N)}}{\partial t} + \dot{\vec{w}} \cdot \nabla f^{(N)} = 0 \\
&\frac{\partial f^{(N)}}{\partial t} + \sum_{i=1}^{N} \left(\dot{\vec{q}}_i \cdot \frac{\partial f^{(N)}}{\partial \vec{q}_i} + \dot{\vec{p}}_i \cdot \frac{\partial f^{(N)}}{\partial \vec{p}_i} \right) = 0 \\
&\frac{\mathrm{d} f^{(N)}}{\mathrm{d} t} = 0 \\
&\frac{\partial f^{(N)}}{\partial t} + \{ f^N, \mathcal{H} \} = 0
\end{aligned}}$$

The second expression follows from the first by simply writing out the terms of the divergence. The third expression follows from the second one upon realizing that $f^{(N)} = f^{(N)}(t, \vec{q}_1, \vec{q}_2, ..., \vec{q}_3, \vec{p}_1, \vec{p}_2, ..., \vec{p}_N)$ and using the fact that for a function $f(x, y)$ the infinitessimal $\mathrm{d}f = (\partial f/\partial x)\,\mathrm{d}x + (\partial f/\partial y)\,\mathrm{d}y$. Finally, the fourth expression follows from the second upon using the Hamiltonian equations of motion and the expression for the Poisson brackets, and will be used abundantly below.

The Liouville equation is basically a complete 'level-1' (see Chapter 2) dynamical theory for fluids. Rather than describing the evolution of a single microstate, $\vec{\Gamma}(t)$, it describes the evolution of an ensemble of microstates (a macrostate). If anything, this makes computations even harder; for starters, the N-point distribution function $f^{(N)}$ is a function of $6N$ variables, which is utterly unmanageable. However, the Liouville equation is an important, powerful starting point for the development of a 'level-2' dynamical theory, from which in turn we can construct a 'level-3' theory.

Recall from Chapter 2, that a level-2 theory seeks to describe the evolution of the phase-space distribution function (DF)

$$f(\vec{q}, \vec{p}) = \frac{\mathrm{d}^6 N}{\mathrm{d}^3 \vec{q}\, \mathrm{d}^3 \vec{p}}$$

which describes the density of particles in 6D phase-space $(\vec{q}, \vec{p})$. In what follows,

we shall refer to this 6-dimensional phase-space as μ-space, to distinguish it from the 6N-dimensional Γ-space. And we shall refer to the above DF as the 1-point DF, $f^{(1)}$, in order to distinguish it from the N-point DF, $f^{(N)}$, which appears in the Liouville equation. Whereas the latter describes the ensemble density of micro-states in Γ-space, the latter describes the density of particles in μ-space.

Kinetic Theory: One can derive an equation for the time-evolution of the 1-point DF, starting from the Liouville equation. First we make the assumption that all particles are (statistically) identical (which is basically always the case). This implies that $f^{(N)}$ is a **symmetric function** of $\vec{w}_i$, such that

$$f^{(N)}(..., \vec{w}_i, ..., \vec{w}_j, ...) = f^{(N)}(..., \vec{w}_j, ..., \vec{w}_i, ...) \qquad \forall (i,j)$$

In words; if you flip the indices of any two particles, nothing changes. This allows us to derive an equation describing the evolution of the 1-point distribution function $f^{(1)}(\vec{w})$, as follows.

We first define the **reduced** or **k-particle DF**, which is obtained by integrating the N-body DF, $f^{(N)}$, over $N-k$ six-vectors $\vec{w}_i$. Since $f^{(N)}$ is symmetric in $\vec{w}_i$, without loss of generality we may choose the integration variables to be $\vec{w}_{k+1}, \vec{w}_{k+2}, ..., \vec{w}_N$:

$$\boxed{f^{(k)}(\vec{w}_1, \vec{w}_2, ..., \vec{w}_k, t) \equiv \frac{N!}{(N-k)!} \int \prod_{i=k+1}^{N} \mathrm{d}^6 \vec{w}_i \, f^{(N)}(\vec{w}_1, \vec{w}_2, ..., \vec{w}_N, t)}$$

where the choice of the prefactor will become clear in what follows.

In particular, the **1-particle distribution function** is

$$f^{(1)}(\vec{w}_1, t) \equiv N \int \prod_{i=2}^{N} \mathrm{d}^6 \vec{w}_i \, f^{(N)}(\vec{w}_1, \vec{w}_2, ..., \vec{w}_N, t)$$

Because of the prefactor, we now have that

$$\int \mathrm{d}^6 \vec{w}_1 \, f^{(1)}(\vec{w}_1, t) = N \int \prod_{i=1}^{N} \mathrm{d}^6 \vec{w}_i \, f^{(N)}(\vec{w}_1, \vec{w}_2, ..., \vec{w}_N, t) = N$$

where we have used the normalization condition of $f^{(N)}$. Hence, $f^{(1)}(\vec{q},\vec{p},t) = \mathrm{d}N/\mathrm{d}^3\vec{q}\,\mathrm{d}^3\vec{p}$ is the number of particles in the phase-space volume $\mathrm{d}^3\vec{q}\,\mathrm{d}^3\vec{p}$ centered on $(\vec{q},\vec{p})$.

That $f^{(1)}(\vec{w},t)$ is an important, relevant DF is evident from the following. Consider an **observable** $Q(\vec{w})$ that involves only quantities that depend additively on the phase-space coordinates of **single, individual particles** [i.e., $Q_{\mathrm{ensemble}} = Q(\vec{w}_1) + Q(\vec{w}_2) + ... + Q(\vec{w}_N)$]. Examples are velocity, kinetic energy, or any other velocity moment v^k. The expectation value, $\langle Q\rangle$, can be written as

$$\langle Q\rangle = \int \mathrm{d}^6\vec{w}_1 ... \mathrm{d}^6\vec{w}_N f^{(N)}(\vec{w}_1,\vec{w}_2,...,\vec{w}_N)\sum_{i=1}^{N} Q_i$$

Since all particles are statistically identical, we can rewrite this as

$$\boxed{\langle Q\rangle = \int \mathrm{d}^6\vec{w}_1\, Q(\vec{w}_1)\, f^{(1)}(\vec{w}_1)}$$

Hence, computing the expectation value for any observable $Q(\vec{w})$ only requires knowledge of the 1-particle DF. And since all our macroscopic continuum properties of the fluid (i.e., ρ, $\vec{u}$, ε) depend additively on the phase-space coordinates, the **1-particle DF** suffices for a macroscopic description of the fluid. Hence, our goal is derive an evolution equation for $f^{(1)}(\vec{q},\vec{p},t)$. We do so as follows.

For the time evolution of each reduced DF we can write

$$\begin{aligned}\frac{\partial f^{(k)}}{\partial t} &= \frac{N!}{(N-k)!}\int \prod_{i=k+1}^{N} \mathrm{d}^6\vec{w}_i \,\frac{\partial f^{(N)}}{\partial t}(\vec{w}_1,\vec{w}_2,...,\vec{w}_N)\\ &= \frac{N!}{(N-k)!}\int \prod_{i=k+1}^{N} \mathrm{d}^6\vec{w}_i \,\{\mathcal{H}, f^{(N)}\}\end{aligned}$$

where the first step simply follows from operating the time derivative on the definition of the reduced k-particle DF, and the second step follows from the **Liouville equation**.

Next we substitute the Hamiltonian, which in general can be written as

$$\boxed{\mathcal{H}(\vec{q}_i,\vec{p}_i)=\sum_{i=1}^{N}\frac{\vec{p}_i^{\,2}}{2m}+\sum_{i=1}^{N}V(\vec{q}_i)+\frac{1}{2}\sum_{i=1}^{N}\sum_{\substack{j=1\\j\neq i}}^{N}U(|\vec{q}_i-\vec{q}_j|)}$$

Note that the Hamiltonian contains three terms; a **kinetic** energy term, a term describing the potential energy due to an **external force** $\vec{F}_i=-\nabla V(\vec{q}_i)$ that only depends on the position of particle i (i.e., an example would be the gravitational field of Earth when describing it's atmosphere), and the potential energy $U(|\vec{q}_i-\vec{q}_j|)$ related to **two-body interactions** between particles i and j. The force on particle i due to the latter depends on the positions of all the other $N-1$ particles. Note that the factor of $1/2$ is to avoid double-counting of the particle pairs. Examples of the two-body interactions can be the VanderWaals force in the case of a liquid, the Coulomb force in the case of a plasma, or the gravitational force in the case of dark matter halo.

Substituting this expression for the Hamiltonian in the equation for the time-evolution of the reduced DF yields, after some tedious algebra (see Appendix J), an expression for the evolution of the k**-particle DF**

$$\boxed{\frac{\partial f^{(k)}}{\partial t}=\{\mathcal{H}^{(k)},f^{(k)}\}+\sum_{i=1}^{k}\int \mathrm{d}^3\vec{q}_{k+1}\,\mathrm{d}^3\vec{p}_{k+1}\,\frac{\partial U(|\vec{q}_i-\vec{q}_{k+1}|)}{\partial\vec{q}_i}\cdot\frac{\partial f^{(k+1)}}{\partial\vec{p}_i}}$$

Here $\mathcal{H}^{(k)}$ is the Hamiltonian for the k-particles, which is simply given by

$$\mathcal{H}^{(k)}(\vec{w}_1,\vec{q}_2,...,\vec{q}_k)=\sum_{i=1}^{k}\frac{\vec{p}_i^{\,2}}{2m}+\sum_{i=1}^{k}V(\vec{q}_i)+\frac{1}{2}\sum_{i=1}^{k}\sum_{\substack{j=1\\j\neq i}}^{k}U(|\vec{q}_i-\vec{q}_j|)$$

Note that the above experssion for the evolution of the k-particle DF is not a closed function; it depends on $f^{(k+1)}$. Hence, if you want to solve for $f^{(k)}$ you first need to solve for $f^{(k+1)}$, which requires that you solve for $f^{(k+2)}$, etc. Thus, we have a hierarcical set of N coupled differential equations, which is called the **BBGKY hierarchy** (after **B**ogoliubov, **B**orn, **G**reen, **K**irkwood and **Y**von, who independently developed this approach between 1935 and 1946).

Of particular interest to us is the expression for the **1-particle DF:**

$$\boxed{\frac{\partial f^{(1)}}{\partial t} = \{\mathcal{H}^{(1)}, f^{(1)}\} + \int \mathrm{d}^3\vec{q}_2\, \mathrm{d}^3\vec{p}_2\, \frac{\partial U(|\vec{q}_1 - \vec{q}_2|)}{\partial \vec{q}_1} \cdot \frac{\partial f^{(2)}}{\partial \vec{p}_1}}$$

Note that $\mathcal{H}^{(1)}$ is the 1-particle Hamiltonian which is simply

$$\mathcal{H}^{(1)} = \mathcal{H}^{(1)}(\vec{q}, \vec{p}) = \frac{p^2}{2m} + V(\vec{q})$$

where we emphasize once more that $V(\vec{x})$ is the external potential. The first term in the evolution equation for the 1-particle DF (the Poisson brackets) is called the **streaming term**; it describes how particles move in the absence of collisions. The second term is called the **collision integral**, and describes how the distribution of particles in phase-space is impacted by two-body collisions. Note that it depends on the the **2-particle DF** $f^{(2)}(\vec{q}_1, \vec{q}_2, \vec{p}_1, \vec{p}_2)$, which shouldn't come as a surprise given that accounting for two-body collisions requires knowledge of the phase-space coordinates of the two particles in question.

Thus, we started with the **Liouville equation**, governing a complicated function of N variable, and it looks like all we have achieved is to replace it with a set of N coupled equations. However, the **BBKGY hierarchy** is useful since it allows us to make some simplifying assumptions (which will be sufficiently accurate under certain conditions), that truncates the series. Also, it is important to point out that the BBGKY hierarchy is completely general; *the only real assumption we have made thus far is that the system obeys Hamiltonian dynamics!*

From here on out, though, we can target specific fluids (i.e., collisionless fluids, neutral fluids, plasmas) by specifying details about the two-body interaction potential $U(|\vec{q}_i - \vec{q}_j|)$ and/or the external potential $V(\vec{q})$. Let us start by considering the easiest example, namely the **collisionless fluid**. Here we have two methods of proceeding. First of all, we can simply set $U(|\vec{q}_i - \vec{q}_j|) = 0$ (i.e., ignore two-body interactions) and realize that we can compute $V(\vec{q})$ from the density distribution

$$\rho(\vec{q}, t) = m \int \mathrm{d}^3\vec{p}\, f^{(1)}(\vec{q}, \vec{p}, t)$$

where m is the particle mass, using the Poisson equation

$$\nabla^2\Phi = 4\pi G\rho$$

where we have used $\Phi(\vec{q},t) = V(\vec{q},t)/m$ to coincide with the standard notation for the gravitational potential used throughout these lecture notes. This implies that the collision integral vanishes, and we are left with a **closed equation** for the 1-particle DF, given by

$$\boxed{\frac{\mathrm{d}f^{(1)}}{\mathrm{d}t} = \frac{\partial f^{(1)}}{\partial t} + \{f^{(1)}, \mathcal{H}^{(1)}\} = \frac{\partial f^{(1)}}{\partial t} + \vec{v}\cdot\frac{\partial f^{(1)}}{\partial \vec{x}} - \nabla\Phi\cdot\frac{\partial f^{(1)}}{\partial \vec{v}} = 0}$$

Here we have used the more common $(\vec{x},\vec{v})$ coordinates in place of the canonical $(\vec{q},\vec{p})$, and the fact that $\dot{\vec{p}} = -m\nabla\Phi$. This equation is the **Collisionless Boltzmann Equation** (CBE) which is the fundamental equation describing a collisionless system (i.e., a galaxy or dark matter halo). It expresses that *the flow of particles in μ-space is incompressible, and that the local phase-space density around any particle is fixed.* The evolution of a collisionless system of particles under this CBE is depicted in the left-hand panel of Fig. 5. Although the CBE is a simple looking equation, recall that $f^{(1)}$ is still a 6D function. Solving the CBE is tedious and not something that is typically done. As we will see in the next Chapter, instead what we do is to (try to) solve **moment equations** of the CBE.

For completeness, let us now derive the CBE using a somewhat different approach. This time we treat the gravity among the individual particles, and we do NOT assume upfront that we can account for gravity in terms of a 'smooth' potential $V(\vec{q})$. Hence, we set $V = 0$, and

$$U(|\vec{q}_1 - \vec{q}_2|) = -\frac{Gm^2}{|\vec{q}_1 - \vec{q}_2|}$$

is now the gravitational potential energy due to particles 1 and 2. Starting from our BBGKY expression for the 1-particle DF, we need to come up with a description for the 2-particle DF. In general, we can always write

$$\boxed{f^{(2)}(\vec{q}_1,\vec{q}_2,\vec{p}_1,\vec{p}_2) = f^{(1)}(\vec{q}_1,\vec{p}_1)\, f^{(1)}(\vec{q}_2,\vec{p}_2) + g(\vec{q}_1,\vec{q}_2,\vec{p}_1,\vec{p}_2)}$$

This the first step in what is called the **Mayer cluster expansion**. We can write this in (a self-explanatory) shorthand notation as

$$f^{(2)}(1,2) = f^{(1)}(1)\, f^{(1)}(2) + g(1,2)$$

The next step in the expansion involves the 3-particle DF:

$$f^{(3)}(1,2,3) = f(1)\,f(2)\,f(3) + f(1)\,g(2,3) + f(2)\,g(1,3) + f(3)\,g(1,2) + h(1,2,3)$$

and so onward for k-particle DFs with $k > 3$. The function $g(1,2)$ is called the **two-point correlation function**. It describes how the phase-space coordinates of two particles are correlated. Note that if they are NOT correlated than $g(1,2) = 0$. This is reminiscent of probability statistics: if x and y are two independent random variables then $P(x,y) = P(x)\,P(y)$. Similarly, $h(1,2,3)$ describes the **three-point correlation function**; the correlation among particles 1, 2 and 3 that is not already captured by their mutual two-point correlations described by $g(1,2)$, $g(2,3)$ and $g(1,3)$.

Now, let's assume that the phase-space coordinates of two particles are uncorrelated; i.e., we set $g(1,2) = 0$. This implies that the 2-particles DF is simply the products of two 1-particle DFs, and thus that the evolution equation for $f^{(1)}$ is closed! In fact, using that $\partial\mathcal{H}^{(1)}/\partial\vec{q} = 0$ and $\partial\mathcal{H}^{(1)}/\partial\vec{p} = \vec{p}/m = \vec{v}$ we obtain that

$$\frac{\partial f^{(1)}}{\partial t} + \vec{v}\cdot\frac{\partial f^{(1)}}{\partial \vec{x}} = \int \mathrm{d}^3\vec{q}_2\,\mathrm{d}^3\vec{p}_2\,f^{(1)}(\vec{q}_2,\vec{p}_2)\,\frac{\partial U(|\vec{q}_1-\vec{q}_2|)}{\partial \vec{q}_1}\cdot\frac{\partial f^{(1)}}{\partial \vec{p}_1}$$

Taking the operator outside of the **collision integral** (note that the $f^{(1)}$ in the operator has $\vec{q}_1$ and $\vec{p}_1$ as arguments), and performing the integral over $\vec{p}_2$ yields

$$\frac{\partial f^{(1)}}{\partial t} + \vec{v}\cdot\frac{\partial f^{(1)}}{\partial \vec{x}} - \frac{\partial f^{(1)}}{\partial \vec{p}_1}\cdot\frac{\partial}{\partial \vec{q}_1}\left[\frac{1}{m}\int \mathrm{d}^3\vec{q}_2\,\rho(\vec{q}_2)\,U(|\vec{q}_1-\vec{q}_2|)\right] = 0$$

Using that

$$\Phi(\vec{x}) = -G\int \mathrm{d}^3\vec{x}'\,\frac{\rho(\vec{x}')}{|\vec{x}-\vec{x}'|}$$

this finally can be written as

$$\frac{\partial f^{(1)}}{\partial t} + \vec{v}\cdot\frac{\partial f^{(1)}}{\partial \vec{x}} - \nabla\Phi\cdot\frac{\partial f^{(1)}}{\partial \vec{v}} = 0$$

which we recognize as the CBE! Thus, *we infer that in a collisionless system the phase-space coordinates of the particles are uncorrelated!* This is an important point. It implies that collisions among particles introduce correlations, and thus that the collisional aspect of a fluid is ultimately captured by the correlation functions $g(1,2)$, $h(1,2,3)$, etc.

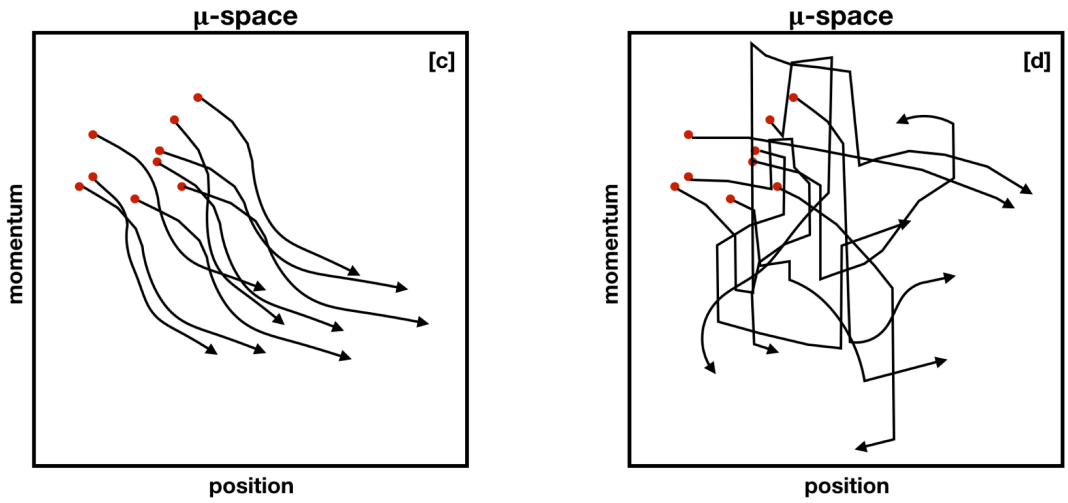

Figure 5: *Illustration of evolution in μ-space. The x- and y-axes represent the* 3*-dimensional position-vector and momentum-vector, respectively. Panel (a) shows the evolution of a collection of particles (indicated by the red dots) in a collisionless system governed by the CBE. As time goes on, the potitions and momentum of all the particles change (according to the Hamiltonian equations of motion), and the particles move around in μ-space smoothly (no abrubt changes) . If the combined potential of all the particle (or the external potential) is time-variable, trajectories of individual particles are allowed to cross each other, unlike trajectories in Γ-space, which can never cross. Panel (b) shows the evolution of a collection of particles in a collisional system (where collisions are highly localized). Collisions cause abrupt changes in momentum. The dynamics of this system is described by the Boltzmann equation.*

If we want to describe say a **collisional, neutral fluid**, we need to decide on how to treat these correlation functions. If we do this for a neutral fluid, which means a fluid in which the interaction potentials are only effective over very small distances (i.e., $U(r) = 0$ for r larger than some small, characteristic collision scale, $r_{\rm coll}$), then one derives what is called the **Boltzmann equation**, which is given by

$$\boxed{\frac{\partial f^{(1)}}{\partial t} + \vec{v} \cdot \frac{\partial f^{(1)}}{\partial \vec{x}} - \nabla\Phi \cdot \frac{\partial f^{(1)}}{\partial \vec{v}} = I[f^{(1)}]}$$

Here $I[f^{(1)}]$ is the collision integral which now is only a function of the 1-particle DF, making the Boltzmann equation a closed equation. It describes how, due to collisions, particles are 'kicked' in and out of certain parts of phase-space. The right-hand panel of Fig. 5 shows an illustration of evolution under the Boltzmann equation.
Rigorously deriving an expression for $I[f^{(1)}]$ from the BBGKY hierarchy is fiddly and outside the scope of this course (see for example the textbook *"Statistical Mechanics"* by Kerson Huang). Instead, in the next Chapter we will use a more heuristic approach, which relies on making the assumptions

- **dilute gas**; density is sufficiently low so that only binary collisions need to be considered
- collisions can be thought of as **instantaneous** and **perfectly localized**.
- **Molecular chaos**: velocities of colliding particles are uncorrelated

The first two assumptions are reasonable, but the **molecular chaos** assumption (introduced by Boltzmann, who referred to it as the **Stosszahlansatz**, which translates to 'assumption regarding number of collisions') has a long and interesting history. Mathematically, the assumption implies that

$$f^{(2)}(\vec{q}, \vec{q}, \vec{p}_1, \vec{p}_2) = f^{(1)}(\vec{q}, \vec{p}_1)\, f^{(1)}(\vec{q}, \vec{p}_2)$$

which thus assumes that $g(\vec{q}, \vec{q}, \vec{p}_1, \vec{p}_2) = 0$. Note that this is different from the assumption we made above when describing collisionless fluids, as here it is only assumed that *at a given location* the *momenta* are correlated. This is a weaker assumption than setting $g(\vec{q}_1, \vec{q}_2, \vec{p}_1, \vec{p}_2) = 0$. At first sight this seems a reasonable assumption; after all, in a dilute gas particles move (relatively) long distances between collisions (i.e., $\lambda_{\rm mfp} \gg r_{\rm coll}$). Although collisions introduce correlations among

the particles, each particle is expected to have many collisions with other particles before colliding with a particular particle again. It seems reasonable to postulate that these intermittent collisions erase correlations again. However, this apparently unremarkable assumption effectively introduces an **arrow of time**, as briefly discussed in the colored text-box at the end of this chapter.

Finally, we point out that if treating a **collisional plasma** in which the interactions are due to long-range Coulomb forces, then the standard approach is to assume that $h(1,2,3) = 0$ (i.e., assume that three-body correlation function is zero). Making several other assumptions (i.e., plasma is spatially homogeneous and the 2-particle correlation function $g(1,2)$ relaxes much faster than the 1-particle DF $f^{(1)}$) this allows one to derive an expression for $g(1,2)$ from the evolution equation of the 2-particle DF, which can then be substituted in the evolution equation of the 1-particles DF. The result is called the **Lenard-Balescu** equation. It is an example of a **Fokker-Planck** equation, which is a generic equation used to describe the time evolution of the probability density function of the velocity of a particle under the influence of stochastic forces (here the Coulomb collisions) that mainly cause small deflections. The Fokker-Planck equation is also used to describe gravitational N-body systems in which the impact of collisions is not negligble (i.e., describing two-body relaxation in a globular cluster).

As a final remark for this Chapter, we have thus far only considered the case of a single species of mono-atoms. If we consider different types of particles, then we have to introduce a separate distribution function for each type. If the different types of particles can interact with each other, this then has to be accounted for in the collision terms.

Molecular Chaos and the Arrow of Time

The assumption of "molecular chaos" (also known as "Stosszahlansatz") which allows one to write down a closed equation for the time-evolution of the 1-point DF, was used by L. Boltzmann to proof his famous **H-Theorem**, which basically states that entropy should always increase (i.e., it is supposed to be a proof of the **second law of thermodynamics**). This in turn implies **time-asymmetry**, giving rise to the thermodynamic **arrow of time**. However, as first brought to bear by J. Loschmidt, it should not be possible to deduce an irreversible process from time-symmetric dynamics and a time-symmetric formalism (i.e., the dynamics that result from the Liouville equation, which has no underlying assumptions, is perfectly time-reversible!). The origin of this **"Loschmidt paradox"**, as it is known, is the questionable assumption of "molecular chaos". After all, once the particles are allowed to collide, their velocity directions and positions in fact do become correlated. Molecular chaos basically assumes that the subsequent collisions with all the other particles somehow erases this correlation again. To what extent this is true, and whether the H-theorem really proofs the second law of thermodynamics is a topic of ongoing debate, especially among philosophers of science.

The material in this text-box is not part of the curriculum for this course

CHAPTER 7

From Boltzmann to Navier-Stokes

In the previous chapter we derived the **BBGKY hierarchy** of equations:

$$\begin{aligned}
&\frac{\partial f^{(1)}}{\partial t} = \{\mathcal{H}^{(1)}, f^{(1)}\} + \int \mathrm{d}^3\vec{q}_2\, \mathrm{d}^3\vec{p}_2\, \frac{\partial U(|\vec{q}_1 - \vec{q}_2|)}{\partial \vec{q}_1} \cdot \frac{\partial f^{(2)}}{\partial \vec{p}_1} \\
&\quad\cdot \\
&\quad\cdot \\
&\quad\cdot \\
&\frac{\partial f^{(k)}}{\partial t} = \{\mathcal{H}^{(k)}, f^{(k)}\} + \sum_{i=1}^{k} \int \mathrm{d}^3\vec{q}_{k+1}\, \mathrm{d}^3\vec{p}_{k+1}\, \frac{\partial U(|\vec{q}_i - \vec{q}_{k+1}|)}{\partial \vec{q}_i} \cdot \frac{\partial f^{(k+1)}}{\partial \vec{p}_i}
\end{aligned}$$

Here $k = 1, 2, ..., N$, $f^{(k)}$ is the k-particle DF, which relates to the N-particle DF ($N > k$) according to

$$f^{(k)}(\vec{w}_1, \vec{w}_2, ..., \vec{w}_k, t) \equiv \frac{N!}{(N-k)!} \int \prod_{i=k+1}^{N} \mathrm{d}^6\vec{w}_i\, f^{(N)}(\vec{w}_1, \vec{w}_2, ..., \vec{w}_N, t)\,,$$

and $\mathcal{H}^{(k)}$ is the k-particle Hamiltonian given by

$$\mathcal{H}^{(k)} = \sum_{i=1}^{k} \frac{\vec{p}_i^{\,2}}{2m} + \sum_{i=1}^{k} V(\vec{q}_i) + \frac{1}{2} \sum_{i=1}^{k} \sum_{\substack{j=1 \\ j\neq i}}^{k} U(|\vec{q}_i - \vec{q}_j|)$$

with $V(\vec{q})$ the potential associated with an external force, and $U(r)$ the two-body interaction potential between two (assumed equal) particles separated by a distance $r = |\vec{q}_i - \vec{q}_j|$.

In order to close this set of N equations, one needs to make certain assumptions that truncate the series. One such assumption is that all particles are uncorrrelated (both spatially and in terms of their momenta), such that

$$f^{(2)}(\vec{q}_1, \vec{q}_2, \vec{p}_1, \vec{p}_2) = f^{(1)}(\vec{q}_1, \vec{p}_1)\, f^{(1)}(\vec{q}_2, \vec{p}_2)$$

which is equivalent to setting the **correlation function** $g(1,2) = 0$. As we have shown in the previous Chapter, the first equation in the BBGKY hierarchy is now closed, and yields the **Collisionless Boltzmann Equation** (CBE), which can be written as

$$\boxed{\frac{\mathrm{d}f}{\mathrm{d}t} = \frac{\partial f}{\partial t} + \dot{\vec{x}} \cdot \frac{\partial f}{\partial \vec{x}} + \dot{\vec{v}} \cdot \frac{\partial f}{\partial \vec{v}} = 0}$$

which is the fundamental evolution equation for collisionless systems. If the forces between particles are gravitational in nature, then $\dot{\vec{v}} = \nabla\Phi$, with $\Phi(\vec{x})$ the **gravitational potential** which related to the density distribution via the **Poisson equation**. NOTE: we have used the shorthand notation f for the 1-particle DF $f^{(1)}$. In what follows *we will adopt that notation throughout, and only use the superscript-notation whenever confusion might arise.*

If, on the other hand, we want to describe a dilute, neutral fluid in which the particles only have short-range interactions (such that $U(r) \simeq 0$ outside of some small distance $r_{\rm coll}$), then we can make the assumption of **molecular chaos** which also allows us to close the BBGKY hierarchy, yielding the **Boltzmann Equation**:

$$\boxed{\frac{\mathrm{d}f}{\mathrm{d}t} = \frac{\partial f}{\partial t} + \dot{\vec{x}} \cdot \frac{\partial f}{\partial \vec{x}} + \dot{\vec{v}} \cdot \frac{\partial f}{\partial \vec{v}} = I[f]}$$

where $I[f]$ is the **collision integral**, which describes how the phase-space density around a particle (or fluid element) changes with time due to collisions.

Let us now take a closer look at this collision integral $I[f]$. It basically expresses the Eulerian time-derivative of the DF due to collisions, i.e.,$I[f] = (\partial f/\partial t)_{\rm coll}$. Recall that we have made the assumption of a dilute gas, so that we only need to consider two-body interactions. In what follows, we make the additional assumption that all collisions are **elastic** [actually, this is sort of implied by the fact that we assume that the dynamics are Hamiltonian]. An example is shown in Figure 1, where $\vec{p}_1 + \vec{p}_2 \rightarrow \vec{p}_1\,' + \vec{p}_2\,'$. Since we assumed a short-range, instantaneous and localized interaction, so that the external potential doesn't significantly vary over the interaction volume (the dashed circle in Fig. 1), we have

$$\begin{aligned} \textbf{momentum conservation:} \quad & \vec{p}_1 + \vec{p}_2 = \vec{p}_1\,' + \vec{p}_2\,' \\ \textbf{energy conservation:} \quad & |\vec{p}_1|^2 + |\vec{p}_2|^2 = |\vec{p}_1\,'|^2 + |\vec{p}_2\,'|^2 \end{aligned}$$

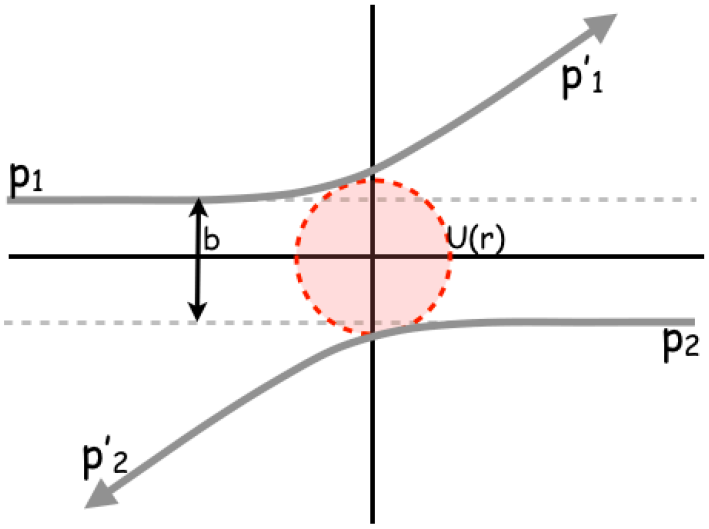

Figure 6: *Illustration of 'collision' between two particles with momenta* p_1 *and* p_2 *due to interaction potential* $U(r)$*. The impact parameter of the collision is* b*.*

where as throughout we have assumed equal mass particles.

We can write the rate at which particles of momentum $\vec{p}_1$ at location $\vec{x}$ experience collisions $\vec{p}_1 + \vec{p}_2 \to \vec{p}_1\,' + \vec{p}_2\,'$ as

$$\mathcal{R} = \omega(\vec{p}_1, \vec{p}_2 | \vec{p}_1\,', \vec{p}_2\,')\, f^{(2)}(\vec{x}, \vec{x}, \vec{p}_1, \vec{p}_2)\, \mathrm{d}^3\vec{p}_2\, \mathrm{d}^3\vec{p}_1\,'\, \mathrm{d}^3\vec{p}_2\,'$$

Here $f^{(2)}(\vec{x}, \vec{x}, \vec{p}_1, \vec{p}_2)$ is the 2-particle DF, expressing the probability that at location $\vec{x}$, you encounter two particles with momenta $\vec{p}_1$ and $\vec{p}_2$, respectively. The function $\omega(\vec{p}_1, \vec{p}_2 | \vec{p}_1\,', \vec{p}_2\,')$ depends on the interaction potential $U(\vec{r})$ and can be calculated (using kinetic theory) via differential cross sections. Note that momentum and energy conservation is encoded in the fact that $\omega(\vec{p}_1, \vec{p}_2 | \vec{p}_1\,', \vec{p}_2\,') \propto \delta^3(\vec{P} - \vec{P}')\, \delta(E - E')$ with $\delta(x)$ the Dirac delta function, $\vec{P} = \vec{p}_1 + \vec{p}_2$ and $\vec{P}' = \vec{p}_1\,' + \vec{p}_2\,'$.

In addition, we have **time-reversibility**, so that it is equally likely that the inverse process $(-\vec{p}_1\,' + -\vec{p}_2\,' \to -\vec{p}_1 + -\vec{p}_2)$ happens. This implies that

$$\omega(\vec{p}_1, \vec{p}_2 | \vec{p}_1\,', \vec{p}_2\,') = \omega(\vec{p}_1\,' \vec{p}_2\,' | \vec{p}_1, \vec{p}_2)$$

Using our assumption of **molecular chaos**, which states that the momenta of the interacting particles are independent, we have that

$$f^{(2)}(\vec{x},\vec{x},\vec{p}_1,\vec{p}_2) = f^{(1)}(\vec{x},\vec{p}_1)\, f^{(1)}(\vec{x},\vec{p}_2)$$

so that the **collision integral** can be written as

$$\boxed{I[f] = \int \mathrm{d}^3\vec{p}_2\, \mathrm{d}^3\vec{p}_1{}'\, \mathrm{d}^3\vec{p}_2{}'\, \omega(\vec{p}_1{}', \vec{p}_2{}'|\vec{p}_1,\vec{p}_2)\, [f(\vec{p}_1{}')\, f(\vec{p}_2{}') - f(\vec{p}_1)\, f(\vec{p}_2)]}$$

where we have suppressed the x arguments of f in order to avoid unnecessary clutter. The first term within the square brackets describes the **replenishing collisions**, in which particles at $(\vec{x},\vec{p}_1{}')$ are scattered into $(\vec{x},\vec{p}_1)$. The second term with the square brackets describes the **depleting collisions**, in which particles at $(\vec{x},\vec{p}_1)$ are kicked out of their phase-space volume into $(\vec{x},\vec{p}_1{}')$.

We can use the above expression to derive that the equilibrium solution for the velocity distribution in a homogeneous fluid is given by the Maxwell-Boltzmann distribution. The expression for an equilibrium distribution function, f_{eq} is that $\partial f_{\mathrm{eq}}/\partial t = 0$ (i.e., the DF at any given location doesn't evolve with time). If we ignore a potential external potential (i.e., $V = 0$), and we take into consideration that an equilibrium solution must indeed be spatially homogeneous, such that $\partial f_{\mathrm{eq}}/\partial \vec{q} = 0$, then we have that the streaming term $\{\mathcal{H}, f_{\mathrm{eq}}\} = 0$. Hence, having an equilibrium requires that the collision integral vanishes as well. As is apparent from the above expression, this will be the case if

$$f(\vec{x},\vec{p}_1{}')\, f(\vec{x},\vec{p}_2{}') - f(\vec{x},\vec{p}_1)\, f(\vec{x},\vec{p}_2) = 0$$

This condition is known as **detailed balance**, and can be written as

$$\log[f(\vec{p}_1)] + \log[f(\vec{p}_2)] = \log[f(\vec{p}_1{}')] + \log[f(\vec{p}_2{}')]$$

This has the form of a conservation law, and implies that $\log[f_{\mathrm{eq}}]$ must be equal to a sum of conserved quantities, $A(\vec{p})$, that obey

$$A(\vec{p}_1) + A(\vec{p}_2) = A(\vec{p}_1{}') + A(\vec{p}_2{}')$$

Quantities $A(\vec{p})$ for which this is the case are called **collisional invariants**. There are three such quantities of interest to us

$A = 1$	**particle number conservations**
$A = \vec{p}$	**momentum conservation**
$A = \vec{p}^{\,2}/(2m)$	**energy conservation**

and we thus expect that

$$\log[f_{\rm eq}(\vec{p})] \propto a_1 \, + a_2 \, \vec{p} + a_3 \, |\vec{p}|^2$$

with a_1, a_2 and a_3 some constants. This notion can be used to demonstrate that the equilibrium distribution must be of the form of a **Maxwell-Boltzmann distribution**

$$f_{\rm eq}(p) = \frac{n}{(2\pi m k_{\rm B} T)^{3/2}} \, \exp\left[-\frac{p^2}{2 m k_{\rm B} T}\right]$$

(see "*Statistical Mechanics*" by Kerson Huang for a detailed derivation).

We have seen that if the logarithm of the DF is a sum of collisional invariants (which it is if the system is in equilibrium), then the collision integral vanishes. In addition, as we will now demonstrate, for a collisional invariant $A(\vec{p})$ we also have that

$$\boxed{\int {\rm d}^3\vec{p} \, A(\vec{p}) \, \left(\frac{\partial f}{\partial t}\right)_{\rm coll} = 0}$$

which will be useful for what follows. To see that this equality holds, we first introduce

$$\mathcal{I}_1 = \int {\rm d}^3\vec{p}_1 \, {\rm d}^3\vec{p}_2 \, {\rm d}^3\vec{p}_1\,' \, {\rm d}^3\vec{p}_2\,' \, \omega(\vec{p}_1\,', \vec{p}_2\,' | \vec{p}_1, \vec{p}_2) \, A(\vec{p}_1) \, \left[f(\vec{p}_1\,') \, f(\vec{p}_2\,') - f(\vec{p}_1) \, f(\vec{p}_2)\right]$$

which is the collision integral multiplied by $A(\vec{p}_1)$ and integrated over $\vec{p}_1$. Note that now *all* momenta are integrated over, such that they are basically nothing but dummy variables. Re-labelling $1 \leftrightarrow 2$, and reordering yields

$$\mathcal{I}_2 = \int {\rm d}^3\vec{p}_1 \, {\rm d}^3\vec{p}_2 \, {\rm d}^3\vec{p}_1\,' \, {\rm d}^3\vec{p}_2\,' \, \omega(\vec{p}_1\,', \vec{p}_2\,' | \vec{p}_1, \vec{p}_2) \, A(\vec{p}_2) \, \left[f(\vec{p}_1\,') \, f(\vec{p}_2\,') - f(\vec{p}_1) \, f(\vec{p}_2)\right]$$

i.e., everything is unchanged except for the argument of our collisional invariant. And since the momenta are dummy variables, we have that $\mathcal{I}_2 = \mathcal{I}_1$. Rather than

swapping indices 1 and 2, we can also swap $\vec{p} \leftrightarrow \vec{p}\,'$. This gives us two additional integrals:

$$\mathcal{I}_3 = -\int \mathrm{d}^3\vec{p}_1\,\mathrm{d}^3\vec{p}_2\,\mathrm{d}^3\vec{p}_1\,'\,\mathrm{d}^3\vec{p}_2\,'\,\omega(\vec{p}_1,\vec{p}_2|\vec{p}_1\,',\vec{p}_2\,')\,A(\vec{p}_1\,')\,[f(\vec{p}_1\,')\,f(\vec{p}_2\,') - f(\vec{p}_1)\,f(\vec{p}_2)]$$

and

$$\mathcal{I}_4 = -\int \mathrm{d}^3\vec{p}_1\,\mathrm{d}^3\vec{p}_2\,\mathrm{d}^3\vec{p}_1\,'\,\mathrm{d}^3\vec{p}_2\,'\,\omega(\vec{p}_1,\vec{p}_2|\vec{p}_1\,',\vec{p}_2\,')\,A(\vec{p}_2\,')\,[f(\vec{p}_1\,')\,f(\vec{p}_2\,') - f(\vec{p}_1)\,f(\vec{p}_2)]$$

where the minus sign comes from the fact that we have reversed $f(\vec{p}_1)\,f(\vec{p}_2) - f(\vec{p}_1\,')\,f(\vec{p}_2\,')$. Because of time-reversibility $\omega(\vec{p}_1\,',\vec{p}_2\,'|\vec{p}_1,\vec{p}_2) = \omega(\vec{p}_1,\vec{p}_2|\vec{p}_1\,',\vec{p}_2\,')$, and we thus have that $\mathcal{I}_4 = \mathcal{I}_3 = \mathcal{I}_2 = \mathcal{I}_1$. Hence $\mathcal{I}_1 = [\mathcal{I}_1 + \mathcal{I}_2 + \mathcal{I}_3 + \mathcal{I}_4]/4$, which can be written as

$$\mathcal{I}_1 = \frac{1}{4}\int \mathrm{d}^3\vec{p}_1\,\mathrm{d}^3\vec{p}_2\,\mathrm{d}^3\vec{p}_1\,'\,\mathrm{d}^3\vec{p}_2\,'\,\omega(\vec{p}_1\,',\vec{p}_2\,'|\vec{p}_1,\vec{p}_2)\times \\ \{A(\vec{p}_1) + A(\vec{p}_2) - A(\vec{p}_1\,') - A(\vec{p}_2\,')\}\,[f(\vec{p}_1\,')\,f(\vec{p}_2\,') - f(\vec{p}_1)\,f(\vec{p}_2)]$$

Since $A(\vec{p})$ is a collisional invariant, the factor in curly brackets vanishes, which in turn assures that $\mathcal{I}_1 = 0$, which completes our proof.

Thus far, we have derived the Boltzmann equation, and we have been able to write down an expression for the collision integral under the assumptions of (i) short-range, elastic collisions and (ii) molecular chaos. How do we proceed from here? The Boltzmann distribution with the above expression for the collision integral is a non-linear integro-differential equation, and solving such an equation is extremely difficult. Fortunately, in the fluid limit we don't really need to. Rather, we are interested what happens to our macroscopic quantities that describe the fluid (ρ, $\vec{u}$, P, ε, etc). We can use the Boltzmann equation to describe the time-evolution of these macroscopic quantities by considering **moment equations** of the Boltzmann equation.

In mathematics, the n^{th}-moment of a real-valued, continuous function $f(x)$ is

$$\mu_n = \int x^n f(x)\,\mathrm{d}x$$

If $f(x)$ is normalized, so that it can be interpreted as a probability function, then $\mu_n = \langle x^n \rangle$.

In our case, consider the scalar function $Q(\vec{v})$. The expectation value for Q at location $\vec{x}$ at time t is given by

$$\langle Q \rangle = \langle Q \rangle(\vec{x}, t) = \frac{\int Q(\vec{v})\, f(\vec{x}, \vec{v}, t)\, \mathrm{d}^3\vec{v}}{\int f(\vec{x}, \vec{v}, t)\, \mathrm{d}^3\vec{v}}$$

Using that

$$n = n(\vec{x}, t) = \int f(\vec{x}, \vec{v}, t)\, \mathrm{d}^3\vec{v}$$

we thus have that

$$\boxed{\int Q(\vec{v})\, f(\vec{x}, \vec{v}, t)\, \mathrm{d}^3\vec{v} = n\, \langle Q \rangle}$$

We will use this abundantly in what follows. In particular, define

$$g(\vec{x}, t) = \int Q(\vec{v})\, f(\vec{x}, \vec{v}, t)\, \mathrm{d}^3\vec{v}$$

Then, in relation to fluid dynamics, there are a few functions $Q(\vec{v})$ that are of particular interest:

$Q(\vec{v}) = 1$	$\Rightarrow$	$g(\vec{x}, t) = n(\vec{x}, t)$	number density
$Q(\vec{v}) = m$	$\Rightarrow$	$g(\vec{x}, t) = \rho(\vec{x}, t)$	mass density
$Q(\vec{v}) = m\, \vec{v}$	$\Rightarrow$	$g(\vec{x}, t) = \rho(\vec{x}, t)\, \vec{u}(\vec{x}, t)$	momentum flux density
$Q(\vec{v}) = \frac{1}{2} m (\vec{v} - \vec{u})^2$	$\Rightarrow$	$g(\vec{x}, t) = \rho(\vec{x}, t)\, \varepsilon(\vec{x}, t)$	specific energy density

where we have used that $\langle \vec{v} \rangle = \vec{u}$, and $\langle (\vec{v} - \vec{u})^2 / 2 \rangle = \varepsilon$.

This indicates that we can obtain dynamical equations for the macroscopic fluid quantities by multiplying the Boltzmann equation with appropriate functions, $Q(\vec{v})$, and integrating over all of velocity space.

Hence, we seek to solve equations of the form

$$\int Q(\vec{v}) \left[\frac{\partial f}{\partial t} + \vec{v}\cdot\nabla f - \nabla\Phi\cdot\frac{\partial f}{\partial \vec{v}}\right] \mathrm{d}^3\vec{v} = \int Q(\vec{v}) \left(\frac{\partial f}{\partial t}\right)_{\mathrm{coll}} \mathrm{d}^3\vec{v}$$

In what follows, we restrict ourselves to $Q(\vec{v})$ that are **collisional invariants** so that the integral on the right-hand side vanishes, and we are left with

$$\int Q(\vec{v})\,\frac{\partial f}{\partial t}\,\mathrm{d}^3\vec{v} + \int Q(\vec{v})\,\vec{v}\cdot\nabla f\,\mathrm{d}^3\vec{v} - \int Q(\vec{v})\,\nabla\Phi\cdot\frac{\partial f}{\partial \vec{v}}\,\mathrm{d}^3\vec{v} = 0$$

Since mass, momentum and energy are all conserved in elastic, short-range collisions we have that the momentum integral over the collision integral will be zero for the zeroth, first and second order moment equations! In other words, *although collisional and collisionless systems solve different Boltzmann equations, their zeroth, first and second moment equations are identical!*

We now split the above equation in three terms:

$$\begin{aligned}
\mathbf{I} \quad & \int Q(\vec{v})\,\frac{\partial f}{\partial t}\,\mathrm{d}^3\vec{v} \\
\mathbf{II} \quad & \int Q(\vec{v})\,v_i\frac{\partial f}{\partial x_i}\,\mathrm{d}^3\vec{v} \\
\mathbf{III} \quad & \int Q(\vec{v})\,\frac{\partial \Phi}{\partial x_i}\,\frac{\partial f}{\partial v_i}\,\mathrm{d}^3\vec{v}
\end{aligned}$$

where we have that $\mathbf{I} + \mathbf{II} - \mathbf{III} = 0$, as long as Q is a collisional invariant.

We now proceed to rewrite each of these three integrals in turn.

Integral I

The first integral can be written as

$$\int Q(\vec{v})\,\frac{\partial f}{\partial t}\,\mathrm{d}^3\vec{v} = \int \frac{\partial Q f}{\partial t}\,\mathrm{d}^3\vec{v} = \frac{\partial}{\partial t}\int Q f\,\mathrm{d}^3\vec{v} = \frac{\partial}{\partial t} n\langle Q\rangle$$

where we have used that both $Q(\vec{v})$ and the integration volume are independent of time.

Integral II

Using similar logic, the second integral can be written as

$$\int Q(\vec{v})\, v_i \frac{\partial f}{\partial x_i}\, \mathrm{d}^3\vec{v} = \int \frac{\partial Q\, v_i\, f}{\partial x_i}\, \mathrm{d}^3\vec{v} = \frac{\partial}{\partial x_i} \int Q\, v_i\, f\, \mathrm{d}^3\vec{v} = \frac{\partial}{\partial x_i}\Big[n\, \langle Q\, v_i \rangle\Big]$$

Here we have used that

$$Q\, v_i\, \frac{\partial f}{\partial x_i} = \frac{\partial (Q\, v_i\, f)}{\partial x_i} - f\, \frac{\partial Q\, v_i}{\partial x_i} = \frac{\partial (Q\, v_i\, f)}{\partial x_i}$$

where the last step follows from the fact that neither v_i nor Q depend on x_i.

Integral III

For the third, and last integral, we are going to define $\vec{F} = \nabla\Phi$ and $\nabla_v \equiv (\partial/\partial v_x, \partial/\partial v_y, \partial/\partial v_z)$, i.e., ∇_v is the equivalent of ∇ but in velocity space. This allows us to write

$$\begin{aligned}
\int Q\, \vec{F} \cdot \nabla_v f\, \mathrm{d}^3\vec{v} &= \int \nabla_v \cdot (Qf\vec{F}) \mathrm{d}^3\vec{v} - \int f\, \nabla_v \cdot (Q\vec{F})\, \mathrm{d}^3\vec{v} \\
&= \int Qf\vec{F} \mathrm{d}^2 S_v - \int f\, \frac{\partial Q F_i}{\partial v_i}\, \mathrm{d}^3\vec{v} \\
&= -\int fQ \frac{\partial F_i}{\partial v_i}\, \mathrm{d}^3\vec{v} - \int f F_i\, \frac{\partial Q}{\partial v_i}\, \mathrm{d}^3\vec{v} \\
&= -\int f \frac{\partial \Phi}{\partial x_i}\, \frac{\partial Q}{\partial v_i}\, \mathrm{d}^3\vec{v} = -\frac{\partial \Phi}{\partial x_i} n \left\langle \frac{\partial Q}{\partial v_i} \right\rangle
\end{aligned}$$

Here we have used Gauss' divergence theorem, and the fact that the integral of $Qf\vec{F}$ over the surface S_v (which is a sphere with radius $|\vec{v}| = \infty$) is equal to zero. This follows from the 'normalization' requirement that $\int f\, \mathrm{d}^3\vec{v} = n$. We have also used that $F_i = \partial\Phi/\partial x_i$ is independent of v_i.

Combining the above expressions for **I**, **II**, and **III**, we obtain that

$$\boxed{\frac{\partial}{\partial t} n\langle Q \rangle + \frac{\partial}{\partial x_i}\Big[n\langle Q v_i \rangle\Big] + \frac{\partial \Phi}{\partial x_i} n \left\langle \frac{\partial Q}{\partial v_i} \right\rangle = 0}$$

In what follows we refer to this as the **master-moment-equation** (in index-form).

Now let us consider $Q = m$, which is indeed a collisional invariant, as required. Substitution in the master-moment equation, and using that $\langle m \rangle = m$, that $mn = \rho$ and that $\langle m v_i \rangle = m \langle v_i \rangle = m u_i$, we obtain

$$\boxed{\frac{\partial \rho}{\partial t} + \frac{\partial \rho u_i}{\partial x_i} = 0}$$

which we recognize as the **continuity equation** in Eulerian index form.

Next we consider $Q = m v_j$, which is also a collisional invariant. Using that $n \langle m v_j v_i \rangle = \rho \langle v_i v_j \rangle$ and that

$$\frac{\partial \Phi}{\partial x_i} n \left\langle \frac{\partial m v_j}{\partial v_i} \right\rangle = \frac{\partial \Phi}{\partial x_i} \rho \left\langle \frac{\partial v_j}{\partial v_i} \right\rangle = \frac{\partial \Phi}{\partial x_i} \rho \delta_{ij} = \rho \frac{\partial \Phi}{\partial x_j}$$

substitution of $Q = m v_j$ in the master-moment equation yields

$$\frac{\partial \rho u_j}{\partial t} + \frac{\partial \rho \langle v_i v_j \rangle}{\partial x_i} + \rho \frac{\partial \Phi}{\partial x_j} = 0$$

Next we use that

$$\frac{\partial \rho u_j}{\partial t} = \rho \frac{\partial u_j}{\partial t} + u_j \frac{\partial \rho}{\partial t} = \rho \frac{\partial u_j}{\partial t} - u_j \frac{\partial \rho u_k}{\partial x_k}$$

where, in the last step, we have used the continuity equation. Substitution in the above equation, and using that k is a mere dummy variable (which can therefore be replaced by i), we obtain that

$$\begin{aligned}
& \rho \frac{\partial u_j}{\partial t} - u_j \frac{\partial \rho u_i}{\partial x_i} + \frac{\partial \rho \langle v_i v_j \rangle}{\partial x_i} + \rho \frac{\partial \Phi}{\partial x_j} = 0 \\
\Leftrightarrow \quad & \rho \frac{\partial u_j}{\partial t} - \left[\frac{\partial \rho u_i u_j}{\partial x_i} - \rho u_i \frac{\partial u_j}{\partial x_i} \right] + \frac{\partial \rho \langle v_i v_j \rangle}{\partial x_i} + \rho \frac{\partial \Phi}{\partial x_j} = 0 \\
\Leftrightarrow \quad & \rho \frac{\partial u_j}{\partial t} + \rho u_i \frac{\partial u_j}{\partial x_i} + \frac{\partial \left[\rho \langle v_i v_j \rangle - \rho u_i u_j \right]}{\partial x_i} + \rho \frac{\partial \Phi}{\partial x_j} = 0
\end{aligned}$$

If we now restrict ourselves to **collisional fluids**, and use that the **stress tensor** can be written as

$$\sigma_{ij} = -\rho\langle w_i w_j\rangle = -\rho\langle v_i v_j\rangle + \rho u_i u_j = -P\delta_{ij} + \tau_{ij}$$

then the equation above can be rewritten as

$$\boxed{\frac{\partial u_j}{\partial t} + u_i\frac{\partial u_j}{\partial x_i} = -\frac{1}{\rho}\frac{\partial P}{\partial x_j} + \frac{1}{\rho}\frac{\partial \tau_{ij}}{\partial x_i} - \frac{\partial \Phi}{\partial x_j}}$$

which we recognize as the **momentum equations** (**Navier-Stokes**) in Eulerian index form. As we have seen in Chapter 3, as long as the fluid is **Newtonian**, the **viscous stress tensor**, τ_{ij}, can be described by two parameters only: the coefficient of shear viscosity, μ, and the coefficient of bulk viscosity, η (which can typically be ignored).

If instead we assume a **collisionless fluid**, then

$$\sigma_{ij} = -\rho\,\langle w_i w_j\rangle = -\rho\langle v_i v_j\rangle + \rho u_i u_j$$

and the momentum equations (now called the **Jeans equations**) reduce to

$$\boxed{\frac{\partial u_j}{\partial t} + u_i\frac{\partial u_j}{\partial x_i} = \frac{1}{\rho}\frac{\partial \sigma_{ij}}{\partial x_i} - \frac{\partial \Phi}{\partial x_j}}$$

In this case, we have no constraints on σ_{ij} other than that it is **manifest symmetric**; *for a collisionless fluid the stress tensor* $\sigma_{ij} = \sigma_{ij}(\vec{x}, t)$ *has a total of 6 unknowns.* The Jeans equations form the basis for building dynamical models of galaxies. However, since they contain many more unknowns than the number of equations, they can in general not be solved unless one makes a number of highly oversimplified assumptions (i.e., the system is spherically symmetric, the velocity structure is isotropic, etc.). This is the topic of **Galactic Dynamics**. Note that adding higher order moment equations ($Q(v) \propto v^a$ with $a \geq 3$) doesn't help in achieving closure since the new equations also add new unknowns, such as $\langle v_i v_j v_k\rangle$, etc. Ultimately, the problem is that collisionless fluids do not have **constitutive equations** such as the **equation of state** for a collisionless fluid.

Finally, it is left as an exersize for the reader (or look at Appendix K) to show that substitution of $Q = mv^2/2$ in the master moment equation yields the **energy equation** (in Lagrangian index form):

$$\boxed{\rho\frac{\mathrm{d}\varepsilon}{\mathrm{d}t} = -P\frac{\partial u_k}{\partial x_k} + \mathcal{V} - \frac{\partial F_{\mathrm{cond},k}}{\partial x_k}}$$

which is exactly the same as what we heuristically derived in Chapter 5, except for the $-\mathcal{L}$ term, which is absent from this derivation based on the Boltzmann equation, since the later does not include the effects of radiation.

Finally, Fig. 7 below summarizes what we have discussed in the last two chapters

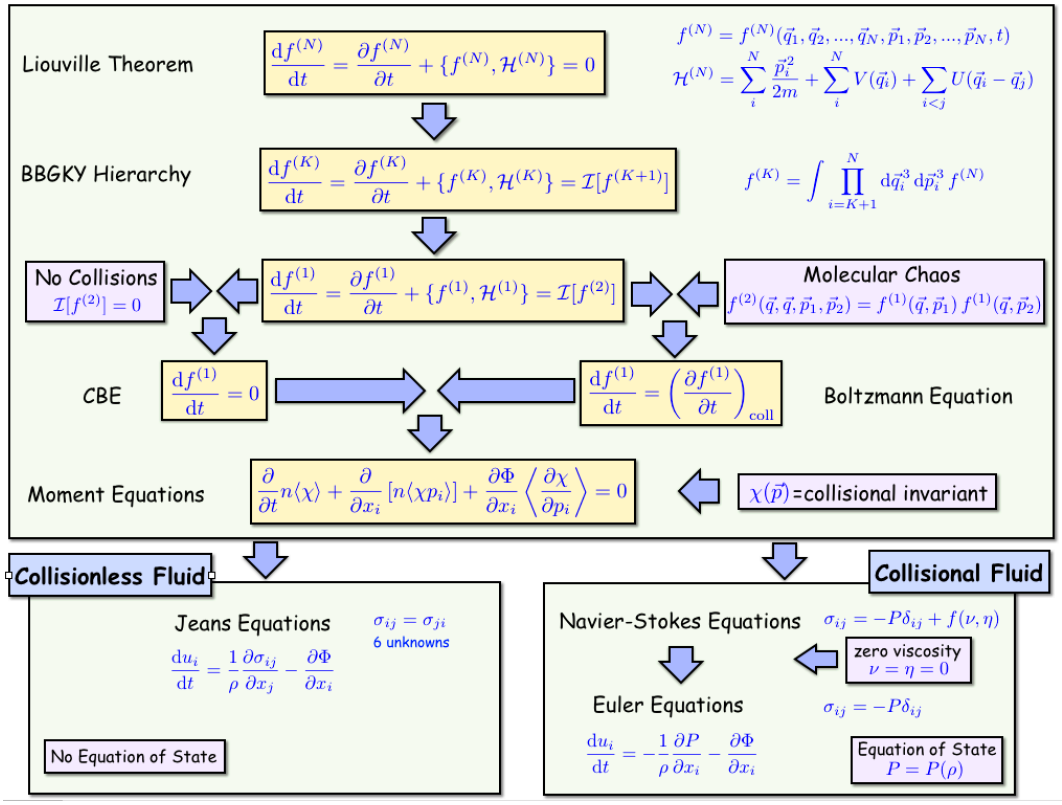

Figure 7: *Flowchart of the origin of the dynamical equations describing fluids.*

CHAPTER 8

Vorticity & Circulation

Vorticity: The vorticity of a flow is defined as the curl of the velocity field:

$$\boxed{\textbf{vorticity}: \qquad \vec{w} = \nabla \times \vec{u}}$$

It is a **microscopic** measure of rotation (vector) at a given point in the fluid, which can be envisioned by placing a paddle wheel into the flow. If it spins about its axis at a rate Ω, then $w = |\vec{w}| = 2\Omega$.

Circulation: The circulation around a closed contour C is defined as the line integral of the velocity along that contour:

$$\boxed{\textbf{circulation}: \qquad \Gamma_C = \oint_C \vec{u} \cdot \mathrm{d}\vec{l} = \int_S \vec{w} \cdot \mathrm{d}\vec{S}}$$

where S is an *arbitrary* surface bounded by C. The circulation is a **macroscopic** measure of rotation (scalar) for a finite area of the fluid.

Irrotational fluid: An irrotational fluid is defined as being curl-free; hence, $\vec{w} = 0$ and therefore $\Gamma_C = 0$ for any C.

Vortex line: a line that points in the direction of the vorticity vector. Hence, a vortex line relates to $\vec{w}$, as a streamline relates to $\vec{u}$ (cf. Chapter 2).

Vortex tube: a bundle of vortex lines. The circularity of a curve C is proportional to the number of vortex lines that thread the enclosed area.

In an **inviscid** fluid the vortex lines/tubes move **with** the fluid: a vortex line anchored to some fluid element remains anchored to that fluid element.

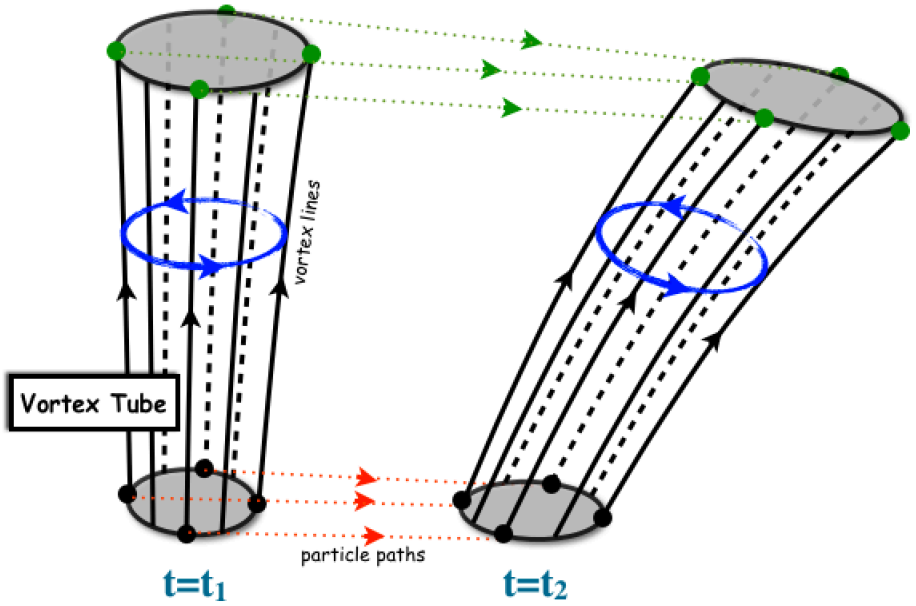

Figure 8: *Evolution of a vortex tube. Solid dots correspond to fluid elements. Due to the shear in the velocity field, the vortex tube is stretched and tilted. However, as long as the fluid is inviscid and barotropic Kelvin's circularity theorem assures that the circularity is conserved with time. In addition, since vorticity is divergence-free ('solenoidal'), the circularity along different cross sections of the same vortex-tube is the same.*

Vorticity equation: The Navier-Stokes momentum equations, in the absence of bulk viscosity, in Eulerian vector form, are given by

$$\frac{\partial \vec{u}}{\partial t} + (\vec{u}\cdot\nabla)\,\vec{u} = -\frac{\nabla P}{\rho} - \nabla\Phi + \nu\left[\nabla^2\vec{u} + \frac{1}{3}\nabla(\nabla\cdot\vec{u})\right]$$

Using the vector identity $(\vec{u}\cdot\nabla)\,\vec{u} = \frac{1}{2}\nabla u^2 + (\nabla\times\vec{u})\times\vec{u} = \nabla(u^2/2) - \vec{u}\times\vec{w}$ allows us to rewrite this as

$$\frac{\partial \vec{u}}{\partial t} - \vec{u}\times\vec{w} = -\frac{\nabla P}{\rho} - \nabla\Phi - \frac{1}{2}\nabla u^2 + \nu\left[\nabla^2\vec{u} + \frac{1}{3}\nabla(\nabla\cdot\vec{u})\right]$$

If we now take the curl on both sides of this equation, and we use that curl(grad S) = 0 for any scalar field S, and that $\nabla\times(\nabla^2\vec{A}) = \nabla^2(\nabla\times\vec{A})$, we obtain the **vorticity equation**:

$$\boxed{\frac{\partial \vec{w}}{\partial t} = \nabla \times (\vec{u} \times \vec{w}) - \nabla \times \left(\frac{\nabla P}{\rho} \right) + \nu \nabla^2 \vec{w}}$$

To write this in Lagrangian form, we first use that $\nabla \times (S\,\vec{A}) = \nabla S \times \vec{A} + S\,(\nabla \times \vec{A})$ [see Appendix A] to write

$$\nabla \times (\frac{1}{\rho}\,\nabla P) = \nabla(\frac{1}{\rho}) \times \nabla P + \frac{1}{\rho}(\nabla \times \nabla P) = \frac{\rho \nabla(1) - 1 \nabla \rho}{\rho^2} \times \nabla P = \frac{\nabla P \times \nabla \rho}{\rho^2}$$

where we have used, once more, that $\mathrm{curl}(\mathrm{grad}\, S) = 0$. Next, using the vector identities from Appendix A, we write

$$\nabla \times (\vec{w} \times \vec{u}) = \vec{w}(\nabla \cdot \vec{u}) - (\vec{w} \cdot \nabla)\vec{u} - \vec{u}(\nabla \cdot \vec{w}) + (\vec{u} \cdot \nabla)\vec{w}$$

The third term vanishes because $\nabla \cdot \vec{w} = \nabla \cdot (\nabla \times \vec{u}) = 0$. Hence, using that $\partial \vec{w}/\partial t + (\vec{u} \cdot \nabla)\vec{w} = \mathrm{d}\vec{w}/\mathrm{d}t$ we finally can write the **vorticity equation in Lagrangian form:**

$$\boxed{\frac{\mathrm{d}\vec{w}}{\mathrm{d}t} = (\vec{w} \cdot \nabla)\vec{u} - \vec{w}(\nabla \cdot \vec{u}) + \frac{\nabla \rho \times \nabla P}{\rho^2} + \nu \nabla^2 \vec{w}}$$

This equation describes how the vorticity of a fluid element evolves with time. We now describe the various terms of the *rhs* of this equation in turn:

- $(\vec{w} \cdot \nabla)\vec{u}$: This term represents the **stretching** and **tilting** of vortex tubes due to velocity gradients. To see this, we pick $\vec{w}$ to be pointing in the z-direction. Then

  $$(\vec{w} \cdot \nabla)\vec{u} = w_z \frac{\partial \vec{u}}{\partial z} = w_z \frac{\partial u_x}{\partial z}\vec{e}_x + w_z \frac{\partial u_y}{\partial z}\vec{e}_y + w_z \frac{\partial u_z}{\partial z}\vec{e}_z +$$

  The first two terms on the *rhs* describe the tilting of the vortex tube, while the third term describes the stretching.

- $\vec{w}(\nabla \cdot \vec{u})$: This term describes **stretching** of vortex tubes due to flow **compressibility**. This term is zero for an incompressible fluid or flow ($\nabla \cdot \vec{u} = 0$). Note that, again under the assumption that the vorticity is pointing in the z-direction,

$$\vec{w}(\nabla \cdot \vec{u}) = w_z \left[\frac{\partial u_x}{\partial x} + \frac{\partial u_y}{\partial y} + \frac{\partial u_z}{\partial z} \right] \vec{e}_z$$

- $(\nabla\rho \times \nabla P)/\rho^2$: This is the **baroclinic** term. It describes the production of vorticity due to a misalignment between pressure and density gradients. This term is zero for a **barotropic** EoS: if $P = P(\rho)$ the pressure and density gradiens are parallel so that $\nabla P \times \nabla\rho = 0$. Obviously, this baroclinic term also vanishes for an incompressible fluid ($\nabla\rho = 0$) or for an isobaric fluid ($\nabla P = 0$). The baroclinic term is responsible, for example, for creating vorticity in pyroclastic flows (see Fig. 4).

- $\nu\nabla^2\vec{w}$: This term describes the **diffusion** of vorticity due to **viscosity**, and is obviously zero for an inviscid fluid ($\nu = 0$). Typically, viscosity generates/creates vorticity at a bounding surface: due to the *no-slip* boundary condition shear arises giving rise to vorticity, which is subsequently diffused into the fluid by the viscosity. In the interior of a fluid, no new vorticity is generated; rather, viscosity diffuses and dissipates vorticity.

- $\nabla \times \vec{F}$: There is a fifth term that can create vorticity, which however does not appear in the vorticity equation above. The reason is that we assumed that the only external force is gravity, which is a conservative force and can therefore be written as the gradient of a (gravitational) potential. More generally, though, there may be non-conservative, external body forces present, which would give rise to a $\nabla \times \vec{F}$ term in the rhs of the vorticity equation. An example of a non-conservative force creating vorticity is the **Coriolis force**, which is responsible for creating hurricanes.

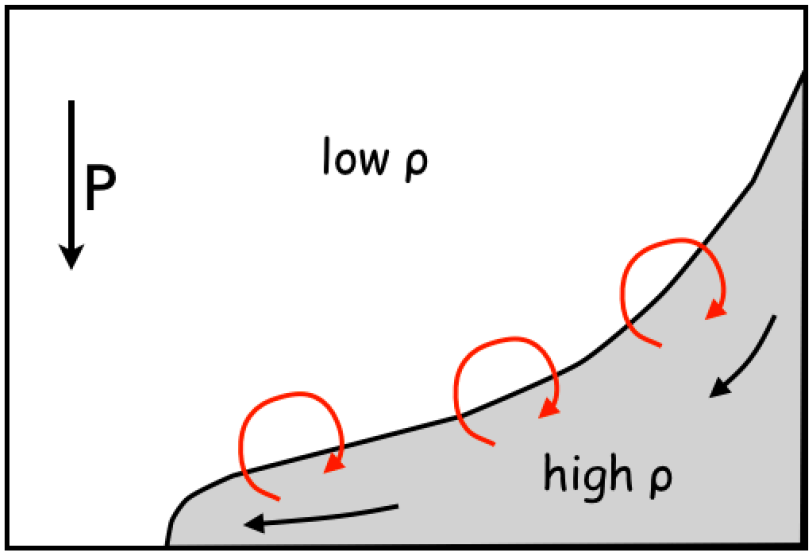

Figure 9: *The baroclinic creation of vorticity in a pyroclastic flow. High density fluid flows down a mountain and shoves itself under lower-density material, thus creating non-zero baroclinicity.*

Using the definition of **circulation**, it can be shown (here without proof) that

$$\frac{\mathrm{d}\Gamma}{\mathrm{d}t} = \int_S \left[\frac{\partial \vec{w}}{\partial t} + \nabla \times (\vec{w} \times \vec{u})\right] \cdot \mathrm{d}\vec{S}$$

Using the **vorticity equation**, this can be rewritten as

$$\boxed{\frac{\mathrm{d}\Gamma}{\mathrm{d}t} = \int_S \left[\frac{\nabla\rho \times \nabla P}{\rho^2} + \nu\nabla^2\vec{w} + \nabla \times \vec{F}\right] \cdot \mathrm{d}\vec{S}}$$

where, for completeness, we have added in the contribution of an external force $\vec{F}$ (which vanishes if $\vec{F}$ is conservative). Using Stokes' Curl Theorem (see Appendix B) we can also write this equation in a line-integral form as

$$\boxed{\frac{\mathrm{d}\Gamma}{\mathrm{d}t} = -\oint \frac{\nabla P}{\rho} \cdot \mathrm{d}\vec{l} + \nu \oint \nabla^2\vec{u} \cdot \mathrm{d}\vec{l} + \oint \vec{F} \cdot \mathrm{d}\vec{l}}$$

which is the form that is more often used.

NOTE: By comparing the equations expressing $\mathrm{d}\vec{w}/\mathrm{d}t$ and $\mathrm{d}\Gamma/\mathrm{d}t$ it is clear that the stretching a tilting terms present in the equation describing $\mathrm{d}\vec{w}/\mathrm{d}t$, are absent in the equation describing $\mathrm{d}\Gamma/\mathrm{d}t$. This implies that stretching and tilting changes the vorticity, but keeps the circularity invariant. This is basically the first theorem of Helmholtz described below.

Kelvin's Circulation Theorem: The number of vortex lines that thread any element of area that moves with the fluid (i.e., the circulation) remains unchanged in time for an inviscid, barotropic fluid, in the absence of non-conservative forces.

The proof of **Kelvin's Circulation Theorem** is immediately evident from the above equation, which shows that $\mathrm{d}\Gamma/\mathrm{d}t = 0$ if the fluid is both **inviscid** ($\nu = 0$), **barotropic** ($P = P(\rho) \Rightarrow \nabla\rho \times \nabla P = 0$), and there are no non-conservative forces ($\vec{F} = 0$).

We end this chapter on vorticity and circulation with the three theorems of Helmholtz, which hold in the absence of non-conservative forces (i.e., $\vec{F} = 0$).

Helmholtz Theorem 1: The **strength** of a vortex tube, which is defined as the circularity of the circumference of any cross section of the tube, is constant along its length. This theorem holds for **any** fluid, and simply derives from the fact that the vorticity field is **divergence-free** (we say **solenoidal**): $\nabla \cdot \vec{w} = \nabla \cdot (\nabla \times \vec{u}) = 0$. To see this, use Gauss' divergence theorem to write that

$$\int_V \nabla \cdot \vec{w}\, \mathrm{d}V = \int_S \vec{w} \cdot \mathrm{d}^2 S = 0$$

Here V is the volume of a subsection of the vortex tube, and S is its bounding surface. Since the vorticity is, by definition, perpendicular to S along the sides of the tube, the only non-vanishing components to the surface integral come from the areas at the top and bottom of the vortex tube; i.e.

$$\int_S \vec{w} \cdot \mathrm{d}^2 \vec{S} = \int_{A_1} \vec{w} \cdot (-\hat{n})\, \mathrm{d}A + \int_{A_2} \vec{w} \cdot \hat{n}\, \mathrm{d}A = 0$$

where A_1 and A_2 are the areas of the cross sections that bound the volume V of the vortex tube. Using Stokes' curl theorem, we have that

$$\int_A \vec{w} \cdot \hat{n} \, \mathrm{d}A = \oint_C \vec{u} \cdot \mathrm{d}\vec{l}$$

Hence we have that $\Gamma_{C_1} = \Gamma_{C_2}$ where C_1 and C_2 are the curves bounding A_1 and A_2, respectively.

Helmholtz Theorem 2: A vortex line cannot end in a fluid. Vortex lines and tubes must appear as closed loops, extend to infinity, or start/end at solid boundaries.

Helmholtz Theorem 3: A barotropic, inviscid fluid that is initially irrotational will remain irrotational in the absence of rotational (i.e., non-conservative) external forces. Hence, such a fluid does not and cannot create vorticity (except across curved shocks, see Chapter 11).

The proof of Helmholtz' third theorem is straightforward. According to Kelvin's circulation theorem, a barotropic, inviscid fluid has $\mathrm{d}\Gamma/\mathrm{d}t = 0$ everywhere. Hence,

$$\frac{\mathrm{d}\Gamma}{\mathrm{d}t} = \int_S \left[\frac{\partial \vec{w}}{\partial t} + \nabla \times (\vec{w} \times \vec{u}) \right] \cdot \mathrm{d}^2 \vec{S} = 0$$

Since this has to hold for any S, we have that $\partial \vec{w}/\partial t = \nabla \times (\vec{u} \times \vec{w})$. Hence, if $\vec{w} = 0$ initially, the vorticity remains zero for ever.

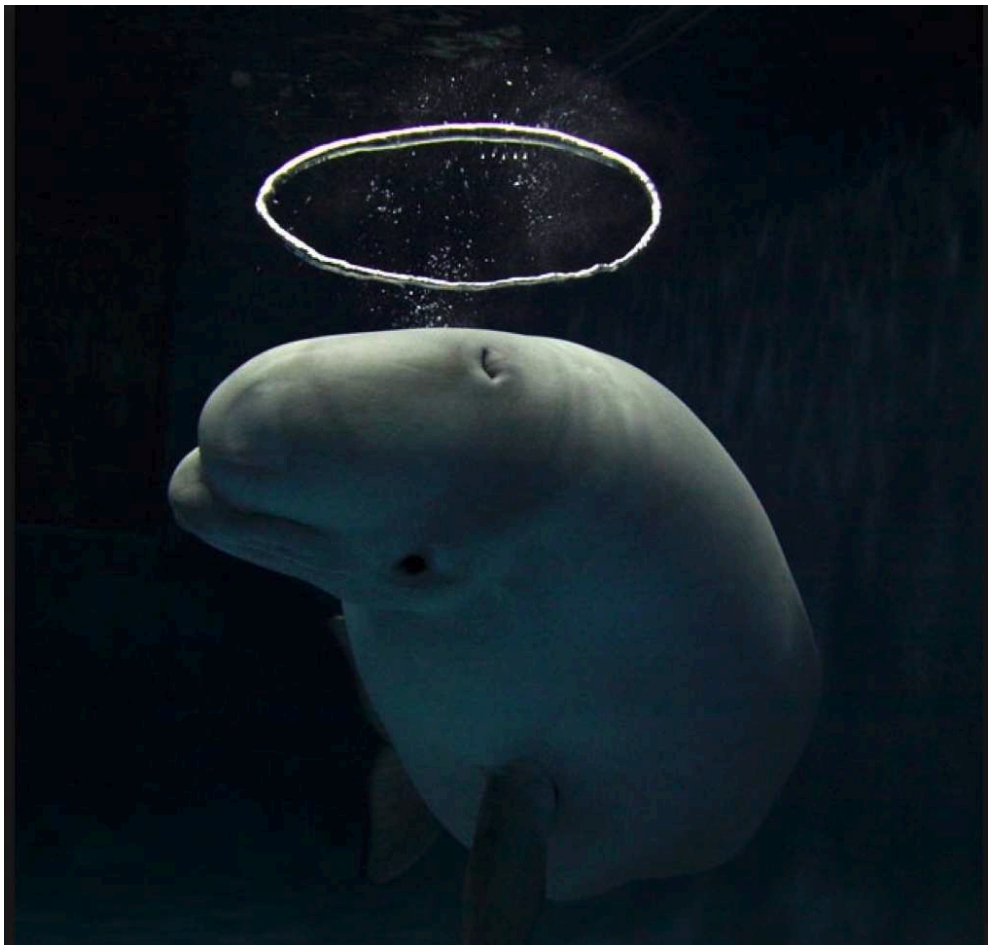

Figure 10: *A beluga whale demonstrating Kelvin's circulation theorem and Helmholtz' second theorem by producing a closed vortex tube under water, made out of air.*

CHAPTER 9

Hydrostatics and Steady Flows

Having derived all the relevant equations for hydrodynamics, we now start examining several specific flows. Since a fully general solution of the Navier-Stokes equation is (still) lacking (this is one of the seven Millenium Prize Problems, a solution of which will earn you $1,000,000), we can only make progress if we make several assumptions.

We start with arguably the simplest possible flow, namely 'no flow'. This is the area of **hydrostatics** in which $\vec{u}(\vec{x},t) = 0$. And since we seek a static solution, we also must have that all $\partial/\partial t$-terms vanish. Finally, in what follows we shall also ignore radiative processes (i.e., we set $\mathcal{L} = 0$).

Applying these restrictions to the continuity, momentum and energy equations (see box at the end of Chapter 5) yields the following two non-trivial equations:

$$\nabla P = -\rho \nabla \Phi$$

$$\nabla \cdot \vec{F}_{\rm cond} = 0$$

The first equation is the well known equation of **hydrostatic equilibrium**, stating that the gravitational force is balanced by pressure gradients, while the second equation states that in a static fluid the **conductive flux** needs to be divergence-free.

To further simplify matters, let's assume (i) spherical symmetry, and (ii) a barotropic equation of state, i.e., $P = P(\rho)$.

The equation of hydrostatic equilibrium now reduces to

$$\frac{{\rm d}P}{{\rm d}r} = -\frac{G\,M(r)\,\rho(r)}{r^2}$$

In addition, if the gas is self-gravitating (such as in a star) then we also have that

$$\boxed{\frac{\mathrm{d}M}{\mathrm{d}r} = 4\pi\rho(r)\, r^2}$$

For a barotropic EoS this is a closed set of equations, and the density profile can be solved for (given proper boundary conditions). Of particular interest in astrophysics, is the case of a **polytropic EoS**: $P \propto \rho^{\Gamma}$, where Γ is the polytropic index. Note that $\Gamma = 1$ and $\Gamma = \gamma$ for isothermal and adiabatic equations of state, respectively. A spherically symmetric, polytropic fluid in HE is called a polytropic sphere.

Lane-Emden equation: Upon substituting the **polytropic EoS** in the equation of **hydrostatic equilibrium** and using the **Poisson equation**, one obtains a single differential equation that completely describes the structure of the polytropic sphere, known as the **Lane-Emden equation**:

$$\frac{1}{\xi^2}\frac{\mathrm{d}}{\mathrm{d}\xi}\left(\xi^2\frac{\mathrm{d}\theta}{\mathrm{d}\xi}\right) = -\theta^n$$

Here $n = 1/(\Gamma - 1)$ is related to the polytropic index (in fact, confusingly, some texts refer to n as the polytropic index),

$$\xi = \left(\frac{4\pi G\rho_{\mathrm{c}}}{\Phi_0 - \Phi_{\mathrm{c}}}\right)^{1/2} r$$

is a dimensionless radius,

$$\theta = \left(\frac{\Phi_0 - \Phi(r)}{\Phi_0 - \Phi_{\mathrm{c}}}\right)$$

with Φ_{c} and Φ_0 the values of the gravitational potential at the center ($r = 0$) and at the surface of the star (where $\rho = 0$), respectively. The density is related to θ according to $\rho = \rho_{\mathrm{c}}\theta^n$ with ρ_{c} the central density.

Solutions to the Lane-Emden equation are called **polytropes of index** n. In general, the Lane-Emden equation has to be solved numerically subject to the boundary conditions $\theta = 1$ and $\mathrm{d}\theta/\mathrm{d}\xi = 0$ at $\xi = 0$. Analytical solutions exist, however, for $n = 0$, 1, and 5. Examples of polytropes are stars that are supported by **degeneracy pressure**. For example, a non-relativistic, degenerate equation of state has $P \propto \rho^{5/3}$

(see Appendix H) and is therefore describes by a polytrope of index $n = 3/2$. In the relativistic case $P \propto \rho^{4/3}$ which results in a polytrope of index $n = 3$.

Another polytrope that is often encountered in astrophysics is the **isothermal sphere**, which has $P \propto \rho$ and thus $n = \infty$. It has $\rho \propto r^{-2}$ at large radii, which implies an infinite total mass. If one truncates the isothermal sphere at some radius and embeds it in a medium with external pressure (to prevent the sphere from expanding), it is called a **Bonnor-Ebert sphere**, which is a structure that is frequently used to describe molecular clouds.

Stellar Structure: stars are gaseous spheres in hydrostatic equilibrium (except for radial pulsations, which may be considered perturbations away from HE). The structure of stars is therefore largely governed by the above equation.

However, in general the **equation of state** is of the form $P = P(\rho, T, \{X_i\})$, where $\{X_i\}$ is the set of the abundances of all emements i. The temperature structure of a star and its abundance ratios are governed by **nuclear physics** (which provides the source of energy) and the various **heat transport mechanisms**.

Heat transport in stars: Typically, ignoring abundance gradients, stars have the equation of state of an ideal gas, $P = P(\rho, T)$. This implies that the equations of stellar structure need to be complemented by an equation of the form

$$\boxed{\frac{\mathrm{d}T}{\mathrm{d}r} = F(r)}$$

Since T is a measure of the internal energy, the rhs of this equation describes the **heat flux**, $F(r)$.

The main heat transport mechanisms in a star are:

- conduction
- convection
- radiation

Note that the fourth heat transport mechanism, advection, is not present in the case of hydrostatic equilibrium, because $\vec{u} = 0$.

Recall from Chapter 4 that the **thermal conductivity** $\mathcal{K} \propto (k_{\rm B}\,T)^{1/2}/\sigma$ where σ is the collisional cross section. Using that $k_{\rm B}T \propto v^2$ and that the mean-free path of the particles is $\lambda_{\rm mfp} = 1/(n\sigma)$, we have that

$$\mathcal{K} \propto n\,\lambda_{\rm mfp}\,v$$

with v the thermal, microscopic velocity of the particles (recall that $\vec{u} = 0$). Since radiative heat transport in a star is basically the conduction of photons, and since $c \gg v_{\rm e}$ and the mean-free part of photons is much larger than that of electrons (after all, the cross section for Thomson scattering, $\sigma_{\rm T}$, is much smaller than the typical cross section for Coulomb interactions), we have that in stars *radiation is a far more efficient heat transport mechanism than conduction*. An exception are relativistic, degenerate cores, for which $v_{\rm e} \sim c$ and photons and electrons have comparable mean-free paths.

Convection: convection only occurs if the **Schwarzschild Stability Criterion** is violated, which happens when the temperature gradient $\mathrm{d}T/\mathrm{d}r$ becomes too large (i.e., larger than the temperature gradient that would exist if the star was adiabatic; see Chapter 13). If that is the case, convection always dominates over radiation as the most efficient heat transport mechanism. In general, as a rule of thumb, more massive stars are *more radiative* and *less convective*.

Trivia: On average it takes ~ 200.000 years for a photon created at the core of the Sun in nuclear burning to make its way to the Sun's photosphere; from there it only takes ~ 8 minutes to travel to the Earth.

Hydrostatic Mass Estimates: Now let us consider the case of an ideal gas, for which

$$P = \frac{k_{\rm B}T}{\mu m_{\rm p}}\rho\,,$$

but this time the gas is not self-gravitating; rather, the gravitational potential may be considered 'external'. A good example is the ICM; the hot gas that permeates clusters. From the EoS we have that

$$\begin{aligned}\frac{\mathrm{d}P}{\mathrm{d}r} &= \frac{\partial P}{\partial \rho}\frac{\mathrm{d}\rho}{\mathrm{d}r} + \frac{\partial P}{\partial T}\frac{\mathrm{d}T}{\mathrm{d}r} = \frac{P}{\rho}\frac{\mathrm{d}\rho}{\mathrm{d}r} + \frac{P}{T}\frac{\mathrm{d}T}{\mathrm{d}r} \\ &= \frac{P}{r}\left[\frac{r}{\rho}\frac{\mathrm{d}\rho}{\mathrm{d}r} + \frac{r}{T}\frac{\mathrm{d}T}{\mathrm{d}r}\right] = \frac{P}{r}\left[\frac{\mathrm{d}\ln\rho}{\mathrm{d}\ln r} + \frac{\mathrm{d}\ln T}{\mathrm{d}\ln r}\right]\end{aligned}$$

Substitution of this equation in the equation for Hydrostatic equilibrium (HE) yields

$$\boxed{M(r) = -\frac{k_\mathrm{B}\,T(r)\,r}{\mu m_\mathrm{p} G}\left[\frac{\mathrm{d}\ln\rho}{\mathrm{d}\ln r} + \frac{\mathrm{d}\ln T}{\mathrm{d}\ln r}\right]}$$

This equation is often used to measure the 'hydrostatic' mass of a galaxy cluster; X-ray measurements can be used to infer $\rho(r)$ and $T(r)$ (after deprojection, which is analytical in the case of spherical symmetry). Substitution of these two radial dependencies in the above equation then yields an estimate for the cluster's mass profile, $M(r)$. Note, though, that this mass estimate is based on three crucial assumptions: (i) sphericity, (ii) hydrostatic equilibrium, and (iii) an ideal-gas EoS. Clusters typically are not spherical, often are turbulent (such that $\vec{u} \neq 0$, violating the assumption of HE), and can have significant contributions from non-thermal pressure due to magnetic fields, cosmic rays and/or turbulence. Including these non-thermal pressure sources the above equation becomes

$$M(r) = -\frac{k_\mathrm{B}\,T(r)\,r}{\mu m_\mathrm{p} G}\left[\frac{\mathrm{d}\ln\rho}{\mathrm{d}\ln r} + \frac{\mathrm{d}\ln T}{\mathrm{d}\ln r} + \frac{P_\mathrm{nt}}{P_\mathrm{th}}\frac{\mathrm{d}\ln P_\mathrm{nt}}{\mathrm{d}\ln r}\right]$$

were P_nt and P_th are the non-thermal and thermal contributions to the total gas pressure. Unfortunately, it is extremely difficult to measure P_nt reliably, which is therefore often ignored. This may result in systematic biases of the inferred cluster mass (typically called the 'hydrostatic mass').

Solar Corona: As a final example of a hydrostatic problem in astrophysics, consider the problem of constructing a static model for the Solar corona.

The Solar corona is a large, spherical region of hot ($T \sim 10^6$K) plasma extending well beyond its photosphere. Let's assume that the heat is somehow (magnetic reconnection?) produced in the lower layers of the corona, and try to infer the density, temperature and pressure profiles under the assumption of hydrostatic equilibrium.

We have the boundary condition of the temperature at the base, which we assume to be $T_0 = 3 \times 10^6$K, at a radius of $r = r_0 \sim R_\odot \simeq 6.96 \times 10^{10}$ cm. The mass of the corona is negligble, and we therefore have that

$$\begin{aligned} \frac{\mathrm{d}P}{\mathrm{d}r} &= -\frac{G\ \mathrm{M}_\odot}{r^2}\,\frac{\mu m_\mathrm{p}}{k_\mathrm{B}}\,\frac{P}{T} \\ \frac{\mathrm{d}}{\mathrm{d}r}\left(\mathcal{K}\, r^2\,\frac{\mathrm{d}T}{\mathrm{d}r}\right) &= 0 \end{aligned}$$

where we have used the ideal gas EoS to substitute for ρ. As we have seen above $\mathcal{K} \propto n\lambda_\mathrm{mfp} T^{1/2}$. In a plasma one furthermore has that $\lambda_\mathrm{mfp} \propto n^{-1}\, T^2$, which implies that $\mathcal{K} \propto T^{5/2}$. Hence, the second equation can be written as

$$r^2 T^{5/2} \frac{\mathrm{d}T}{\mathrm{d}r} = \text{constant}$$

which implies

$$T = T_0\,\left(\frac{r}{r_0}\right)^{-2/7}$$

Note that this equation satisfies our boundary condition, and that $T_\infty = \lim_{r\to\infty} T(r) = 0$. Substituting this expression for T in the HE equation yields

$$\frac{\mathrm{d}P}{P} = -\frac{G\ \mathrm{M}_\odot\,\mu m_\mathrm{p}}{k_\mathrm{B} T_0\, r_0^{2/7}}\,\frac{\mathrm{d}r}{r^{12/7}}$$

Solving this ODE under the boundary condition that $P = P_0$ at $r = r_0$ yields

$$P = P_0\,\exp\left[-\frac{7}{5}]\,\frac{G\ \mathrm{M}_\odot\,\mu m_\mathrm{p}}{k_\mathrm{B} T_0\, r_0}\,\left\{\left(\frac{r}{r_0}\right)^{-5/7} - 1\right\}\right]$$

Note that

$$\lim_{r\to\infty} P = P_0\,\exp\left[-\frac{7}{5}\,\frac{G\ \mathrm{M}_\odot\,\mu m_\mathrm{p}}{k_\mathrm{B} T_0\, r_0}\right] \neq 0$$

Hence, you need an external pressure to confine the corona. Well, that seems OK, given that the Sun is embedded in an ISM, whose pressure we can compute taking

characteristic values for the warm phase ($T \sim 10^4$K and $n \sim 1\,\mathrm{cm}^{-3}$). Note that the other phases (cold and hot) have the same pressure. Plugging in the numbers, we find that

$$\frac{P_\infty}{P_{\rm ISM}} \sim 10 \frac{\rho_0}{\rho_{\rm ISM}}$$

Since $\rho_0 \gg \rho_{\rm ISM}$ we thus infer that the ISM pressure falls short, by orders of magnitude, to be able to confine the corona....

As first inferred by Parker in 1958, the correct implicication of this puzzling result is that a hydrostatic corona is impossible; instead, Parker made the daring suggestion that there should be a **solar wind**, which was observationally confirmed a few years later.

Having addressed hydrostatics ('no flow'), we now consider the next simplest flow; **steady flow**, which is characterised by $\vec{u}(\vec{x},t) = \vec{u}(\vec{x})$. For steady flow $\partial\vec{u}/\partial t = 0$, and fluid elements move along the **streamlines** (see Chapter 2).

Using the vector identity $(\vec{u}\cdot\nabla)\,\vec{u} = \frac{1}{2}\nabla u^2 + (\nabla\times\vec{u})\times\vec{u} = \nabla(u^2/2) - \vec{u}\times\vec{w}$, allows us to write the Navier-Stokes equation for a steady flow of ideal fluid as

$$\boxed{\nabla\left(\frac{u^2}{2}+\Phi\right) + \frac{\nabla P}{\rho} - \vec{u}\times\vec{w} = 0}$$

This equation is known as **Crocco's theorem**. In order to write this in a more 'useful' form, we first proceed to demonstrate that $\nabla P/\rho$ an be written in terms of the gradients of the **specific enthalpy**, h, and the **specific entropy**, s:

The **enthalpy**, H, is a measure for the total energy of a thermodynamic system that includes the **internal** energy, U, and the amount of energy required to make room for it by displacing its environment and establishing its volume and pressure:

$$H = U + PV$$

The differential of the enthalpy can be written as

$$\mathrm{d}H = \mathrm{d}U + P\,\mathrm{d}V + V\,\mathrm{d}P$$

Using the first law of thermodynamics, according to which $\mathrm{d}U = \mathrm{d}Q - P\mathrm{d}V$, and the second law of thermodynamics, according to which $\mathrm{d}Q = T\mathrm{d}S$, we can rewrite this as

$$\mathrm{d}H = T\,\mathrm{d}S + V\,\mathrm{d}P$$

which, in specific form, becomes

$$\mathrm{d}h = T\mathrm{d}s + \frac{\mathrm{d}P}{\rho}$$

(i.e., we have $s = S/m$). This relation is one of the **Gibbs relations** frequently encountered in thermodynamics. NOTE: for completeness, we point out that this expression ignores changes in the chemical potential (see Appendix L).

The above expression for $\mathrm{d}h$ implies that

$$\boxed{\frac{\nabla P}{\rho} = \nabla h - T\,\nabla s}$$

(for a formal proof, see at the end of this chapter). Now recall from the previous chapter on vorticity that the **baroclinic term** is given by

$$\nabla \times \left(\frac{\nabla P}{\rho}\right) = \frac{\nabla\rho \times \nabla P}{\rho^2}$$

Using the above relation, and using that the curl of the gradient of a scalar vanishes, we can rewrite this baroclinic term as $\nabla \times (T\,\nabla s)$. This implies that *one can create vorticity by creating a gradient in (specific) entropy*! One way to do this, which is one of the most important mechanisms of creating vorticity in astrophysics, is via **curved shocks**; when an irrotational, isentropic fluid comes across a curved shock, different streamlines will experience a different jump in entropy (Δs will depend on the angle under which you cross the shock). Hence, in the post-shocked gas there will be a gradient in entropy, and thus vorticity.

Intermezzo: isentropic vs. adiabatic

We consider a flow to be **isentropic** if it conserves (specific) entropy, which implies that $\mathrm{d}s/\mathrm{d}t = 0$. Note that an ideal fluid is a fluid without dissipation (viscosity) and conduction (heat flow). Hence, any flow of ideal fluid is isentropic. A fluid is said to be isentropic if $\nabla s = 0$. A process is said to be **adiabatic** if $\mathrm{d}Q/\mathrm{d}t = 0$. Note that, according to the second law of thermodynamics, $T\mathrm{d}S \geq \mathrm{d}Q$. Equality only holds for a **reversible** process; in other words, only if a process is adiabatic and reversible do we call it isentropic. An irreversible, adiabatic process, therefore, can still create entropy.

Using the momentum equation for a steady, ideal fluid, and substituting $\nabla P/\rho \rightarrow \nabla h - T\,\nabla s$, we obtain

$$\boxed{\nabla B = T\,\nabla s + \vec{u} \times \vec{w}}$$

where we have introduced the **Bernoulli function**

$$\boxed{B \equiv \frac{u^2}{2} + \Phi + h = \frac{u^2}{2} + \Phi + \varepsilon + P/\rho}$$

which obviously is a measure of energy. The above equation is sometimes referred to as **Crocco's theorem**. It relates entropy gradients to vorticity and gradients in the Bernoulli function.

Let's investigate what happens to the Bernoulli function for an ideal fluid in a steady flow. Since we are in a steady state we have that

$$\frac{\mathrm{d}B}{\mathrm{d}t} = \frac{\partial B}{\partial t} + (\vec{u} \cdot \nabla)B = (\vec{u} \cdot \nabla)B$$

Next we use that

$$
\begin{aligned}
(\vec{u}\cdot\nabla)B &= (\vec{u}\cdot\nabla)\left[\frac{u^2}{2}+\Phi+h\right] \\
&= (\vec{u}\cdot\nabla)\left[\frac{u^2}{2}+\Phi\right]+\vec{u}\cdot\frac{\nabla P}{\rho}+T\,(\vec{u}\cdot\nabla s) \\
&= (\vec{u}\cdot\left[\nabla\left(\frac{u^2}{2}+\Phi\right)+\frac{\nabla P}{\rho}\right]+T\,(\vec{u}\cdot\nabla s) \\
&= \vec{u}\cdot(\vec{u}\times\vec{w})+T\,(\vec{u}\cdot\nabla s) \\
&= 0
\end{aligned}
$$

Here we have used that the cross-product of $\vec{u}$ and $\vec{w}$ is perpendicular to $\vec{u}$, and that in an ideal fluid $\vec{u}\cdot\nabla s = 0$. The latter follow from the fact that in an ideal fluid $\mathrm{d}s/\mathrm{d}t = 0$, and the fact that $\mathrm{d}s/\mathrm{d}t = \partial s/\partial t + \vec{u}\cdot\nabla s$. Since all $\partial/\partial t$ terms vanish for a steady flow, we see that $\vec{u}\cdot\nabla s = 0$ for a steady flow of ideal fluid. And as a consequence, we thus also have that

$$
\boxed{\frac{\mathrm{d}B}{\mathrm{d}t} = 0}
$$

Hence, *in a steady flow of ideal fluid, the Bernoulli function is conserved*. Using the definition of the Bernoulli function we can write this as

$$
\frac{\mathrm{d}B}{\mathrm{d}t} = \vec{u}\cdot\frac{\mathrm{d}\vec{u}}{\mathrm{d}t}+\frac{\mathrm{d}\Phi}{\mathrm{d}t}+T\,\frac{\mathrm{d}s}{\mathrm{d}t}+\frac{1}{\rho}\frac{\mathrm{d}P}{\mathrm{d}t} = 0
$$

Since $\mathrm{d}s/\mathrm{d}t = 0$ for an ideal fluid, we have that if the flow is such that the gravitational potential along the flow doesn't change significantly (such that $\mathrm{d}\Phi/\mathrm{d}t \simeq 0$), we find that

$$
\boxed{\vec{u}\cdot\frac{\mathrm{d}\vec{u}}{\mathrm{d}t} = -\frac{1}{\rho}\,\frac{\mathrm{d}P}{\mathrm{d}t}}
$$

This is known as **Bernoulli's theorem**, and states that as the speed of a steady flow increases, the internal pressure of the ideal fluid must decrease. Applications of Bernoulli's theorem discussed in class include the shower curtain and the pitot tube (a flow measurement device used to measure fluid flow velocity).

Potential flow: The final flow to consider in this chapter is potential flow. Consider an irrotational flow, which satisfies $\vec{w} \equiv \nabla \times \vec{u} = 0$ everywhere. This implies that there is a scalar function, $\phi_u(x)$, such that $\vec{u} = \nabla \phi_u$, which is why $\phi_u(x)$ is called the **velocity potential**. The corresponding flow $\vec{u}(\vec{x})$ is called potential flow.

If the fluid is ideal (i.e., $\nu = \mathcal{K} = 0$), and barotropic or isentropic, such that the flow fluid has vanishing baroclinicity, then **Kelvin's circulation theorem** assures that the flow will remain irrotational throughout (no vorticity can be created), provided that all forces acting on the fluid are conservative.

If the fluid is **incompressible**, in addition to being irrotational, then we have that both the curl and the divergence of the velocity field vanish. This implies that

$$\nabla \cdot \vec{u} = \nabla^2 \phi_u = 0$$

This is the well known **Laplace equation**, familiar from electrostatics. Mathematically, this equation is of the elliptic PDE type which requires well defined boundary conditions in order for a solution to both exist and be unique. A classical case of potential flow is the flow around a solid body placed in a large fluid volume. In this case, an obvious boundary condition is the one stating that the velocity component perpendicular to the surface of the body at the body (assumed at rest) is zero. This is called a *Neumann* boundary condition and is given by

$$\frac{\partial \phi_u}{\partial n} = \vec{n} \cdot \nabla \phi_u = 0$$

with $\vec{n}$ the normal vector. The Laplace equation with this type of boundary condition constitutes a well-posed problem with a unique solution. An example of potential flow around a solid body is shown in Fig. 2 in Chapter 2. We will not examine any specific examples of potential flow, as this means having to solve a Laplace equation, which is purely a mathematical exersize. We end, though, by pointing out that real fluids are never perfectly inviscid (ideal fluids don't exist). And any flow past a surface involves a boundary layer inside of which viscosity creates vorticity (due to no-slip boundary condition, which states that the tangential velocity at the surface of the body must vanish). Hence, potential flow can never fully describe the flow around a solid body; otherwise one would run into **d'Alembert's paradox** which is that steady potential flow around a body exerts zero force on the body; in other words, it costs no energy to move a body through the fluid at constant speed. We know from everyday experience that this is indeed not true. The solution to the

paradox is that viscosity created in the boundary layer, and subsequently dissipated, results in friction.

Although potential flow around an object can thus never be a full description of the flow, in many cases, the boundary layer is very thin, and away from the boundary layer the solutions of potential flow still provide an accurate description of the flow.

As promised in the text, we end this chapter by demonstrating that

$$\mathrm{d}h = T\,\mathrm{d}s + \frac{\mathrm{d}P}{\rho} \qquad \Longleftrightarrow \qquad \nabla h = T\,\nabla s + \frac{\nabla P}{\rho}$$

To see this, use that the natural variables of h are the specific entropy, s, and the pressure P. Hence, $h = h(s, P)$, and we thus have that

$$\mathrm{d}h = \frac{\partial h}{\partial s}\,\mathrm{d}s + \frac{\partial h}{\partial P}\,\mathrm{d}P$$

From a comparison with the previous expression for $\mathrm{d}h$, we see that

$$\frac{\partial h}{\partial s} = T\,, \qquad\qquad \frac{\partial h}{\partial P} = \frac{1}{\rho}$$

which allows us to derive

$$\begin{aligned}
\nabla h &= \frac{\partial h}{\partial x}\,\vec{e}_x + \frac{\partial h}{\partial y}\,\vec{e}_y + \frac{\partial h}{\partial z}\,\vec{e}_z \\
&= \left(\frac{\partial h}{\partial s}\,\frac{\partial s}{\partial x} + \frac{\partial h}{\partial P}\,\frac{\partial P}{\partial x}\right)\vec{e}_x + \left(\frac{\partial h}{\partial s}\,\frac{\partial s}{\partial y} + \frac{\partial h}{\partial P}\,\frac{\partial P}{\partial y}\right)\vec{e}_y + \left(\frac{\partial h}{\partial s}\,\frac{\partial s}{\partial z} + \frac{\partial h}{\partial P}\,\frac{\partial P}{\partial z}\right)\vec{e}_z \\
&= \frac{\partial h}{\partial s}\left(\frac{\partial s}{\partial x}\,\vec{e}_x + \frac{\partial s}{\partial y}\,\vec{e}_y + \frac{\partial s}{\partial z}\,\vec{e}_z\right) + \frac{\partial h}{\partial P}\left(\frac{\partial P}{\partial x}\,\vec{e}_x + \frac{\partial P}{\partial y}\,\vec{e}_y + \frac{\partial P}{\partial z}\,\vec{e}_z\right) \\
&= T\nabla s + \frac{1}{\rho}\nabla P
\end{aligned}$$

which completes our proof.

CHAPTER 10

Viscous Flow and Accretion Flow

As we have seen in our discussion on potential flow in the previous chapter, realistic flow past an object always involves a boundary layer in which viscosity results in vorticity. Even if the viscosity of the fluid is small, the no-slip boundary condition typically implies a region where the shear is substantial, and viscocity thus manifests itself.

In this chapter we examine two examples of **viscous flow**. We start with a well-known example from engineering, known as **Poiseuille-Hagen flow** through a pipe. Although not really an example of astrophysical flow, it is a good illustration of how viscosity manifests itself as a consequence of the **no-slip boundary condition**. The second example that we consider is viscous flow in a thin accretion disk. This flow, which was first worked out in detail in a famous paper by Shakura & Sunyaev in 1973, is still used today to describe accretion disks in AGN and around stars.

Pipe Flow: Consider the steady flow of an incompressible viscous fluid through a circular pipe of radius $R_{\rm pipe}$ and lenght L. Let ρ be the density of the fluid as it flows through the pipe, and let $\nu = \mu/\rho$ be its **kinetic viscosity**. Since the flow is incompressible, we have that fluid density will be ρ throughout. If we pick a Cartesian coordinate system with the z-axis along the symmetry axis of the cylinder, then the velocity field of our flow is given by

$$\vec{u} = u_z(x, y, z)\, \vec{e}_z$$

In other words, $u_x = u_y = 0$.

Starting from the **continuity equation**

$$\frac{\partial \rho}{\partial t} + \nabla \cdot \rho \vec{u} = 0$$

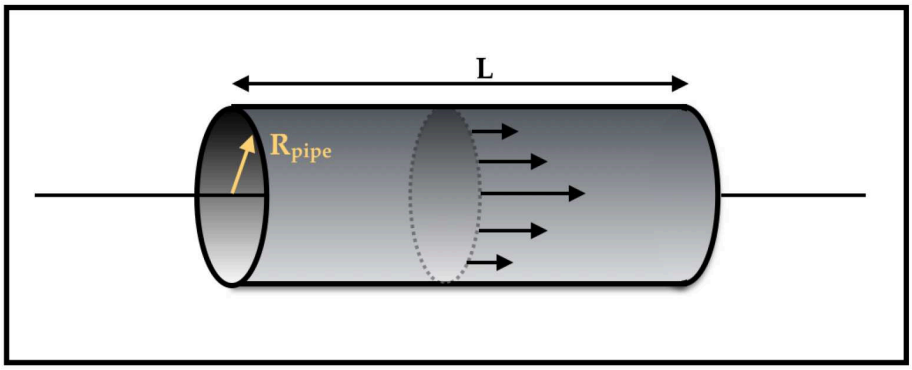

Figure 11: *Poiseuille-Hagen flow of a viscous fluid through a pipe of radius* R_{pipe} *and lenght* L*.*

and using that all partial time-derivatives of a steady flow vanish, we obtain that

$$\frac{\partial \rho u_x}{\partial x} + \frac{\partial \rho u_y}{\partial y} + \frac{\partial \rho u_z}{\partial z} = 0 \qquad \Rightarrow \qquad \frac{\partial u_z}{\partial z} = 0$$

where we have used that $\partial\rho/\partial z = 0$ because of the incompressibility of the flow. Hence, we can update our velocity field to be $\vec{u} = u_z(x, y)\,\vec{e}_z$.

Next we write down the **momentum equations** for a steady, incompressible flow, which are given by

$$(\vec{u} \cdot \nabla)\vec{u} = -\frac{\nabla P}{\rho} + \nu \nabla^2 \vec{u} - \nabla \Phi$$

In what follows we assume the pipe to be perpendicular to $\nabla\Phi$, so that we may ignore the last term in the above expression. For the x- and y- components of the momentum equation, one obtains that $\partial P/\partial x = \partial P/\partial y = 0$. For the z-component, we instead have

$$u_z \frac{\partial u_z}{\partial z} = -\frac{1}{\rho}\frac{\partial P}{\partial z} + \nu \nabla^2 u_z$$

Combining this with our result from the continuity equation, we obtain that

$$\boxed{\frac{1}{\rho}\frac{\partial P}{\partial z} = \nu \nabla^2 u_z}$$

Next we use that $\partial P/\partial z$ cannot depend on z; otherwise u_z would depend on z, but according to the continuity equation $\partial u_z/\partial z = 0$. This means that the pressure

gradient in the z-direction must be constant, which we write as $-\Delta P/L$, where ΔP is the pressure different between the beginning and end of the pipe, and the minus sign us used to indicate the the fluid pressure declines as it flows throught the pipe.

Hence, we have that

$$\nabla^2 u_z = -\frac{\Delta P}{\rho\,\nu\,L} = \text{constant}$$

At this point, it is useful to switch to **cylindrical coordinates**, (R, θ, z), with the z-axis as before. Because of the symmetries involved, we have that $\partial/\partial\theta = 0$, and thus the above expression reduces to

$$\frac{1}{R}\frac{\mathrm{d}}{\mathrm{d}R}\left(R\frac{\mathrm{d}u_z}{\mathrm{d}R}\right) = -\frac{\Delta P}{\rho\,\nu\,L}$$

(see Appendix D). Rewriting this as

$$\mathrm{d}u_z = -\frac{1}{2}\frac{\Delta P}{\rho\,\nu\,L}\,R\,\mathrm{d}R$$

and integrating from R to R_{pipe} using the no-slip boundary condition that $u_z(R_{\text{pipe}}) = 0$, we finally obtain the flow solution

$$\boxed{u_z(R) = \frac{\Delta P}{4\rho\,\nu\,L}\,\left[R_{\text{pipe}}^2 - R^2\right]}$$

This solution is called **Poiseuille flow** or **Poiseuille-Hagen flow**.

As is evident from the above expression, for a given pressure difference ΔP, the flow speed $u \propto \nu^{-1}$ (i.e., a more viscous fluid will flow slower). In addition, for a given fluid viscosity, applying a larger pressure difference ΔP results in a larger flow speed ($u \propto \Delta P$).

Now let us compute the amount of fluid that flows through the pipe per unit time:

$$\dot{M} = 2\pi \int_0^{R_{\text{pipe}}} \rho\,u_z(R)\,R\,\mathrm{d}R = \frac{\pi}{8}\,\frac{\Delta P}{\nu\,L}\,R_{\text{pipe}}^4$$

Note the strong dependence on the pipe radius; this makes it clear that a clogging of the pipe has a drastic impact on the mass flow rate (relevant for both arteries and oil-pipelines). The above expression also gives one a relatively easy method to measure

the viscosity of a fluid: take a pipe of known $R_{\rm pipe}$ and L, apply a pressure difference ΔP across the pipe, and measure the mass flow rate, $\dot{M}$; the above expression allows one to then compute ν.

The Poiseuille velocity flow field has been experimentally confirmed, *but only for slow flow*! When $|\vec{u}|$ gets too large (i.e., ΔP is too large), then the flows becomes irregular in time and space; turbulence develops and $|\vec{u}|$ drops due to the enhanced drag from the turbulence. This will be discussed in more detail in Chapter 11.

Accretion Disks: We now move to a viscous flow that is more relevant for astrophysics; accretion flow. Consider a thin accretion disk surrounding an accreting object of mass $M_\bullet \gg M_{\rm disk}$ (such that we may ignore the disk's self-gravity). Because of the symmetries involved, we adopt **cylindrical coordinates**, (R, θ, z), with the z-axis perpendicular to the disk. We also have that $\partial/\partial\theta$ is zero, and we set $u_z = 0$ throuhout.

We expect u_θ to be the main velocity component, with a small u_R component representing the radial accretion flow. We also take the flow to be **incompressible**.

Let's start with the **continuity equation**, which in our case reads

$$\frac{\partial \rho}{\partial t} + \frac{1}{R}\frac{\partial}{\partial R}\left(R\,\rho\,u_R\right) = 0$$

(see Appendix D for how to express the divergence in cylindrical coordinates).

Next up is the **Navier-Stokes equations**. For now, we only consider the θ-component, which is given by

$$\begin{aligned}\frac{\partial u_\theta}{\partial t} \;+\; & u_R\frac{\partial u_\theta}{\partial R} + \frac{u_\theta}{R}\frac{\partial u_\theta}{\partial \theta} + u_z\frac{\partial u_\theta}{\partial z} + \frac{u_R\,u_\theta}{R} = -\frac{1}{\rho}\frac{\partial P}{\partial \theta} \\ & + \;\nu\left[\frac{\partial^2 u_\theta}{\partial R^2} + \frac{1}{R^2}\frac{\partial^2 u_\theta}{\partial \theta^2} + \frac{\partial^2 u_\theta}{\partial z^2} + \frac{1}{R}\frac{\partial u_\theta}{\partial R} + \frac{2}{R^2}\frac{\partial u_R}{\partial \theta} - \frac{u_\theta}{R^2}\right] + \frac{\partial \Phi}{\partial \theta}\end{aligned}$$

NOTE: There are several terms in the above expression that may seem 'surprising'. The important thing to remember in writing down the equations in curvi-linear

coordinates is that operators can also act on unit-direction vectors. For example, the θ-component of $\nabla^2\vec{u}$ is NOT $\nabla^2 u_\theta$. That is because the operator ∇^2 acts on $u_R\vec{e}_R + u_\theta\vec{e}_\theta + u_z\vec{e}_z$, and the directions of $\vec{e}_R$ and $\vec{e}_\theta$ depend on position! The same holds for the convective operator $(\vec{u}\cdot\nabla)\,\vec{u}$. The full expressions for both cylindrical and spherical coordinates are written out in Appendix D.

Setting all the terms containing $\partial/\partial\theta$ and/or u_z to zero, the Navier-Stokes equation simplifies considerably to

$$\rho\left[\frac{\partial u_\theta}{\partial t} + u_R\frac{\partial u_\theta}{\partial R} + \frac{u_R\,u_\theta}{R}\right] = \mu\left[\frac{\partial^2 u_\theta}{\partial R^2} + \frac{\partial^2 u_\theta}{\partial z^2} + \frac{1}{R}\frac{\partial u_\theta}{\partial R} - \frac{u_\theta}{R^2}\right]$$

where we have replaced the **kinetic viscosity**, ν, with $\mu = \nu\rho$.

Integrating over z and writing

$$\int_{-\infty}^{\infty}\rho\,\mathrm{d}z = \Sigma$$

where Σ is the surface density, as well as neglecting variation of ν, u_R and u_θ with z (a reasonable approximation), the continuity and Navier-Stokes equation become

$$\begin{aligned}\frac{\partial\Sigma}{\partial t} + \frac{1}{R}\frac{\partial}{\partial R}\left(R\,\Sigma\,u_R\right) &= 0\\ \Sigma\left(\frac{\partial u_\theta}{\partial t} + u_R\frac{\partial u_\theta}{\partial R} + \frac{u_R\,u_\theta}{R}\right) &= \mathcal{F}(\mu,R)\end{aligned}$$

where $\mathcal{F}(\mu,R)$ describes the various **viscous terms**.

Next we multiply the continuity equation by Ru_θ which we can then write as

$$\frac{\partial(\Sigma\,R\,u_\theta)}{\partial t} - \Sigma\frac{\partial(Ru_\theta)}{\partial t} + \frac{\partial(\Sigma\,R\,u_R\,u_\theta)}{\partial R} - R\,\Sigma\,u_R\frac{\partial u_\theta}{\partial R} = 0$$

Adding this to R times the Navier-Stokes equation, and rearranging terms, yields

$$\frac{\partial(\Sigma\,R\,u_\theta)}{\partial t} + \frac{\partial(\Sigma\,R\,u_R\,u_\theta)}{\partial R} + \Sigma\,u_R\,u_\theta = \mathcal{G}(\mu,R)$$

where $\mathcal{G}(\mu,R) = R\mathcal{F}(\mu)$. Next we introduce the **angular frequency** $\Omega \equiv u_\theta/R$ which allows us to rewrite the above expression as

$$\boxed{\frac{\partial(\Sigma\,R^2\,\Omega)}{\partial t} + \frac{1}{R}\frac{\partial}{\partial R}\left(\Sigma\,R^3\,\Omega\,u_R\right) = \mathcal{G}(\mu,R)}$$

Note that $\Sigma\, R^2\, \Omega = \Sigma\, R\, u_\theta$ is the *angular momentum per unit surface density*. Hence the above equation describes the evolution of angular momentum in the accretion disk. It is also clear, therefore, that $\mathcal{G}(\mu, R)$ must describe the **viscous torque** on the disk material, per unit surface area. To derive an expression for it, recall that

$$\mathcal{G}(\mu, R) = R \int \mathrm{d}z\, \mu \left[\frac{\partial^2 u_\theta}{\partial R^2} + \frac{1}{R} \frac{\partial u_\theta}{\partial R} - \frac{u_\theta}{R^2} \right]$$

where we have ignored the $\partial^2 u_\theta / \partial z^2$ term which is assumed to be small. Using that $\mu = \nu \rho$ and that μ is independent of R and z (this is an assumption that underlies the Navier-Stokes equation from which we started) we have that

$$\mathcal{G}(\mu, R) = \nu\, R\, \Sigma \left[\frac{\partial^2 u_\theta}{\partial R^2} + \frac{1}{R} \frac{\partial u_\theta}{\partial R} - \frac{u_\theta}{R^2} \right]$$

Next we use that $u_\theta = \Omega\, R$ to write

$$\frac{\partial u_\theta}{\partial R} = \Omega + R \frac{\mathrm{d}\Omega}{\mathrm{d}R}$$

Substituting this in the above expression for $\mathcal{G}(\mu, R)$ yield

$$\mathcal{G}(\mu, R) = \nu\, \Sigma \left[R^2 \frac{\mathrm{d}^2 \Omega}{\mathrm{d}R^2} + 3R \frac{\mathrm{d}\Omega}{\mathrm{d}R} \right] = \frac{1}{R} \frac{\partial}{\partial R} \left(\nu\, \Sigma\, R^3 \frac{\mathrm{d}\Omega}{\mathrm{d}R} \right)$$

Substituting this expression for the viscous torque in the evolution equation for the angular momentum per unit surface density, we finally obtain the full set of equations that govern our thin accretion disk:

$$\frac{\partial}{\partial t} \left(\Sigma\, R^2\, \Omega \right) + \frac{1}{R} \frac{\partial}{\partial R} \left(\Sigma\, R^3\, \Omega\, u_R \right) = \frac{1}{R} \frac{\partial}{\partial R} \left(\nu\, \Sigma\, R^3 \frac{\mathrm{d}\Omega}{\mathrm{d}R} \right)$$

$$\frac{\partial \Sigma}{\partial t} + \frac{1}{R} \frac{\partial}{\partial R} \left(R\, \Sigma\, u_R \right) = 0$$

$$\Omega = \left(\frac{G\, M_\bullet}{R^3} \right)^{1/2}$$

These three equations describe the dynamics of a thin, viscous accretion disk. The third equation indicates that we assume that the fluid is in Keplerian motion around the accreting object of mass $M_\bullet$. As discussed further below, this is a reasonable assumption as long as the accretion disk is thin.

Note that the non-zero u_R results in a **mass inflow rate**

$$\dot{M}(R) = -2\pi\Sigma\, R\, u_R$$

(a positive u_R reflects outwards motion).

Now let us consider a **steady accretion disk**. This implies that $\partial/\partial t = 0$ and that $\dot{M}(R) = \dot{M} \equiv \dot{M}_\bullet$ (the mass flux is constant throughout the disk, otherwise $\partial\Sigma/\partial t \neq 0$). In particular, the continuity equation implies that

$$R\,\Sigma\, u_R = C_1$$

Using the above expression for the mass inflow rate, we see that

$$\boxed{C_1 = -\frac{\dot{M}_\bullet}{2\pi}}$$

Similarly, for the Navier-Stokes equation, we have that

$$\Sigma\, R^3\, \Omega\, u_R - \nu\, \Sigma\, R^3\, \frac{\mathrm{d}\Omega}{\mathrm{d}R} = C_2$$

Using the boundary condition that at the radius of the accreting object, $R_\bullet$, the disk material must be dragged into rigid rotation (a no-slip boundary condition), which implies that $\mathrm{d}\Omega/\mathrm{d}R = 0$ at $R = R_\bullet$, we obtain that

$$\boxed{C_2 = R_\bullet^2\, \Omega_\bullet\, C_1 = -\frac{\dot{M}_\bullet}{2\pi}\, (G\, M_\bullet\, R_\bullet)^{1/2}}$$

Substituting this in the above expression, and using that

$$\frac{\mathrm{d}\Omega}{\mathrm{d}R} = \frac{\mathrm{d}}{\mathrm{d}R}\left(\frac{G\, M_\bullet}{R^3}\right)^{1/2} = -\frac{3}{2}\,\frac{\Omega}{R}$$

we have that

$$\begin{aligned}\nu\,\Sigma &= -\frac{\dot{M}_\bullet}{2\pi}\left[R^2\Omega + (G\,M_\bullet\,R_\bullet)^{1/2}\right]\left(R^3\frac{\mathrm{d}\Omega}{\mathrm{d}R}\right)^{-1} \\ &= +\frac{\dot{M}_\bullet}{3\pi}\left[1-\left(\frac{R_\bullet}{R}\right)^{1/2}\right]\end{aligned}$$

This shows that *the mass inflow rate and kinetic viscosity depend linearly on each other*.

The gravitational energy lost by the inspiraling material is converted into heat. This is done through **viscous dissipation**: viscosity robs the disk material of angular momentum which in turn causes it to spiral in.

We can work out the **rate of viscous dissipation** using

$$\mathcal{V} = \pi_{ij}\,\frac{\partial u_i}{\partial x_j}$$

where we have that the **viscous stress tensor** is

$$\pi_{ij} = \mu\left[\frac{\partial u_i}{\partial x_j} + \frac{\partial u_j}{\partial x_i} - \frac{2}{3}\delta_{ij}\frac{\partial u_k}{\partial x_k}\right]$$

(see Chapter 4). Note that the last term in the above expression vanishes because the fluid is incompressible, such that

$$\mathcal{V} = \mu\left[\left(\frac{\partial u_i}{\partial x_j}\right)^2 + \frac{\partial u_j}{\partial x_i}\,\frac{\partial u_i}{\partial x_j}\right]$$

(remember to apply the Einstein summation convention here!).

In our case, using that $\partial/\partial\theta = \partial/\partial z = 0$ and that $u_z = 0$, the only surviving terms are

$$\mathcal{V} = \mu\left[\left(\frac{\partial u_R}{\partial R}\right)^2 + \left(\frac{\partial u_\theta}{\partial R}\right)^2 + \frac{\partial u_R}{\partial R}\,\frac{\partial u_R}{\partial R}\right] = \mu\left[2\left(\frac{\partial u_R}{\partial R}\right)^2 + \left(\frac{\partial u_\theta}{\partial R}\right)^2\right]$$

If we make the reasonable assumption that $u_R \ll u_\theta$, we can ignore the first term, such that we finally obtain

$$\boxed{\mathcal{V} = \mu \left(\frac{\partial u_\theta}{\partial R}\right)^2 = \mu R^2 \left(\frac{\mathrm{d}\Omega}{\mathrm{d}R}\right)^2}$$

which expresses the viscous dissipation *per unit volume*. Note that $\partial u_\theta/\partial R = \Omega + \mathrm{d}\Omega/\mathrm{d}R$. Hence, even in a solid body rotation ($\mathrm{d}\Omega/\mathrm{d}R = 0$) there is a radial derivative of u_θ. However, when $\mathrm{d}\Omega/\mathrm{d}R = 0$ there is no velocity shear in the disk, which shows that the Ω term cannot contribute to the viscous dissipation rate.

As before, we now proceed by integrating over the z-direction, to obtain

$$\frac{\mathrm{d}E}{\mathrm{d}t} = \int \mu\, R^2 \left(\frac{\mathrm{d}\Omega}{\mathrm{d}R}\right)^2 \mathrm{d}z = \nu\, \Sigma\, R^2 \left(\frac{\mathrm{d}\Omega}{\mathrm{d}R}\right)^2$$

Using our expression for $\nu\Sigma$ derived above, we can rewrite this as

$$\frac{\mathrm{d}E}{\mathrm{d}t} = \frac{\dot{M}_\bullet}{3\pi}\, R^2 \left[1 - \left(\frac{R_\bullet}{R}\right)^{1/2}\right] \left(\frac{\mathrm{d}\Omega}{\mathrm{d}R}\right)^2$$

Using once more that $\mathrm{d}\Omega/\mathrm{d}R = -(3/2)\Omega/R$, and integrating over the entire disk yields the accretion luminosity of a thin accretion disk:

$$\boxed{L_{\rm acc} \equiv 2\pi \int_{R_\bullet}^{\infty} \frac{\mathrm{d}E}{\mathrm{d}t}\, R\, \mathrm{d}R = \frac{G\, M_\bullet\, \dot{M}_\bullet}{2\, R_\bullet}}$$

To put this in perspective, realize that the gravitation energy of mass m at radius $R_\bullet$ is $G\, M_\bullet m/\, R_\bullet$. Thus, $L_{\rm acc}$ is exactly half of the gravitational energy lost due to the inflow. This obviously begs the question where the other half went...The answer is simple; it is stored in kinetic energy at the 'boundary' radius $R_\bullet$ of the accreting flow.

We end our discussion on accretion disks with a few words of caution. First of all, our entire derivation is only valid for a <u>thin</u> accretion disk. In a thin disk, the

pressure in the disk must be small (otherwise it would puff up). This means that the $\partial P/\partial R$ term in the R-component of the Navier-Stokes equation is small compared to $\partial\Phi/\partial R = GM/R^2$. This in turn implies that the gas will indeed be moving on Keplerian orbits, as we have assumed. If the accretion disk is thick, the situation is much more complicated, something that will not be covered in this course.

Finally, let us consider the time scale for accretion. As we have seen above, the energy loss rate per unit surface area is

$$\nu\,\Sigma\,R^2\left(\frac{\mathrm{d}\Omega}{\mathrm{d}R}\right)^2 = \frac{9}{4}\nu\,\frac{G\,M_\bullet}{R^3}$$

We can compare this with the gravitation potential energy of disk material per unit surface area, which is

$$E = \frac{G\,M_\bullet\Sigma}{R}$$

This yields an accretion time scale

$$\boxed{t_{\rm acc} \equiv \frac{E}{\mathrm{d}E/\mathrm{d}t} = \frac{4}{9}\frac{R^2}{\nu} \sim \frac{R^2}{\nu}}$$

Too estimate this time-scale, we first estimate the molecular viscosity. Recall that $\nu \propto \lambda_{\rm mfp} v$ with v a typical velocity of the fluid particles. In virtually all cases encountered in astrophysics, we have that the size of the accretion disk, R, is many, many orders of magnitude larger than $\lambda_{\rm mfp}$. As a consequence, the corresponding $t_{\rm acc}$ easily exceeds the Hubble time!

The conclusion is that **molecular viscosity** is way too small to result in any significant accretion in objects of astrophysical size. Hence, other source of viscosity are required, which is a topic of ongoing discussion in the literature. Probably the most promising candidates are turbulence (in different forms), and the magneto-rotational instability (MRI). Given the uncertainties involved, it is common practive to simply write

$$\nu = \alpha\,\frac{P}{\rho}\,\frac{1}{R}\,\left(\frac{\mathrm{d}\Omega}{\mathrm{d}R}\right)^{-1}$$

where α is a 'free parameter'. A thin accretion disk modelled this way is often called an **alpha-accretion disk**. If you wonder what the origin is of the above expression;

Figure 12: *Image of the central region of NGC 4261 taken with the Hubble Space Telescope. It reveals a* $\sim 100pc$ *scale disk of dust and gas, which happens to be perpendicular to a radio jet that emerges from this galaxy. This is an alledged 'accretion disk' supplying fuel to the central black hole in this galaxy. This image was actually analyzed by the author as part of his thesis.*

it simply comes from assuming that the only non-vanishing off-diagonal term of the stress tensor is taken to be αP (where P is the value along the diagonal of the stress tensor).

CHAPTER 11

Turbulence

Non-linearity: The Navier-Stokes equation is non-linear. This non-linearity arises from the convective (material) derivative term

$$\vec{u} \cdot \nabla \vec{u} = \frac{1}{2} \nabla u^2 - \vec{u} \times \vec{w}$$

which describes the "inertial acceleration" and is ultimately responsible for the origin of the **chaotic character** of many flows and of **turbulence**. Because of this non-linearity, we cannot say whether a solution to the Navier-Stokes equation with nice and smooth initial conditions will remain nice and smooth for all time (at least not in 3D).

Laminar flow: occurs when a fluid flows in parallel layers, without lateral mixing (no cross currents perpendicular to the direction of flow). It is characterized by high momentum diffusion and low momentum convection.

Turbulent flow: is characterized by chaotic and stochastic property changes. This includes low momentum diffusion, high momentum convection, and rapid variation of pressure and velocity in space and time.

The Reynold's number: In order to gauge the importance of viscosity for a fluid, it is useful to compare the ratio of the inertial acceleration $(\vec{u} \cdot \nabla \vec{u})$ to the viscous acceleration $(\nu \left[\nabla^2 \vec{u} + \frac{1}{3} \nabla (\nabla \cdot \vec{u})\right])$. This ratio is called the Reynold's number, $\mathcal{R}$, and can be expressed in terms of the typical velocity scale $U \sim |\vec{u}|$ and length scale $L \sim 1/\nabla$ of the flow, as

$$\boxed{\mathcal{R} = \left| \frac{\vec{u} \cdot \nabla \vec{u}}{\nu \left[\nabla^2 \vec{u} + \frac{1}{3} \nabla (\nabla \cdot \vec{u})\right]} \right| \sim \frac{U^2/L}{\nu U/L^2} = \frac{U\,L}{\nu}}$$

If $\mathcal{R} \gg 1$ then viscosity can be ignored (and one can use the Euler equations to describe the flow). However, if $\mathcal{R} \ll 1$ then viscosity is important.

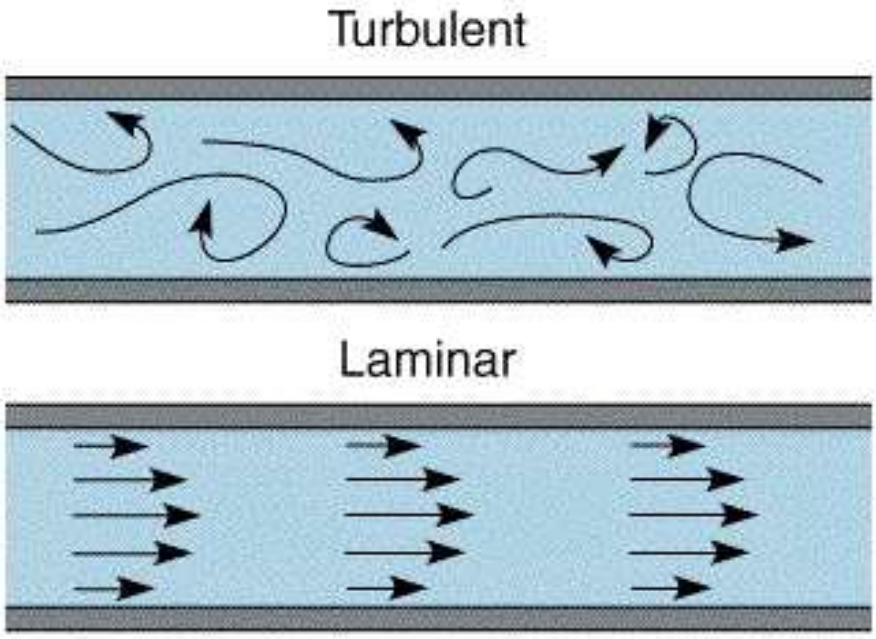

Figure 13: *Illustration of laminar vs. turbulent flow.*

Similarity: Flows with the same Reynold's number are similar. This is evident from rewriting the Navier-Stokes equation in terms of the following dimensionless variables

$$\tilde{u} = \frac{\vec{u}}{U} \qquad \tilde{x} = \frac{\vec{x}}{L} \qquad \tilde{t} = t\,\frac{U}{L} \qquad \tilde{p} = \frac{P}{\rho\,U^2} \qquad \tilde{\Phi} = \frac{\Phi}{U^2} \qquad \tilde{\nabla} = L\,\nabla$$

This yields (after multiplying the Navier-Stokes equation with L/U^2):

$$\boxed{\frac{\partial \tilde{u}}{\partial \tilde{t}} + \tilde{u}\cdot\tilde{\nabla}\tilde{u} + \tilde{\nabla}\tilde{p} + \tilde{\nabla}\tilde{\Phi} = \frac{1}{\mathcal{R}}\left[\tilde{\nabla}^2\tilde{u} + \frac{1}{3}\tilde{\nabla}(\tilde{\nabla}\cdot\tilde{u})\right]}$$

which shows that the form of the solution depends only on $\mathcal{R}$. This principle is extremely powerful as it allows one to making scale models (i.e., when developing airplanes, cars etc). NOTE: the above equation is only correct for an incompressible fluid, i.e., a fluid that obeys $\nabla\rho = 0$. If this is not the case the term $\tilde{P}\,(\nabla\rho/\rho)$ needs to be added at the rhs of the equation, braking its scale-free nature.

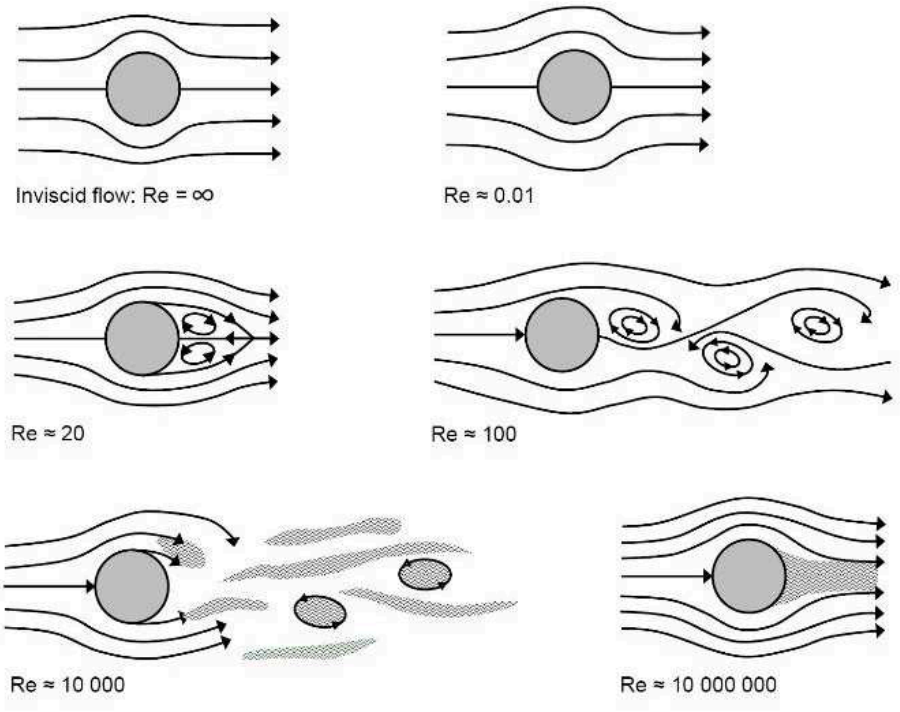

Figure 14: *Illustration of flows at different Reynolds number.*

As a specific example, consider fluid flow past a cylinder of diameter L:

- $\mathcal{R} \ll 1$: "creeping flow". In this regime the flow is viscously dominated and (nearly) symmetric upstream and downstream. The inertial acceleration $(\vec{u} \cdot \nabla \vec{u})$ can be neglected, and the flow is (nearly) time-reversible.
- $\mathcal{R} \sim 1$: Slight asymmetry develops
- $10 \leq \mathcal{R} \leq 41$: Separation occurs, resulting in two counter-rotating votices in the wake of the cylinder. The flow is still steady and laminar, though.
- $41 \leq \mathcal{R} \leq 10^3$: "von Kármán vortex street"; **unsteady laminar flow** with counter-rotating vortices shed periodically from the cylinder. Even at this stage the flow is still 'predictable'.
- $\mathcal{R} > 10^3$: vortices are unstable, resulting in a **turbulent wake** behind the cylinder that is 'unpredictable'.

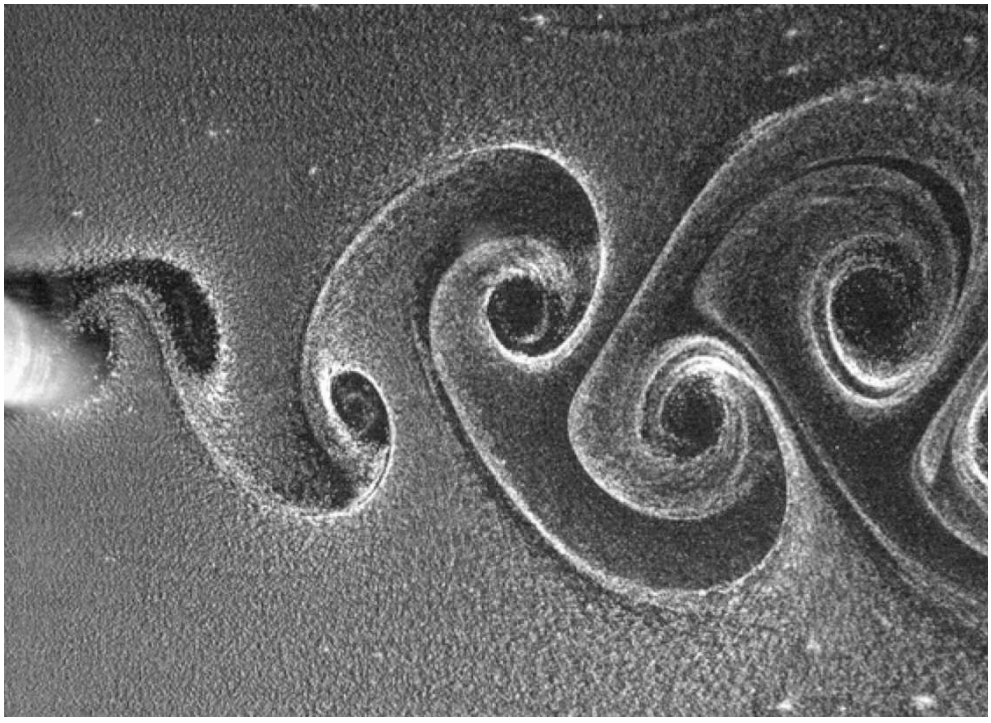

Figure 15: *The image shows the von Kármán Vortex street behind a 6.35 mm diameter circular cylinder in water at Reynolds number of 168. The visualization was done using hydrogen bubble technique.* `Credit:` *Sanjay Kumar & George Laughlin, Department of Engineering, The University of Texas at Brownsville*

The following movie shows a $\mathcal{R} = 250$ flow past a cylinder. Initially one can witness separation, and the creation of two counter-rotating vortices, which then suddenly become 'unstable', resulting in the von Kármán vortex street:

`http://www.youtube.com/watch?v=IDeGDFZSYo8`

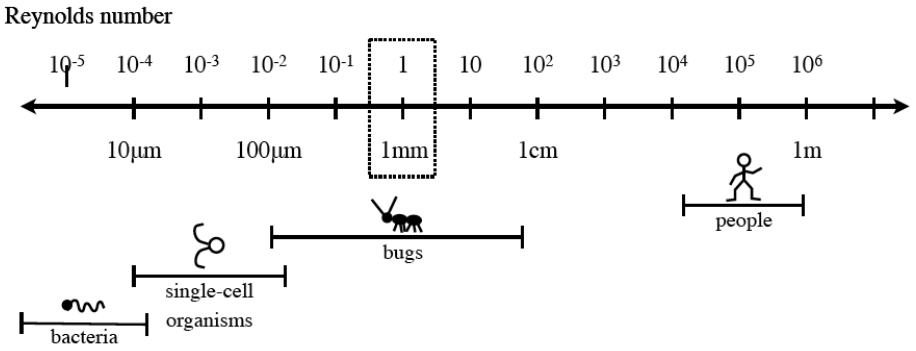

Figure 16: *Typical Reynolds numbers for various biological organisms. Reynolds numbers are estimated using the length scales indicated, the rule-of-thumb in the text, and material properties of water.*

Locomotion at Low-Reynolds number: Low Reynolds number corresponds to high kinetic visocisity *for a given U and L.* In this regime of 'creeping flow' the flow past an object is (nearly) time-reversible. Imagine trying to move (swim) in a highly viscous fluid (take honey as an example). If you try to do so by executing time-symmetric movements, you will not move. Instead, you need to think of a symmetry-breaking solution. Nature has found many solutions for this problem. If we make the simplifying "rule-of-thumb" assumption that an animal of size L meters moves roughly at a speed of $U = L$ meters per second (yes, this is very, very rough, but an ant *does* move close to 1 mm/s, and a human at roughly 1 m/s), then we have that $\mathcal{R} = UL/\nu \simeq L^2/\nu$. Hence, with respect to a fixed substance (say water, for which $\nu \sim 10^{-2}\text{cm}^2/s$), smaller organisms move at lower Reynolds number (effectively in a fluid of higher viscosity). Scaling down from a human to bacteria and single-cell organisms, the motion of the latter in water has $\mathcal{R} \sim 10^{-5} - 10^{-2}$. Understanding the locomotion of these organisms is a fascinating sub-branch of bio-physics.

Boundary Layers: Even when $\mathcal{R} \gg 1$, viscosity always remains important in thin boundary layers adjacent to any solid surface. This boundary layer must exist in order to satisfy the **no-slip boundary condition**. If the Reynolds number exceeds a critical value, the boundary layer becomes turbulent. Turbulent layes and their associated turbulent wakes exert a much bigger drag on moving bodies than their laminar counterparts.

Momentum Diffusion & Reynolds stress: This gives rise to an interesting phenomenon. Consider flow through a pipe. If you increase the viscosity (i.e., decrease $\mathcal{R}$), then it requires a larger force to achieve a certain flow rate (think of how much harder it is to push honey through a pipe compared to water). However, this trend is not monotonic. For sufficiently low viscosity (large $\mathcal{R}$), one finds that the trend reverses, and that is becomes harder again to push the fluid through the pipe. This is a consequence of turbulence, which causes **momentum diffusion** within the flow, which acts very much like viscosity. However, this momentum diffusion is not due to the **viscous stress tensor**, τ_{ij}, but rather to the **Reynolds stress tensor** R_{ij}. To understand the 'origin' of the Reynolds stress tensor,consider the following:

For a turbulent flow, $\vec{u}(t)$, it is advantageous to decompose each component of $\vec{u}$ into a 'mean' component, $\bar{u}_i$, and a 'fluctuating' component, u'_i, according to

$$u_i = \bar{u}_i + u'_i$$

This is knowns as the **Reynolds decomposition**. The 'mean' component can be a time-average, a spatial average, or an ensemble average, depending on the detailed characteristics of the flow. Note that this is reminiscent of how we decomposed the microscopic velocities of the fluid particles in a 'mean' velocity (describing the fluid elements) and a 'random, microscopic' velocity ($\vec{v} = \vec{u} + \vec{w}$).

Substituting this into the Navier-Stokes equation, and taking the average of that, we obtain

$$\frac{\partial \bar{u}_i}{\partial t} + \bar{u}_j \frac{\partial \bar{u}_i}{\partial x_j} = \frac{1}{\rho} \frac{\partial}{\partial x_j} \left[\overline{\tau}_{ij} - \rho \overline{u'_i u'_j} \right]$$

where, for simplicity, we have ignored gravity (the $\nabla\Phi$-term). This equation looks identical to the Navier-Stokes equation (in absence of gravity), except for the $-\rho\overline{u'_i u'_j}$ term, which is what we call the Reynolds stress tensor:

$$R_{ij} = -\rho\overline{u_i' u_j'}$$

Note that $\overline{u_i' u_j'}$ means the same averaging (time, space or ensemble) as above, but now for the product of u_i' and u_j'. Note that $\bar{u_i'} = 0$, by construction. However, the expectation value for the product of u_i' and u_j' is generally not. As is evident from the equation, the **Reynolds stresses** (which reflect momentum diffusion due to turbulence) act in exactly the same way as the **viscous stresses**. However, they are only present when the flow is turbulent.

Note also that the Reynolds stress tensor is related to the **two-point correlation tensor**

$$\xi_{ij}(\vec{r}) \equiv \overline{u_i'(\vec{x}, t)\, u_j'(\vec{x} + \vec{r}, t)}$$

in the sense that $R_{ij} = \xi_{ij}(0)$. At large separations, $\vec{r}$, the fluctuating velocities will be uncorrelated so that $\lim_{r\to\infty} \xi_{ij} = 0$. But on smaller scales the fluctuating velocities will be correlated, and there will be a 'characteristic' scale associated with these correlations, called the **correlation length**.

Turbulence: Turbulence is still considered as one of the last "unsolved problems of classical physics" [Richard Feynman]. What we technically mean by this is that we do not yet know how to calculate $\xi_{ij}(\vec{r})$ (and higher order correlation functions, like the three-point, four-point, etc) in a particular situation from a fundamental theory. Salmon (1998) nicely sums up the challenge of defining **turbulence**:

> Every aspect of turbulence is controversial. Even the definition of fluid turbulence is a subject of disagreement. However, nearly everyone would agree with some elements of the following description:
>
> - Turbulence requires the presence of vorticity; irrotational flow is smooth and steady to the extent that the boundary conditions permit.
> - Turbulent flow has a complex structure, involving a broad range of space and time scales.
> - Turbulent flow fields exhibit a high degree of apparent randomness and disorder. However, close inspection often reveals the presence of embedded cohererent flow structures

- Turbulent flows have a high rate of viscous energy dissipation.
- Advected tracers are rapidly mixed by turbulent flows.

However, one further property of turbulence seems to be more fundamental than all of these because it largely explains why turbulence demands a statistical treatment...turbulence is chaotic.

The following is a brief, qualitative description of turbulence:

Turbulence kicks in at sufficiently high Reynolds number (typically $\mathcal{R} > 10^3 - 10^4$). Turbulent flow is characterized by irregular and seemingly random motion. Large vortices (called **eddies**) are created. These contain a large amount of kinetic energy. Due to **vortex stretching** these eddies are stretched thin until they 'break up' in smaller eddies. This results in a **cascade** in which the turbulent energy is transported from large scales to small scales. This cascade is largely **inviscid**, conserving the total turbulent energy. However, once the length scale of the eddies becomes comparable to the mean free path of the particles, the energy is dissipated; the kinetic energy associated with the eddies is transformed into internal energy. The scale at which this happens is called the **Kolmogorov length scale**. The length scales between the scale of turbulence 'injection' and the Kolomogorov length scale at which it is dissipated is called the **inertial range**. Over this inertial range turbulence is believed/observed to be scale invariant. The ratio between the injection scale, L, and the dissipation scale, l, is proportional to the **Reynolds number** according to $L/l \propto \mathcal{R}^{3/4}$. Hence, two turbulent flows that look similar on large scales (comparable L), will dissipate their energies on different scales, l, if their Reynolds numbers are different.

Molecular clouds: an example of turbulence in astrophysics are molecular clouds. These are gas clouds of masses $10^5 - 10^6 M_\odot$, densities $n_H \sim 100 - 500\,\mathrm{cm}^{-3}$, and temperatures $T \sim 10$K. They consist mainly of molecular hydrogen and are the main sites of **star formation**. Observations show that their velocity linewidths are $\sim 6-10$km/s, which is much higher than their sound speed ($c_\mathrm{s} \sim 0.2$km/s). Hence, they are supported against (gravitational) collapse by **supersonic turbulence**. On small scales, however, the turbulent motions compress the gas to high enough densities that stars can form. A numerical simulation of a molecular cloud with supersonic turbulence is available here:
`http://www.youtube.com/watch?v=3z9ZKAkbMhY`

CHAPTER 12

Sound Waves

If a (compressible) fluid in equilibrium is perturbed, and the perturbation is sufficiently small, the perturbation will propagate through the fluid as a **sound wave** (aka acoustic wave) , which is a mechanical, longitudinal wave (i.e, a displacement in the same direction as that of propagation).

If the perturbation is small, we may assume that the velocity gradients are so small that viscous effects are negligble (i.e., we can set $\nu = 0$). In addition, we assume that the time scale for conductive heat transport is large, so that energy exchange due to conduction can also safely be ignored. In the absence of these dissipative processes, the wave-induced changes in gas properties are **adiabatic**.

Before proceeding, let us examine the **Reynold's number** of a (propagating) sound wave. Using that $\mathcal{R} = U\,L/\nu$, and setting $U = c_{\rm s}$ (the typical velocity involved is the sound speed, to be defined below), $L = \lambda$ (the characteristic scale of the flow is the wavelength of the acoustic wave), we have that $\mathcal{R} = \lambda\, c_{\rm s}/\nu$. Using the expressions for the viscosity $\mu = \nu\rho$ from the constitutive relations in Chapter 5, we see that $\nu \propto \lambda_{\rm mfp}\, c_{\rm s}$. Hence, we have that

$$\mathcal{R} \equiv \frac{U\,L}{\nu} \propto \frac{\lambda}{\lambda_{\rm mfp}}$$

Thus, as long as the wave-length of the acoustic wave is much larger than the mean-free path of the fluid particles, we have that the Reynolds number is large, and thus that viscosity and conduction can be ignored.

Let $(\rho_0, P_0, \vec{u}_0)$ be a **uniform, equilibrium solution** of the Euler fluid equations (i.e., ignore viscosity). Also, in what follows we will ignore gravity (i.e., $\nabla\Phi = 0$).

Uniformity implies that $\nabla\rho_0 = \nabla P_0 = \nabla\vec{u}_0 = 0$. In addition, since the only allowed motion is uniform motion of the entire system, we can always use a Galilean coordinate transformation so that $\vec{u}_0 = 0$, which is what we adopt in what follows.

Substitution into the continuity and momentum equations, one obtains that $\partial\rho_0/\partial t = \partial\vec{u}_0/\partial t = 0$, indicative of an **equilibrium** solution as claimed.

Perturbation Analysis: Consider a small perturbation away from the above equilibrium solution:

$$\begin{aligned} \rho_0 &\rightarrow \rho_0 + \rho_1 \\ P_0 &\rightarrow P_0 + P_1 \\ \vec{u}_0 &\rightarrow \vec{u}_0 + \vec{u}_1 = \vec{u}_1 \end{aligned}$$

where $|\rho_1/\rho_0| \ll 1$, $|P_1/P_0| \ll 1$ and $\vec{u}_1$ is small (compared to the sound speed, to be derived below).

Substitution in the **continuity** and **momentum** equations yields

$$\begin{aligned} \frac{\partial(\rho_0+\rho_1)}{\partial t} + \nabla(\rho_0+\rho_1)\vec{u}_1 &= 0 \\ \frac{\partial\vec{u}_1}{\partial t} + \vec{u}_1\cdot\nabla\vec{u}_1 &= -\frac{\nabla(P_0+P_1)}{(\rho_0+\rho_1)} \end{aligned}$$

which, using that $\nabla\rho_0 = \nabla P_0 = \nabla\vec{u}_0 = 0$ reduces to

$$\begin{aligned} \frac{\partial\rho_1}{\partial t} + \rho_0\nabla\vec{u}_1 + \nabla(\rho_1\vec{u}_1) &= 0 \\ \frac{\partial\vec{u}_1}{\partial t} + \frac{\rho_1}{\rho_0}\frac{\partial\vec{u}_1}{\partial t} + \vec{u}_1\cdot\nabla\vec{u}_1 + \frac{\rho_1}{\rho_0}\,\vec{u}_1\cdot\nabla\vec{u}_1 &= -\frac{\nabla P_1}{\rho_0} \end{aligned}$$

The latter follows from first multiplying the momentum equations with $(\rho_0+\rho_1)/\rho_0$. Note that we don't need to consider the **energy equation**; this is because (i) we have assumed that conduction is negligble, and (ii) the disturbance is adiabatic (meaning $\mathrm{d}Q = 0$, and there is thus no heating or cooling).

Next we **linearize** these equations, which means we use that the perturbed values are all small such that terms that contain products of two or more of these quantities are always negligible compared to those that contain only one such quantity. Hence, the above equations reduce to

$$\begin{aligned} \frac{\partial\rho_1}{\partial t} + \rho_0\nabla\vec{u}_1 &= 0 \\ \frac{\partial\vec{u}_1}{\partial t} + \frac{\nabla P_1}{\rho_0} &= 0 \end{aligned}$$

These equations describe the evolution of perturbations in an **inviscid** and **uniform** fluid. As always, these equations need an additional equation for closure. As mentioned above, we don't need the **energy equation**: instead, we can use that the flow is adiabatic, which implies that $P \propto \rho^\gamma$.

Using Taylor series expansion, we then have that

$$P(\rho_0 + \rho_1) = P(\rho_0) + \left(\frac{\partial P}{\partial \rho}\right)_0 \rho_1 + \mathcal{O}(\rho_1^2)$$

where we have used $(\partial P/\partial \rho)_0$ as shorthand for the partial derivative of $P(\rho)$ at $\rho = \rho_0$. And since the flow is isentropic, we have that the partial derivative is for constant entropy. Using that $P(\rho_0) = P_0$ and $P(\rho_0 + \rho_1) = P_0 + P_1$, we find that, when linearized,

$$P_1 = \left(\frac{\partial P}{\partial \rho}\right)_0 \rho_1$$

Note that $P_1 \neq P(\rho_1)$; rather P_1 is the perturbation in pressure associated with the perturbation ρ_1 in the density.

Substitution in the fluid equations of our perturbed quantities yields

$$\begin{aligned} \frac{\partial \rho_1}{\partial t} + \rho_0 \nabla \vec{u}_1 &= 0 \\ \frac{\partial \vec{u}_1}{\partial t} + \left(\frac{\partial P}{\partial \rho}\right)_0 \frac{\nabla \rho_1}{\rho_0} &= 0 \end{aligned}$$

Taking the partial time derivative of the above **continuity** equation, and using that $\partial \rho_0/\partial t = 0$, gives

$$\frac{\partial^2 \rho_1}{\partial t^2} + \rho_0 \nabla \cdot \frac{\partial \vec{u}_1}{\partial t} = 0$$

Substituting the above **momentum equation**, and realizing that $(\partial P/\partial \rho)_0$ is a constant, then yields

$$\boxed{\frac{\partial^2 \rho_1}{\partial t^2} - \left(\frac{\partial P}{\partial \rho}\right)_0 \nabla^2 \rho_1 = 0}$$

which we recognize as a **wave equation**, whose solution is a **plane wave**:

$$\rho_1 \propto e^{i(\vec{k}\cdot\vec{x} - \omega t)}$$

with $\vec{k}$ the **wavevector**, $k = |\vec{k}| = 2\pi/\lambda$ the **wavenumber**, λ the **wavelength**, $\omega = 2\pi\nu$ the **angular frequency**, and ν the **frequency**.

To gain some insight, consider the 1D case: $\rho_1 \propto e^{i(kx-\omega t)} \propto e^{ik(x-v_{\rm p}t)}$, where we have defined the **phase velocity** $v_{\rm p} \equiv \omega/k$. This is the velocity with which the wave pattern propagates through space. For our perturbation of a compressible fluid, this phase velocity is called the **sound speed**, $c_{\rm s}$. Substituting the solution $\rho_1 \propto e^{i(kx-\omega t)}$ into the wave equation, we see that

$$\boxed{c_{\rm s} = \frac{\omega}{k} = \sqrt{\left(\frac{\partial P}{\partial \rho}\right)_s}}$$

where we have made it explicit that the flow is assumed to be isentropic. Note that the partial derivative is for the unperturbed medium. This sound speed is sometimes called the **adiabatic speed of sound**, to emphasize that it relies on the assumption of an adiabatic perturbation. If the fluid is an ideal gas, then

$$c_{\rm s} = \sqrt{\gamma \frac{k_{\rm B}T}{\mu\, m_{\rm p}}}$$

which shows that the adiabatic sound speed of an ideal fluid increases with temperature.

We can repeat the above derivation by relaxing the assumption of isentropic flow, and assuming instead that (more generally) the flow is **polytropic**. In that case, $P \propto \rho^\Gamma$, with Γ the **polytropic index** (Note: a polytropic EoS is an example of a **barotropic** EoS). The only thing that changes is that now the sound speed becomes

$$c_{\rm s} = \sqrt{\frac{\partial P}{\partial \rho}} = \sqrt{\Gamma \frac{P}{\rho}}$$

which shows that the sound speed is larger for a stiffer EoS (i.e., a larger value of Γ).

Note also that, for our barotropic fluid, the sound speed is independent of ω. This implies that all waves move equally fast; the shape of a wave packet is preserved

as it moves. We say that an ideal (inviscid) fluid with a barotropic EoS is a **non-dispersive medium**.

To gain further insight, let us look once more at the (1D) solution for our perturbation:

$$\rho_1 \propto e^{i(kx-\omega t)} \propto e^{ikx}\, e^{-i\omega t}$$

Recalling **Euler's formula** ($e^{i\theta} = \cos\theta + i\sin\theta$), we see that:

- The e^{ikx} part describes a periodic, spatial oscillation with wavelength $\lambda = 2\pi/k$.
- The $e^{-i\omega t}$ part describes the time evolution:
  - If ω is **real**, then the solution describes a **sound wave** which propagates through space with a sound speed c_s.
  - If ω is **imaginary** then the perturation is either exponentially growing ('unstable') or decaying ('damped') with time.

We will return to this in Chapter 14, when we discuss the **Jeans stability criterion**.

As discussed above, acoustic waves result from disturbances in a compressible fluid. These disturbances may arise from objects being moved through the fluid. However, sound waves can also be sourced by fluid motions themselves. A familiar example is the noise from jet-engines; the noise emenates from the turbulent wake created by engines. In astrophysics, turbulence will also typically create sound waves. In general these sound waves will not have an important impact on the physics. A potential exception is the heating of the ICM by sound waves created by turbulent wakes created by AGN feedback. We now derive the main equation that describes how fluid motion can source sound waves.

In the linear perturbation theory used earlier in this chapter, we neglected the inertial acceleration term $\vec{u}\cdot\nabla\vec{u}$ since it is quadratic in the (assumed small) velocity. When developing a theory in which the sound waves are sourced by fluid, the velocities are not necessarily small, and we cannot neglect the inertial acceleration term. To

proceed, it is advantageous to start from the Euler equation in flux-conservative form (see Chapter 3)

$$\frac{\partial \rho u_i}{\partial t} + \frac{\partial \Pi_{ij}}{\partial x_j} = 0$$

Here Π_{ij} is the **momentum flux density tensor** which, for an inviscid fluid, is given by

$$\Pi_{ij} = P\delta_{ij} + \rho u_i u_j$$

We now set $\rho = \rho_0 + \rho_1$ and $P = P_0 + P_1$, where the subscript '0' indicates the unperturbed equilibrium flow, and '1' refers to the perturbed quantities. Using that, $\partial\rho_0/\partial t = 0$, the continuity equation reduces to

$$\frac{\partial \rho_1}{\partial t} + \frac{\partial \rho u_i}{\partial x_i} = 0$$

In addition, using the fact that we can ignore P_0, since the pressure only enters the Euler equation via its gradient, and $\nabla P_0 = 0$ (i.e., the unperturbed medium is in pressure equilibrium), we can write the momentum flux density tensor as

$$\Pi_{ij} = \rho u_i u_j + P_1\delta_{ij} + c_{\rm s}^2\rho_1\delta_{ij} - c_{\rm s}^2\rho_1\delta_{ij} = c_{\rm s}^2\rho_1\delta_{ij} + Q_{ij}$$

where we have introduced the tensor

$$\boxed{Q_{ij} \equiv \rho u_i u_j + (P_1 - c_{\rm s}^2\rho_1)\delta_{ij}}$$

which describes the departure of Π_{ij} from linear theory. To see this, recall that in linear theory any term that is quadratic in velocity is ignored, and that in linear theory the perturbed pressure and density are related according to $P_1 = c_{\rm s}^2\rho_1$. Hence, in linear theory $Q_{ij} = 0$.

Substituting the above expression for Π_{ij} in the Euler equation in flux-conservative form yields

$$\frac{\partial \rho u_i}{\partial t} + c_{\rm s}^2\frac{\partial \rho_1}{\partial x_i} = -\frac{\partial Q_{ij}}{\partial x_j}$$

Next we take the time-derivative of the continuity equation to obtain

$$\frac{\partial^2 \rho_1}{\partial t^2} + \frac{\partial}{\partial x_i}\left[\frac{\partial \rho u_i}{\partial t}\right] = 0$$

Substituting the Euler equation finally yields the **inhomogeneous wave equation**

$$\boxed{\frac{\partial^2 \rho_1}{\partial t^2} - c_{\rm s}^2 \frac{\partial^2 \rho_1}{\partial x_i^2} = \frac{\partial^2 Q_{ij}}{\partial x_i \partial x_j}}$$

which is known as the **Lighthill equation**, after M.J. Lighthill who first derived it in 1952. It is an example of an **inhomogeneous wave equation**; the term on the rhs is a **source term**, and its presence makes the PDE inhomogeneous.

Inhomogeneous wave equations are well known in Electrodynamics. In particular, introducing the (scalar) electric potential, ϕ, and the (vector) magnetic potential $\vec{A}$, defined from the $\vec{E}$ and $\vec{B}$ fields by

$$\vec{E} = -\nabla\phi - \frac{\partial \vec{A}}{\partial t} \qquad \vec{B} = \nabla \times \vec{A}$$

and adopting the **Lorenz gauge condition**

$$\frac{1}{c^2}\frac{\partial \phi}{\partial t} + \nabla \cdot \vec{A} = 0$$

the four **Maxwell equations** in a vacuum with charge ρ and current $\vec{J}$ reduce to two uncoupled, inhomogeneous wave equations that are symmetric in the potentials:

$$\begin{aligned} \nabla^2 \phi - \frac{1}{c^2}\frac{\partial^2 \phi}{\partial t^2} &= -\frac{\rho}{\varepsilon_0} \\ \nabla^2 \vec{A} - \frac{1}{c^2}\frac{\partial^2 \vec{A}}{\partial t^2} &= -\mu_0 \, \vec{J}. \end{aligned}$$

As discussed in many standard textbooks on electromagnetism, the general solution of the inhomogeneous wave equation

$$\frac{\partial^2 \rho_1}{\partial t^2} - c_{\rm s}^2 \frac{\partial^2 \rho_1}{\partial x_i^2} = \mathcal{G}(\vec{x}, t)$$

is given by

$$\rho_1(\vec{x}, t) = \frac{1}{4\pi c_{\rm s}^2} \int \frac{\mathcal{G}(\vec{x}', t - |\vec{x} - \vec{x}'|/c_{\rm s})}{|\vec{x} - \vec{x}'|} \, {\rm d}V'$$

This represent a superposition of spherical acoustic waves traveling outward from their sources located at $\vec{x}'$.

Thus, we have seen that keeping the higher-order velocity terms yields a source term of acoustic waves, given by

$$\mathcal{G}(\vec{x},t) = \frac{\partial^2}{\partial x_i \partial x_j}\left[\rho u_i u_j + (P_1 - c_{\rm s}^2 \rho_1)\delta_{ij}\right]$$

Note that this is a scalar quantity (Einstein summation). Although this equation gives some insight as to how fluid motion can spawn sound waves, actually solving the Lighthill equation for a turbulent velocity field $\vec{u}(\vec{x},t)$ is obviously horrendously difficult.

We end this chapter by considering the impact of **viscosity** and **conductivity**. As we stated at the beginning of this chapter, these transport mechanisms can be ignored as long as the wavelength of the sound wave is much larger than the mean-free path of the fluid particles. However, in the long run viscosity and conductivity will cause some level of momentum dissipation and energy diffusion, which will cause the sound waves to die out. In fact, for a non-ideal fluid the **momentum flux density tensor** is given by

$$\Pi_{ij} \equiv \rho\langle v_i v_j\rangle = \rho u_i u_j + P\delta_{ij} - \tau_{ij}$$

Hence, the **viscous stress tensor**, τ_{ij}, enters the tensor Q_{ij} that describes the departure of Π_{ij} from linear theory. Hence, viscosity can simply be included in the source (or sink) term of the Lighthill equation. Note that in its derivation we did NOT linearize; we did NOT make the assumptions that $\rho_1 \ll \rho_0$ or $P_1 \ll P_0$. The Lighthill equation is therefore valid *in general* as long as ρ_1 and P_1 are perturbations away from an equilibrium solution with $\partial\rho_0/\partial t = 0$ and $\nabla P_0 = 0$.

CHAPTER 13

Shocks

When discussing sound waves in the previous chapter, we considered small (linear) perturbations. In this Chapter we consider the case in which the perturbations are large (non-linear). Typically, a large disturbance results in an abrupt **discontinuity** in the fluid, called a **shock**. Note: not all discontinuities are shocks, but all shocks are discontinuities.

Consider a **polytropic** EoS:

$$P = P_0 \left(\frac{\rho}{\rho_0}\right)^{\Gamma}$$

The sound speed is given by

$$c_{\rm s} = \left(\frac{\partial P}{\partial \rho}\right)^{1/2} = \sqrt{\Gamma \frac{P}{\rho}} = c_{\rm s,0} \left(\frac{\rho}{\rho_0}\right)^{(\Gamma-1)/2}$$

If $\Gamma = 1$, i.e., the EoS is **isothermal**, then the sound speed is a constant, independent of density of pressure. However, if $\Gamma \neq 1$, then the sound speed varies with the local density. An important example, often encountered in (astro)physics is the **adiabatic** EoS, for which $\Gamma = \gamma$ ($\gamma = 5/3$ for a mono-atomic gas). In that case we have that $c_{\rm s}$ increases with density (and pressure, and temperature).

In our discussion of sound waves (Chapter 13), we used perturbation theory, in which we neglected the $\vec{u}_1 \cdot \nabla \vec{u}_1$ term. However, when the perturbations are not small, this term is no longer negligble, and causes non-linearities to develop. The most important of those, is the fact that the sound speed itself varies with density (as we have seen above). This implies that the wave-form of the acoustic wave changes with time; the wave-crest is moving faster than the wave-trough, causing an overall steepening of the wave-form. This steepening continues until the wave-crest tries to overtake the wave-trough, which is not allowed, giving rise to a shock front.

Mach Number: if v is the flow speed of the fluid, and $c_{\rm s}$ is the sound speed, then

the Mach number of the flow is defined as

$$\boxed{\mathcal{M} = \frac{v}{c_{\rm s}}}$$

Note: *simply accelerating a flow to supersonic speeds does* **not** *necessarily generate a shock*. Shocks only arise when an obstruction in the flow causes a deceleration of fluid moving at supersonic speeds. The reason is that disturbances cannot propagate upstream, so that the flow cannot 'adjust itself' to the obstacle because there is no way of propagating a signal (which always goes at the sound speed) in the upstream direction. Consequently, the flow remains undisturbed until it hits the obstacle, resulting in a discontinuous change in flow properties; a shock.

Structure of a Shock: Fig. 17 shows the structure of a planar shock. The shock has a finite, non-zero width (typically a few mean-free paths of the fluid particles), and separates the 'up-stream', pre-shocked gas, from the 'down-stream', shocked gas.

For reasons that will become clear in what follows, it is useful to split the downstream region in two sub-regions; one in which the fluid is out of thermal equilibrium, with net cooling $\mathcal{L} > 0$, and, further away from the shock, a region where the downstream gas is (once again) in thermal equilibrium (i.e., $\mathcal{L} = 0$). If the transition between these two sub-regions falls well outside the shock (i.e., if $x_3 \gg x_2$) the shock is said to be **adiabatic**. In that case, we can derive a relation between the upstream (pre-shocked) properties (ρ_1, P_1, T_1, u_1) and the downstream (post-shocked) properties (ρ_2, P_2, T_2, u_2); these relations are called the **Rankine-Hugoniot jump conditions**. Linking the properties in region three (ρ_3, P_3, T_3, u_3) to those in the pre-shocked gas is in general not possible, except in the case where $T_3 = T_1$. In this case one may consider the shock to be **isothermal**.

Rankine-Hugoniot jump conditions: We now derive the relations between the up- and down-stream quantities, under the assumption that the shock is adiabatic. Consider a rectangular volume V that encloses part of the shock; it has a thickness $\mathrm{d}x > (x_2 - x_1)$ and is centered in the x-direction on the middle of shock. At fixed x the volume is bounded by an area A. If we ignore variations in ρ and $\vec{u}$ in the y-

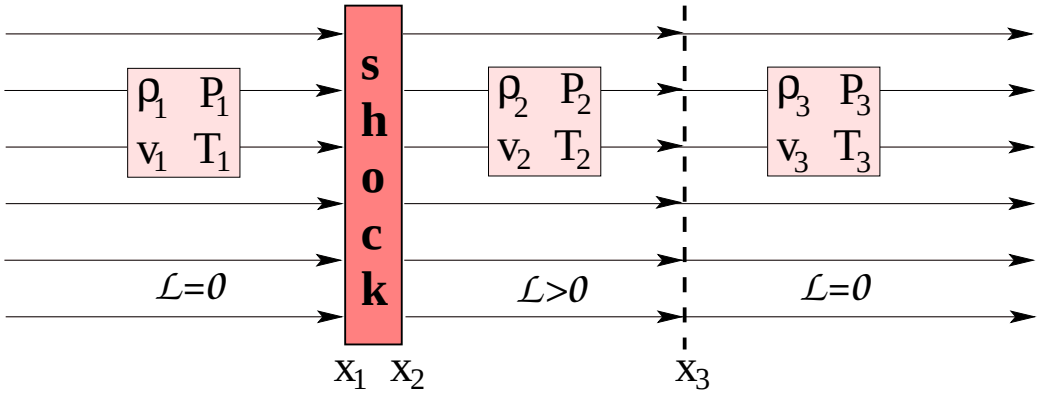

Figure 17: *Structure of a planar shock.*

and z-directions, the **continuity equation** becomes

$$\frac{\partial \rho}{\partial t} + \frac{\partial}{\partial x}(\rho\, u_x) = 0$$

If we integrate this equation over our volume V we obtain

$$\begin{aligned} & \int\int\int \frac{\partial \rho}{\partial t}\,\mathrm{d}x\,\mathrm{d}y\,\mathrm{d}z + \int\int\int \frac{\partial}{\partial x}(\rho u_x)\,\mathrm{d}x\,\mathrm{d}y\,\mathrm{d}z = 0 \\ \Leftrightarrow\quad & \frac{\partial}{\partial t}\int \rho\,\mathrm{d}x\,\mathrm{d}y\,\mathrm{d}z + A\int \frac{\partial}{\partial x}(\rho u_x)\,\mathrm{d}x = 0 \\ \Leftrightarrow\quad & \frac{\partial M}{\partial t} + \int \mathrm{d}(\rho u_x) = 0 \end{aligned}$$

Since there is no mass accumulation in the shock, and mass does not dissapear in the shock, we have that

$$\rho u_x|_{+\mathrm{d}x/2} = \rho u_x|_{-\mathrm{d}x/2}$$

In terms of the upstream (index 1) and downstream (index 2) quantities:

$$\boxed{\rho_1\, u_1 = \rho_2\, u_2}$$

This equation describes **mass conservation** across a shock.

The momentum equation in the x-direction, ignoring viscosity, is given by

$$\frac{\partial}{\partial t}(\rho\, u_x) = -\frac{\partial}{\partial x}(\rho\, u_x\, u_x + P) - \rho\frac{\partial \Phi}{\partial x}$$

Integrating this equation over V and ignoring any gradient in Φ across the shock, we obtain

$$\boxed{\rho_1\, u_1^2 + P_1 = \rho_2\, u_2^2 + P_2}$$

This equation describes how the shock **converts ram pressure into thermal pressure**.

Finally, applying the same to the **energy equation** under the assumption that the shock is adiabatic (i.e., $\mathrm{d}Q/\mathrm{d}t = 0$), one finds that $(E + P)u$ has to be the same on both sides of the shock, i.e.,

$$\left[\frac{1}{2}u^2 + \Phi + \varepsilon + \frac{P}{\rho}\right]\, \rho\, u = \text{constant}$$

We have already seen that $\rho\, u$ is constant. Hence, if we once more ignore gradients in Φ across the shock, we obtain that

$$\boxed{\frac{1}{2}u_1^2 + \varepsilon_1 + P_1/\rho_1 = \frac{1}{2}u_2^2 + \varepsilon_2 + P_2/\rho_2}$$

This equation describes how the shock **converts kinetic energy into enthalpy**. Qualitatively, a shock converts an ordered flow upstream into a disordered (hot) flow downstream.

The three equations in the rectangular boxes are known as the **Rankine-Hugoniot (RH) jump conditions for an adiabatic shock**. Using straightforward but tedious algebra, these RH jump conditions can be written in a more useful form using the **Mach number** $\mathcal{M}_1$ of the upstream gas:

$$\begin{aligned}
\frac{\rho_2}{\rho_1} &= \frac{u_1}{u_2} = \left[\frac{1}{\mathcal{M}_1^2} + \frac{\gamma-1}{\gamma+1}\left(1 - \frac{1}{\mathcal{M}_1^2}\right)\right]^{-1} \\
\frac{P_2}{P_1} &= \frac{2\gamma}{\gamma+1}\,\mathcal{M}_1^2 - \frac{\gamma-1}{\gamma+1} \\
\frac{T_2}{T_1} &= \frac{P_2\,\rho_2}{P_1\,\rho_1} = \frac{\gamma-1}{\gamma+1}\left[\frac{2}{\gamma+1}\left(\gamma\mathcal{M}_1^2 - \frac{1}{\mathcal{M}_1^2}\right) + \frac{4\gamma}{\gamma-1} - \frac{\gamma-1}{\gamma+1}\right]
\end{aligned}$$

Here we have used that for an **ideal gas**

$$P = (\gamma - 1)\,\rho\,\varepsilon = \frac{k_{\rm B}\,T}{\mu\,m_{\rm p}}\,\rho$$

Given that $\mathcal{M}_1 > 1$, we see that $\rho_2 > \rho_1$ (shocks **compress**), $u_2 < u_1$ (shocks **decelerate**), $P_2 > P_1$ (shocks **increase pressure**), and $T_2 > T_1$ (shocks **heat**). The latter may seem surprising, given that the shock is considered to be **adiabatic**: although the process has been adiabatic, in that $\mathrm{d}Q/\mathrm{d}t = 0$, the gas **has** changed its adiabat; its entropy has increased as a consequence of the shock converting kinetic energy into thermal, internal energy. In general, in the presence of **viscosity**, a change that is adiabatic does not imply that the states before and after are simply linked by the relation $P = K\,\rho^{\gamma}$, with K some constant. Shocks are always viscous, which causes K to change across the shock, such that the entropy increases; it is this aspect of the shock that causes **irreversibility**, thus defining an "arrow of time".

Back to the RH jump conditions: in the limit $\mathcal{M}_1 \gg 1$ we have that

$$\rho_2 = \frac{\gamma + 1}{\gamma - 1}\,\rho_1 = 4\,\rho_1$$

where we have used that $\gamma = 5/3$ for a monoatomic gas. Thus, with an **adiabatic shock** you can achieve a maximum compression in density of a factor four! Physically, the reason why there is a maximal compression is that the pressure and temperature of the downstream fluid diverge as $\mathcal{M}_1^2$. This huge increase in downstream pressure inhibits the amount of compression of the downstream gas. However, this is only true under the assumption that the shock is **adiabtic**. The downstream, post-shocked gas is out of thermal equilibrium, and in general will be cooling (i.e., $\mathcal{L} > 0$). At a certain distance past the shock (i.e., when $x = x_3$ in Fig. 15), the fluid will re-establish **thermal equilibrium** (i.e., $\mathcal{L} = 0$). In some special cases, one can obtain the properties of the fluid in the new equilibrium state; one such case is the example of an **isothermal shock**, for which the downstream gas has the same temperature as the upstream gas (i.e., $T_3 = T_1$).

In the case of an **isothermal shock**, the first two **Rankine-Hugoniot jump con-**

ditions are still valid, i.e.,

$$\begin{aligned} \rho_1\, u_1 &= \rho_3\, u_3 \\ \rho_1\, u_1^2 + P_1 &= \rho_3\, u_3^2 + P_3 \end{aligned}$$

However, the third condition, which derives from the energy equation, is no longer valid. After all, in deriving that one we had assumed that the shock was adiabatic. In the case of an isothermal shock we have to replace the third RH jump condition with $T_1 = T_3$. The latter implies that $c_{\rm s}^2 = P_3/\rho_3 = P_1/\rho_1$, and allows us to rewrite the second RH condition as

$$\begin{aligned} & \rho_1(u_1^2 + c_{\rm s}^2) = \rho_3(u_3^2 + c_{\rm s}^2) \\ \Leftrightarrow \quad & u_1^2 - \tfrac{\rho_3}{\rho_1} u_3^2 = \tfrac{\rho_3}{\rho_1} c_{\rm s}^2 - c_{\rm s}^2 \\ \Leftrightarrow \quad & u_1^2 - u_1 u_3 = (\tfrac{u_1}{u_3} - 1)\, c_{\rm s}^2 \\ \Leftrightarrow \quad & u_1 u_3 (u_1 - u_3) = (u_1 - u_3)\, c_{\rm s}^2 \\ \Leftrightarrow \quad & c_{\rm s}^2 = u_1 u_3 \end{aligned}$$

Here the second step follows from using the first RH jump condition. If we now substitute this result back into the first RH jump condition we obtain that

$$\frac{\rho_3}{\rho_1} = \frac{u_1}{u_3} = \left(\frac{u_1}{c_{\rm s}}\right)^2 = \mathcal{M}_1^2$$

Hence, in the case of **isothermal shock** (or an adiabatic shock, but sufficiently far behind the shock in the downstream fluid), we have that there is no restriction to how much compression the shock can achieve; depending on the Mach number of the shock, the compression can be huge.

Figure 18: *An actual example of a supernova blastwave. The red colors show the optical light emitted by the supernova ejecta, while the green colors indicate X-ray emission coming from the hot bubble of gas that has been shock-heated when the blast-wave ran over it.*

Supernova Blastwave: An important example of a shock in astrophysics are supernova blastwaves. When a supernova explodes, it blasts a shell of matter (the 'ejecta') at high (highly supersonic) speed into the surrounding medium. The kinetic energy of this shell material is roughly $E_{\rm SN} = 10^{51}$ erg. This is roughly 100 times larger than the amount of energy emitted in radiation by the supernova explosion (which is what we 'see'). For comparison, the entire Milky Way has a luminosity of $\sim 10^{10}\,{\rm L}_\odot \simeq 4 \times 10^{43}\,{\rm erg} s^{-1}$, which amounts to an energy emitted by stars over an entire year that is of the order of 1.5×10^{51} erg. Hence, the kinetic energy released by a single SN is larger than the energy radiated by stars, by the entire galaxy, in an entire year!
The mass of the ejecta is of the order of 1 Solar mass, which implies (using that $E_{\rm SN} = \frac{1}{2} M_{\rm ej} v_{\rm ej}^2$), that the ejecta have a velocity of $\sim 10,000\,{\rm km\,s^{-1}}$!! Initially, this shell material has a mass that is much larger than the mass of the surroundings swept up by the shock, and to lowest order the shell undergoes free expansion. This phase is therefore called the **free-expansion phase**. As the shock moves out, it engulves more and more interstellar material, which is heated (and compressed) by the shock. Hence, the interior of the shell (=shock) is a super-hot bubble of over-pressurized

gas, which 'pushes' the shock outwards. As more and more material is swept-up, and accelerated outwards, the mass of the shell increases, which causes the velocity of the shell to decelerate. At the early stages, the cooling of the hot bubble is negligble, and the blastwave is said to be in the **adiabatic phase**, also known as the **Sedov-Taylor phase**. At some point, though, the hot bubble starts to cool, radiating awaiting the kinetic energy of the supernova, and lowering the interior pressure up to the point that it no longer pushes the shell outwards. This is called the **radiative phase**. From this point on, the shell expands purely by its inertia, being slowed down by the work it does against the surrounding material. This phase is called the **snow-plow phase**. Ultimately, the velocity of the shell becomes comparable to the sound speed of the surrounding material, after which it continues to move outward as a sound wave, slowly dissipating into the surroundings.

During the adiabatic phase, we can use a simple dimensional analysis to solve for the evolution of the shock radius, $r_{\rm sh}$, with time. Since the only physical parameters that can determine $r_{\rm sh}$ in this adiabatic phase are time, t, the initial energy of the SN explosion, ε_0, and the density of the surrounding medium, ρ_0, we have that

$$r_{\rm sh} = f(t, \varepsilon_0, \rho_0) = A t^{\eta}\, \varepsilon_0^{\alpha}\, \rho_0^{\beta}$$

It is easy to check that there is only one set of values for η, α and β for which the product on the right has the dimensions of length (which is the dimension of $r_{\rm sh}$. This solution has $\eta = 2/5$, $\alpha = 1/5$ and $\beta = -1/5$, such that

$$r_{\rm sh} = A \left(\frac{\varepsilon}{\rho_0}\right)^{1/5} t^{2/5}$$

and thus

$$v_{\rm sh} = \frac{{\rm d}r_{\rm sh}}{{\rm d}t} = \frac{2A}{5} \left(\frac{\varepsilon}{\rho_0}\right)^{1/5} t^{-3/5}$$

which shows that indeed the shock decelerates as it moves outwards.

CHAPTER 14

Fluid Instabilities

In this Chapter we discuss the following instabilities:

- convective instability (Schwarzschild criterion)
- interface instabilities (Rayleigh-Taylor & Kelvin-Helmholtz)
- gravitational instability (Jeans criterion)
- thermal instability (Field criterion)

Convective Instability: In astrophysics we often need to consider fluids heated from "below" (e.g., stars, Earth's atmosphere where Sun heats surface, etc.)[2]. This results in a temperature gradient: hot at the base, colder further "up". Since warmer fluids are more buoyant ('lighter'), they like to be further up than colder ('heavier') fluids. The question we need to address is under what conditions this adverse temperature gradient becomes unstable, developing "overturning" motions known as thermal **convection**.

Consider a blob with density $\rho_{\rm b}$ and pressure $P_{\rm b}$ embedded in an ambient medium of density ρ and pressure P. Suppose the blob is displaced by a small distance δz upward. After the displacement the blob will have conditions $(\rho_{\rm b}^*, P_{\rm b}^*)$ and its new ambient medium is characterized by (ρ', P'), where

$$\rho' = \rho + \frac{{\rm d}\rho}{{\rm d}z}\,\delta z \qquad\qquad P' = P + \frac{{\rm d}P}{{\rm d}z}\,\delta z$$

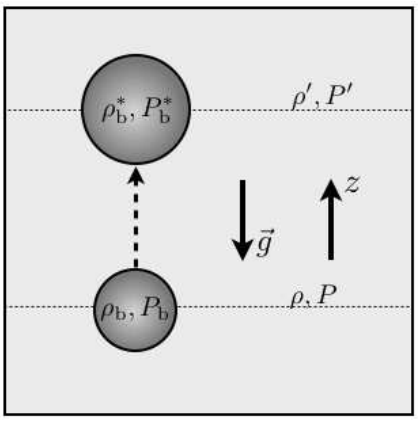

Initially the blob is assumed to be in **mechanical** and **thermal equilibrium** with its ambient medium, so that $\rho_{\rm b} = \rho$ and $P_{\rm b} = P$. After the displacement the blob needs to re-establish a new mechanical and thermal equilibrium. In general, the time scale on which it re-establishes mechanical (pressure) equilibrium is the sound crossing

[2]Here and in what follows, 'up' refers to the direction opposite to that of gravity.

time, $\tau_{\rm s}$, while re-establishing thermal equilibrium
proceeds much slower, on the conduction time, $\tau_{\rm c}$. Given that $\tau_{\rm s} \ll \tau_{\rm c}$ we can assume that $P_{\rm b}^* = P'$, and treat the displacement as **adiabatic**. The latter implies that the process can be described by an adiabatic EoS: $P \propto \rho^\gamma$. Hence, we have that

$$\rho_{\rm b}^* = \rho_{\rm b} \left(\frac{P_{\rm b}^*}{P_{\rm b}}\right)^{1/\gamma} = \rho_{\rm b} \left(\frac{P'}{P}\right)^{1/\gamma} = \rho_{\rm b} \left[1 + \frac{1}{P}\frac{{\rm d}P}{{\rm d}z}\,\delta z\right]^{1/\gamma}$$

In the limit of small displacements δz, we can use Taylor series expansion to show that, to first order,

$$\rho_{\rm b}^* = \rho + \frac{\rho}{\gamma\,P}\,\frac{{\rm d}P}{{\rm d}z}\,\delta z$$

where we have used that initially $\rho_{\rm b} = \rho$, and that the Taylor series expansion, $f(x) \simeq f(0)+f'(0)x+\frac{1}{2}f''(0)x^2+...$, of $f(x) = [1+x]^{1/\gamma}$ is given by $f(x) \simeq 1+\frac{1}{\gamma}x+....$ Suppose we have a stratified medium in which ${\rm d}\rho/{\rm d}z < 0$ and ${\rm d}P/{\rm d}z < 0$. In that case, if $\rho_{\rm b}^* > \rho'$ the blob will be heavier than its surrounding and it will sink back to its original position; the system is stable to convection. If, on the other hand, $\rho_{\rm b}^* < \rho'$ then the displacement has made the blob more buoyant, resulting in **instability**. Hence, using that $\rho' = \rho + ({\rm d}\rho/{\rm d}z)\,\delta z$ we see that stability requires that

$$\frac{{\rm d}\rho}{{\rm d}z} < \frac{\rho}{\gamma\,P}\,\frac{{\rm d}P}{{\rm d}z}$$

This is called the **Schwarzschild criterion for convective stability**.

It is often convenient to rewrite this criterion in a form that contains the temperature. Using that

$$\rho = \rho(P,T) = \frac{\mu\,m_{\rm p}}{k_{\rm B}T}P$$

it is straightforward to show that

$$\frac{{\rm d}\rho}{{\rm d}z} = \frac{\rho}{P}\,\frac{{\rm d}P}{{\rm d}z} - \frac{\rho}{T}\,\frac{{\rm d}T}{{\rm d}z}$$

Substitution in $\rho' = \rho + ({\rm d}\rho/{\rm d}z)\,\delta z$ then yields that

$$\rho_{\rm b}^* - \rho' = \left[-(1-\frac{1}{\gamma})\frac{\rho}{P}\frac{{\rm d}P}{{\rm d}z} + \frac{\rho}{T}\frac{{\rm d}T}{{\rm d}z}\right]\,\delta z$$

Since stability requires that $\rho_{\rm b}^* - \rho' > 0$, and using that $\delta z > 0$, $\mathrm{d}P/\mathrm{d}z < 0$ and $\mathrm{d}T/\mathrm{d}z < 0$ we can rewrite the above Schwarzschild criterion for stability as

$$\left|\frac{\mathrm{d}T}{\mathrm{d}z}\right| < \left(1 - \frac{1}{\gamma}\right) \frac{T}{P} \left|\frac{\mathrm{d}P}{\mathrm{d}z}\right|$$

This shows that if the temperature gradient becomes too large the system becomes convectively unstable: blobs will rise up until they start to loose their thermal energy to the ambient medium, resulting in convective energy transport that tries to "overturn" the hot (high entropy) and cold (low entropy) material. In fact, without any proof we mention that in terms of the **specific entropy**, s, one can also write the Schwarzschild criterion for convective stability as $\mathrm{d}s/\mathrm{d}z > 0$.

To summarize, the **Schwarzschild criterion for convective stability** is given by either of the following three expressions:

$$\left|\frac{\mathrm{d}T}{\mathrm{d}z}\right| < \left(1 - \frac{1}{\gamma}\right) \frac{T}{P} \left|\frac{\mathrm{d}P}{\mathrm{d}z}\right|$$

$$\frac{\mathrm{d}\rho}{\mathrm{d}z} < \frac{\rho}{\gamma\, P} \frac{\mathrm{d}P}{\mathrm{d}z}$$

$$\frac{\mathrm{d}s}{\mathrm{d}z} > 0$$

Rayleigh-Taylor Instability: The Rayleigh-Taylor (RT) instability is an instability of an interface between two fluids of different densities that occurs when one of the fluids is accelerated into the other. Examples include supernova explosions in which expanding core gas is accelerated into denser shell gas and the common terrestrial example of a denser fluid such as water suspended above a lighter fluid such as oil in the Earth's gravitational field.

It is easy to see where the RT instability comes from. Consider a fluid of density ρ_2 sitting on top of a fluid of density $\rho_1 < \rho_2$ in a gravitational field that is pointing in the downward direction. Consider a small perturbation in which the initially horizontal interface takes on a small amplitude, sinusoidal deformation. Since this

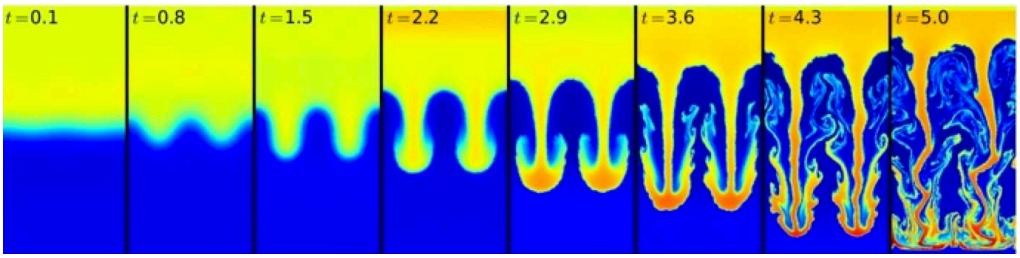

Figure 19: *Example of Rayleigh-Taylor instability in a hydro-dynamical simulation.*

implies moving a certain volume of denser material down, and an equally large volume of the lighter material up, it is immediately clear that the potential energy of this 'perturbed' configuration is lower than that of the initial state, and therefore energetically favorable. Simply put, the initial configuration is unstable to small deformations of the interface.

Stability analysis (i.e., perturbation analysis of the fluid equations) shows that the **dispersion relation** corresponding to the RT instability is given by

$$\omega = \pm i\, k \sqrt{\frac{g}{k}\, \frac{\rho_2 - \rho_1}{\rho_2 + \rho_1}}$$

where g is the gravitational acceleration, and the factor $(\rho_2 - \rho_1)/(\rho_2 + \rho_1)$ is called the **Atwood number**. Since the wavenumber of the perturbation $k > 0$ we see that ω is imaginary, which implies that the perturbations will grow exponentially (i.e., the system is unstable). If $\rho_1 > \rho_2$ though, ω is real, and the system is stable (perturbations to the interface propagate as waves).

Kelvin-Helmholtz Instability: the Kelvin-Helmholtz (KH) instability is an interface instability that arises when two fluids with different densities have a velocity difference across their interface. Similar to the RT instability, the KH instability manifests itself as a small wavy pattern in the interface which develops into turbulence and which causes **mixing**. Examples where KH instability plays a role are wind blowing over water, (astrophysical) jets, the cloud bands on Jupiter (in particular the famous red spot), and clouds of denser gas falling through the hot, low density intra-cluster medium (ICM).

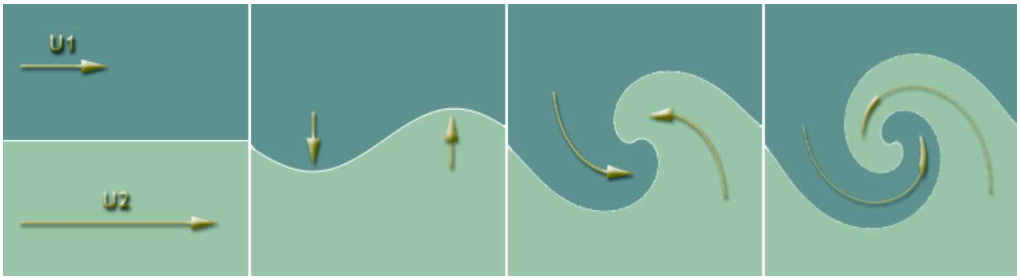

Figure 20: *Illustration of onset of Kelvin-Helmholtz instability*

Stability analysis (i.e., perturbation analysis of the fluid equations) shows that the the **dispersion relation** corresponding to the KH instability is given by

$$\frac{\omega}{k} = \frac{(\rho_1 u_1 + \rho_2 u_2) \pm i\,(u_1 - u_2)\,(\rho_1 \rho_2)^{1/2}}{\rho_1 + \rho_2}$$

Note that this dispersion relation has both real and imaginary parts, given by

$$\frac{\omega_{\rm R}}{k} = \frac{(\rho_1 u_1 + \rho_2 u_2)}{\rho_1 + \rho_2}$$

and

$$\frac{\omega_{\rm I}}{k} = (u_1 - u_2)\,\frac{(\rho_1 \rho_2)^{1/2}}{\rho_1 + \rho_2}$$

Since the imaginary part is non-zero, except for $u_1 = u_2$, we we have that, in principle, *any* velocity difference across an interface is KH unstable. In practice, **surface tension** can stabilize the short wavelength modes so that typically **KH instability** kicks in above some velocity treshold.

As an example, consider a cold cloud of radius $R_{\rm c}$ falling into a cluster of galaxies. The latter contains a hot intra-cluster medium (ICM), and as the cloud moves through this hot ICM, KH instabilities can develop on its surface. If the cloud started out at a large distance from the cluster with zero velocity, than at infall it has a velocity $v \sim v_{\rm esc} \sim c_{\rm s,h}$, where the latter is the sound speed of the hot ICM, assumed to be in hydrostatic equilibrium. Defining the cloud's overdensity $\delta = \rho_{\rm c}/\rho_{\rm h} - 1$, we can write the (imaginary part of the) dispersion relation as

$$\omega = \frac{\rho_{\rm h}\,(\rho_{\rm c}/\rho_{\rm h})^{1/2}}{\rho_{\rm h}[1 + (\rho_{\rm c}/\rho_{\rm h})]}\,c_{\rm s,h}\,k = \frac{(\delta+1)^{1/2}}{\delta+2}\,c_{\rm s,h}\,k$$

The mode that will destroy the cloud has $k \sim 1/R_{\rm c}$, so that the time-scale for cloud destruction is

$$\tau_{\rm KH} \simeq \frac{1}{\omega} \simeq \frac{R_{\rm c}}{c_{\rm s,h}} \frac{\delta+2}{(\delta+1)^{1/2}}$$

Assuming pressure equilibrium between cloud and ICM, and adopting the EoS of an ideal gas, implies that $\rho_{\rm h}\, T_{\rm h} = \rho_{\rm c}\, T_{\rm c}$, so that

$$\frac{c_{\rm s,h}}{c_{\rm s,c}} = \frac{T_{\rm h}^{1/2}}{T_{\rm c}^{1/2}} = \frac{\rho_{\rm c}^{1/2}}{\rho_{\rm h}^{1/2}} = (\delta+1)^{1/2}$$

Hence, one finds that the **Kelvin-Helmholtz time** for cloud destruction is

$$\tau_{\rm KH} \simeq \frac{1}{\omega} \simeq \frac{R_{\rm c}}{c_{\rm s,c}} \frac{\delta+2}{\delta+1}$$

Note that $\tau_{\rm KH} \sim \zeta(R_{\rm c}/c_{\rm s,c}) = \zeta\tau_{\rm s}$, with $\zeta = 1(2)$ for $\delta \gg 1 (\ll 1)$. Hence, the **Kelvin-Helmholtz instability** will typically destroy clouds falling into a hot "atmosphere" on a time scale between one and two **sound crossing times**, $\tau_{\rm s}$, of the cloud. Note, though, that magnetic fields and/or radiative cooling at the interface may stabilize the clouds.

Gravitational Instability: In our discussion of sound waves we used perturbation analysis to derive a dispersion relation $\omega^2 = k^2\, c_{\rm s}^2$. In deriving that equation we ignored gravity by setting $\nabla\Phi = 0$ (see Chapter 12). If you do not ignore gravity, then you add one more perturbed quantity; $\Phi = \Phi_0 + \Phi_1$ and one more equation, namely the **Poisson equation** $\nabla^2\Phi = 4\pi G\rho$.
It is not difficult to show that this results in a modified **dispersion relation**:

$$\boxed{\omega^2 = k^2\, c_{\rm s}^2 - 4\pi G\rho_0 = c_{\rm s}^2\, \left(k^2 - k_{\rm J}^2\right)}$$

where we have introduced the **Jeans wavenumber**

$$k_{\rm J} = \frac{\sqrt{4\pi G\rho_0}}{c_{\rm s}}$$

to which we can also associate a **Jeans length**

$$\boxed{\lambda_{\rm J} \equiv \frac{2\pi}{k_{\rm J}} = \sqrt{\frac{\pi}{G\rho_0}}\, c_{\rm s}}$$

and a **Jeans mass**

$$M_{\rm J} = \frac{4}{3}\pi\rho_0 \left(\frac{\lambda_{\rm J}}{2}\right)^3 = \frac{\pi}{6}\,\rho_0\,\lambda_{\rm J}^3$$

From the dispersion relation one immediately sees that the system is **unstable** (i.e., ω is imaginary) if $k < k_{\rm J}$ (or, equivalently, $\lambda > \lambda_{\rm J}$ or $M > M_{\rm J}$). This is called the **Jeans criterion for gravitational instability**. It expresses when pressure forces (which try to disperse matter) are no longer able to overcome gravity (which tries to make matter collapse), resulting in exponential gravitational collapse on a time scale

$$\boxed{\tau_{\rm ff} = \sqrt{\frac{3\,\pi}{32\,G\,\rho}}}$$

known as the **free-fall time** for gravitational collapse.

The Jeans stability criterion is of utmost importance in astrophysics. It is used to describes the formation of galaxies and large scale structure in an expanding space-time (in this case the growth-rate is not exponential, but only power-law), to describe the formation of stars in molecular clouds within galaxies, and it may even play an important role in the formation of planets in protoplanetary disks.

In deriving the Jeans Stability criterion you will encounter a somewhat puzzling issue. Consider the **Poisson equation** for the unperturbed medium (which has density ρ_0 and gravitational potential Φ_0):

$$\nabla^2\Phi_0 = 4\pi G\rho_0$$

Since the initial, unperturbed medium is supposed to be homogeneous there can be no gravitational force; hence $\nabla\Phi_0 = 0$ everywhere. The above Poisson equation then implies that $\rho_0 = 0$. In other words, an unperturbed, homogeneous density field of non-zero density does not seem to exist. Sir James Jeans 'ignored' this 'nuisance' in his derivation, which has since become known as the **Jeans swindle**. The problem arises because Newtonian physics is not equipped to deal with systems of infinite extent (a requirement for a perfectly homogeneous density distribution). See Kiessling (1999; arXiv:9910247) for a detailed discussion, including an elegant demonstration that the Jeans swindle is actually vindicated!

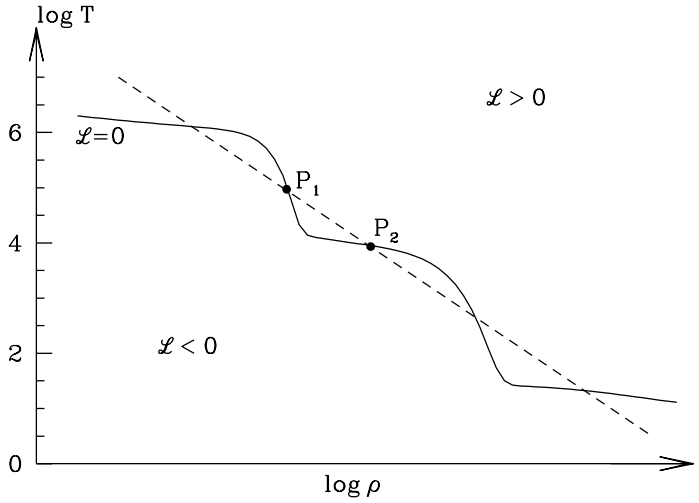

Figure 21: *The locus of thermal equilibrium ($\mathcal{L} = 0$) in the (ρ, T) plane, illustrating the principle of thermal instability. The dashed line indicates a line of constant pressure.*

Thermal Instability: Let $\mathcal{L} = \mathcal{L}(\rho, T) = \mathcal{C} - \mathcal{H}$ be the net cooling rate. If $\mathcal{L} = 0$ the system is said to be in **thermal equilibrium** (TE), while $\mathcal{L} > 0$ and $\mathcal{L} < 0$ correspond to cooling and heating, respectively.

The condition $\mathcal{L}(\rho, T) = 0$ corresponds to a curve in the (ρ, T)-plane with a shape similar to that shown in Fig. 11. It has flat parts at $T \sim 10^6$K, at $T \sim 10^4$K, at $T \sim 10 - 100$K. This can be understood from simple atomic physics (see for example § 8.5.1 of Mo, van den Bosch & White, 2010). Above the TE curve we have that $\mathcal{L} > 0$ (net cooling), while below it $\mathcal{L} < 0$ (net heating). The dotted curve indicates a line of constant pressure ($T \propto \rho^{-1}$). Consider a blob in thermal and mechanical (pressure) equilibrium with its ambient medium, and with a pressure indicated by the dashed line. There are five possible solutions for the density and temperature of the blob, two of which are indicated by P_1 and P_2; here confusingly the P refers to 'point' rather than 'pressure'. Suppose I have a blob located at point P_2. If I heat the blob, displacing it from TE along the constant pressure curve (i.e., the blob is assumed small enough that the sound crossing time, on which the blob re-established mechanical equilibrium, is short). The blob now finds itself in the region where $\mathcal{L} > 0$ (i.e, net cooling), so that it will cool back to its original location on the TE-curve; the blob is **stable**. For similar reasons, it is easy to see that a blob located at point P_1 is **unstable**. This instability is called **thermal instability**, and it explains why the ISM is a **three-phase** medium, with gas of three different temperatures ($T \sim 10^6\,\mathrm{K}, 10^4\,\mathrm{K}$, and $\sim 10 - 100\,\mathrm{K}$) coexisting in pressure equilibrium. Gas at any other temperature but in pressure equilibrium is thermally unstable.

It is easy to see that the requirement for **thermal instability** translates into

$$\left(\frac{\partial \mathcal{L}}{\partial T}\right)_P < 0$$

which is known as the **Field criterion for thermal instability** (after astrophysicist George B. Field).

Fragmentation and Shattering: Consider the Jeans criterion, expressing a balance between gravity and pressure. Using that the **Jeans mass** $M_{\rm J} \propto \rho\, \lambda_{\rm J}^3$ and that $\lambda_{\rm J} \propto \rho^{-1/2}\, c_{\rm s}$, we see that

$$M_{\rm J} \propto \rho^{-1/2}\, T^{3/2}$$

where we have used that $c_{\rm s} \propto T^{1/2}$. Now consider a **polytropic equation of state**, which has $P \propto \rho^{\Gamma}$, with Γ the **polytropic index**. Assuming an ideal gas, such that

$$P = \frac{k_{\rm B}\, T}{\mu\, m_{\rm p}} \rho$$

we thus see that a polytropic ideal gas must have that $T \propto \rho^{\Gamma-1}$. Substituting that in the expression for the Jeans mass, we obtain that

$$M_{\rm J} \propto \rho^{\frac{3}{2}\Gamma-2} = \rho^{\frac{3}{2}(\Gamma-\frac{4}{3})}$$

Thus, we see that for $\Gamma > 4/3$ the Jeans mass will increase with increasing density, while the opposite is true for $\Gamma < 4/3$. Now consider a system that is (initially) larger than the Jeans mass. Since pressure can no longer support it against its own gravity, the system will start to collapse, which increases the density. If $\Gamma < 4/3$, the Jeans mass will becomes smaller as a consequence of the collapse, and now small subregions of the system will find themselves having a mass larger than the Jeans mass $\Rightarrow$ the system will start to **fragment**.

If the collapse is adiabatic (i.e., we can ignore cooling), then $\Gamma = \gamma = 5/3 > 4/3$ and there will be no fragmentation. However, if cooling is very efficient, such that while the cloud collapses it maintains the same temperature, the EoS is now isothermal, which implies that $\Gamma = 1 < 4/3$: the cloud will fragment into smaller collapsing clouds. Fragmentation is believed to underly the formation of star clusters.

A very similar process operates related to the **thermal instability**. In the discussion of the **Field criterion** we had made the assumption *"the blob is assumed small enough that the sound crossing time, on which the blob re-established mechanical equilibrium, is short"*. Here 'short' means compared to the cooling time of the cloud. Let's define the **cooling length** $l_{\rm cool} \equiv c_{\rm s}\tau_{\rm cool}$, where $c_{\rm s}$ is the cloud's sound speed and $\tau_{\rm cool}$ is the cooling time (the time scale on which it radiates away most of its internal energy). The above assumption thus implies that the size of the cloud, $l_{\rm cloud} \ll l_{\rm cool}$. As a consequence, whenever the cloud cools somewhat, it can immediately re-establish pressure equilibrium with its surrounding (i.e., the sound crossing time, $\tau_{\rm s} = l_{\rm cloud}/c_{\rm s}$ is much smaller than the cooling time $\tau_{\rm cool} = l_{\rm cool}/c_{\rm s}$).

Now consider a case in which $l_{\rm cloud} \gg l_{\rm cool}$ (i.e., $\tau_{\rm cool} \ll \tau_{\rm s}$). As the cloud cools, it cannot maintain pressure equilibrium with its surroundings; it takes too long for mechanical equilibrium to be established over the entire cloud. What happens is that smaller subregions, of order the size $l_{\rm cool}$, will fragment. The smaller fragments will be able to maintain pressure equilibrium with their surroundings. But as the small cloudlets cool further, the cooling length $l_{\rm cool}$ shrinks. To see this, realize that when T drops this lowers the sound speed and decreases the cooling time; after all, we are in the regime of thermal instability, so $(\partial\mathcal{L}/\partial T)_P < 0$. As a consequence, $l_{\rm cool} = c_{\rm s}\tau_{\rm cool}$ drops as well. So the small cloudlett soon finds itself larger than the cooling length, and it in turn will fragment. This process of **shattering** continues until the cooling time becomes sufficiently long and the cloudletts are no longer thermally unstable (see McCourt et al., 2018, MNRAS, **473**, 5407 for details).

This process of **shattering** is believed to play an important role in the inter-galactic medium (IGM) in between galaxies, and the circum-galactic medium (CGM) in the halos of galaxies.

CHAPTER 15

Collisionless Dynamics: CBE & Jeans Equations

In this chapter we consider collisionless fluids, such as galaxies and dark matter halos. As discussed in previous chapters, their dynamics is governed by the **Collisionless Boltzmann equation** (CBE)

$$\boxed{\frac{\mathrm{d}f}{\mathrm{d}t} = \frac{\partial f}{\partial t} + v_i \frac{\partial f}{\partial x_i} - \frac{\partial \Phi}{\partial x_i}\frac{\partial f}{\partial v_i} = 0}$$

By taking the velocity moment of the CBE (see Chapter 7), we obtain the **Jeans equations**

$$\boxed{\frac{\partial u_i}{\partial t} + u_i \frac{\partial u_j}{\partial x_i} = -\frac{1}{\rho}\frac{\partial \hat{\sigma}_{ij}}{\partial x_i} - \frac{\partial \Phi}{\partial x_i}}$$

which are the equivalent of the Navier-Stokes equations (or Euler equations), but for a collisionless fluid. The quantity $\hat{\sigma}_{ij}$ in the above expression is the **stress tensor**, defined as

$$\hat{\sigma}_{ij} = \rho \left\langle w_i w_j \right\rangle = \rho \langle v_i v_j \rangle - \rho \langle v_i \rangle \left\langle v_j \right\rangle$$

In this chapter, we write a hat on top of the stress tensor, in order to distinguish it from the **velocity dispersion tensor** given by

$$\boxed{\sigma^2_{ij} = \left\langle v_i v_j \right\rangle - \left\langle v_i \right\rangle \left\langle v_j \right\rangle = \frac{\hat{\sigma}_{ij}}{\rho}}$$

This notation may cause some confusion, but it is adapted here in order to be consistent with the notation in standard textbooks on galactic dynamics. For the same reason, in what follows we will write $\langle v_i \rangle$ in stead of u_i.

As we have discussed in detail in chapters 4 and 5, for a collisional fluid the stress tensor is given by

$$\hat{\sigma}_{ij} = \rho \sigma^2_{ij} = -P\delta_{ij} + \tau_{ij}$$

and therefore completely specified by two scalar quantities; the pressure P and the shear viscosity μ (as always, we ignore bulk viscosity). Both P and μ are related to ρ and T via **constitutive equations**, which allow for closure in the equations.

In the case of a collisionless fluid, though, no consistutive relations exist, and the (symmetric) velocity dispersion tensor has 6 unknowns. As a consequence, the Jeans equations do not form a closed set. Adding higher-order moment equations of the CBE will yield more equations, but this also adds new, higher-order unknowns such as $\langle v_i v_j v_k \rangle$, etc. As a consequence, the set of CBE moment equations never closes!

Note that σ_{ij}^2 is a **local** quantity; $\sigma_{ij}^2 = \sigma_{ij}^2(\vec{x})$. At each point $\vec{x}$ it defines the **velocity ellipsoid**; an ellipsoid whose principal axes are defined by the orthogonal eigenvectors of σ_{ij}^2 with lengths that are proportional to the square roots of the respective eigenvalues.

Since these eigenvalues are typically not the same, a collisionless fluid experiences **anisotropic** pressure-like forces. In order to be able to close the set of Jeans equations, it is common to make certain assumptions about the symmetry of the fluid. For example, a common assumption is that the fluid is **isotropic**, such that the (local) velocity dispersion tensor is specified by a single quantity; the local velocity dispersion σ^2. Note, though, that if with this approach, a solution is found, the solution may not correspond to a physical distribution function (DF) (i.e., in order to be physical, $f \geq 0$ everywhere). Thus, although any real DF obeys the Jeans equations, not every solution to the Jeans equations corresponds to a physical DF!!!

As a worked out example, we now derive the Jeans equations under **cylindrical symmetry**. We therefore write the Jeans equations in the cylindrical coordinate system (R, ϕ, z). The first step is to write the CBE in cylindrical coordinates.

$$\frac{\mathrm{d}f}{\mathrm{d}t} = \frac{\partial f}{\partial t} + \dot{R}\frac{\partial f}{\partial R} + \dot{\phi}\frac{\partial f}{\partial \phi} + \dot{z}\frac{\partial f}{\partial z} + \dot{v}_R\frac{\partial f}{\partial v_R} + \dot{v}_\phi\frac{\partial f}{\partial v_\phi} + \dot{v}_z\frac{\partial f}{\partial v_z}$$

Recall from vector calculus (see Appendices A and D) that

$$\vec{v} = \dot{R}\vec{e}_R + R\dot{\phi}\vec{e}_\phi + \dot{z}\vec{e}_z = v_R\vec{e}_R + v_\phi\vec{e}_\phi + v_z\vec{e}_z$$

from which we obtain the acceleration vector

$$\vec{a} = \frac{\mathrm{d}\vec{v}}{\mathrm{d}t} = \ddot{R}\vec{e}_R + \dot{R}\dot{\vec{e}}_R + \dot{R}\dot{\phi}\vec{e}_\phi + R\ddot{\phi}\vec{e}_\phi + R\dot{\phi}\dot{\vec{e}}_\phi + \ddot{z}\vec{e}_z + \dot{z}\dot{\vec{e}}_z$$

Using that $\dot{\vec{e}}_R = \dot{\phi}\vec{e}_\phi$, $\dot{\vec{e}}_\phi = -\dot{\phi}\vec{e}_R$, and $\dot{\vec{e}}_z = 0$ we have that

$$\vec{a} = \left[\ddot{R} - R\dot{\phi}^2\right]\vec{e}_R + \left[2\dot{R}\dot{\phi} + R\ddot{\phi}\right]\vec{e}_\phi + \ddot{z}\vec{e}_z$$

Next we use that

$$\begin{aligned} v_R = \dot{R} &\Rightarrow \dot{v}_R = \ddot{R} \\ v_\phi = R\dot{\phi} &\Rightarrow \dot{v}_\phi = \dot{R}\dot{\phi} + R\ddot{\phi} \\ v_z = \dot{z} &\Rightarrow \dot{v}_z = \ddot{z} \end{aligned}$$

to write the acceleration vector as

$$\vec{a} = \left[\dot{v}_R - \frac{v_\phi^2}{R}\right]\vec{e}_R + \left[\frac{v_R v_\phi}{R} + \dot{v}_\phi\right]\vec{e}_\phi + \dot{v}_z\,\vec{e}_z$$

Newton's equation of motion in vector form reads

$$\vec{a} = -\nabla\Phi = \frac{\partial\Phi}{\partial R}\,\vec{e}_R + \frac{1}{R}\frac{\partial\Phi}{\partial\phi}\,\vec{e}_\phi + \frac{\partial\Phi}{\partial z}\,\vec{e}_z$$

Combining this with the above we see that

$$\begin{aligned} \dot{v}_R &= -\tfrac{\partial\Phi}{\partial R} + \tfrac{v_\phi^2}{R} \\ \dot{v}_\phi &= -\tfrac{1}{R}\tfrac{\partial\Phi}{\partial R} + \tfrac{v_R v_\phi}{R} \\ \dot{v}_z &= -\tfrac{\partial\Phi}{\partial z} \end{aligned}$$

which allows us to the write the **CBE in cylindrical coordinates** as

$$\boxed{\frac{\partial f}{\partial t} + v_R\frac{\partial f}{\partial R} + \frac{v_\phi}{R}\frac{\partial f}{\partial\phi} + v_z\frac{\partial f}{\partial z} + \left[\frac{v_\phi^2}{R} - \frac{\partial\Phi}{\partial R}\right]\frac{\partial f}{\partial v_R} - \frac{1}{R}\left[v_R v_\phi + \frac{\partial\Phi}{\partial\phi}\right]\frac{\partial f}{\partial v_\phi} - \frac{\partial\Phi}{\partial z}\frac{\partial f}{\partial v_z} = 0}$$

The **Jeans equations** follow from multiplication with v_R, v_ϕ, and v_z and integrating over velocity space. Note that the **cylindrical symmetry** requires that all derivatives with respect to ϕ vanish. The remaining terms are:

$$
\begin{aligned}
\int v_R \frac{\partial f}{\partial t} \mathrm{d}^3\vec{v} &= \frac{\partial}{\partial t}\int v_R f \mathrm{d}^3\vec{v} = \frac{\partial(\rho\langle v_R\rangle)}{\partial t} \\
\int v_R^2 \frac{\partial f}{\partial R} \mathrm{d}^3\vec{v} &= \frac{\partial}{\partial R}\int v_R^2 f \mathrm{d}^3\vec{v} = \frac{\partial(\rho\langle v_R^2\rangle)}{\partial R} \\
\int v_R v_z \frac{\partial f}{\partial z} \mathrm{d}^3\vec{v} &= \frac{\partial}{\partial z}\int v_R v_z f \mathrm{d}^3\vec{v} = \frac{\partial(\rho\langle v_R v_z\rangle)}{\partial z} \\
\int \frac{v_R v_\phi^2}{R} \frac{\partial f}{\partial v_R} \mathrm{d}^3\vec{v} &= \frac{1}{R}\left[\int \frac{\partial(v_R v_\phi^2 f)}{\partial v_R}\mathrm{d}^3\vec{v} - \int \frac{\partial(v_R v_\phi^2)}{\partial v_R} f \mathrm{d}^3\vec{v}\right] = -\rho\frac{\langle v_\phi^2\rangle}{R} \\
\int v_R \frac{\partial\Phi}{\partial R}\frac{\partial f}{\partial v_R} \mathrm{d}^3\vec{v} &= \frac{\partial\Phi}{\partial R}\left[\int \frac{\partial(v_R f)}{\partial v_R}\mathrm{d}^3\vec{v} - \int \frac{\partial v_R}{\partial v_R} f \mathrm{d}^3\vec{v}\right] = -\rho\frac{\partial\Phi}{\partial R} \\
\int \frac{v_R^2 v_\phi}{R} \frac{\partial f}{\partial v_\phi} \mathrm{d}^3\vec{v} &= \frac{1}{R}\left[\int \frac{\partial(v_R^2 v_\phi f)}{\partial v_\phi}\mathrm{d}^3\vec{v} - \int \frac{\partial(v_R^2 v_\phi)}{\partial v_\phi} f \mathrm{d}^3\vec{v}\right] = -\rho\frac{\langle v_R^2\rangle}{R} \\
\int v_R \frac{\partial\Phi}{\partial z}\frac{\partial f}{\partial v_z} \mathrm{d}^3\vec{v} &= \frac{\partial\Phi}{\partial z}\left[\int \frac{\partial(v_R f)}{\partial v_z}\mathrm{d}^3\vec{v} - \int \frac{\partial v_z}{\partial v_R} f \mathrm{d}^3\vec{v}\right] = 0
\end{aligned}
$$

Working out the similar terms for the other Jeans equations we finally obtain the **Jeans Equations in Cylindrical Coordinates**:

$$
\frac{\partial(\rho\langle v_R\rangle)}{\partial t} + \frac{\partial(\rho\langle v_R^2\rangle)}{\partial R} + \frac{\partial(\rho\langle v_R v_z\rangle)}{\partial z} + \rho\left[\frac{\langle v_R^2\rangle - \langle v_\phi^2\rangle}{R} + \frac{\partial\Phi}{\partial R}\right] = 0
$$

$$
\frac{\partial(\rho\langle v_\phi\rangle)}{\partial t} + \frac{\partial(\rho\langle v_R v_\phi\rangle)}{\partial R} + \frac{\partial(\rho\langle v_\phi v_z\rangle)}{\partial z} + 2\rho\frac{\langle v_R v_\phi\rangle}{R} = 0
$$

$$
\frac{\partial(\rho\langle v_z\rangle)}{\partial t} + \frac{\partial(\rho\langle v_R v_z\rangle)}{\partial R} + \frac{\partial(\rho\langle v_z^2\rangle)}{\partial z} + \rho\left[\frac{\langle v_R v_z\rangle}{R} + \frac{\partial\Phi}{\partial z}\right] = 0
$$

These are 3 equations with 9 unknowns, which can only be solved if we make additional assumptions. In particular, one often makes the following assumptions:

1 System is static $\Rightarrow$ the $\frac{\partial}{\partial t}$-terms are zero and $\langle v_R\rangle = \langle v_z\rangle = 0$.

2 Velocity dispersion tensor is diagonal $\Rightarrow \langle v_i v_j\rangle = 0$ (if $i \neq j$).

3 Meridional isotropy $\Rightarrow \langle v_R^2\rangle = \langle v_z^2\rangle = \sigma_R^2 = \sigma_z^2 \equiv \sigma^2$.

Under these assumptions we have 3 unknowns left: $\langle v_\phi \rangle$, $\langle v_\phi^2 \rangle$, and σ^2, and the Jeans equations reduce to

$$\boxed{\begin{array}{l} \dfrac{\partial(\rho\sigma^2)}{\partial R} + \rho\left[\dfrac{\sigma^2 - \langle v_\phi^2 \rangle}{R} + \dfrac{\partial\Phi}{\partial R}\right] = 0 \\ \\ \dfrac{\partial(\rho\sigma^2)}{\partial z} + \rho\dfrac{\partial\Phi}{\partial z} = 0 \end{array}}$$

Since we now only have two equations left, the system is still not closed. If from the surface brightness we can estimate the mass density, $\rho(R,z)$, and hence (using the Poisson equation) the potential $\Phi(R,z)$, we can solve the second of these Jeans equations for the **meridional velocity dispersion**:

$$\sigma^2(R,z) = \frac{1}{\rho}\int_z^\infty \rho\frac{\partial\Phi}{\partial z}\mathrm{d}z$$

and the first Jeans equation then gives the **mean square azimuthal velocity** $\langle v_\phi^2 \rangle = \langle v_\phi \rangle^2 + \sigma_\phi^2$:

$$\langle v_\phi^2 \rangle(R,z) = \sigma^2(R,z) + R\frac{\partial\Phi}{\partial R} + \frac{R}{\rho}\frac{\partial(\rho\sigma^2)}{\partial R}$$

Thus, although $\langle v_\phi^2 \rangle$ is uniquely specified by the Jeans equations, we don't know how it splits in the actual **azimuthal streaming**, $\langle v_\phi \rangle$, and the **azimuthal dispersion**, σ_ϕ^2. Additional assumptions are needed for this.

A similar analysis, but for a spherically symmetric system, using the spherical coordinate system (r, θ, ϕ), gives the following **Jeans equations in Spherical Symmetry**

$$\boxed{\begin{aligned}
&\frac{\partial(\rho\langle v_r\rangle)}{\partial t} + \frac{\partial(\rho\langle v_r^2\rangle)}{\partial r} + \frac{\rho}{r}\left[2\langle v_r^2\rangle - \langle v_\theta^2\rangle - \langle v_\phi^2\rangle\right] + \rho\frac{\partial\Phi}{\partial r} = 0 \\
&\frac{\partial(\rho\langle v_\theta\rangle)}{\partial t} + \frac{\partial(\rho\langle v_r v_\theta\rangle)}{\partial r} + \frac{\rho}{r}\left[3\langle v_r v_\theta\rangle + \left(\langle v_\theta^2\rangle - \langle v_\phi^2\rangle\right)\cot\theta\right] = 0 \\
&\frac{\partial(\rho\langle v_\phi\rangle)}{\partial t} + \frac{\partial(\rho\langle v_r v_\phi\rangle)}{\partial r} + \frac{\rho}{r}\left[3\langle v_r v_\phi\rangle + 2\langle v_\theta v_\phi\rangle\cot\theta\right] = 0
\end{aligned}}$$

If we now make the additional assumptions that the system is **static** and that also the *kinematic* properties of the system are spherically symmetric, then there can be *no streaming motions* and all mixed second-order moments vanish. Consequently, the **velocity dispersion tensor** is diagonal with $\sigma_\theta^2 = \sigma_\phi^2$. Under these assumptions only one of the three Jeans equations remains:

$$\boxed{\frac{\partial(\rho\sigma_r^2)}{\partial r} + \frac{2\rho}{r}\left[\sigma_r^2 - \sigma_\theta^2\right] + \rho\frac{\partial\Phi}{\partial r} = 0}$$

Notice that this single equation still constains two unknown, $\sigma_r^2(r)$ and $\sigma_\theta^2(r)$ (if we assume that the density and potential are known), and can thus not be solved.
It is useful to define the **anisotropy parameter**

$$\boxed{\beta(r) \equiv 1 - \frac{\sigma_\theta^2(r) + \sigma_\phi^2(r)}{2\sigma_r^2(r)} = 1 - \frac{\sigma_\theta^2(r)}{\sigma_r^2(r)}}$$

where the second equality only holds under the assumption that the kinematics are spherically symmetric.

With β thus defined the (spherical) Jeans equation can be written as

$$\frac{1}{\rho}\frac{\partial(\rho\langle v_r^2\rangle)}{\partial r} + 2\frac{\beta\langle v_r^2\rangle}{r} = -\frac{\mathrm{d}\Phi}{\mathrm{d}r}$$

If we now use that $\mathrm{d}\Phi/\mathrm{d}r = GM(r)/r$, we can write the following expression for the

enclosed (dynamical) mass:

$$\boxed{M(r) = -\frac{r\langle v_r^2\rangle}{G}\left[\frac{\mathrm{d}\ln\rho}{\mathrm{d}\ln r} + \frac{\mathrm{d}\ln\langle v_r^2\rangle}{\mathrm{d}\ln r} + 2\beta\right]}$$

Hence, if we know $\rho(r)$, $\langle v_r^2\rangle(r)$, and $\beta(r)$, we can use the **spherical Jeans equation** to infer the mass profile $M(r)$.

Consider an external, spherical galaxy. Observationally, we can measure the projected **surface brightness** profile, $\Sigma(R)$, which is related to the 3D **luminosity density** $\nu(r) = \rho(r)/\Upsilon(r)$

$$\Sigma(R) = 2\int_R^\infty \frac{\nu\, r\, \mathrm{d}r}{\sqrt{r^2 - R^2}}$$

with $\Upsilon(r)$ the **mass-to-light ratio**. Similarly, the **line-of-sight velocity dispersion**, $\sigma_\mathrm{p}^2(R)$, which can be inferred from spectroscopy, is related to both $\langle v_r^2\rangle(r)$ and $\beta(r)$ according to (see Figure 22)

$$\begin{aligned}
\Sigma(R)\sigma_p^2(R) &= 2\int_R^\infty \langle (v_r\cos\alpha - v_\theta\sin\alpha)^2\rangle \frac{\nu\, r\, \mathrm{d}r}{\sqrt{r^2 - R^2}} \\
&= 2\int_R^\infty \left(\langle v_r^2\rangle\cos^2\alpha + \langle v_\theta^2\rangle\sin^2\alpha\right)\frac{\nu\, r\, \mathrm{d}r}{\sqrt{r^2 - R^2}} \\
&= 2\int_R^\infty \left(1 - \beta\frac{R^2}{r^2}\right)\frac{\nu\,\langle v_r^2\rangle\, r\, \mathrm{d}r}{\sqrt{r^2 - R^2}}
\end{aligned}$$

The 3D luminosity density is trivially obtained from the observed $\Sigma(R)$ using the **Abel transform**

$$\nu(r) = -\frac{1}{\pi}\int_r^\infty \frac{\mathrm{d}\Sigma}{\mathrm{d}R}\frac{\mathrm{d}R}{\sqrt{R^2 - r^2}}$$

In general, we have three unknowns: $M(r)$ [or equivalently $\rho(r)$ or $\Upsilon(r)$], $\langle v_r^2\rangle(r)$ and $\beta(r)$. With our two observables $\Sigma(R)$ and $\sigma_\mathrm{p}^2(R)$, these can only be determined if we make additional assumptions.

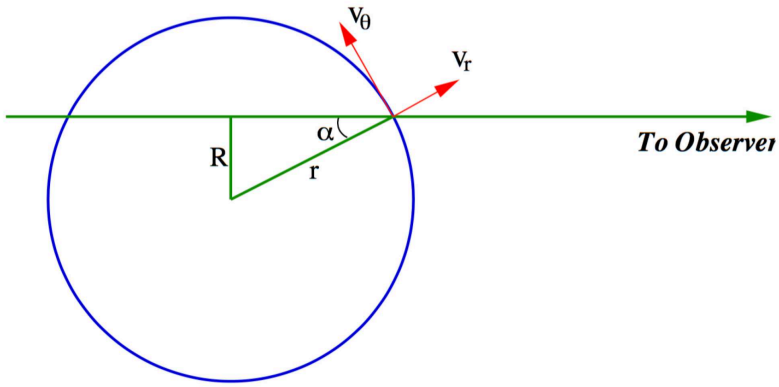

Figure 22: *Geometry related to projection*

EXAMPLE 1: Assume isotropy: $\beta(r) = 0$. In this case we can use the **Abel transform** to obtain

$$\nu(r)\langle v_r^2\rangle(r) = -\frac{1}{\pi}\int_r^\infty \frac{\mathrm{d}(\Sigma\sigma_p^2)}{\mathrm{d}R}\frac{\mathrm{d}R}{\sqrt{R^2-r^2}}$$

and the enclosed mass follows from the Jeans equation

$$M(r) = -\frac{r\langle v_r^2\rangle}{G}\left[\frac{\mathrm{d}\ln\nu}{\mathrm{d}\ln r} + \frac{\mathrm{d}\ln\langle v_r^2\rangle}{\mathrm{d}\ln r}\right]$$

Note that the first term uses the *luminosity* density $\nu(r)$ rather than the *mass* density $\rho(r)$. This is because σ_{p}^2 is weighted by light rather than mass.
The mass-to-light ratio now follows from

$$\Upsilon(r) = \frac{M(r)}{4\pi\int_0^r \nu(r)\, r^2\,\mathrm{d}r}$$

which can be used to constrain the mass of a potential dark matter halo or central supermassive black hole (but always under assumption that the system is isotropic).

EXAMPLE 2: Assume a constant mass-to-light ratio: $\Upsilon(r) = \Upsilon_0$. In this case the luminosity density $\nu(r)$ immediately yields the enclosed mass:

$$M(r) = 4\pi\Upsilon_0\int_0^r \nu(r)\, r^2\,\mathrm{d}r$$

We can now use the **spherical Jeans Equation** to write $\beta(r)$ in terms of $M(r)$, $\nu(r)$ and $\langle v_r^2 \rangle(r)$. Substituting this in the equation for $\Sigma(R)\sigma_p^2(R)$ yields a solution for $\langle v_r^2 \rangle(r)$, and thus for $\beta(r)$. As long as $\beta(r) \leq 1$ the model is said to be **self-consistent** within the context of the Jeans equations.

Almost always, radically different models (based on radically different assumptions) can be constructed, that are all consistent with the data and the Jeans equations. This is often referred to as the **mass-anisotropy degeneracy**. Note, however, that none of these models need to be physical: they can still have $f < 0$.

Integrals of Motion: An integral of motion is a function $I(\vec{x}, \vec{v})$ of the phase-space coordinates that is constant along all orbits, i.e.,

$$I[\vec{x}(t_1), \vec{v}(t_1)] = I[\vec{x}(t_2), \vec{v}(t_2)]$$

for any t_1 and t_2. The value of the integral of motion can be the same for different orbits. Note that an integral of motion can not depend on time. Orbits can have from zero to five integrals of motion. If the Hamiltonian does not depend on time, then energy is always an integral of motion.

Integrals of motion come in two kinds:

- **Isolating Integrals of Motion:** these reduce the dimensionality of the particle's trajectory in 6-dimensional phase-space by one. Therefore, an orbit with n isolating integrals of motion is restricted to a $6 - n$ dimensional manifold in 6-dimensional phase-space. Energy is always an isolating integral of motion.
- **Non-Isolating Integrals of Motion:** these are integrals of motion that do *not* reduce the dimensionality of the particle's trajectory in phase-space. They are of essentially no practical value for the dynamics of the system.

Orbits: If in a system with n degrees of freedom a particular orbit admits n independent isolating integrals of motion, the orbit is said to be **regular**, and its corresponding trajectory $\Gamma(t)$ is confined to a $2n - n = n$ dimensional manifold in phase-space. Topologically this manifold is called an **invariant torus** (or torus for short), and is uniquely specified by the n isolating integrals. A regular orbit has n fundamental frequencies, ω_i, with which it circulates or librates in its n-dimensional manifold. If two or more of these frequencies are commensurable (i.e., $l\omega_i + m\omega_j = 0$

with l and m integers), then the orbit is a **resonant orbit**, and has a dimensionality that is one lower than that of the non-resonant regular orbits (i.e., $l\omega_i + m\omega_j$ is an extra isolating integral of motion). Orbits with fewer than n isolating integrals of motion are called **irregular** or **stochastic**.

Every spherical potential admits at least four isolating integrals of motion, namely energy, E, and the three components of the angular momentum vector $\vec{L}$. Orbits in a flattened, axisymmetric potential frequently (but not always) admit three isolating integrals of motion: E, L_z (where the z-axis is the system's symmetry axis), and a **non-classical** third integral I_3 (the integral is called non-classical since there is no analytical expression of I_3 as function of the phase-space variables).

Since an integral of motion, $I(\vec{x}, \vec{v})$ is constant along an orbit, we have that

$$\frac{\mathrm{d}I}{\mathrm{d}t} = \frac{\partial I}{\partial x_i}\frac{\mathrm{d}x_i}{\mathrm{d}t} + \frac{\partial I}{\partial v_i}\frac{\mathrm{d}v_i}{\mathrm{d}t} = \vec{v}\cdot\nabla I - \nabla\Phi\cdot\frac{\partial I}{\partial \vec{v}} = 0$$

Compare this to the **CBE** for a steady-state (static) system:

$$\vec{v}\cdot\nabla f - \nabla\Phi\cdot\frac{\partial f}{\partial \vec{v}} = 0$$

Thus the condition for I to be an **integral of motion** is identical with the condition for I to be a **steady-state solution of the CBE**. This implies the following:

Jeans Theorem: *Any steady-state solution of the CBE depends on the phase-space coordinates only through integrals of motion. Any function of these integrals is a steady-state solution of the CBE.*

Strong Jeans Theorem: *The DF of a steady-state system in which almost all orbits are regular can be written as a function of the independent isolating integrals of motion.*

Hence, the DF of any steady-state spherical system can be expressed as $f = f(E, \vec{L})$. If the system is spherically symmetric in *all* its properties, then $f = f(E, L^2)$, i.e., the DF can only depend on the magnitude of the angular momentum vector, not on its direction.

An even simpler case to consider is the one in which $f = f(E)$: Since $E = \Phi(\vec{r}) + \frac{1}{2}[v_r^2 + v_\theta^2 + v_\phi^2]$ we have that

$$\begin{aligned}
\langle v_r^2 \rangle &= \frac{1}{\rho} \int \mathrm{d}v_r \mathrm{d}v_\theta \mathrm{d}v_\phi \, v_r^2 \, f \left(\Phi + \frac{1}{2}[v_r^2 + v_\theta^2 + v_\phi^2] \right) \\
\langle v_\theta^2 \rangle &= \frac{1}{\rho} \int \mathrm{d}v_r \mathrm{d}v_\theta \mathrm{d}v_\phi \, v_\theta^2 \, f \left(\Phi + \frac{1}{2}[v_r^2 + v_\theta^2 + v_\phi^2] \right) \\
\langle v_\phi^2 \rangle &= \frac{1}{\rho} \int \mathrm{d}v_r \mathrm{d}v_\theta \mathrm{d}v_\phi \, v_\phi^2 \, f \left(\Phi + \frac{1}{2}[v_r^2 + v_\theta^2 + v_\phi^2] \right)
\end{aligned}$$

Since these equations differ only in the labelling of one of the variables of integration, it is immediately evident that $\langle v_r^2 \rangle = \langle v_\theta^2 \rangle = \langle v_\phi^2 \rangle$. Hence, assuming that $f = f(E)$ is identical to assuming that the system is **isotropic** (and thus $\beta(r) = 0$). And since

$$\langle v_i \rangle = \frac{1}{\rho} \int \mathrm{d}v_r \mathrm{d}v_\theta \mathrm{d}v_\phi \, v_i \, f \left(\Phi + \frac{1}{2}[v_r^2 + v_\theta^2 + v_\phi^2] \right)$$

it is also immediately evident that $\langle v_r \rangle = \langle v_\theta \rangle = \langle v_\phi \rangle = 0$. Thus, a system with $f = f(E)$ has no net sense of rotation.

The more general $f(E, L^2)$ models typically are **anisotropic**. Models with $0 < \beta \leq 1$ are radially anisotropic. In the extreme case of $\beta = 1$ all orbits are purely radial and $f = g(E)\,\delta(L)$, with $g(E)$ some function of energy. Tangentially anisotropic models have $\beta < 0$, with $\beta = -\infty$ corresponding to a model in which all orbits are circular. In that case $f = g(E)\,\delta[L - L_{\max}(E)]$, where $L_{\max}(E)$ is the maximum angular momentum for energy E. Another special case is the one in which $\beta(r) = \beta$ is constant; such models have $f = g(E)\,L^{-2\beta}$.

Next we consider **axisymmetric** systems. If we only consider systems for which most orbits are regular, then the **strong Jeans Theorem** states that, in the most general case, $f = f(E, L_z, I_3)$. For a static, axisymmetric system

$$\langle v_R \rangle = \langle v_z \rangle = 0 \qquad \langle v_R v_\phi \rangle = \langle v_z v_\phi \rangle = 0$$

but note that, in this general case, $\langle v_R v_z \rangle \neq 0$; Hence, in general, in a three-integral model with $f = f(E, L_z, I_3)$ the **velocity ellipsoid** is not aligned with (R, ϕ, z), and the velocity dispersion tensor contains four unknowns: $\langle v_R^2 \rangle$, $\langle v_\phi^2 \rangle$, $\langle v_z^2 \rangle$, and $\langle v_R v_z \rangle$. In this case there are two non-trivial Jeans Equations:

$$\boxed{\begin{aligned}&\frac{\partial(\rho\langle v_R^2\rangle)}{\partial R}+\frac{\partial(\rho\langle v_R v_z\rangle)}{\partial z}+\rho\left[\frac{\langle v_R^2\rangle-\langle v_\phi^2\rangle}{R}+\frac{\partial\Phi}{\partial R}\right]=0\\&\frac{\partial(\rho\langle v_R v_z\rangle)}{\partial R}+\frac{\partial(\rho\langle v_z^2\rangle)}{\partial z}+\rho\left[\frac{\langle v_R v_z\rangle}{R}+\frac{\partial\Phi}{\partial z}\right]=0\end{aligned}}$$

which clearly doesn't suffice to solve for the four unknowns (modelling three-integral axisymmetric systems is best done using the Schwarzschild orbit superposition technique). To make progress with Jeans modeling, one has to make additional assumptions. A typical assumption is that the DF has the **two-integral form** $f = f(E, L_z)$.

In that case, $\langle v_R v_z\rangle = 0$ [velocity ellipsoid now *is* aligned with (R, ϕ, z)] and $\langle v_R^2\rangle = \langle v_z^2\rangle$ (see Binney & Tremaine 2008), so that the **Jeans equations** reduce to

$$\boxed{\begin{aligned}&\frac{\partial(\rho\langle v_R^2\rangle)}{\partial R}+\rho\left[\frac{\langle v_R^2\rangle-\langle v_\phi^2\rangle}{R}+\frac{\partial\Phi}{\partial R}\right]=0\\&\frac{\partial(\rho\langle v_z^2\rangle)}{\partial z}+\rho\frac{\partial\Phi}{\partial z}=0\end{aligned}}$$

which is a closed set for the two unknowns $\langle v_R^2\rangle$ $(= \langle v_z^2\rangle)$ and $\langle v_\phi^2\rangle$. Note, however, that the Jeans equations provide no information about how $\langle v_\phi^2\rangle$ splits in streaming and random motions. In practice one often writes that

$$\langle v_\phi\rangle = k\left[\langle v_\phi^2\rangle - \langle v_R^2\rangle\right]$$

with k a free parameter. When $k = 1$ the azimuthal dispersion is $\sigma_\phi^2 \equiv \langle v_\phi^2\rangle - \langle v_\phi\rangle^2 = \sigma_R^2 = \sigma_z^2$ everywhere. Such models are called **oblate isotropic rotators**.

The final topics to be briefly discussed in this chapter are the **Virial Theorem** and the **negative heat capacity** of gravitational systems.

Consider a gravitational system consisting of N particles (e.g., stars, fluid elements). The **total energy** of the system is $E = K + W$, where

$$\textbf{Total Kinetic Energy:} \quad K = \sum_{i=1}^{N} \tfrac{1}{2}\, m_i\, v_i^2$$

$$\textbf{Total Potential Energy:} \quad W = -\tfrac{1}{2} \sum_{i=1}^{N} \sum_{j \neq i} \tfrac{G\, m_i m_j}{|\vec{r}_i - \vec{r}_j|}$$

The latter follows from the fact that **gravitational binding energy** between a pair of masses is proportional to the product of their masses, and inversely proportional to their separation. The factor $1/2$ corrects for double counting the number of pairs.

Potential Energy in Continuum Limit: To infer an expression for the gravitational potential energy in the continuum limit, it is useful to rewrite the above expression as

$$W = \frac{1}{2} \sum_{i=1}^{N} m_i\, \Phi_i$$

where

$$\Phi_i = -\sum_{j \neq i} \frac{G\, m_j}{r_{ij}}$$

where $r_{ij} = |\vec{r}_i - \vec{r}_j|$. In the continuum limit this simply becomes

$$W = \frac{1}{2} \int \rho(\vec{x})\, \Phi(\vec{x})\, \mathrm{d}^3\vec{x}$$

One can show (see e.g., Binney & Tremaine 2008) that this is equal to the trace of the **Chandrasekhar Potential Energy Tensor**

$$W_{ij} \equiv -\int \rho(\vec{x})\, x_i\, \frac{\partial \Phi}{\partial x_j}\, \mathrm{d}^3\vec{x}$$

In particular,

$$W = \mathrm{Tr}(W_{ij}) = \sum_{i=1}^{3} W_{ii} = -\int \rho(\vec{x})\, \vec{x} \cdot \nabla\Phi \, \mathrm{d}^3\vec{x}$$

which is another, equally valid, expression for the gravitational potential energy in the continuum limit.

Virial Theorem: A stationary, gravitational system obeys

$$\boxed{2K + W = 0}$$

Actually, the correct virial equation is $2K + W + \Sigma = 0$*, where* Σ *is the surface pressure. In many, but certainly not all, applications in astrophysics this term can be ignored. Many textbooks don't even mention the surface pressure term.*

Combining the **virial equation** with the expression for the total energy, $E = K + W$, we see that for a system that obeys the virial theorem

$$\boxed{E = -K = W/2}$$

Example: Consider a cluster consisting of N galaxies. If the cluster is in virial equilibrium then

$$2\sum_{i=1}^{N} \frac{1}{2} m\, v_i^2 - \frac{1}{2}\sum_{i=1}^{N}\sum_{j\neq i} \frac{G\, m_i m_j}{r_{ij}} = 0$$

If we assume, for simplicity, that all galaxies have equal mass then we can rewrite this as

$$N\, m\, \frac{1}{N}\sum_{i=1}^{N} v_i^2 - \frac{G\,(Nm)^2}{2}\, \frac{1}{N^2}\sum_{i=1}^{N}\sum_{j\neq i} \frac{1}{r_{ij}} = 0$$

Using that $M = N\, m$ and $N(N-1) \simeq N^2$ for large N, this yields

$$M = \frac{2\,\langle v^2 \rangle}{G\,\langle 1/r \rangle}$$

with

$$\langle 1/r \rangle = \frac{1}{N(N-1)} \sum_{i=1}^{N} \sum_{j \neq i} \frac{1}{r_{ij}}$$

It is useful to define the **gravitational radius** $r_{\rm g}$ such that

$$W = -\frac{G\,M^2}{r_{\rm g}}$$

Using the relations above, it is clear that $r_{\rm g} = 2/\langle 1/r \rangle$. We can now rewrite the above equation for M in the form

$$M = \frac{r_{\rm g} \langle v^2 \rangle}{G}$$

Hence, one can infer the mass of our cluster of galaxies from its velocity dispersion and its gravitation radius. In general, though, neither of these is observable, and one uses instead

$$M = \alpha \frac{R_{\rm eff} \langle v_{\rm los}^2 \rangle}{G}$$

where $v_{\rm los}$ is the line-of-sight velocity, $R_{\rm eff}$ is some measure for the 'effective' radius of the system in question, and α is a parameter of order unity that depends on the radial distribution of the galaxies. Note that, under the assumption of **isotropy**, $\langle v_{\rm los}^2 \rangle = \langle v^2 \rangle / 3$ and one can also infer the mean reciprocal pair separation from the projected pair separations; in other words under the assumption of isotropy one can infer α, and thus use the above equation to compute the total, gravitational mass of the cluster. This method was applied by **Fritz Zwicky** in 1933, who inferred that the total dynamical mass in the Coma cluster is much larger than the sum of the masses of its galaxies. This was the first observational evidence for **dark matter**, although it took the astronomical community until the late 70's to generally accept this notion.

For a self-gravitating fluid

$$K = \sum_{i=1}^{N} \frac{1}{2} m_i v_i^2 = \frac{1}{2} N m \langle v^2 \rangle = \frac{3}{2} N k_{\rm B} T$$

where the last step follows from the kinetic theory of ideal gases of monoatomic particles. In fact, we can use the above equation for *any* fluid (including a collisionless one), if we interpret T as an **effective** temperature that measures the rms velocity of the constituent particles. If the system is in virial equilibrium, then

$$E = -K = -\frac{3}{2} N k_{\rm B} T$$

which, as we show next, has some important implications...

Heat Capacity: the amount of heat required to increase the temperature by one degree Kelvin (or Celsius). For a self-gravitating fluid this is

$$C \equiv \frac{{\rm d}E}{{\rm d}T} = -\frac{3}{2} N k_{\rm B}$$

which is negative! This implies that **by losing energy, a gravitational system gets hotter**!! This is a very counter-intuitive result, that often leads to confusion and wrong expectations. Below we give three examples of implications of the **negative heat capacity** of gravitating systems,

Example 1: Drag on satellites Consider a satellite orbiting Earth. When it experiences friction against the (outer) atmosphere, it loses energy. This causes the system to become more strongly bound, and the orbital radius to shrink. Consequently, the energy loss results in the gravitational potential energy, W, becoming more negative. In order for the satellite to re-establish virial equilibrium ($2K + W = 0$), its kinetic energy needs to **increase**. Hence, contrary to common intuition, *friction causes the satellite to speed up*, as it moves to a lower orbit (where the circular velocity is higher).

Example 2: Stellar Evolution A star is a gaseous, self-gravitating sphere that radiates energy from its surface at a luminosity L. Unless this energy is replenished (i.e., via some energy production mechanism in the star's interior), the star will react by shrinking (i.e., the energy loss implies an increase in binding energy, and thus a

potential energy that becomes more negative). In order for the star to remain in virial equilibrium its kinetic energy, which is proportional to temperature, has to increase; *the star's energy loss results in an increase of its temperature.*

In the Sun, hydrogen burning produces energy that replenishes the energy loss from the surface. As a consequence, the system is in equilibrium, and will not contract. However, once the Sun has used up all its hydrogren, it will start to contract and heat up, because of the **negative heat capacity**. This continues until the temperature in the core becomes sufficiently high that helium can start to fuse into heavier elements, and the Sun settles in a new equilibrium.

Example 3: Core Collapse *a system with negative heat capacity in contact with a heat bath is thermodynamically unstable.* Consider a self-gravitating fluid of 'temperature' T_1, which is in contact with a heat bath of temperature T_2. Suppose the system is in thermal equilibrium, so that $T_1 = T_2$. If, due to some small disturbance, a small amount of heat is tranferred from the system to the heat bath, the negative heat capacity implies that this results in $T_1 > T_2$. Since heat always flows from hot to cold, more heat will now flow from the system to the heat bath, further increasing the temperature difference, and T_1 will continue to rise without limit. This run-away instability is called the **gravothermal catastrophe**. An example of this instability is the **core collapse of globular clusters:** Suppose the formation of a gravitational system results in the system having a declining velocity dispersion profile, $\sigma^2(r)$ (i.e., σ decreases with increasing radius). This implies that the central region is (dynamically) hotter than the outskirts. **IF** heat can flow from the center to those outskirts, the gravothermal catastrophe kicks in, and σ in the central regions will grow without limits. Since $\sigma^2 = GM(r)/r$, the central mass therefore gets compressed into a smaller and smaller region, while the outer regions expand. This is called **core collapse**. Note that this does NOT lead to the formation of a supermassive black hole, because regions at smaller r always shrink faster than regions at somewhat larger r. In dark matter halos, and elliptical galaxies, the velocity dispersion profile is often declining with radius. However, in those systems the two-body relaxation time is soo long that there is basically no heat flow (which requires two-body interactions). However, globular clusters, which consist of $N \sim 10^4$ stars, and have a crossing time of only $t_{\rm cross} \sim 5 \times 10^6$yr, have a two-body relaxation time of only $\sim 5 \times 10^8$yr. Hence, heat flow in globular clusters is not negligible, and they can (and do) undergo core collapse. The collapse does not proceed indefinitely, because of binaries (see `Galactic Dynamics` by Binney & Tremaine for more details).

CHAPTER 16

Collisions & Encounters of Collisionless Systems

Consider an encounter between two collisionless N-body systems (i.e., dark matter halos or galaxies): a perturber P and a system S. Let q denote a particle of S and let b be the impact parameter, v_∞ the initial speed of the encounter, and R_0 the distance of closest approach (see Fig. 14).

Typically what happens in an encounter is that **orbital energy** (of P wrt S) **is converted into random motion energy** of the constituent particles of P and S (i.e., q gains kinetic energy wrt S).

The **velocity impulse** $\Delta\vec{v}_{\rm q} = \int \vec{g}(t)\,{\rm d}t$ of q due to the gravitational field $\vec{g}(t)$ from P decreases with increasing v_∞ (simply because Δt will be shorter). Consequently, when v_∞ increases, less and less orbital energy is transferred to random motion, and there is a critical velocity, $v_{\rm crit}$, such that

$$\begin{aligned} v_\infty > v_{\rm crit} \quad &\Rightarrow \quad S \text{ and } P \text{ escape from each other} \\ v_\infty < v_{\rm crit} \quad &\Rightarrow \quad S \text{ and } P \text{ merge together} \end{aligned}$$

There are only two cases in which we can calculate the outcome of the encounter analytically:

- **high speed encounter** ($v_\infty \gg v_{\rm crit}$). In this case the encounter is said to be **impulsive** and one can use the impulsive approximation to compute its outcome.
- **large mass ratio** ($M_{\rm P} \ll M_{\rm S}$). In this case one can use the treatment of **dynamical friction** to describe how P loses orbital energy and angular momentum to S.

In all other cases, one basically has to resort to numerical simulations to study the outcome of the encounter. In what follows we present treatments of first the impulse approximation and then dynamical friction.

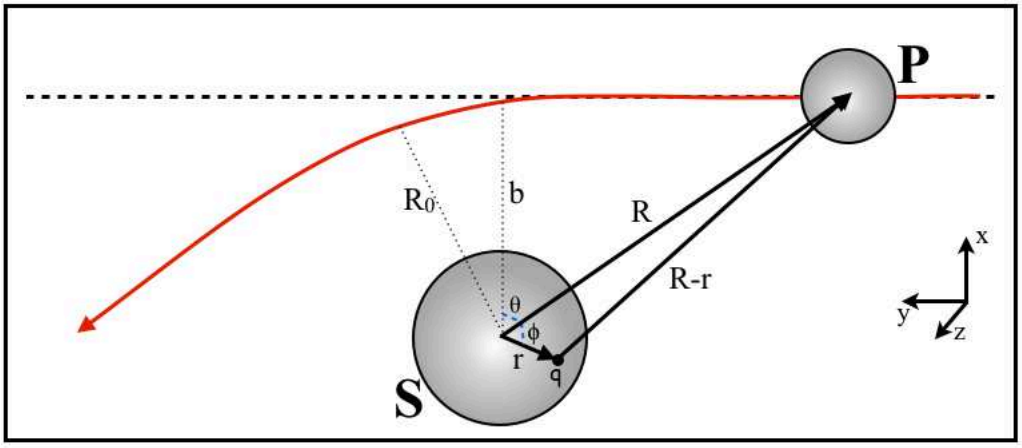

Figure 23: *Schematic illustration of an encounter with impact parameter b between a perturber P and a subject S.*

Impulse Approximation: In the limit where the encounter velocity v_∞ is much larger than the internal velocity dispersion of S, the change in the internal energy of S can be approximated analytically. The reason is that, in a high-speed encounter, the time-scale over which the tidal forces from P act on q is much shorter than the dynamical time of S (or q). Hence, we may consider q to be stationary (fixed wrt S) during the encounter. Consequently, q only experiences a change in its **kinetic** energy, while its potential energy remains unchanged:

$$\Delta E_{\rm q} = \frac{1}{2}(\vec{v}+\Delta\vec{v})^2 - \frac{1}{2}\vec{v}^2 = \vec{v}\cdot\Delta\vec{v} + \frac{1}{2}|\Delta\vec{v}|^2$$

We are interested in $\Delta E_{\rm S} = \sum_q \Delta E_{\rm q}$, where the summation is over all its constituent particles:

$$\Delta E_{\rm S} = \int \Delta E(\vec{r})\,\rho(r)\,{\rm d}^3\vec{r} \simeq \frac{1}{2}\int |\Delta\vec{v}|^2\,\rho(r){\rm d}^3\vec{r}$$

where we have used that, because of symmetry, the integral

$$\int \vec{v}\cdot\Delta\vec{v}\,\rho(r)\,{\rm d}^3\vec{r} \simeq 0$$

In the large v_∞ limit, we have that the distance of closest approach $R_0 \to b$, and the velocity of P wrt S is $v_{\rm P}(t) \simeq v_\infty\vec{e}_y \equiv v_{\rm P}\vec{e}_y$. Consequently, we have that

$$\vec{R}(t) = (b, v_{\rm P}t, 0)$$

Let $\vec{r}$ be the position vector of q wrt S and adopt the **distant encounter approximation**, which means that $b \gg \max[R_{\rm S}, R_{\rm P}]$, where $R_{\rm S}$ and $R_{\rm P}$ are the sizes of S and P, respectively. This means that we may treat P as a point mass $M_{\rm P}$, so that

$$\Phi_{\rm P}(\vec{r}) = -\frac{GM_{\rm P}}{|\vec{r} - \vec{R}|}$$

Using geometry, and defining ϕ as the angle between $\vec{r}$ and $\vec{R}$, we we have that

$$|\vec{r} - \vec{R}|^2 = (R - r\cos\phi)^2 + (r\sin\phi)^2$$

so that

$$|\vec{r} - \vec{R}| = \sqrt{R^2 - 2rR\cos\phi + r^2}$$

Next we use the series expansion

$$\frac{1}{\sqrt{1+x}} = 1 - \frac{1}{2}x + \frac{1}{2}\frac{3}{4}x^2 - \frac{1}{2}\frac{3}{4}\frac{5}{6}x^3 + ...$$

to write

$$\frac{1}{|\vec{r} - \vec{R}|} = \frac{1}{R}\left[1 - \frac{1}{2}\left(-2\frac{r}{R}\cos\phi + \frac{r^2}{R^2}\right) + \frac{3}{8}\left(-2\frac{r}{R}\cos\phi + \frac{r^2}{R^2}\right)^2 + ...\right]$$

Substitution in the expression for the potential of P yields

$$\Phi_{\rm P}(\vec{r}) = -\frac{GM_{\rm P}}{R} - \frac{GM_{\rm P}r}{R^2}\cos\phi - \frac{GM_{\rm P}r^2}{R^3}\left(\frac{3}{2}\cos^2\phi - \frac{1}{2}\right) + \mathcal{O}[(r/R)^3]$$

- The first term on rhs is a constant, not yielding any force (i.e., $\nabla_r \Phi_{\rm P} = 0$).
- The second term on the rhs describes how the center of mass of S changes its velocity due to the encounter with P.
- The third term on the rhs corresponds to the **tidal force** per unit mass and is the term of interest to us.

It is useful to work in a rotating coordinate frame (x', y', z') centered on S and with the x'-axis pointing towards the instantaneous location of P, i.e., x' points along $\vec{R}(t)$. Hence, we have that $x' = r'\cos\phi$, where $r'^2 = x'^2 + y'^2 + z'^2$. In this new coordinate frame, we can express the third term of $\Phi_{\rm P}(\vec{r})$ as

$$\begin{aligned}\Phi_3(\vec{r}) &= -\frac{GM_{\rm P}}{R^3}\left(\frac{3}{2}r'^2\cos^2\phi - \frac{1}{2}r'^2\right)\\ &= -\frac{GM_{\rm P}}{R^3}\left(x'^2 - \frac{1}{2}y'^2 - \frac{1}{2}z'^2\right)\end{aligned}$$

Hence, the tidal force is given by

$$\vec{F}'_{\rm tid}(\vec{r}) \equiv -\nabla\Phi_{\rm P} = \frac{GM_{\rm P}}{R^3}(2x', -y', -z')$$

We can relate the components of $\vec{F}'_{\rm tid}$ to those of the corresponding tidal force, $\vec{F}_{\rm tid}$ in the (x, y, z)-coordinate system using

$$\begin{aligned} x' &= x\cos\theta - y\sin\theta & \qquad F_x &= F_{x'}\cos\theta + F_{y'}\sin\theta\\ y' &= x\sin\theta + y\cos\theta & F_y &= -F_{x'}\sin\theta + F_{y'}\cos\theta\\ z' &= z & F_z &= F_{z'}\end{aligned}$$

where θ is the angle between the x and x' axes, with $\cos\theta = b/R$ and $\sin\theta = v_P t/R$. After some algebra one finds that

$$\begin{aligned}F_x &= \frac{GM_{\rm P}}{R^3}\left[x(2-3\sin^2\theta) - 3y\sin\theta\cos\theta\right]\\ F_y &= \frac{GM_{\rm P}}{R^3}\left[y(2-3\cos^2\theta) - 3x\sin\theta\cos\theta\right]\\ F_x &= -\frac{GM_{\rm P}}{R^3}z\end{aligned}$$

Using these, we have that

$$\Delta v_x = \int \frac{{\rm d}v_x}{{\rm d}t}\,{\rm d}t = \int F_x\,{\rm d}t = \int_{-\pi/2}^{\pi/2} F_x\,\frac{{\rm d}t}{{\rm d}\theta}\,{\rm d}\theta$$

with similar expressions for Δv_y and Δv_z. Using that $\theta = \tan^{-1}(v_{\rm P}t/b)$ one has that ${\rm d}t/{\rm d}\theta = b/(v_{\rm P}\cos^2\theta)$. Substituting the above expressions for the tidal force, and using that $R = b/\cos\theta$, one finds, after some algebra, that

$$\Delta\vec{v} = (\Delta v_x, \Delta v_y, \Delta v_z) = \frac{2GM_{\rm P}}{v_{\rm P}b^2}(x, 0, -z)$$

Substitution in the expression for $\Delta E_{\rm S}$ yields

$$\Delta E_{\rm S} = \frac{1}{2}\int |\Delta\vec{v}|^2\,\rho(r)\,{\rm d}^3\vec{r} = \frac{2\,G^2\,M_{\rm P}^2}{v_{\rm P}^2\,b^4}\,M_{\rm S}\,\langle x^2+z^2\rangle$$

Under the assumption that S is spherically symmetric we have that $\langle x^2+z^2\rangle = \frac{2}{3}\langle x^2+y^2+z^2\rangle = \frac{2}{3}\langle r^2\rangle$ and we obtain the final expression for the energy increase of S as a consequence of the impulsive encounter with P:

$$\boxed{\Delta E_{\rm S} = \frac{4}{3}G^2 M_{\rm S}\left(\frac{M_{\rm P}}{v_{\rm P}}\right)^2\frac{\langle r^2\rangle}{b^4}}$$

This derivation, which is originally due to Spitzer (1958), is surprisingly accurate for encounters with $b > 5{\rm max}[R_{\rm P}, R_{\rm S}]$, even for relatively slow encounters with $v_\infty \sim \sigma_S$. For smaller impact parameters one has to make a correction (see `Galaxy Formation and Evolution` by Mo, van den Bosch & White 2010 for details).

The **impulse approximation** shows that high-speed encounters can pump energy into the systems involved. This energy is tapped from the orbital energy of the two systems wrt each other. Note that $\Delta E_{\rm S} \propto b^{-4}$, so that close encounters are far more important than distant encounters.

Let $E_{\rm b} \propto GM_{\rm S}/R_{\rm S}$ be the **binding energy** of S. Then, it is tempting to postulate that if $\Delta E_{\rm S} > E_{\rm b}$ the impulsive encounter will lead to the **tidal disruption** of S. However, this is not at all guaranteed. What is important for disruption is how that energy $\Delta E_{\rm S}$ is distributed over the consistituent particles of S. Since $\Delta E \propto r^2$, particles in the outskirts of S typically gain much more energy than those in the center. However, particles in the outskirts are least bound, and thus require the least amount of energy to become unbound. Particles that are strongly bound (with small r) typically gain very little energy. As a consequence, a significant fraction of the mass can remain bound even if $\Delta E_{\rm S} \gg E_{\rm b}$ (see van den Bosch et al., 2019, MNRAS, **474**, 3043 for details).

After the encounter, S has gained **kinetic energy** (in the amount of $\Delta E_{\rm S}$), but its **potential energy** has remained unchanged (recall, this is the assumption that underlies the impulse approximation). As a consequence, after the encounter S will no longer be in **virial equilibrium**; S will have to readjust itself to re-establish virial equilibrium.

Let K_0 and E_0 be the initial (pre-encounter) kinetic and total energy of S. The **virial theorem** ensures that $E_0 = -K_0$. The encounter causes an increase of (kinetic) energy, so that $K_0 \rightarrow K_0 + \Delta E_{\rm S}$ and $E_0 \rightarrow E_0 + \Delta E_{\rm S}$. After S has re-established virial equilibrium, we have that $K_1 = -E_1 = -(E_0 + \Delta E_{\rm S}) = K_0 - \Delta E_{\rm S}$. Thus, we see that virialization after the encounter changes the kinetic energy of S from $K_0 + \Delta E_{\rm S}$ to $K_0 - \Delta E_{\rm S}$! The gravitational energy after the encounter is $W_1 = 2E_1 = 2E_0 + 2\Delta E_{\rm S} = W_0 + 2\Delta E_{\rm S}$, which is less negative than before the encounter. Using the definition of the **gravitational radius** (see Chapter 12), $r_{\rm g} = GM_{\rm S}^2/|W|$, from which it is clear that the (gravitational) radius of S increases due to the impulsive encounter. Note that here we have ignored the complication coming from the fact that the injection of energy $\Delta E_{\rm S}$ may result in unbinding some of the mass of S.

Dynamical Friction: Consider the motion of a subject mass $M_{\rm S}$ through a medium of individual particles of mass $m \ll M_{\rm S}$. The subject mass $M_{\rm S}$ experiences a "drag force", called dynamical friction, which transfers orbital energy and angular momentum from $M_{\rm S}$ to the sea of particles of mass m.

There are three different "views" of dynamical friction:

1. Dynamical friction arises from **two-body encounters** between the subject mass and the particles of mass m, which drives the system twowards **equipartition**. i.e., towards $\frac{1}{2}M_{\rm S}v_{\rm S}^2 = \frac{1}{2}m\langle v_m^2\rangle$. Since $M_{\rm S} \gg m$, the system thus evolves towards $v_{\rm S} \ll v_m$ (i.e., $M_{\rm S}$ slowes down).

2. Due to **gravitational focussing** the subject mass $M_{\rm S}$ creates an overdensity of particles behind its path (the "wake"). The gravitational back-reaction of this wake on $M_{\rm S}$ is what gives rise to dynamical friction and causes the subject mass to slow down.

3. The subject mass $M_{\rm S}$ causes a perturbation $\delta\Phi$ in the potential of the collection of particles of mass m. The gravitational interaction between the **response density** (the density distribution that corresponds to $\delta\Phi$ according to the Poisson equation) and the subject mass is what gives rise to dynamical friction (see Fig. 13).

Although these views are similar, there are some subtle differences. For example, according to the first two descriptions dynamical friction is a **local** effect. The

third description, on the other hand, treats dynamical friction more as a **global** effect. As we will see, there are circumstances under which these views make different predictions, and if that is the case, the third and latter view presents itself as the better one.

Chandrasekhar derived an expression for the dynamical friction force which, although it is based on a number of questionable assumptions, yields results in reasonable agreement with simulations. This so-called **Chandrasekhar dynamical friction** force is given by

$$\boxed{\vec{F}_{\rm df} = M_{\rm S}\,\frac{{\rm d}\vec{v}_S}{{\rm d}t} = -\frac{4\pi\,G^2\,M_{\rm S}^2}{v_{\rm S}^2}\,\ln\Lambda\,\rho(<v_{\rm S})\,\frac{\vec{v}_{\rm S}}{v_{\rm S}}}$$

Here $\rho(<v_{\rm S})$ is the density of particles of mass m that have a speed $v_m < v_{\rm S}$, and $\ln\Lambda$ is called the **Coulomb logarithm**. It's value is uncertain (typically $3 \lesssim \ln\Lambda \lesssim 30$). One often approximates it as $\ln\Lambda \sim \ln(M_{\rm h}/M_{\rm S})$, where $M_{\rm h}$ is the total mass of the system of particles of mass m, but this should only be considered a very rough estimate at best. The uncertainties for the Coulomb logarithm derive from the oversimplified assumptions made by Chandrasekhar, which include that the medium through which the subject mass is moving is infinite, uniform and with an isotropic velocity distribution $f(v_m)$ for the sea of particles.

Similar to **frictional drag** in fluid mechanics, $\vec{F}_{\rm df}$ is always pointing in the direction **opposite** of $v_{\rm S}$.

Contrary to **frictional drag** in fluid mechanics, which always increases in strength when $v_{\rm S}$ increases, dynamical friction has a more complicated behavior: In the low-$v_{\rm S}$ limit, $F_{\rm df} \propto v_{\rm S}$ (similar to hydrodynamical drag). However, in the high-$v_{\rm S}$ limit one has that $F_{\rm df} \propto v_{\rm S}^{-2}$ (which arises from the fact that the factor $\rho(<v_{\rm S})$ saturates).

Note that $\vec{F}_{\rm df}$ is **independent** of the mass m of the constituent particles, and proportional to $M_{\rm S}^2$. The latter arises, within the second or third view depicted above, from the fact that the wake or response density has a mass that is proportional to $M_{\rm S}$, and the gravitational force between the subject mass and the wake/response density therefore scales as $M_{\rm S}^2$.

One shortcoming of Chandrasekhar's dynamical friction description is that it treats

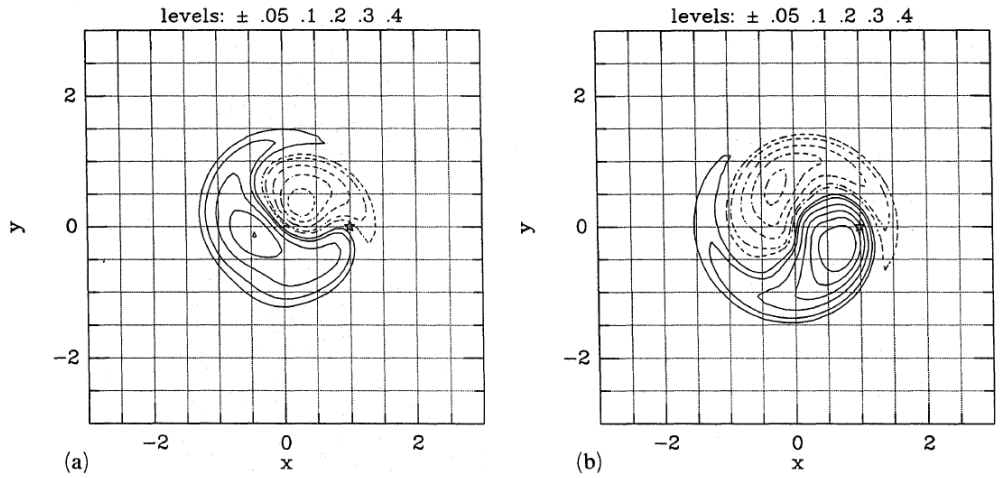

Figure 24: *Examples of the response density in a host system due to a perturber orbiting inside it. The back-reaction of this response density on the perturber causes the latter to experience dynamical friction. The position of the perturber is indicated by an asterisk. [*`Source:`* Weinberg, 1989, MNRAS, 239, 549]*

dynamical friction as a purely **local phenomenon**; it is treated as the cumulative effect of many **uncorrelated** two-body encounters between the subject masss and the individual field particles. That this local treatment is incomplete is evident from the fact that an object A orbiting **outside** of an N-body system B still experiences dynamical friction. This can be understood with the picture sketched under view 3 above, but not in a view that treats dynamical friction as a local phenomenon.

Orbital decay: As a consequence of dynamical friction, a subject mass $M_{\rm S}$ orbiting inside (or just outside) of a larger N-body system of mass $M_{\rm h} > M_{\rm S}$, will transfer its orbital energy and angular momentum to the constituent particles of the 'host' mass. As a consequence it experiences orbital decay.

Let us assume that the host mass is a **singular isothermal sphere** with density and potential given by

$$\rho(r) = \frac{V_{\rm c}^2}{4\pi G r^2} \qquad\qquad \Phi(r) = V_{\rm c}^2 \ln r$$

where $V_{\rm c}^2 = GM_{\rm h}/r_{\rm h}$ with $r_{\rm h}$ the radius of the host mass. If we further assume that this host mass has, at each point, an **isotropic** and **Maxwellian** velocity distrubution, then

$$f(v_m) = \frac{\rho(r)}{(2\pi\sigma^2)^{3/2}} \exp\left[-\frac{v_m^2}{2\sigma^2}\right]$$

with $\sigma = V_c/\sqrt{2}$.

NOTE: the assumption of a singular isothermal sphere with an isotropic, Maxwellian velocity distribution is unrealistic, but it serves the purpose of the order-of-magnitude estimate for the orbital decay rate presented below.

Now consider a subject of mass $M_{\rm S}$ moving on a **circular orbit** ($v_{\rm S} = V_{\rm c}$) through this host system of mass $M_{\rm h}$. The **Chandrasekhar dynamical friction** that this subject mass experiences is

$$F_{\rm df} = -\frac{4\pi\,\ln\Lambda\,G^2\,M_{\rm S}^2\,\rho(r)}{V_{\rm c}^2}\left[{\rm erf}(1) - \frac{2}{\sqrt{\pi}}{\rm e}^{-1}\right] \simeq -0.428\,\ln\Lambda\,\frac{GM_{\rm S}^2}{r^2}$$

The subject mass has **specific angular momentum** $L = rv_{\rm S}$, which it loses due to dynamical friction at a rate

$$\frac{{\rm d}L}{{\rm d}t} = r\frac{{\rm d}v_{\rm S}}{{\rm d}t} = r\frac{F_{\rm df}}{M_{\rm S}} \simeq -0.428\,\ln\Lambda\,\frac{GM_{\rm S}}{r}$$

Due to this angular momentum loss, the subject mass moves to a smaller radius, while it continues to move on a circular orbit with $v_{\rm S} = V_{\rm c}$. Hence, the rate at which the orbital radius changes obeys

$$V_{\rm c}\frac{{\rm d}r}{{\rm d}t} = \frac{{\rm d}L}{{\rm d}t} = -0.428\ln\Lambda\,\frac{GM_{\rm S}}{r}$$

Solving this differential equation subject to the initial condition that $r(0) = r_i$, one finds that the subject mass $M_{\rm S}$ reaches the center of the host after a time

$$\boxed{t_{\rm df} = \frac{1.17}{\ln\Lambda}\,\frac{r_i^2\,V_{\rm c}}{G\,M_{\rm S}} = \frac{1.17}{\ln\Lambda}\left(\frac{r_i}{r_{\rm h}}\right)^2\,\frac{M_{\rm h}}{M_{\rm S}}\,\frac{r_{\rm h}}{V_{\rm c}}}$$

In the case where the host system is a **virialized dark matter halo** we have that

$$\frac{r_{\rm h}}{V_{\rm c}} \simeq \frac{1}{10H(z)} = 0.1t_{\rm H}$$

where $t_{\rm H}$ is called the **Hubble time**, and is approximately equal to the age of the Universe corresponding to redshift z (the above relation derives from the fact

that virialized dark matter halos all have the same average density). Using that $\ln\Lambda \sim \ln(M_{\rm h}/M_{\rm S})$ and assuming that the subject mass starts out from an initial radius $r_i = r_{\rm h}$, we obtain a dynamical friction time

$$t_{\rm df} = 0.12\,\frac{M_{\rm h}/M_{\rm S}}{\ln(M_{\rm h}/M_{\rm S})}\,t_{\rm H}$$

Hence, the time $t_{\rm df}$ on which dynamical friction brings an object of mass $M_{\rm S}$ moving in a host of mass $M_{\rm h}$ from an initial radius of $r_i = r_{\rm h}$ to $r = 0$ is shorter than the Hubble time as long as $M_{\rm S} \gtrsim M_{\rm h}/30$. Hence, dynamical friction is only effective for fairly massive objects, relative to the mass of the host. In fact, if you take into account that the subject mass experiences mass stripping as well (due to the tidal interactions with the host), the dynamical friction time increases by a factor 2 to 3, and $t_{\rm df} < t_{\rm H}$ actually requires that $M_{\rm S} \gtrsim M_{\rm h}/10$.

For a more detailed treatment of collisions and encounters of collisionless systems, see Chapter 12 of `Galaxy Formation and Evolution` by Mo, van den Bosch & White.

Computational Hydrodynamics

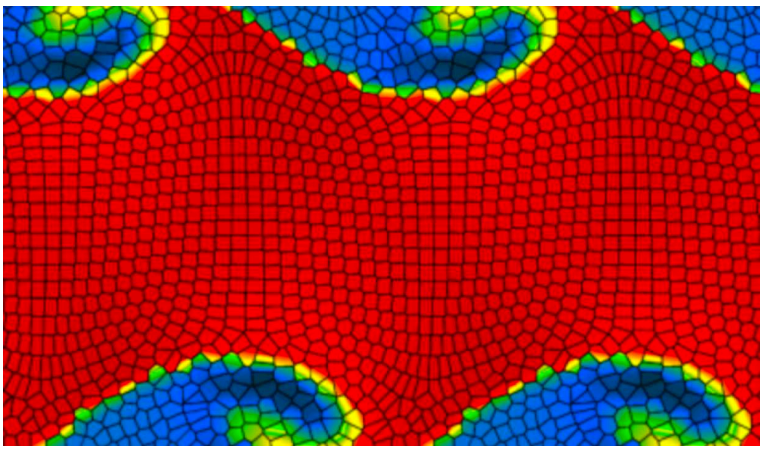

The following chapters give an elementary introduction into computational hydrodynamics; i.e., the topic of how to solve the equations of hydrodynamics numerically. Students are expected to be somewhat familiar with (partial) differential equations. For those who want a quick reminder, Appendix E lists some of the basics.

Numerical, or computational, hydrodynamics is a rich topic, and one could easily devote an entire course to it. The following chapters therefore only scratch the surface of this rich topic. Readers who want to get more indepth information are referred to the following excellent textbooks

- *Numerical Solution of Partial Differential Equations* by K. Morton & D. Mayers
- *Numerical Methods for Partial Differential Equations* by W. Ames
- *Difference Methods for Initial Value Problems* by R. Richtmyer
- *Numerical Methods for Engineers and Scientists* by J. Hoffman
- *Riemann Solvers and Numerical Methods for Fluid Dynamics* by E. Toro

CHAPTER 17

Solving PDEs with Finite Difference Methods

Having discussed the theory of fluid dynamics, we now focus on how to actually solve the **partial differential equations** (PDEs) that describe the time-evolution of the various hydrodynamical quantities. Solving PDEs analytically is complicated (see Appendix E for some background) and typically only possible for highly idealized flows. In general, we are forced to solve the PDEs numerically. How this is done is the topic of this and subsequent chapters.

The first thing to realize is that a computer will only solve a discrete representation of the actual PDE. We call this approximation a **finite difference approximation** (FDA). In addition, we need to represent the physical data (i.e., our hydrodynamical quantities of interest) in a certain finite physical region of interest, called the **computational domain**). Typically this is done by subdividing the computational domain using a *computational mesh*; the data is specified at a finite number of grid points or cells. Throughout these chapters on numerical hydrodynamics we will consider regular, cartesian meshes, but more complicated, even time-dependent meshes can be adopted as well. There are two different 'methods' (or 'philosophies') for how to formulate the problem. On the one hand, one can think of the data as literally being placed at the grid *points*. This yields a **finite difference formulation**. Alternatively, one can envision the data being spread our over the mesh cell (or 'zone'), yielding a **finite volume formulation**. In practice. finite difference formulations are a bit faster, and easier to comprehend, which is why much of what follows adopts the finite difference formulation. In Chapter 19, though, we will transition to finite volume formulation, which is the formulation most often adopted in modern computational fluid dynamics.

Before proceeding with discussing finite difference formulations of our hydrodynamical equations on a mesh, we point out that **particle based methods** have also been developed. Smoothed Particle Hydrodynamics (SPH) is the main example, which is quite often used in astrophysics (but rarely in engineering problems). SPH has the advantage of being Lagrangian, which is desirable in certain applications, but it is typically much harder to proof that the SPH scheme converges to the actual physical

equations being modelled. In what follows we therefore adhere to Eulerian methods based on computational domains that are discretized on a mesh.

In numerical hydrodynamics it is common and most convenient to write the hydrodynamical equations in **conservative form**

$$\frac{\partial q}{\partial t} + \nabla \cdot \vec{f}(q) = S$$

Here $q(\vec{x}, t)$ is a state variable of the fluid (either scalar or vector), $\vec{f}(q)$ describes the flux of q, and S describes the various sources and/or sinks of q. As we have seen in Chapter 3, for an **ideal** (i.e., **inviscid** and **non-conductive**) fluid, *which is what we consider throughout these chapters on numerical hydrodynamics*, the continuity, momentum and energy equations in conservative form are:

$$\begin{aligned}
\frac{\partial \rho}{\partial t} + \nabla \cdot (\rho \vec{u}) &= 0 \\
\frac{\partial \rho \vec{u}}{\partial t} + \nabla \cdot (\rho \vec{u} \otimes \vec{u} + P) &= -\rho \nabla \Phi \\
\frac{\partial \rho(\frac{1}{2}u^2 + \Phi + \varepsilon)}{\partial t} + \nabla \cdot \left[\left(\frac{1}{2}u^2 + \Phi + \varepsilon + \frac{P}{\rho} \right) \rho \vec{u} \right] &= \rho \frac{\partial \Phi}{\partial t} - \mathcal{L}
\end{aligned}$$

The latter, the energy equation, can be rewritten as

$$\frac{\partial \rho(\frac{1}{2}u^2 + \varepsilon)}{\partial t} + \nabla \cdot \left[\left(\frac{1}{2}u^2 + \varepsilon + \frac{P}{\rho} \right) \rho \vec{u} \right] = -\rho \vec{u} \cdot \nabla \Phi - \mathcal{L}$$

In order to see this, use that

$$\begin{aligned}
\rho \frac{\partial \Phi}{\partial t} - \frac{\partial \rho \Phi}{\partial t} - \frac{\partial \rho \Phi u_k}{\partial x_k} &= -\Phi \frac{\partial \rho}{\partial t} - \nabla \cdot (\rho \Phi \vec{u}) \\
&= -\Phi \frac{\partial \rho}{\partial t} - \Phi \nabla \cdot \rho \vec{u} - \rho \vec{u} \cdot \nabla \Phi \\
&= -\Phi \left[\frac{\partial \rho}{\partial t} + \nabla \cdot \rho \vec{u} \right] - \rho \vec{u} \cdot \nabla \Phi = -\rho \vec{u} \cdot \nabla \Phi
\end{aligned}$$

Thus, ignoring radiation ($\mathcal{L} = 0$) and gravity ($\Phi = 0$), in addition to viscosity and conduction, the equations of hydrodynamics in conservative form are

$$\frac{\partial \vec{q}}{\partial t} + \nabla \cdot \vec{f} = 0 \qquad \text{or,} \qquad \frac{\partial q_i}{\partial t} + \frac{\partial f_i}{\partial q_i} = 0$$

where

$$\vec{q} = \begin{pmatrix} \rho \\ \rho\vec{u} \\ \frac{1}{2}\rho u^2 + \rho\varepsilon \end{pmatrix} \qquad \text{and} \qquad \vec{f}(\vec{q}) = \begin{pmatrix} \rho\vec{u} \\ \rho\vec{u} \otimes \vec{u} + P \\ (\frac{1}{2}u^2 + \varepsilon + P/\rho)\,\rho\vec{u} \end{pmatrix}$$

Depending on the number of spatial dimensions, this is a set of 3-5 coupled PDEs, and our goal is to come up with a scheme how to numerically solve these. Note that we are considering a highly oversimplified case, ignoring gravity, radiation, viscosity and conduction. As discussed later, adding viscosity and conduction changes the character of the PDE, while gravity and radiation can be added as source and/or sink terms, something we will not cover in these lecture notes.

Typically, one can numerically solve this set of PDEs using the following procedure:

1. Define a spatial grid, $\vec{x}_i$, where here the index refers to the grid point.
2. Specify initial conditions for $\vec{q}(\vec{x}, t)$ at $t = 0$ at all $\vec{x}_i$, and specify suitable boundary conditions on the finite computational domain used.
3. Compute ρ, $\vec{u}$ and ε at all $\vec{x}_i$.
4. Compute the fluxes $\vec{f}(\vec{q})$ at all $\vec{x}_i$.
5. Take a small step in time, Δt, and compute the new $\vec{q}(\vec{x}_i, t + \Delta t)$.
6. Go back to [3]

Although this sounds simple, there are many things that can go wrong. By far the most tricky part is step [5], as we will illustrate in what follows.

Let us start with some basics. The above *set* of PDEs is **hyperbolic**. Mathematically this means the following. Consider the Jacobian matrix of the flux function

$$F_{ij}(\vec{q}) \equiv \frac{\partial f_i}{\partial q_j}$$

The set of PDEs is hyperbolic if, for each value of $\vec{q}$, *all* the eigenvalues of $\mathbf{F}$ are **real**, and $\mathbf{F}$ is **diagonizable**.

In a system described by a hyperbolic PDE, information travels at a finite speed (c_s in the example here). Information is not transmitted until the wave arrives. The smoothness of the solution to a hyperbolic PDE depends on the smoothness of the initial and boundary conditions. For instance, if there is a jump in the data at the start or at the boundaries, then the jump will propagate as a shock in the solution. If, in addition, the PDE is nonlinear (which is the case for the Euler equations), then shocks may develop even though the initial conditions and the boundary conditions are smooth.

If we were to consider the **Navier-Stokes equation**, rather than the Euler equations, then we add 'non-ideal' terms (referring to the fact that these terms are absent for an ideal fluid) related to **viscosity** and **conduction**. These terms come with a second-order spatial derivative, describing diffusive processes. Such terms are called **parabolic**, and they have a different impact on the PDE. See the box on the next page.

Hence, we are faced with the problem of simultaneously solving a **hyperbolic** set of 3-5 PDEs, some of which are **non-linear**, and some of which may contain **parabolic** terms. This is a formidable problem, and one could easily devote an entire course to it. Readers who want to get more indepth information are referred to the textbooks listed at the start of this section on numerical hydrodynamics.

The Nature of Hyperbolic and Parabolic PDEs

Consider the first-order PDE

$$\frac{\partial \rho}{\partial t} + v\frac{\partial \rho}{\partial x} = 0$$

As we will see later on, this is the 1D linear advection equation, and it describes how density features are being propagated (i.e., advected) with constant speed v. To get some insight, let's consider the formal solution

$$\rho = \rho_0 + \rho_1 \mathrm{e}^{i(kx-\omega t)}$$

which consists of a constant part, ρ_0, plus a wave-like perturbation. Substituting this in the PDE yields

$$\omega = kv \qquad \Rightarrow \qquad \rho(x,t) = \rho_0 + \rho_1 \mathrm{e}^{ik(x-vt)}$$

This is a travelling wave, and ω is always real. We also see that the group velocity $\partial\omega/\partial k = v$ is constant, and independent of k; all modes propagate at the same speed, and the wave-solution is thus non-dispersive. This is characteristic of a **hyperbolic PDE**. Next consider the **heat equation**

$$\frac{\partial T}{\partial t} = \kappa \frac{\partial^2 T}{\partial x^2}$$

This equation describes how heat diffuses in a 1D system with diffusion coefficient κ. Substituting the same formal solution as above, we obtain that

$$\omega = -i\kappa k^2 \qquad \Rightarrow \qquad \rho(x,t) = \rho_0 + \rho_1 \mathrm{e}^{ikx}\mathrm{e}^{-\kappa k^2 t}$$

Note that ω is now imaginary, and that the solution has an exponentially decaying term. This describes how the perturbation will 'die out' over time due to dissipation. This is characteristic of a **parabolic PDE**.

In what follows, rather than tackling the problem of numerically solving the Euler or Navier-Stokes equations, we focus on a few simple limiting cases that result in fewer equations, which will give valuable insight to aspects of the various numerical schemes. In particular, we restrict ourselves to the **1D** case, and continue to assume an **ideal** fluid for which we can ignore **radiation** and **gravity**. The hydrodynamic equations now reduce to the following set of 3 PDEs:

$$\begin{aligned} \frac{\partial \rho}{\partial t} + \frac{\partial}{\partial x}(\rho u) &= 0 \\ \frac{\partial}{\partial t}(\rho u) + \frac{\partial}{\partial x}(\rho u u + P) &= 0 \\ \frac{\partial}{\partial t}\left(\frac{1}{2}\rho u^2 + \rho\varepsilon\right) + \frac{\partial}{\partial x}\left(\left[\frac{1}{2}\rho u^2 + \rho\varepsilon + P\right] u\right) &= 0 \end{aligned}$$

If we now, in addition, assume **constant pressure**, P, and a **constant flow velocity**, u, then this system reduces to 2 separate, linear PDEs given by

$$\frac{\partial \rho}{\partial t} + u\frac{\partial \rho}{\partial x} = 0 \qquad \text{and} \qquad \frac{\partial \varepsilon}{\partial t} + u\frac{\partial \varepsilon}{\partial x} = 0$$

These are identical equations, known as the **linear advection equation**. They describe the **passive transport** of the quantities ρ and ε in the flow with constant velocity u. This equation has a well-known, rather trivial solution: If the initial ($t = 0$) conditions are given by $\rho_0(x)$ and $\varepsilon_0(x)$, the the general solutions are

$$\rho(x,t) = \rho_0(x - ut) \qquad \text{and} \qquad \varepsilon(x,t) = \varepsilon_0(x - ut)$$

Since the analytical solution to this linear advection equation is (trivially) known, it is an ideal equation on which to test our numerical scheme(s). As we will see, even this extremely simple example will proof to be surprisingly difficult to solve numerically.

The Courant-Friedrich-Lewy condition: Due to the finite travelling speed of waves, hyperbolic PDEs have a **finite physical domain of dependence**. This implies that any scheme used to solve a hyperbolic PDE must obey the Courant-Friedrich-Lewy (CFL) condition (often called the Courant condition, for short). In particular, if u is the speed at which information propagates, and grid cells are interspaced by Δx, then the time-step Δt used in the numerical integration must obey

$$\boxed{|u\,\Delta t/\Delta x| \equiv |\alpha_{\rm c}| \leq 1}$$

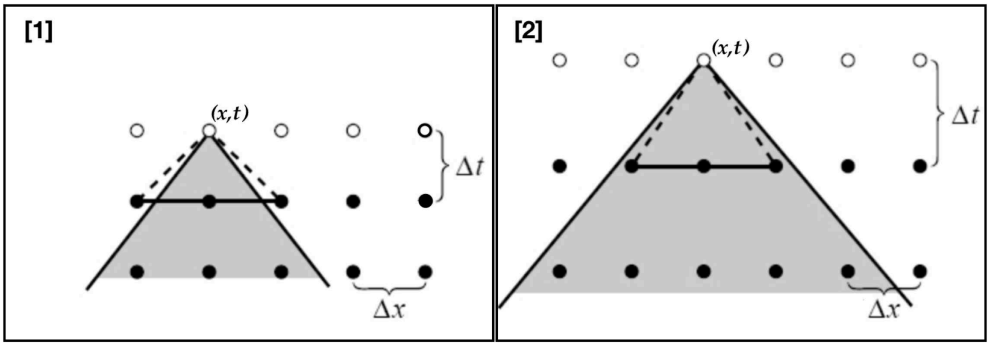

Figure 25: *Filled and open dots indicate the grid points (horizontal) and time steps (vertical). The grey region is the physical domain of dependence for the* (x,t)*-grid point, and the CFL-condition states that the numerical domain of dependence must contain this physical domain. The triangle formed by the two dashed lines and solid black line indicates this numerical domain in the case of the* **explicit Euler scheme** *of integration discussed below. It relies on the properties of the neighboring grid points at the previous time-step. The time-step in panel [1] DOES meet the CFL-criterion, while that in panel [2] does NOT.*

Here the parameter α_c is often called the CFL, or Courant, parameter. Note that this CFL condition is *necessary* for stability, but not *sufficient*. In other words, obeying the CFL condition does not guarantee stability, as we will see shortly.

The principle behind the CFL condition is simple: if a wave is moving across a discrete spatial grid and we want to compute its amplitude at discrete time steps of equal duration, Δt, then this duration must be less than the time for the wave to travel to adjacent grid points. As a corollary, when the grid point separation is reduced, the upper limit for the time step also decreases. In essence, *the numerical domain of dependence of any point in space and time must include the analytical domain of dependence* (wherein the initial conditions have an effect on the exact value of the solution at that point) to assure that the scheme can access the information required to form the solution. This is illustrated in Fig. 25.

IMPORTANT: change in notation: From here on out, following standard notation in many textbooks on this topic, we are going to write the function to be solved as $u(x,t)$, without implying that this u is velocity (as has been our notation thus far). Although this may cause some confusion, it is in line with the standard notation

in computational hydrodynamics and much of the literature on solving differential equations. In this new notation our linear advection equation is given by

$$\frac{\partial u}{\partial t} + v\,\frac{\partial u}{\partial x} = 0$$

where v is now the constant advection speed, and u is the property being advected. Throughout we adopt a discretization in time and space given by

$$\begin{aligned} t^n &= t_0 + n\Delta t \\ x_i &= x_0 + i\Delta x \end{aligned}$$

Note that subscripts indicate the spatial index, while superscripts are used to refer to the temporal index. Hence, u_i^{n+1} refers to the value of u at grid location i at time-step $n+1$, etc. The key to numerically solving differential equations is find how to express derivatives in terms of the discretized quantities. This requires a **finite difference scheme**. Using Taylor series expansion, we have that

$$\begin{aligned} u_{i+1} &\equiv u(x_i + \Delta x) = u(x_i) + \Delta x \frac{\partial u}{\partial x}(x_i) + \frac{(\Delta x)^2}{2}\frac{\partial^2 u}{\partial x^2}(x_i) + \frac{(\Delta x)^3}{6}\frac{\partial^3 u}{\partial x^3}(x_i) + \mathcal{O}(\Delta x^4) \\ u_i &\equiv u(x_i) \\ u_{i-1} &\equiv u(x_i - \Delta x) = u(x_i) - \Delta x \frac{\partial u}{\partial x}(x_i) + \frac{(\Delta x)^2}{2}\frac{\partial^2 u}{\partial x^2}(x_i) - \frac{(\Delta x)^3}{6}\frac{\partial^3 u}{\partial x^3}(x_i) + \mathcal{O}(\Delta x^4) \end{aligned}$$

By subtracting the first two expression, and dividing by Δx, we obtain the following finite difference approximation for the first derivative

$$\boxed{u_i' \approx \frac{u_{i+1} - u_i}{\Delta x} - \frac{1}{2}\frac{\partial^2 u}{\partial x^2}(x_i)\Delta x}$$

The first term is the finite difference approximation (FDA) for the first derivative, and is known as the **forward difference**. The second term gives the **truncation error**, which shows that this FDA is first-order accurate (in Δx).

We can obtain an alternative FDA for the first derivative by subtracting the latter two expressions, and again dividing by Δx:

$$\boxed{u_i' \approx \frac{u_i - u_{i-1}}{\Delta x} - \frac{1}{2}\frac{\partial^2 u}{\partial x^2}(x_i)\Delta x}$$

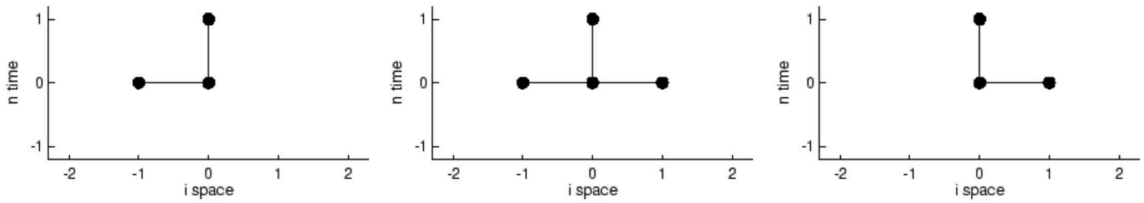

Figure 26: *Stencil diagrams for the Backward-Space FTBS scheme (left-hand panel), the Central-Space FTCS scheme (middle panel), and the Forward-Space FTFS scheme (right-hand panel). All of these are examples of explicite Euler integration schemes.*

which is also first-order accurate in Δx (i.e., the numerical error in u' is proportional to Δx). This finite difference scheme is known as **backward difference**.

Combining the two Taylor series approximations, and subtracting one from the other, yields yet another FDA for the first derivative, given by

$$\boxed{u'_i \approx \frac{u_{i+1} - u_{i-1}}{2\Delta x} - \frac{1}{3}\frac{\partial^3 u}{\partial x^3}(x_i)(\Delta x)^2}$$

which is known as the **centred difference** scheme. Note that this FDA is second-order accurate in Δx.

Using the same approach, one can also obtain FDAs for higher-order derivatives. For example, by *adding* the two Taylor series expressions above, we find that

$$\boxed{u''_i \approx \frac{u_{i+1} - 2u_i + u_{i-1}}{(\Delta x)^2} - \frac{1}{12}\frac{\partial^4 u}{\partial x^4}(x_i)(\Delta x)^2}$$

Similarly, by folding in Taylor series expressions for u_{i+2} and u_{i-2}, one can obtain higher-order FDAs. For example, the first derivative can then be written as

$$\boxed{u'_i \approx \frac{-u_{i+2} + 8u_{i+1} - 8u_{i-1} + u_{i-2}}{12\Delta x}}$$

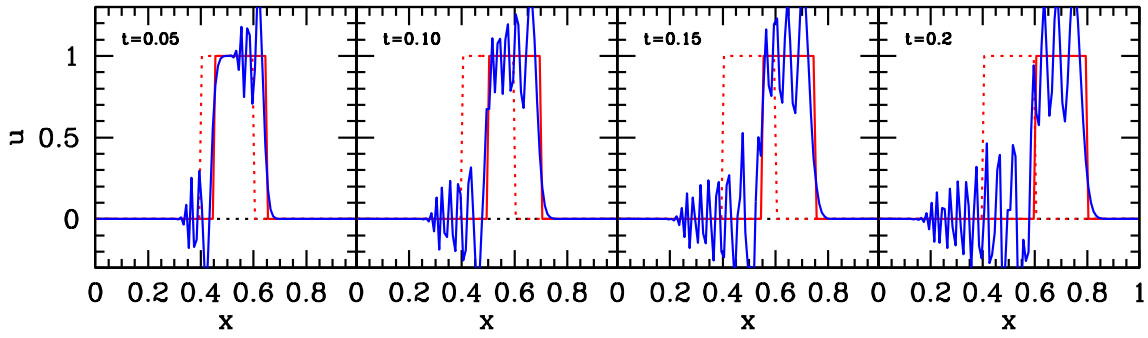

Figure 27: *The results of using the FTCS scheme to propate the initial conditions, indicated by the red dotted lines, using the 1D linear advection equation. Despite the fact that* $\alpha_c = v\Delta t/\Delta x = 0.1$*, thus obeying the CFL-condition, the numerically solution (in blue) develops growing oscillations, a manifestation of its inherent unstable nature. The red solid lines in each panel show the corresponding analytical solutions. These results are based on a linear spatial grid using 100 spatial cells over the domain* $[0, 1]$*, with a time step* $\Delta t = 0.001$*. The advection velocity is* $v = 1.0$*.*

which is fourth-order accurate in Δx. Typically, higher-order is better (if stable, see next chapter), but it also is computationally more expensive (slower).

Now let us return to our linear advection equation. Since we only know $u(x, t)$ in the past, but not in the future, we have to use the backward difference scheme to approximate $\partial\rho/\partial t$. For the spatial derivative it seems natural to pick the centred difference scheme, which is higher order than the forward or backward difference schemes. Hence, we have that

$$\frac{\partial u}{\partial t} \to \frac{u_i^{n+1} - u_i^n}{\Delta t} \qquad \frac{\partial u}{\partial x} \to \frac{u_{i+1}^n - u_{i-1}^n}{2\Delta x}$$

which allows us to write

$$\boxed{u_i^{n+1} = u_i^n - v\,\frac{\Delta t}{2\Delta x}\,\left(u_{i+1}^n - u_{i-1}^n\right)}$$

This scheme for solving the linear advection equation numerically is called the **explicit Euler scheme** or **FTCS-scheme** for **F**orward-**T**ime-**C**entral-**S**pace.

We can define similar explicit schemes based on the forward and backward difference

schemes. In particular, we have the **FTBS** (Forward-Time-Backward-Space) scheme

$$\boxed{u_i^{n+1} = u_i^n - v\,\frac{\Delta t}{\Delta x}\,\left(u_i^n - u_{i-1}^n\right)}$$

and the **FTFS** (Forward-Time-Forward-Space) scheme

$$\boxed{u_i^{n+1} = u_i^n - v\,\frac{\Delta t}{\Delta x}\,\left(u_{i+1}^n - u_i^n\right)}$$

It is useful to illustrate the dependencies in these schemes using so-called **stencil diagrams**. These are depicted for the FTBS, FTCS and FTFS schemes in Fig. 26.

Figure 27 shows the results of the FTCS-scheme applied to a simple initial condition in which $u = 1$ for $0.4 \leq x \leq 0.6$ and zero otherwise (red, dotted lines). These conditions are advected with a constant, uniform velocity $v = 1.0$. The blue curves show the results obtained using the FTCS scheme with $\Delta x = 0.01$ (i.e., the domain $[0, 1]$ is discretized using 100 spatial cells) and $\Delta t = 0.001$. Results are shown after 50, 100, 150 and 200 time-steps, as indicated. The solid, red curves in the four panels show the corresponding analytical solution, which simply correspond to a horizontal displacement of the initial conditions.

Despite the fact that the CFL-condition is easily met ($|v\,\Delta t/\Delta x = 0.1$), the solution develops large oscillations that grow with time, rendering this scheme useless.

Let's now try another scheme. Let's pick the **FTBS** scheme, whose stencil is given by the left-hand panel of Fig. 26. The results are shown in Fig. 28. Surprisingly, this scheme, which is also known as the **upwind** or **donor-cell** scheme yields very different solutions. The solutions are smooth (no growing oscillations), but they are substantial 'smeared out', as if **diffusion** is present.

For completeness, Fig. 29 shows the same results but for the **FTFS** scheme (stencil shown in right-hand panel of Fig. 26). This scheme is even more unstable as the FTCS scheme, with huge oscillations developing rapidly.

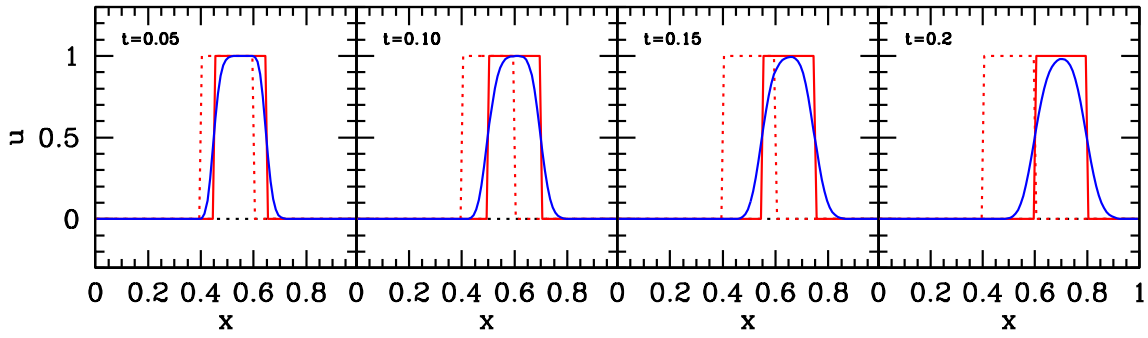

Figure 28: *Same as Figure 27, but for the FCBS scheme (stencil in left-hand panel of Fig. 26). This scheme is stable, yielding smooth solutions, but it suffers from significant numerical diffusion.*

Before we delve into other integration schemes, and an indepth analysis of why subtly different schemes perform so dramatically differently, we first take a closer look at the 1D **conservation equation**

$$\frac{\partial u}{\partial t} + \frac{\partial f}{\partial x} = 0$$

where $f = f(u)$ is the flux associated with u (which, in the case of linear advection is give by $f = vu$). We can write this equation in **integral form** as

$$\int_{x_{i-\frac{1}{2}}}^{x_{i+\frac{1}{2}}} \mathrm{d}x \int_{t^n}^{t^{n+1}} \mathrm{d}t \left[\frac{\partial u}{\partial t} + \frac{\partial f}{\partial x}\right] = 0$$

where the integration limits are the boundaries of cell i, which we denote by $x_{i-\frac{1}{2}}$ and $x_{i+\frac{1}{2}}$, and the boundaries of the time step $t^n \to t^{n+1}$. If we now consider u as being constant over a cell, and the flux is assumed constant during a time step, we can write this as

$$\int_{x_{i-\frac{1}{2}}}^{x_{i+\frac{1}{2}}} \mathrm{d}x \left[u(x, t^{n+1}) - u(x, t^n)\right] + \int_{t^n}^{t^{n+1}} \mathrm{d}t \left[f(x_{i+\frac{1}{2}}, t) - f(x_{i-\frac{1}{2}}, t)\right] =$$

$$u(x_i, t^{n+1})\Delta x - u(x_i, t^n)\Delta x + f_{i+\frac{1}{2}}^{n+\frac{1}{2}}\Delta t - f_{i-\frac{1}{2}}^{n+\frac{1}{2}}\Delta t = 0$$

This yields the following **update formula in conservation form:**

$$\boxed{u_i^{n+1} = u_i^n - \frac{\Delta t}{\Delta x}\left(f_{i+\frac{1}{2}}^n - f_{i-\frac{1}{2}}^n\right)}$$

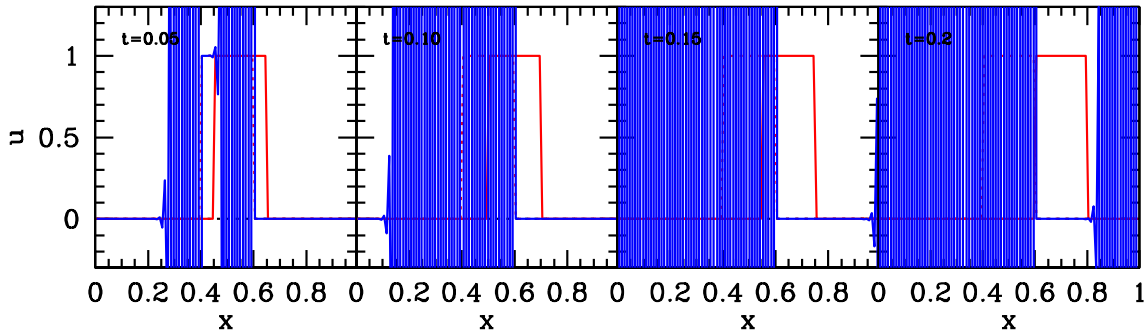

Figure 29: *Same as Figure 27, but for the FCFS scheme (stencil in right-hand panel of Fig. 26). Clearly, this scheme is utterly unstable and completely useless.*

This is called 'conservation form' because it expresses that property u in cell i only changes due to a flux of u through its boundaries. With this formulation, we can describe any integration scheme by simply specifying the flux $f^n_{i+\frac{1}{2}}$. For example, the three integration schemes discussed thus far are specified by $f^n_{i+\frac{1}{2}} = f(u^n_i)$ (FTBS), $f^n_{i+\frac{1}{2}} = \frac{1}{2}[f(u^n_{i+1}) + f(u^n_i)]$ (FTCS), and $f^n_{i+\frac{1}{2}} = f(u^n_{i+1})$ (FTFS). See also the Table on the next page.

So far we have considered three integration schemes, which are all examples of explicit Euler schemes. When a direct computation of the dependent variables can be made in terms of known quantities, the computation is said to be **explicit**. In contrast, when the dependent variables are defined by coupled sets of equations, and either a matrix or iterative technique is needed to obtain the solution, the numerical method is said to be **implicit**. An example of an implicit scheme is the following FDA of the heat equation (see Problem Set 3)

$$\frac{u^{n+1}_i - u^n_i}{\Delta t} = \kappa \left(\frac{u^{n+1}_{i+1} - 2u^{n+1}_i + u^{n+1}_{i-1}}{\Delta x^2} \right)$$

Note that the second-order spatial derivative on the rhs is evaluated at time t^{n+1}, rather than t^n, which is what makes this scheme implicit. Since explicit schemes are much easier to code up, we will not consider any implicit schemes in these lecture notes. We emphasize, though, the sometimes implicit schemes are powerful alternatives.

Neither of the three (explicit) schemes considered thus far are satisfactory; the FTCS

and FTFS schemes are unstable, yielding oscillations that grow rapidly, while the FTBS scheme suffers from a large amount of **numerical dissipation**. Fortunately, there are many alternative schemes, both explicit and implicit. The Table on the next page lists 7 explicit finite difference methods that have been suggested in the literature. In addition to the three Euler methods discussed above, this includes the **Lax-Friedrichs** method, which is basically a FTCS-method with an added **artificial viscosity** term. Similar to the FTCS method, it is second order accurate in space, and first-order accurate in time. The performance of this method is evident from the upper-right panel in Fig. 30. Clearly, the artificial viscosity suppresses the onset of growing oscillations, which is good, but the numerical diffusion is much worse than in the FCBS upwind (or donor-cell) scheme, rendering this method not very useful, except when the initial conditions are very smooth.

All the finite-difference methods encountered thus far are first-order accurate in time. The table also lists three schemes that are **second-order** accurate in both space and time, i.e., with an error that is $\mathcal{O}(\Delta x^2, \Delta t^2)$. The first of these is the **Lax-Wendroff** method. As is evident from the lower-left panel of Fig. 30 it results in some oscillations, but these don't grow much beyond a certain point (unlike, for example, the first-order Euler-FTCS scheme shown in the upper-left panel). Another, similar scheme, is the **Beam-Warming** method, whose performance, shown in the lower-middle panel of Fig 30, is only marginally better. Finally, the lower-right panel shows the performace of the **Fromm** method, which is basically the average of the Lax-Wendroff and Beam-Warming schemes, i.e., $f^n_{i+\frac{1}{2},\mathrm{Fromm}} = \frac{1}{2}[f^n_{i+\frac{1}{2},\mathrm{LW}} + f^n_{i+\frac{1}{2},\mathrm{BW}}]$. As is evident, this is clearly the most successfull method encountered thus far.

Explicit Finite Difference Methods for 1D Linear Advection Problem

Euler FTBS	$f^n_{i+\frac{1}{2}} = f(u^n_i)$ $u^{n+1}_i = u^n_i - \alpha_{\rm c}[u^n_i - u^n_{i-1}]$
Euler FTCS	$f^n_{i+\frac{1}{2}} = \frac{1}{2}[f(u^n_{i+1}) + f(u^n_i)]$ $u^{n+1}_i = u^n_i - \frac{\alpha_{\rm c}}{2}[u^n_{i+1} - u^n_{i-1}]$
Euler FTFS	$f^n_{i+\frac{1}{2}} = f(u^n_{i+1})$ $u^{n+1}_i = u^n_i - \alpha_{\rm c}[u^n_{i+1} - u^n_i]$
Lax-Friedrichs	$f^n_{i+\frac{1}{2}} = \frac{1}{2}[f(u^n_{i+1}) + f(u^n_i)] - \frac{1}{2}\frac{\Delta x}{\Delta t}[u^n_{i+1} - u^n_i]$ $u^{n+1}_i = u^n_i - \frac{\alpha_{\rm c}}{2}[u^n_{i+1} - u^n_{i-1}] + \frac{1}{2}[u^n_{i+1} - 2u^n_i + u^n_{i-1}]$
Lax-Wendroff	$f^n_{i+\frac{1}{2}} = \frac{1}{2}[f(u^n_{i+1}) + f(u^n_i)] - \frac{v^2}{2}\frac{\Delta t}{\Delta x}[u^n_{i+1} - u^n_i]$ $u^{n+1}_i = u^n_i - \frac{\alpha_{\rm c}}{2}[u^n_{i+1} - u^n_{i-1}] + \frac{\alpha^2_{\rm c}}{2}[u^n_{i+1} - 2u^n_i + u^n_{i-1}]$
Beam-Warming	$f^n_{i+\frac{1}{2}} = \frac{1}{2}[3f(u^n_i) - f(u^n_{i-1})] - \frac{v^2}{2}\frac{\Delta t}{\Delta x}[u^n_i - u^n_{i-1}]$ $u^{n+1}_i = u^n_i - \frac{\alpha_{\rm c}}{2}[3u^n_i - 4u^n_{i-1} + u^n_{i-2}] + \frac{\alpha^2_{\rm c}}{2}[u^n_i - 2u^n_{i-1} + u^n_{i-2}]$
Fromm	$f^n_{i+\frac{1}{2}} = \frac{1}{4}[f(u^n_{i+1}) + 4f(u^n_i) - f(u^n_{i-1})] - \frac{v^2}{4}\frac{\Delta t}{\Delta x}[u^n_{i+1} - u^n_i - u^n_{i-1} + u^n_{i-2}]$ $u^{n+1}_i = u^n_i - \frac{\alpha_{\rm c}}{4}[u^n_{i+1} + 3u^n_i - 5u^n_{i-1} + u^n_{i-2}] + \frac{\alpha^2_{\rm c}}{4}[u^n_{i+1} - u^n_i - u^n_{i-1} + u^n_{i-2}]$

Table listing all the explicit integration schemes discussed in the text. For each entry the first line indicates the flux, while the second line indicate the conservative update formula for the 1D linear advection equation, for which $f(u) = vu$, with v the constant advection speed. The parameter $\alpha_{\rm c}$ is the Courant (or CFL) parameter given by $\alpha_{\rm c} = v\,\Delta t/\Delta x$.

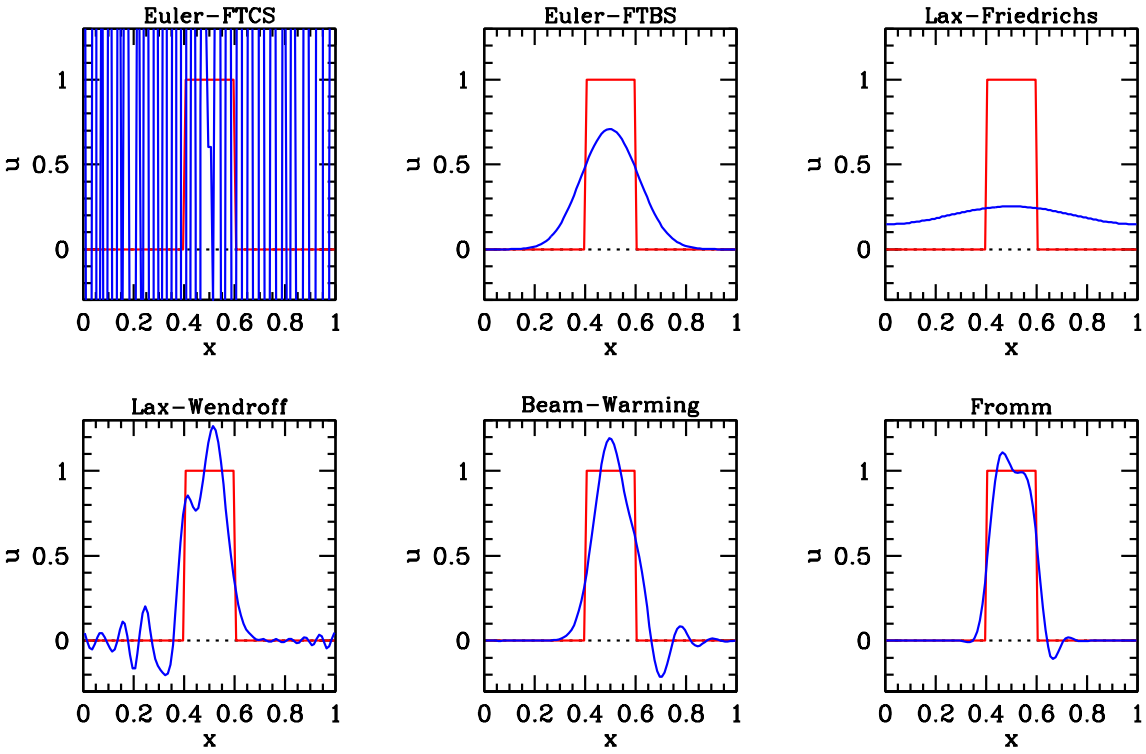

Figure 30: *The result of using 6 different explicit integration schemes, as indicated, to propagate the initial conditions indicated by red using the 1D linear advection equation with a constant velocity* $v = 1.0$. *All schemes use a Courant parameter* $\alpha_c = 0.1$, *and 100 grid points to sample* $u(x)$ *over the* x*-interval* $[0, 1]$, *assuming periodic boundary conditions. The blue curves show the results after 1000 time steps of* $\Delta t = 0.001$, *which covers exactly one full period.*

CHAPTER 18

Consistency, Stability, and Convergence

In the previous chapter we have explored a variety of finite difference methods, applied to a super-simple PDE, namely the 1D linear advection equation (whose analytical solution is trivially known). And we have seen that each method has its own shortcomings. In some cases, large oscillations develop, that continue to grow, in other cases, numerical diffusion washes away any sharp features.

In this chapter we address the question how one can test/assess the performance of finite difference schemes. We start by introducing some relevant terms:

Consistency: A numerical scheme is consistent if its *discrete* operator (with finite differences) converges towards the *continuous* operator (with derivatives) of the PDE in the limit $\Delta t, \Delta x \to 0$ (which is the limit of vanishing truncation error).

Stability: A numerical scheme is stable if numerical noise, from initial conditions, round-off errors, etc., does not grow.

Convergence: A numerical scheme converges if its solution converges towards the real solution of the PDE in the limit $\Delta t, \Delta x \to 0$.

The three 'aspects' of a numerical scheme are related through what is known as **Lax's equivalance theorem:** It states that *for a consistent finite difference method, for a well-posed linear initial value problem, the method is convergent if and only if it is stable.*

The theorem is important since it allows one to assess **convergence** of a finite difference method, which is ultimately what one is interested in, by establishing whether the method is **consistent** and **stable**. Consistency, the requirement that the finite difference scheme approximates the correct PDE is straightforward to verify, and stability is typically much easier to test than convergence. In the remainder of this chapter we discuss how to test for stability, and we introduce the concept of the

modified equation, which is useful to develop a feeling for the behavior of a finite difference method.

Truncation error: As we have seen in the previous chapter, the finite differences are typically obtained using Taylor series expansion up to some order in Δx and/or Δt. This introduces truncation errors, errors that derive from the fact that the series is truncated at some finite order. The forward and backward Euler schemes are first order in both space and time, we write $\mathcal{O}(\Delta t, \Delta x)$, the FTCS and Lax-Friedrichs schemes are first order in time, but second order in space, i.e., $\mathcal{O}(\Delta t, \Delta x^2)$, and the Lax-Wendroff, Beam-Warming and Fromm methods are all second order in both space and time, i.e., $\mathcal{O}(\Delta t^2, \Delta x^2)$. Typically higher order yields better accuracy, if stable. Or, put differently, one can achieve the same accuracy but using a coarser grid/mesh.

As we have seen in the previous chapter, the first-order method that appears stable (the upwind/donor cell methods) yields smeared solutions, while the second-order methods (Lax-Wendroff, Beam-Warming and Fromm) give rise to oscillations. This qualitively different behavior of first and second order methods is typical and can be understood using an analysis of what is called the **modified equation**. Recall that the discrete equation used (i.e., the finite difference scheme adopted) is to approximate the original PDE (in the cases discussed thus far, the 1D linear advection equation). However, the discrete equation may be an *even better approximation* of a modified version of the original PDE (one that corresponds to a higher order of the truncation error). Analyzing this modified equation gives valuable insight into the qualitative behavior of the numerical scheme in question.

As an example, consider the Euler FTCS method, which replaces the actual PDE

$$\frac{\partial u}{\partial t} + v \frac{\partial u}{\partial x} = 0$$

with the following discrete equation

$$\frac{u_i^{n+1} - u_i^n}{\Delta t} + v \frac{u_{i+1}^n - u_{i-1}^n}{2\Delta x} = 0$$

Using Taylor series expansion in time up to second order, we have that

$$u_i^{n+1} = u_i^n + \Delta t \left(\frac{\partial u}{\partial t}\right) + \frac{(\Delta t)^2}{2} \left(\frac{\partial^2 u}{\partial t^2}\right) + \mathcal{O}(\Delta t^3)$$

which implies that

$$\frac{u_i^{n+1} - u_i^n}{\Delta t} = \frac{\partial u}{\partial t} + \frac{\Delta t}{2}\left(\frac{\partial^2 u}{\partial t^2}\right) + \mathcal{O}(\Delta t^2)$$

Similarly, using Taylor series expansion in space up to second order, we have that

$$u_{i+1}^n = u_i^n + \Delta x\left(\frac{\partial u}{\partial x}\right) + \frac{(\Delta x)^2}{2}\left(\frac{\partial^2 u}{\partial x^2}\right) + \mathcal{O}(\Delta x^3)$$

$$u_{i-1}^n = u_i^n - \Delta x\left(\frac{\partial u}{\partial x}\right) + \frac{(\Delta x)^2}{2}\left(\frac{\partial^2 u}{\partial x^2}\right) + \mathcal{O}(\Delta x^3)$$

which implies that

$$\frac{u_{i+1}^n - u_{i-1}^n}{2\Delta x} = \frac{\partial u}{\partial x} + \mathcal{O}(\Delta x^2)$$

Hence, our **modified equation** is

$$\frac{\partial u}{\partial t} + v\frac{\partial u}{\partial x} = -\frac{\Delta t}{2}\frac{\partial^2 u}{\partial t^2} + \mathcal{O}(\Delta t^2, \Delta x^2)$$

Using that

$$\frac{\partial^2 u}{\partial t^2} = \frac{\partial}{\partial t}\left(\frac{\partial u}{\partial t}\right) = -v\frac{\partial}{\partial t}\left(\frac{\partial u}{\partial x}\right) = -v\frac{\partial}{\partial x}\left(\frac{\partial u}{\partial t}\right) = v^2\frac{\partial^2 u}{\partial x^2}$$

where in the second and final step we have used the original PDE to relate the temporal derivate to the spatial derivative. Using this, we can write our **modified equation** as

$$\frac{\partial u}{\partial t} + v\frac{\partial u}{\partial x} = -v^2\frac{\Delta t}{2}\frac{\partial^2 u}{\partial x^2} + \mathcal{O}(\Delta t^2, \Delta x^2)$$

Note that the first term on the right-hand side is a **diffusion term**, with a diffusion coefficient

$$\mathcal{D} = -v^2\frac{\Delta t}{2}$$

Hence, to second order, the discrete equation of the 1D linear advection equation based on the FTCS method, actually solves what is known as an **advection-diffusion equation**. But, most importantly, the corresponding diffusion coeffient is negative. This implies that the FTCS scheme is **unconditionally unstable**; i.e., there are no Δx and/or Δt for which the FTCS method will yield a stable solution of the 1D linear advection equation.

Let us now apply the same method to the FTBS scheme, whose discrete equation for the 1D linear advection equation is given by

$$\frac{u_i^{n+1} - u_i^n}{\Delta t} + v\,\frac{u_i^n - u_{i-1}^n}{\Delta x} = 0$$

Using Taylor series expansions as above, one finds that

$$\frac{u_i^n - u_{i-1}^n}{\Delta x} = \frac{\partial u}{\partial x} - \frac{\Delta x}{2}\frac{\partial^2 u}{\partial x^2} + \mathcal{O}(\Delta x^2)$$

Hence, our **modified equation** is

$$\frac{\partial u}{\partial t} + v\,\frac{\partial u}{\partial x} = -\frac{\Delta t}{2}\frac{\partial^2 u}{\partial t^2} + v\,\frac{\Delta x}{2}\frac{\partial^2 u}{\partial x^2} + \mathcal{O}(\Delta t^2, \Delta x^2)$$

which can be recast in the **advection-diffusion equation** form with

$$\mathcal{D} = v\,\frac{\Delta x}{2} - v^2\,\frac{\Delta t}{2} = v\,\frac{\Delta x}{2}\left(1 - v\,\frac{\Delta t}{\Delta x}\right) = v\,\frac{\Delta x}{2}\,(1 - \alpha_{\mathrm{c}})$$

Thus we see that we can achieve **stable diffusion** (meaning $\mathcal{D} > 0$) if $v > 0$ and $\alpha_{\mathrm{c}} < 1$ (the latter is the CFL-condition, which has to be satisfied anyways). This explains the diffuse nature of the FTBS scheme (see Fig. 28). It also shows that if $v < 0$ one needs to use the FTFS scheme, to achieve similar stability. The **upwind** or **donor cell** scheme is generic term to refer to the FTBS (FTFS) scheme if $v > 0$ ($v < 0$). Or, put differently, in the upwind method the *spatial differencing is performed using grid points on the side from which information flows.*

The student is encouraged to apply this method to other finite difference schemes. For example, applying it to the Lax-Friedrichs method yields once again a modified equation of the advection-diffusion form, but this time with a diffusion coefficient

$$\mathcal{D} = \frac{\Delta x^2}{2\Delta t}(1 - \alpha_{\mathrm{c}}^2)$$

which results in stable diffusion ($\mathcal{D} > 0$) as long as the CFL-criterion is satisfied.

For Lax-Wendroff and Beam-Warming one obtains modified equations of the form

$$\frac{\partial u}{\partial t} + v\,\frac{\partial u}{\partial x} = \eta\,\frac{\partial^3 u}{\partial x^3} + \mathcal{O}(\Delta t^3, \Delta x^3)$$

with

$$\eta = \frac{v\Delta x^2}{6}\left(\alpha_c^2 - 1\right) \qquad \text{Lax-Wendroff}$$
$$\eta = \frac{v\Delta x^2}{6}\left(2 - 3\alpha_c + \alpha_c^2\right) \qquad \text{Beam-Warming}$$

In order to understand the behavior of the explicit, second-order schemes, consider the modified equation

$$\frac{\partial u}{\partial t} + v\,\frac{\partial u}{\partial x} = \eta\,\frac{\partial^3 u}{\partial x^3}$$

Applying this to a linear wave with frequency ω and wave number k, i.e., $u \propto \exp[\pm i(kx - wt)]$, yields a **dispersion relation**

$$-i\omega + i\,v\,k = -i\,\eta\,k^3 \qquad \Rightarrow \qquad \omega = v\,k + \eta\,k^3$$

and thus a **group velocity**

$$c_g \equiv \frac{\partial \omega}{\partial k} = v + 3\eta k^2$$

Hence, different waves move with a different group velocity, which means that the solution of the above equation is **dispersive**. Numerical noise due to (for example) the truncation error can be written as a Fourier series, and different modes will propagate at different speeds. In particular, if we satisfy the CFL criterion, such that $|\alpha_c| < 1$, then we see that $\eta < 0$ for the Lax-Wendroff scheme. This in turn implies that $c_g < v$, and thus that the noise-modes will start to trail with respect to the advection. This explains why the noise in this scheme is present downwind (see lower-left panel of Fig. 30). In the case of the Beam-Warming method, we have that $\eta > 0$ (if CFL-criterion is satisfied), and thus $c_g > v$; indeed, for this method the noise-induced oscillations lead the advection (see lower middle panel of Fig. 30).

We now turn our attention to the stability of finite difference schemes. In the case where the original PDE is linear, one can assess the stability of the finite difference method using a **von Neumann stability analysis**. This analysis models the numerical noise as a Fourier series, and investigates whether the amplitude of the Fourier modes will grow or not. To see how this works, consider once again the 1D linear advection equation, as discretized by the FTCS method:

$$u_i^{n+1} = u_i^n - \frac{\alpha_c}{2}\left[u_{i+1}^n - u_{i-1}^n\right]$$

Since the underlying PDE is linear, the numerical noise, which is what is added to the actual solution, also obeys the above equation. The von Neumann stability analysis therefore starts by writing the present solution as a Fourier series (representing the numerical noise), i.e.,

$$u_i^n = \sum_k A_k^n \exp(-ikx_i)$$

where we have assumed period boundary conditions, such that we have a discrete sum of modes. Substitution in the above equation yields

$$\begin{aligned} A_k^{n+1} &= A_k^n \left[1 - \frac{\alpha_c}{2}\exp(-ik\Delta x) + \frac{\alpha_c}{2}\exp(+ik\Delta x)\right] \\ &= A_k^n \left[1 + i\alpha_c \sin(k\Delta x)\right] \end{aligned}$$

where we have used that $\sin x = (e^{ix} - e^{-ix})/2i$. The evolution of the mode amplitudes is thus given by

$$\zeta^2 \equiv \frac{|A_k^{n+1}|^2}{|A_k^n|^2} = 1 + \alpha_c^2 \sin^2(k\Delta x)$$

As is evident, we have that $\zeta > 1$, for all k. Hence, for any k the mode amplitude will grow, indicating that the FTCS method is inherently, **unconditionally unstable**.

Now let's apply the same analysis to the upwind scheme (FTBS), for which the discrete equation is given by

$$u_i^{n+1} = u_i^n - \alpha_c \left[u_i^n - u_{i-1}^n\right]$$

Substituting the Fourier series yields

$$\begin{aligned} A_k^{n+1} &= A_k^n \left[1 - \alpha_c + \alpha_c \exp(+ik\Delta x)\right] \\ &= A_k^n \left[1 - \alpha_c + \alpha_c \cos(k\Delta x) + i\alpha_c \sin(k\Delta x)\right] \end{aligned}$$

After a bit of algebra, one finds that the evolution of the mode amplitudes is thus given by

$$\zeta^2 \equiv \frac{|A_k^{n+1}|^2}{|A_k^n|^2} = 1 - 2\alpha_c(1-\alpha_c)[1 - \cos(k\Delta x)]$$

Upon inspection, this has $\zeta < 1$ if $\alpha_c < 1$; Hence, *the upwind scheme is stable as long as the CFL condition is satisfied.* Note, though, that the fact that $\zeta < 1$ implies not only that the numerical noise will not grow, but also that the actual solution will decline with time. Pure advection, which is what the actual PDE describes, show have $\zeta = 1$, i.e., solutions only move, they don't grow or decay with time. Hence, the

fact that our FDA has $\zeta < 1$ is not physical; rather, this represents the numerical diffusion that is present in the upwind scheme.

In Problem Set 3, the students will perform a similar von Neumann stability analysis for an explicit FDA of the heat equation.

CHAPTER 19

Reconstruction and Slope Limiters

In the previous two chapters we discussed how numerically solving the equations of hydrodynamics means that we have to develop a FDA of the PDE (typically hyperbolic, potentially with non-ideal parabolic terms). We discussed how we can obtain insight as to the behavior of the FDA by examining the corresponding modified equation, and by performing a von Neumann stability analysis.

We have compared various FDA schemes to solve the 1D linear advection equation, but found all of them to have serious shortcomings. These became especially apparent when we examined the advection of ICs that contained discontinuities. The first-order FDA schemes were too diffusive and dissipative, while the second order schemes gave rise to spurious over- and undershoots. The latter can be fatal whenever the property to be advected is inherently positive (i.e., mass density). In fact, this relates to an important theorem due to Godunov,

Godunov Theorem: *there are no linear higher-order schemes for treating linear advection that retain positivity of the solution.*

So how are we to proceed? The solution, originally proposed by Dutch astrophysicist Bram van Leer from Leiden, is to use a *non-linear* scheme to treat *linear* advection. This is sometimes called **non-linear hybridization**. These non-linear schemes, though, are based on the **finite volume formulation**, rather than the finite difference formulation adopted thus far. We can transition to the finite volume formulation by taking the **integral form** of the linear advection equation. This is obtained by integrating the **advection equation in conservative form**,

$$\frac{\partial u}{\partial t} + \frac{\partial f}{\partial x} = 0$$

over each cell, which is bounded by $x_{i-\frac{1}{2}} \equiv x_i - \Delta x/2$ and $x_{i+\frac{1}{2}} \equiv x_i + \Delta x/2$, and by t^n and $t^{n+1} = t^n + \Delta t$. Note that, in the case of linear advection considered here $f = vu$ with v the constant advection speed, and u the property that is advected. However, what follows is valid for any flux f.

The above equation in integral form is simply

$$\int_{x_{i-\frac{1}{2}}}^{x_{i+\frac{1}{2}}} \mathrm{d}x \int_{t^n}^{t^{n+1}} \mathrm{d}t \left[\frac{\partial u}{\partial t} + \frac{\partial f}{\partial x}\right] = 0$$

which reduces to

$$\int_{x_{i-\frac{1}{2}}}^{x_{i+\frac{1}{2}}} \mathrm{d}x \left[u(x,t^{n+1}) - u(x,t^n)\right] + \int_{t^n}^{t^{n+1}} \mathrm{d}t \left[f(x_{i+\frac{1}{2}},t) - f(x_{i-\frac{1}{2}},t)\right] = 0$$

If we now introduce the cell-averaged quantities

$$U_i^n \equiv \frac{1}{\Delta x}\int_{x_{i-\frac{1}{2}}}^{x_{i+\frac{1}{2}}} u(x,t^n)\mathrm{d}x\,, \qquad U_i^{n+1} \equiv \frac{1}{\Delta x}\int_{x_{i-\frac{1}{2}}}^{x_{i+\frac{1}{2}}} u(x,t^{n+1})\mathrm{d}x$$

and

$$F_{i-\frac{1}{2}}^{n+\frac{1}{2}} \equiv \frac{1}{\Delta t}\int_{t^n}^{t^{n+1}} f(x_{i-\frac{1}{2}},t)\mathrm{d}t\,, \qquad F_{i+\frac{1}{2}}^{n+\frac{1}{2}} \equiv \frac{1}{\Delta t}\int_{t^n}^{t^{n+1}} f(x_{i+\frac{1}{2}},t)\mathrm{d}t$$

then the update formula for the advection equation becomes

$$\boxed{U_i^{n+1} = U_i^n - \frac{\Delta t}{\Delta x}\left(F_{i+\frac{1}{2}}^{n+\frac{1}{2}} - F_{i-\frac{1}{2}}^{n+\frac{1}{2}}\right)}$$

This is similar to the update formula for the conservation equation that we derived in chapter 17, expect that here the quantities are volume averaged. Note that this equation is <u>exact</u> (it is not a numerical scheme), as long as the U and F involved are computed using the above integrations.

Computing the precise fluxes, though, requires knowledge of $u(x,t)$ over each cell, and at each time. This is easy to see within the context of the linear advection equation: Let $u(x,t^n)$ be the continuous description of u at time t^n. Then, the amount of u advected to the neighboring downwind cell in a timestep Δt is simply given by $\Delta u = \int_{x+\frac{1}{2}-v\Delta t}^{x+\frac{1}{2}} u(x,t^n)\mathrm{d}x$ (assuming that $v\Delta t < \Delta x$), and the time-averaged flux

through the corresponding cell face is $F_{i+\frac{1}{2}}^{n+\frac{1}{2}} = \Delta u/\Delta t$. If the continuous $u(x, t^n)$ is known, this flux can be computed, and the advection equation (in integral form) can be solved exactly. However, because of the discrete nature of sampling, we only know u at finite positions x_i, and the best we can hope to do is to *approximate* Δu, and thus the corresponding flux. Once such approximations are introduced, the update formula becomes a numerical scheme, called a **Godunov scheme**.

One ingredient of such a scheme is **reconstruction**, which refers to a method to reconstruct the continuous $u(x, t^n)$ from the discrete $u_i^n = u(x_i, t^n)$. In Godunovs first order method, it is assumed that $u(x, t)$ is **piecewise constant**; i.e., $u(x, t^n) = U_i^n$ for $x_{i-\frac{1}{2}} \leq x \leq x_{i+\frac{1}{2}}$. Obviously this is basically the simplest, lowest-order approximation one can make. Godunov then used the fact that the discontinuities between adjacent cells, if interpreted as real, basically consistitute what is called a **Riemann problem**, for which a solution can (often) be found analytically. This then allows one to compute the fluxes $F_{i\pm\frac{1}{2}}^{n+\frac{1}{2}}$, which in turn allows one to update $U_i^n \rightarrow U_i^{n+1}$. We will discuss the Riemann problem, and (approximate) Riemann solvers in Chapter 21. Here, we will apply this first-order Godunov scheme to our 1D linear advection equation.

The left-hand panel of Fig. 31 shows the condition for some particular $u(x_i)$ at time t^n. Only 5 cells are shown, for the sake of clarity. The cells are assumed to have a constant distribution of u (i.e., we have made the piecewise constant assumption). Let us now focus on cell i, which straddles a discontinuity in u. Advection with a constant $v > 0$ simply implies that in a time step Δt the piecewise constant profile of $u(x)$ shifts right-ward by an amount $v\Delta t$. This right-ward shift is indicated in the right-hand panel of Fig. 31 by the dashed lines. At the end of the time-step, i.e., at time t^{n+1}, we once again want the fluid to be represented in a piecewise constant fashion over the cells. This is accomplished, for cell i, by integrating $u(x)$ under the dashed lines from $x_{i-\frac{1}{2}}$ to $x_{i+\frac{1}{2}}$ and dividing it by Δx to obtain the new cell-averaged value U_i^{n+1}. The new U_i thus obtained are indicated by the solid lines in the right-hand panel. The U_i^{n+1} differs from U_i^n because some amount of u has flown into cell i from cell $i-1$ (indicated by the light-gray shading), and some amount of u has flown from i into cell $i+1$ (indicated by the dark-gray shading). The corresponding time-averaged fluxes obey

$$\Delta t\, F_{i-\frac{1}{2}}^{n+\frac{1}{2}} = (v\,\Delta t)\, U_{i-1}^n\,, \qquad \text{and} \qquad \Delta t\, F_{i+\frac{1}{2}}^{n+\frac{1}{2}} = (v\,\Delta t)\, U_i^n$$

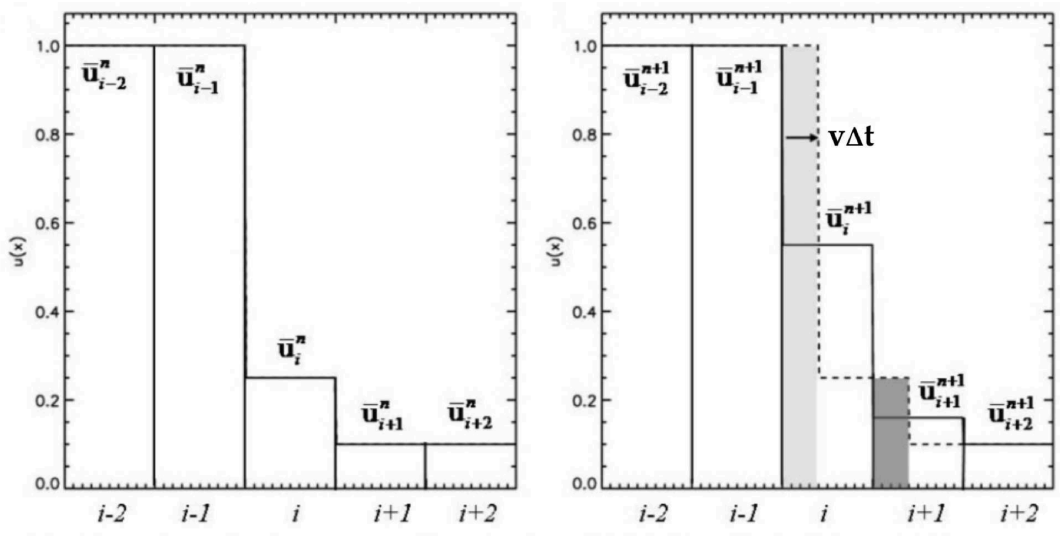

Figure 31: *A single time step in the linear advection of a fluid modelled using piecewise constant reconstruction. The left-hand panel (a) shows the conditions at time t^n. The right-hand panel (b) shows the slabs of fluid after they have been advected for a time Δt (dashed lines) as well as the final profile of $u(x)$ at the end of the time step (solid lines). The total amount of fluid entering (leaving) cell i is shaded light-gray (dark-gray). [Figure adapted from Prof. D. Balsara's lecture notes on "Numerical PDE Techniques for Scientists and Engineers"].*

By invoking conservation of u, we then have that

$$\Delta x\, U_i^{n+1} = \Delta x\, U_i^n + \Delta t\, F_{i-\frac{1}{2}}^{n+\frac{1}{2}} - \Delta t\, F_{i+\frac{1}{2}}^{n+\frac{1}{2}}$$

which implies that

$$U_i^{n+1} = U_i^n - v\frac{\Delta t}{\Delta x}\left(U_i^n - U_{i-1}^n\right) = U_i^n - \alpha_{\rm c}\left(U_i^n - U_{i-1}^n\right)$$

Note that this is exactly the **first-order accurate FTBS upwind (or donor-cell) scheme** from Chapter 17, but now applied to the volume average quantities.

So, one might wonder, what is so 'special' about this **Godunov scheme**? Well, the ingenious aspect of Godunov's method is that is yields an upwind scheme for a general, non-linear system of hyperbolic PDEs. For a linear system of equations, upwind schemes can only be used if all velocities of all waves in the problem (recall

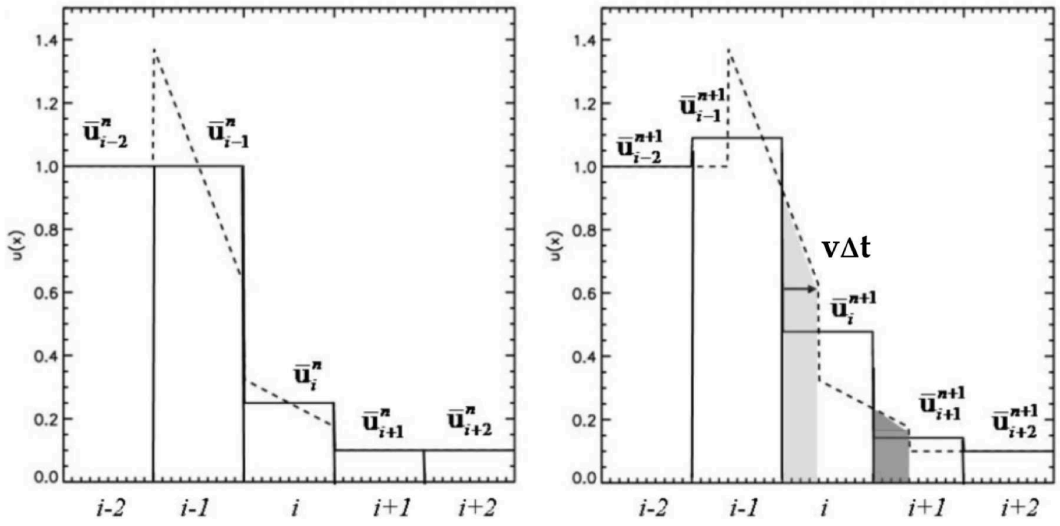

Figure 32: *Same as Fig. 31, but this time piecewise linear reconstruction is used, based on right-sided slopes (thus giving rise to the Lax-Wendroff scheme). Note how the linear reconstruction has introduced a new, higher-than-before, extremum in cell* $i+1$*, which is ultimately responsible for the spurious oscillations characteristic of second-order schemes. As discussed in the text, the solution is to develop a Total Variation Diminishing (TVD) scheme with the use of slope-limiters. [Figure adapted from Prof. D. Balsara's lecture notes on "Numerical PDE Techniques for Scientists and Engineers"].*

that hyperbolic PDEs describe travelling waves) have the same sign. If mixed signs are present, one can typically split the flux $F(u)$ in two components: F^+ and F^- which correspond to the fluxes in opposite directions. This is called **Flux Vector Splitting**. The linearity of the PDE(s) then assures that the solution of the PDE is simply given by the sum of the PDEs for F^+ and F^- separately. However, for a non-linear system (we will encounter such systems in the next chapter) this approach will not work. This is where Godunov's method really brings its value to bear.

For now, though, we apply it to the 1D linear advection equation, in which case it simply becomes identical to the first-order accurate FTBS scheme. And as we have already seen, this scheme suffers from a large amount of numerical diffusion. But, within the Godunov scheme, we can now try to overcome this by going to higher-order. In terms of **reconstruction**, this implies going beyond piecewise constant reconstruction.

The logical next-order step in reconstruction is to assume that within each cell $u(x)$ follows a linear profile, with a slope that is determined by the values of U at its neighboring cells. This is called **piecewise linear reconstruction**. As always, we have three choices for the slope: a right-sided finite difference $\delta U_i^n = U_{i+1}^n - U_i^n$, a left-sided difference $\delta U_i^n = U_i^n - U_{i-1}^n$ and a central difference $\delta U_i^n = (U_{i+1}^n - U_{i-1}^n)/2$. In what follows we shall refer to δU_i^n as the **slope**, eventhough it really is only an **undivided difference**.

The left-hand panel of Fig. 32 shows the same mesh function as in Fig 31, but this time the dashed lines indicate the reconstructed profile based on the right-sided slopes. For cells $i-2$, $i+1$ and $i+2$, this right-sided slope is zero, and the reconstruction is thus identical to that for the piecewise constant case. However, for cells $i-1$ and i reconstruction has endowed the cells with a non-zero slope. For example, the profile of $u(x)$ in cell i is given by

$$u_i^n(x) = U_i^n + \frac{\delta U_i^n}{\Delta x}(x - x_i)$$

where x_i is the central position of cell i. It is easy to see (the student should do this), that upon substitution of this profile in the integral expression for U_i^n, one obtains that $U_i^n = u_i^n$, as required.

Advecting the fluid *with second-order accuracy* is equivalent to shifting the *piecewise linear profile* rightwards by a distance $v\Delta t$. The resulting, shifted profile is shown in the right-hand panel of Fig. 32. As in Fig. 31, the light-gray and dark-gray shaded regions indicate the amount of u that is entering cell i from cell $i-1$, and leaving cell i towards $i+1$, respectively. With a little algebra, one finds that the associated time-averaged fluxes obey

$$\Delta t\, F_{i-\frac{1}{2}}^{n+\frac{1}{2}} = (v\Delta t)\left[U_{i-1}^n + \frac{1}{2}(1-\alpha_{\rm c})\delta U_{i-1}^n\right]$$

and

$$\Delta t\, F_{i+\frac{1}{2}}^{n+\frac{1}{2}} = (v\Delta t)\left[U_{i}^n + \frac{1}{2}(1-\alpha_{\rm c})\delta U_{i}^n\right]$$

As before, invoking conservation of u then implies that

$$\boxed{U_i^{n+1} = U_i^n - \alpha_{\rm c}\left(U_i^n - U_{i-1}^n\right) - \frac{\alpha_{\rm c}}{2}(1-\alpha_{\rm c})\left(\delta U_i^n - \delta U_{i-1}^n\right)}$$

A comparison with the update formula in the piecewise constant case, we see that we have added an extra term proportional to $(\Delta t/\Delta x)^2$ that depends on the slopes. Hence, this is indeed a second-order scheme. By substituting the expressions for the right-sided bias adopted here, the update formula becomes identical to that of the **Lax-Wendroff scheme** that we encountered in Chapter 17, but with u_i replaced by U_i. Similarly, it is easy to show that using the left-sided slopes, yields an update formula equal to that for the **Beam-Warming scheme**, while the central slopes yield an update formula identical to **Fromm's scheme**.

Piecewise Constant Reconstruction	$\rightarrow$	Upwind scheme
Piecewise Linear Reconstruction		
+ right-sided slopes	$\rightarrow$	Lax-Wendroff scheme
+ central slopes	$\rightarrow$	Fromm scheme
+ left-sided slopes	$\rightarrow$	Beam-Warming scheme

Finite volume reconstruction methods and their link to finite difference schemes.

As we have seen in Chapter 17, these second-order accurate schemes all give rise to large oscillations; large over- and undershoots. And as we know from **Godunov's theorem**, these schemes are not positivity-conserving. Fig. 32 makes it clear where these problems come from. Advection of the linearly reconstructed $u(x)$ has caused a spurious overshoot in cell $i-1$ at time t^{n+1}. Upon inspection, it is clear that this overshoot arises because our reconstruction has introduced values for $u(x)$ that are higher than any u_i present at t^n. Once such an unphysical extremum has been introduced, it has a tendency to grow in subsequent time-steps. Using the centered slopes would cause a similar overshoot (albeit somewhat smaller), while the left-sided slopes will result in an *under*shoot in cell $i+1$.

This insight shows us that the over- and under-shoots have their origin in the fact that the linear reconstruction introduces new extrema that were not present initially. The solution, which was originally suggested by Bram van Leer, is to *limit* the piecewise linear profile within each cell such that no new extrema are introduced. This is accomplished by introducing **slope-limiters** (or, very similar, **flux-limiters**). The idea is simple: limit the slopes δU_i^n, such that no new extrema are introduced. Over the years, many different slope-limiters have been introduced by the computational

fluid dynamics community. All of these use some combination of the left- and right-sided slopes defined above. An incomplete list of slope-limiters is presented in the Table below.

An incomplete list of Slope Limiters

van Leer	$\delta U_i^n = \ Q(\delta_{\rm L}, \delta_{\rm R}) \, \frac{\delta_{\rm L}\, \delta_{\rm R}}{\lvert\delta_{\rm L}\rvert + \lvert\delta_{\rm R}\rvert}$
MinMod	$\delta U_i^n = \frac{1}{2} Q(\delta_{\rm L}, \delta_{\rm R}) \min(\lvert\delta_{\rm L}\rvert, \lvert\delta_{\rm R}\rvert)$
Monotized Central	$\delta U_i^n = \frac{1}{2} Q(\delta_{\rm L}, \delta_{\rm R}) \min(\frac{1}{2}\lvert\delta_{\rm L} + \delta_{\rm R}\rvert, 2\lvert\delta_{\rm L}\rvert, 2\lvert\delta_{\rm R}\rvert)$
Superbee	$\delta U_i^n = \frac{1}{2} Q(\delta_{\rm L}, \delta_{\rm R}) \max\left[\min(2\lvert\delta_{\rm L}\rvert, \lvert\delta_{\rm R}\rvert), \min(\lvert\delta_{\rm L}\rvert, 2\lvert\delta_{\rm R}\rvert)\right]$

Here $\delta_{\rm L}$ *and* $\delta_{\rm R}$ *are the left- and right-sided slopes, and* $Q(\delta_{\rm L}, \delta_{\rm R}) = [\mathrm{sgn}(\delta_{\rm L}) + \mathrm{sgn}(\delta_{\rm R})]$ *with* $\mathrm{sgn}(x)$ *the sign-function, defined as* $+1$ *for* $x \geq 0$ *and* -1 *for* $x < 0$.

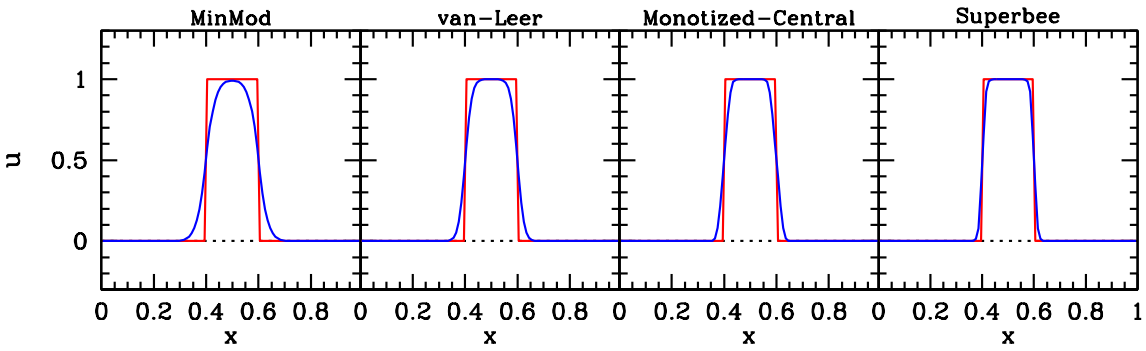

Figure 33: *The result of using Piecewise Linear Reconstruction combined with 4 different slope limiters (as indicated at the top of each panel). to linearly advect the initial conditions shown in red. As in Fig. 30, the advection speed is* $v = 1.0$*, and 100 grid points are used to sample* $u(x)$ *over the* x*-interval* $[0, 1]$*, assuming periodic boundary conditions. The Courant parameter* $\alpha_c = 0.5$*. The blue curves show the results after 1000 time steps of* $\Delta t = 0.001$*, which covers exactly one full period. Note the drastic improvement compared to the finite difference schemes used in Fig. 30!!*

Fig. 33 shows the results of applying our Piecewise Linear Reconstruction with four different slope-limiters (as indicated) to the 1D linear advection of initial conditions indicated by the red top-hat. The blue curves show the results obtained after one period (using periodic boundary conditions) using an advection speed $v = 1.0$, a mesh with 100 grid points on the domain $x \in [0, 1]$, and a Courant parameter $\alpha_c = 0.5$. As can be seen, all limiters produce oscillation-free propogation of the top-hat profile, and with a numerical diffusion that is much smaller than in the case of the upwind finite difference scheme used in Chapter 17 (i.e., compare Fig. 33 to the results in Fig. 30). Clearly, by using a **finite volume formulation** with **non-linear hybridizatrion** in the form of **piecewise linear reconstruction** with the use of **slope limiters** has drastically improved our ability to advect discontinuous features in the fluid.

What is it that makes these slope-limiters so succcessful? In short, the reason is that they are **total variation dimishing**, or **TVD** for short. The total variation, TV of a discrete set $U = U_1, U_2, ..., U_N$ is defined as

$$\boxed{TV(U^n) \equiv \sum_{i=1}^{N} \left| U_{i+1}^n - U_i^n \right|}$$

and an integration scheme is said to be **TVD** iff the total variation does NOT increase with time, i.e.,

$$\boxed{\textbf{TVD} \qquad \Leftrightarrow \qquad TV(U^{n+1}) \leq TV(U^n)}$$

Clearly, whenever a scheme introduces spurious oscillations, the TV will go up, violating the **TVD**-condition. Or, put differently, if a scheme is **TVD**, then it will not allow for the formation of spurious over- and/or under-shoots. Readers interested in finding a quick method to test whether a scheme is **TVD** are referred to the paper *"High Resolution schemes for Conservation Laws"* by Harten (1983) in the Journal of Computational Physics. Here we merely point out that the schemes used in this chapter are all **TVD**.

As we have seen, using reconstruction combined with slope-limiters yields integration schemes that do very well for our 1D linear advection problem. A natural extention to even high-order can be achieved by using high-order in the reconstruction. For example, one could use piecewise parabolic reconstruction, which is third-order accurate in space, and indeed, such schemes have been developed and are in use. It is important, though, to realize that as long as one uses a "piecewise" reconstruction, that discontinuities between neighboring cells persist. And it is these discustinuities that typically cause problems.

This begs the question: why can't we use a continuous reconstruction, i.e., connect all the u_i $(i = 1, 2, ..., N)$ using say an N^{th}-order polynomial. That would assure smoothness and differentiability across the entire computational domain. However, this is not an option, for the simple reason that, as we will see in the next Chapter, discontinuities can be real. An obvious example is a shock, which is a natural outcome of the Euler equations due to its **non-linear** character. Using continuous reconstruction would fail to capture such discontinuities.

As we will see, the solution is to use **Godunov schemes** that rely on use piecewise reconstruction (be it constant, linear or parabolic) and Riemann solvers to compute the fluxes across the resulting discontinuities between adjacent cells. Before we examine this approach in detail, though, we will first take a closer look at non-linearity.

CHAPTER 20

Burgers' Equation & Method of Characteristics

In the previous chapters we examined a number of different numerical schemes to solve the 1D linear advection equation. We derived this equation from the set of hydro-equations by ignoring gravity and radiation, and by assuming constant pressure and velocity (clearly a highly simplified case).

The linear advection equation is an ideal test case because its solution is trivially known (or can be derived using the **method of characteristics** discussed below). In this chapter we are going to consider another equation, which appears very similar to the linear advection equation, except that it is non-linear. As before, we consider the 1D case, and we ignore radiation and gravity. But rather than assuming both P and $\vec{u}$ to be constant, we only assume a constant pressure. This implies that the continuity equation is given by

$$\frac{\partial \rho}{\partial t} + \frac{\partial \rho u}{\partial x} = \frac{\partial \rho}{\partial t} + \rho \frac{\partial u}{\partial x} + u \frac{\partial \rho}{\partial x} = 0$$

while the momentum equation reduces to

$$\frac{\partial \rho u}{\partial t} + \frac{\partial}{\partial x}\left[\rho u u + P\right] = \rho \frac{\partial u}{\partial t} + u \frac{\partial \rho}{\partial t} + \rho u \frac{\partial u}{\partial x} + u \frac{\partial \rho u}{\partial x} = 0$$

where we have used that $\partial P / \partial x = 0$. Multiplying the continuity equation with u and subtracting this from the momentum equation yields

$$\boxed{\frac{\partial u}{\partial t} + u \frac{\partial u}{\partial x} = 0}$$

This equation is known as **Burgers' equation**. Unlike the similar looking advection equation, this is a **non-linear** equation. In fact, it is one of the few non-linear PDEs for which an analytical solution can be found for a select few ICs (see below). The importance of Burgers' equation is that it highlights the quintessential non-linearity of the Euler equations.

Note that the above form of Burgers' equation is not in conservative form. Rather this form is called **quasi-linear**. However, it is trivial to recast Burgers' equation in conservative form:

$$\boxed{\frac{\partial u}{\partial t} + \frac{\partial \frac{1}{2}u^2}{\partial x} = 0}$$

Let's devise finite difference upwind schemes for both (assuming $u > 0$). The results are shown in the table below.

quasi-linear	$\frac{\partial u}{\partial t} + u\frac{\partial u}{\partial x}$	$u_i^{n+1} = u_i^n - \frac{\Delta t}{\Delta x} u_i^n \left[u_i^n - u_{i-1}^n\right]$
conservative	$\frac{\partial u}{\partial t} + \frac{\partial \frac{1}{2}u^2}{\partial x}$	$u_i^{n+1} = u_i^n - \frac{\Delta t}{2\Delta x} \left[(u_i^n)^2 - (u_{i-1}^n)^2\right]$

Forms of Burgers' equation and the corresponding numerical upwind scheme.

Let's use these two schemes to numerically solve Burgers' equation on the domain $x \in [0, 1]$ (using periodic boundary conditions) for an initial velocity field $u(x, 0)$ given by a Gaussian centered at $x = 0.5$, and with a dispersion equal to $\sigma = 0.1$. The initial density is assumed to be uniform. The results for a Courant parameter $\alpha_c = 0.5$ are shown in Fig. 34, where the initial conditions are shown in red, the results from the quasi-linear scheme in magenta (dashed) and the results from the conservative scheme in blue (solid). Note how, in the region where $\partial u/\partial x > 0$ a **rarefaction wave** develops, causing a reduction in the density. Over time, this rarefied region grows larger and larger. In the region where $\partial u/\partial x < 0$ a **compression wave** forms, which steepens over time. As discussed in Chapter 13, because of the non-linear nature of the Euler equations such waves steepen to give rise to shocks, representing discontinuities in flow speed.

Note, though, that at late times the numerical schemes based on the conservative and quasi-linear forms of Burgers' equation yield different predictions for the location of this shock. As it turns out, and as we demonstrate explicitely below, the correct prediction is that coming from the conservative form. This highlights the importance of using a conservative scheme, which is expressed by the following theorem:

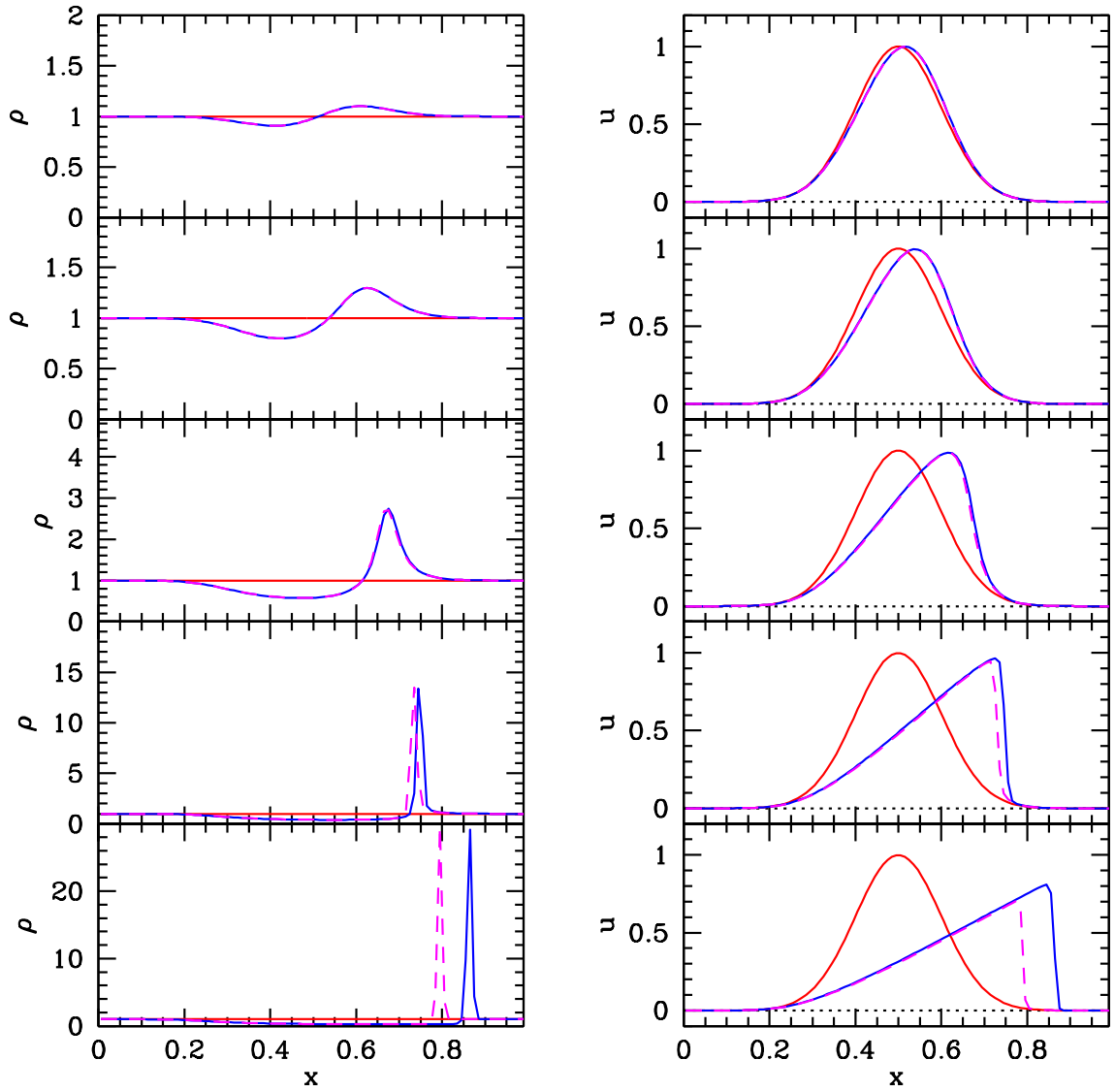

Figure 34: *Evolution as governed by Burgers' equation for an initial, uniform density with the 1D velocity field given by the red Gaussian. Left and right-hand panels show the evolution in density and velocity, respectively. Red lines indicate the initial conditions, while blue (solid) and magenta (dashed) lines indicate the numerical results obtained using the conservative and quasi-linear equations, respectively. Both are solved using the upwind scheme with a Courant parameter* $\alpha_c = 0.5$*, and sampling the* $x = [0, 1]$ *domain using 100 grid points. Note how a shock develops due to the non-linear nature of Burgers' equation, but that the location of the shock differs in the two schemes. Only the conservative scheme yields the correct answer.*

Lax-Wendroff theorem: *If the numerical solution of a conservative scheme converges, it converges towards a weak solution.*

In mathematics, a weak solution (also called a generalized solution) to an ordinary or partial differential equation is a function for which the derivatives may not all exist but which is nonetheless deemed to satisfy the equation in some precisely defined sense. Practically, what the Lax-Wendroff theorem indicates is that the use of equations in conservation form assures that shocks move at the correct speed, and thus converge to the correct location on the mesh.

In order to develop some understanding of the shock and rarefaction, we are going to solve Burgers' equation analytically using the 'method of characteristics', which is a powerful method to solve hyperbolic PDEs.

Method of Characteristics: The idea behind the method of characteristics is to find curves, called *chararacteristics* or *characteristic curves*, along which the PDE becomes an ODE. Once the ODE corresponding to the characteristics is found, these can be solved along the characteristic and transformed into a solution of the PDE. Rather than going through a detailed description of the **method of characteristics**, which can be found in any good textbook on differential calculus[3], we are going to give an example; we will use the method of characteristics to solve the 1D **Burgers equation** which, as discussed above, describes the non-linear evolution of the velocity field in a case without gravity, without radiation, and with a constant pressure (no pressure gradients).

Let the ICs of Burgers' equation be given by the initial velocity field $u(x,0) = f(x)$. Now consider an 'observer' moving with the flow (i.e., an observer 'riding' a fluid element). Let $x(t)$ be the trajectory of this observer. At $t = 0$ the observer is located at x_0 and has a velocity $u_0 = f(x_0)$. We want to know how the velocity of the observer changes as function of time, i.e., along this trajectory. Hence, we want to know

$$\frac{\mathrm{d}u}{\mathrm{d}t} = \frac{\mathrm{d}}{\mathrm{d}t}u(x(t),t) = \frac{\partial u}{\partial t} + \frac{\partial u}{\partial x}\,\frac{\mathrm{d}x}{\mathrm{d}t}$$

[3]or, for an elementary introduction, see https://www.youtube.com/watch?v=tNP286WZw3o

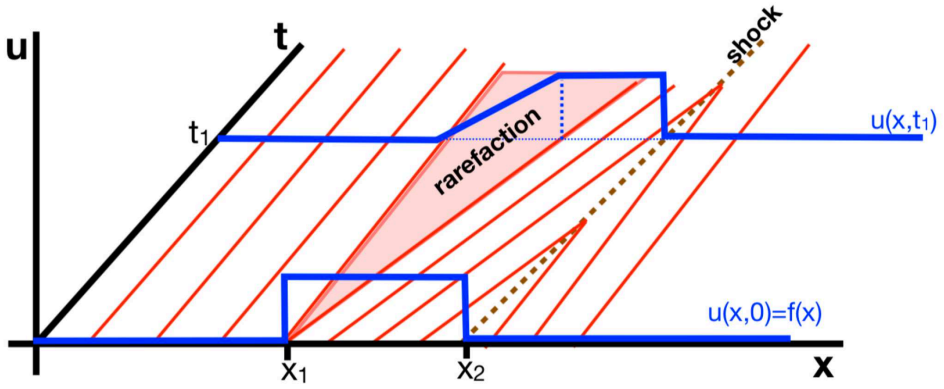

Figure 35: *Solving the Burgers equation for the initial conditions indicated by the blue curve at $t = 0$ using the method of characteristics. The red lines are characteristics; lines along which the velocity remains fixed to the intial value. Not the formation of a rarefaction fan, where the method of characteristics fails to provide a solution, and the formation of a shock where-ever characeristics collide together.*

We see that this equation is equal to Burgers' equation that we seek to solve if $\mathrm{d}x/\mathrm{d}t = u(x,t)$. And in that case we thus have that $\mathrm{d}u/\mathrm{d}t = 0$. Hence, we see that solving the Burgers equation (a quasi-linear, first-order PDE), is equivalent to solving the ODE $\mathrm{d}u/\mathrm{d}t = 0$ along characteristic curves (characteristics) given by $\mathrm{d}x/\mathrm{d}t = u(x,t)$. The solution is simple: $u(x,t) = u_0(x_0,0) = f(x_0)$ where $x_0 = x - u_0 t$. Hence, this can be solved implicitly: for given x and t find the x_0 that solves $x_0 = x - f(x_0)t$. Then, the instantaneous velocity at (x,t) is given by $f(x_0)$.

Fig. 35 illustrates an example. The blue curve indicates the initial conditions; i.e., the initial velocity as function of position x at $t = 0$. It shows a sudden jump (increase) in velocity at x_1 and a sudden decrease at $x = x_2$. The red lines are characteristics, i.e., lines along which the velocity remains constant; their slope is the inverse of the initial velocity at the location x_0 where they cross the $t = 0$ axis. From point x_1, a **rarefraction fan** emenates, which corresponds to a region where the density will decline since neighboring elements spread apart. The method of characteristics does not give a solution in this regime, simply because no characteristics enter here...the solution in this regime turns out to be a linear interpolation between the beginning and end-point of the fan at a given t. From point x_2 a **shock** emenates. Here characteristic from $x_0 < x_2$ 'merge' with characteristics emerging from $x_0 > x_2$. When two characteristics meet, they stop and a discontinuity in the solution emerges (which manifests as a shock).

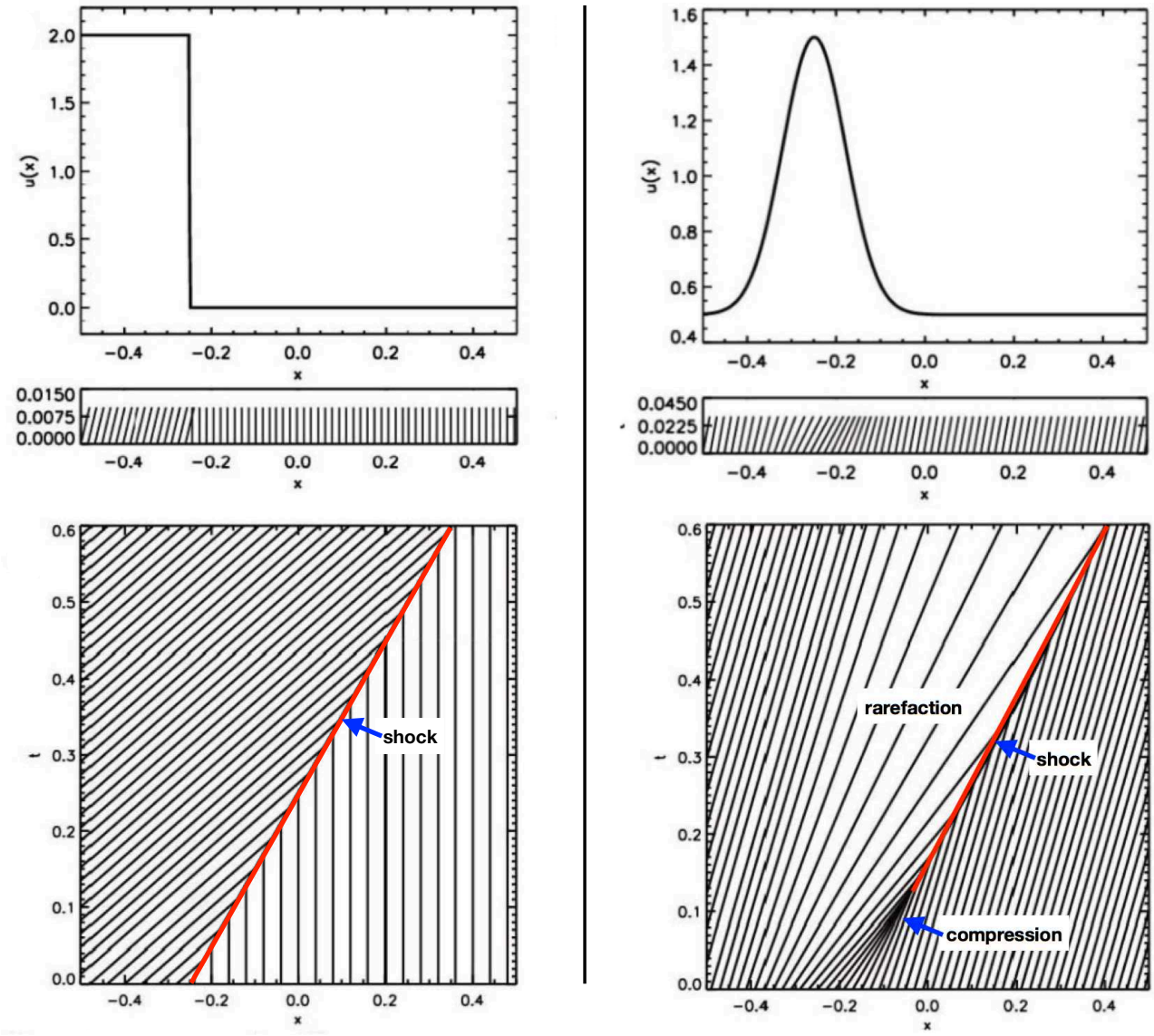

Figure 36: *Initial conditions of $u(x)$ (top panels), and the corresponding characteristics (bottom panels). Note the formation of shocks, and, in the right-hand panel, of a rarefaction wave. Clearly, characteristics give valuable insight into the solution of a hyperbolic PDE.*

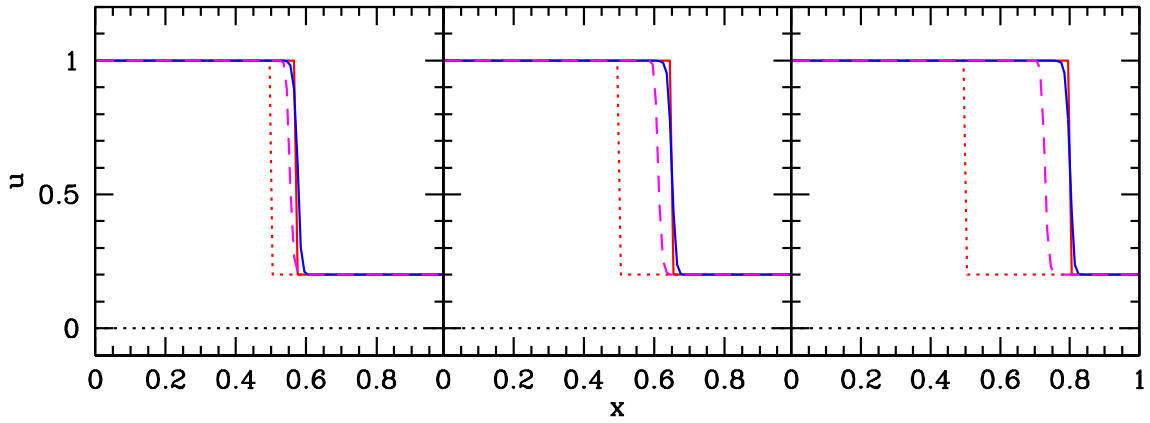

Figure 37: *Evolution of a shock wave in velocity. The initial discontinuity in* $u(x)$ *at* $x = 0.5$ *introduces a shock wave which propagates to the right. The solid red curve panels show the analytical solution (a shock propagating at* $u_{\rm shock} = [u(x < 0.5) + u(x > 0.5)]/2$*), while the red dotted curve shows the ICs. As in Fig. 34, the blue and magenta curves indicate the numerical solutions obtained using conservative and quasi-linear schemes, respectively. Note how the latter fails to reproduce the correct shock speed.*

This is further illustrated in Fig. 36. Upper panels show the initial conditions, with the little bar under the panel indicating with little line-segments the velocity (as reflected by the slope of the line-segment) as function of position. The lower panels plot the characteristics (in a t vs. x plot). Where characteristics merge, a shock forms. It is apparent from the left-hand panels, that the shock in this case will propagate with a speed that is simply the median of the upwind and downwind material, i.e., $u_{\rm shock} = [u(x_2+) + u(x_2-)]/2$. The right-hand panels show the characteristics in the case of the Gaussian ICs also considered in Fig. 34; note how one can see the formation of both a **rarefaction fan** as well as a **shock**.

The example shown in the left-hand panels of Fig. 36 presents us with a situation in which the shock speed is known analytically. We can use this as a test-case to determine which of our numerical schemes (quasi-linear vs. conservative) best reproduces this. We set up ICs in which $u(x) = 1.0$ for $x < 0.5$ and $u(x) = 0.2$ for $x > 0.5$. We solve this numerically using both schemes (with $\alpha_{\rm c} = 0.5$), and compare the outcome to our analytical solution (the shock is moving right-ward with a speed $v_{\rm shock} = (1.0 + 0.2)/2 = 0.6$). The results are shown in Fig. 37. Note

how the solutions from the conservative scheme (in blue) nicely overlap with the analytical solution (in red), while that from the quasi-linear scheme (in magenta) trails behind. This demonstrates the **Lax-Wendroff theorem**, and makes it clear that conservative schemes are required to correctly model the propogation of shocks.

Shock-formation is a natural outcome of the non-linear behavior of the **Burgers' equation**. And since Burgers' equation is a simplified case of the general **Euler equations**, we are to be prepared to deal with shocks and discontinuities in our attempt to numerically solve the hydrodynamic equations. Practically, as we have seen here, this means that we need to consider the Euler equations in conservative form.
%hfill

CHAPTER 21

The Riemann Problem & Godunov Schemes

Thus far, rather than trying to numerically solve the full set of hydrodynamics equations, we instead considered two very special, much simpler cases, namely the **linear advection equation**, and the **non-linear Burgers' equation**, both in 1D. We derived these equation from the set of hydro-equations by assuming an ideal fluid, ignoring gravity and radiation, by assuming constant pressure, and, in the case of the advection equation, also constant velocity. Clearly these are highly simplified cases, but they have the advantage that analytical solution exist, thus allowing us to test our numerical schemes.

We have seen, though, that numerically solving even these super-simple PDEs using finite difference schemes is far from trivial. First order schemes, if stable, suffer from significant numerical diffusion, while second order schemes have a tendency to develop oscillations. As we will discuss in this chapter, and briefly touched upon in Chapter 19, the way forward is to use **Godunov schemes** with **Riemann solvers**.

A **Godunov scheme** is a **Finite Volume Formulation** for solving **conservation laws**, that relies on **reconstruction**. The order of the scheme is related to the method of reconstruction used: **piece-wise constant reconstruction** yields Godunov's first-order scheme. In Chapter 19 we applied this to the linear advection problem, and obtained exactly the first-order Euler FTBS upwind scheme. The power of the first-order Godunov scheme, though, is that it is an upwind scheme for a general, linear or non-linear, system of hyperbolic PDEs; not only for the linear advection equation. If one uses **piece-wise linear reconstruction**, one obtains a scheme that is second-order accurate. As **Godunov's theorem** states, though, a linear higher-order scheme does not preserve positivity, and we have seen the consequences of that in Chapter 17 in the form of large over- and undershoots. As we discussed in Chapter 19, the solution for that is to use a non-linear scheme that involves **slope-limiters**. Applying that to the linear advection equation yields very satisfactory results indeed. And one can in principle take this to even higher accuracy (third-order) by using **piece-wise parabolic reconstruction**, which is something we won't discuss in any detail in these lecture notes (for the interested reader, see Colella & Woodward, 1984).

In this Chapter we are going to see how to apply **Godunov schemes** to the (1D) Euler equations. This will involve **Riemnann solvers**, which are numerical schemes for solving **Riemann problems**, which describes the evolution of a discontinuity in fluid properties. We will discuss how to solve a Riemann problem, apply it to the **SOD shock tube**, and then end by briefly discussing **approximate Riemann solvers**.

Let us first give a brief review of the basics behind the **Godunov scheme**. In the absence of **source/sink terms** (i.e., gravity and radiation), and ignoring viscocity and conduction (which add **parabolic terms**), the hydrodynamic equations reduce to a set of **hyperbolic** PDEs that can be written in **conservation form** as

$$\frac{\partial \vec{u}}{\partial t} + \nabla \cdot \vec{f}(\vec{u}) = 0$$

(see Chapter 17). The update-formula for this equation, in the Finite Volume formulation, is given by

$$\boxed{U_i^{n+1} = U_i^n - \frac{\Delta t}{\Delta x}\left(F_{i+\frac{1}{2}}^{n+\frac{1}{2}} - F_{i-\frac{1}{2}}^{n+\frac{1}{2}}\right)}$$

where the cell-averaged quantities are defined as

$$U_i^n \equiv \frac{1}{\Delta x}\int_{x_{i-\frac{1}{2}}}^{x_{i+\frac{1}{2}}} u(x,t^n)\mathrm{d}x\,, \qquad U_i^{n+1} \equiv \frac{1}{\Delta x}\int_{x_{i-\frac{1}{2}}}^{x_{i+\frac{1}{2}}} u(x,t^{n+1})\mathrm{d}x$$

and

$$F_{i-\frac{1}{2}}^{n+\frac{1}{2}} \equiv \frac{1}{\Delta t}\int_{t^n}^{t^{n+1}} f(x_{i-\frac{1}{2}},t)\mathrm{d}t\,, \qquad F_{i+\frac{1}{2}}^{n+\frac{1}{2}} \equiv \frac{1}{\Delta t}\int_{t^n}^{t^{n+1}} f(x_{i+\frac{1}{2}},t)\mathrm{d}t$$

Reconstruction basically means that one models the continuous $u(x,t)$ from the discrete u_i^n on the mesh. This means that, for $x_{i-\frac{1}{2}} \le x \le x_{i+\frac{1}{2}}$, one assumes that

$$u(x,t^n) = u_i^n \qquad \text{piecewise constant}$$

$$u(x,t^n) = u_i^n + \frac{\delta U_i^n}{\Delta x}(x - x_i) \quad \text{piecewise linear}$$

In the latter δU_i^n is a **slope**, which can be computed centered, left-sided or right-sided. Once such a reconstruction scheme is adopted, one can compute the U_i^n using the integral expression given above. Next, the Godunov schemes use (approximate) Riemann solvers to infer the (time-averaged) fluxes $F_{i-\frac{1}{2}}^{n+\frac{1}{2}}$ and $F_{i+\frac{1}{2}}^{n+\frac{1}{2}}$. The idea is that reconstruction (be it piecewise constant, piecewise linear or piecewise parabolic) leaves discontinuities between adjacent cells. Godunov' insight was to treat these as 'real' and to solve them analytically as Riemann problems. That implies that one now has, at each cell-interface, a solution for $u(x,t)$, which can be integrated over time to infer $F_{i-\frac{1}{2}}^{n+\frac{1}{2}}$ and $F_{i+\frac{1}{2}}^{n+\frac{1}{2}}$. Next, one uses the update formula to compute U_i^{n+1}, and one proceeds cell-by-cell, and time-step by time-step. In what follows we take a closer look at this Riemann problem and how it may be solved.

Riemann Problem: A Riemann problem, named after the mathematician Bernhard Riemann, is a specific initial value problem composed of a conservation equation together with piecewise constant initial data which has a single discontinuity in the domain of interest. Let L and R denote the states to the left and right of the discontuity. Each of these states is described by three quantities. These can be the **conserved quantities** ρ, ρu and $E = \frac{1}{2}\rho u^2 + \rho\varepsilon$, or what are called the **primitive variables** ρ, u, and P.

The solution of the Riemann problem, i.e., the time-evolution of this discontinuous initial state, can comprise

- 0 or 1 contact discontinuitieas (also called entropy jumps)
- 0, 1 or 2 shocks
- 0, 1 or 2 rarefaction waves (or fans)

but, the total number of shocks *plus* rarefaction fans cannot exceed two. All these shocks, entropy jumps and rarefaction waves appear as **characteristics** in the solution. In particular, the velocities of the features are given by the eigenvalues of the Jacobian matrix of the flux function (called the **characteristic matrix**), which is given by

$$A_{ij}(\vec{q}) \equiv \frac{\partial f_i}{\partial q_j}$$

where $\vec{f}(\vec{q})$ is the flux in the Euler equations in conservative form.

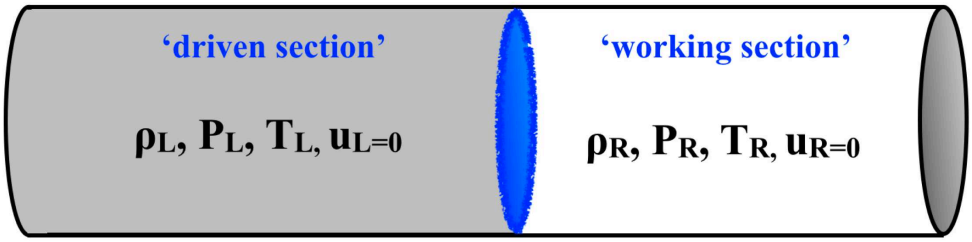

Figure 38: *Initial conditions for the Sod shock tube. The left region has the higher pressure (i.e., $P_{\rm L} > P_{\rm R}$) and is therefore called the driven section, while the region on the right is called the working section. The two regions are initially separated by a diaphragm (in blue), which is instantaneously removed at $t = 0$. Both the fluid on the left and right are assumed to be ideal fluids with an ideal equation of state.*

The solution for a completely general Riemann problem can be tedious, and will not be discussed here. Rather, we will look at a famous special case, the **Sod shock tube problem**, named after Gary Sod who discussed this case in 1978. It is a famous example of a 1D Riemann problem for which the solution is analytical, and which is often used as a typical test-case for numerical hydro-codes.

The shock tube is a long one-dimensional tube, closed at its ends and initially divided into two equal size regions by a thin diagragm (see Fig. 38). Each region is filled with the same gas (assumed to have an ideal equation of state), but with different thermodynamic parameters (pressure, density and temperature). The gas to the left, called the **driven section**, has a higher pressure than that to the right, called the **working section** (i.e., $P_{\rm L} > P_{\rm R}$), and both gases are initially at rest (i.e., $u_{\rm L} = u_{\rm R} = 0$). At $t = 0$, the diagragm, which we consider located at $x = x_0$ is instantaneously removed, resulting in a high speed flow, which propagates into the working section. The high-pressure gas originally in the driven section expands, creating an **expansion or rarefaction wave**, and flows into the working section, pushing the gas of this part. The rarefaction is a continuous process and takes place inside a well-defined region, called the **rarefaction fan**, which grows in width with time (see also Chapter 20). The **compression** of the low-pressure gas results in a **shock wave** propagating into the working section. The expanded fluid (originally part of the driven section) is separated from the compressed gas (originally part of the working section) by a **contact discontinuity**, across which there is a jump in entropy. The velocities and pressures on both sides of the contact discotinuity, though, are identical (otherwise it would be a shock).

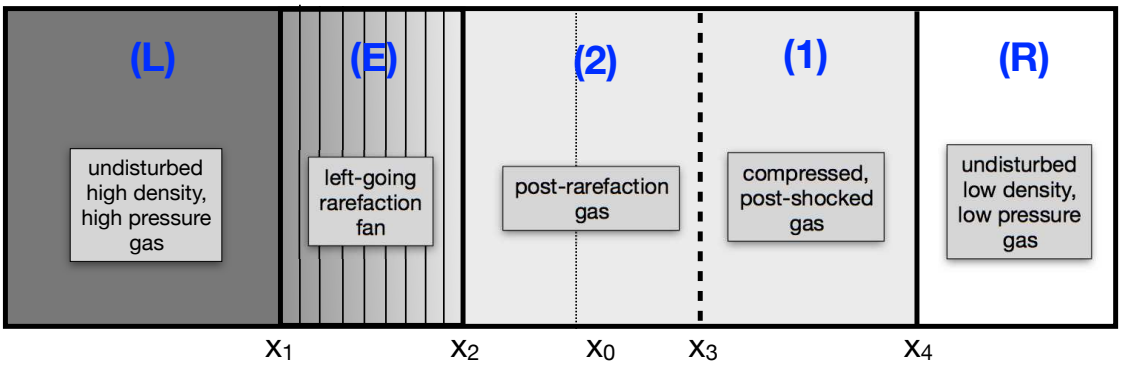

Figure 39: *Illustration of the different zones present in the SOD shock tube. The original diaphragm, which was removed at $t = 0$, was located at x_0 indicated by the dotted line. The solid line at x_4 marks the location of the right-going shock, while the dashed line at x_3 corresponds to a contact discontuity. The region marked (E), between x_1 and x_2, indicates the left-going rarefaction fan. Regions (L) and (R) are not yet affected by the removal of the diaphragm and thus reflect the initial conditions Left and Right of x_0.*

Fig. 39 illustrates the different zones at a time before either the shock wave or the rarefaction fan has been able to reach the end of the tube. Hence, the regions to the far left and far right are still in their original, undisturbed states, to which we refer as the 'L' and 'R' states, respectively. In between, we distinguish three different zones; a rarefaction fan 'E', a region of gas (region '2') that originally came from the driven section but has been rarefied due to expansion, and a region with gas (region '1') that originally belonged to the working section but that has been compressed (it has been overrun by the shock wave). Note that regions 1 and 2 are separated by a contact discontinuity (aka entropy jump).

Our goal is to compute $\rho(x,t)$, $u(x,t)$, and $P(x,t)$ in each zone, as well as the locations x_1, x_2, x_3 and x_4 of the boundaries between each of these zones. This is a typical Riemann problem. It can be solved using the **method of characteristics**, but since we are focussing on numerical hydrodynamics here, we are not going to give the detailed derivation; interested readers are referred to textbooks on this topic. Another useful resource is the paper by Lora-Clavijo et al. 2013, Rev. Mex. de Fisica, 29-50, which gives a detailed description of exact solutions to 1D Riemann problems.

However, even without the method of characteristics, we can use our physical insight developed in these lectures notes to obtain most of the solution. This involves the following steps:

[**1**] First we realize that we can infer the conditions in region '1' from the known conditions in region 'R' using the **Ranking-Hugoniot jump conditions** (see Chapter 13) for a non-radiative shock. If we refer to the **Mach number** of the shock (to be derived below) as $\mathcal{M}_{\rm s} \equiv u_{\rm s}/c_{\rm s,R}$, with $c_{\rm s,R} = \sqrt{\gamma P_{\rm R}/\rho_{\rm R}}$ the sound speed in region 'R', then we have that

$$\begin{aligned} P_1 &= P_{\rm R}\left[\frac{2\gamma}{\gamma+1}\mathcal{M}_{\rm s}^2 - \frac{\gamma-1}{\gamma+1}\right] \\ \rho_1 &= \rho_{\rm R}\left[\frac{2}{\gamma+1}\frac{1}{\mathcal{M}_{\rm s}^2} + \frac{\gamma-1}{\gamma+1}\right]^{-1} \\ u_1 &= \frac{2}{\gamma+1}\left[\mathcal{M}_{\rm s} - \frac{1}{\mathcal{M}_{\rm s}}\right] \end{aligned}$$

Note that for the latter, one first needs to convert to the rest-frame of the shock, in which the velocities in regions 'R' and '1' are given by $u'_{\rm R} = u_{\rm R} - u_{\rm s} = -u_{\rm s}$ and $u'_1 = u_1 + u_{\rm s}$. One then solves for u'_1 and converts to u_1. Finally, if needed one can infer the temperature T_1 from $T_{\rm R}$ using the corresponding RH jump condition according to which $T_1/T_{\rm R} = (P_1\rho_1/P_{\rm R}\rho_{\rm R})$.

[**2**] Having established the properties in zone '1', the next step is to infer the properties in zone '2'. Here we use that the velocity and pressure are constant across a contact discontinuity to infer that $P_2 = P_1$ and $u_2 = u_1$. For the density, we need to link it to $\rho_{\rm L}$, which we can do using the fact that rarefraction is an adiabatic process, for which $P \propto \rho^\gamma$. Hence, we have that $\rho_2 = \rho_{\rm L}(P_2/P_{\rm L})^{1/\gamma}$.

[**3**] What remains is to compute the shock speed, $u_{\rm s}$, or its related Mach number, $\mathcal{M}_{\rm s}$. This step is not analytical, though. Using insight that can be gained from the method of characteristics, not discussed here, one can infer that the Mach number is a solution to the following implicit, non-linear equation, which needs to be solved numerically using a root finder:

$$\mathcal{M}_{\rm s} - \frac{1}{\mathcal{M}_{\rm s}} = c_{\rm s,L}\frac{\gamma+1}{\gamma-1}\left\{1 - \left[\frac{P_{\rm R}}{P_{\rm L}}\left(\frac{2\gamma}{\gamma+1}\mathcal{M}_{\rm s}^2 - \frac{\gamma-1}{\gamma+1}\right)\right]^{\frac{\gamma-1}{2\gamma}}\right\}$$

with $c_{\rm s,L} = \sqrt{\gamma P_{\rm L}/\rho_{\rm L}}$ the sound speed in region 'L'. Once the value of $\mathcal{M}_{\rm s}$ has been

determined, it can be used in steps [1] and [2] to infer all the parameters of (uniform) zones 1 and 2.

[**4**] To determine the internal structure of the rarefraction fan, one once again has to rely on the method of characteristics. Without any derivation, we simply give the solution:

$$\begin{aligned} u(x) &= \frac{2}{\gamma+1}\left(c_{\rm s,L} + \frac{x-x_0}{t}\right) \\ c_{\rm s}(x) &= c_{\rm s,L} - \frac{1}{2}(\gamma-1)u(x) \\ P(x) &= P_{\rm L}\left[\frac{c_{\rm s}(x)}{c_{\rm s,L}}\right]^{\frac{2\gamma}{\gamma-1}} \\ \rho(x) &= \gamma\frac{P(x)}{c_{\rm s}^2(x)} \end{aligned}$$

[**5**] Finally we need to determine the locations of the zone boundaries, indicated by x_1, x_2, x_3 and x_4 (see Fig. 39). The shock wave is propagating with speed $u_{\rm s} = \mathcal{M}_{\rm s}c_{\rm s,R}$. The contact discontinuity is propagating with a speed $u_2 = u_1$. The far left-edge of the rarefaction wave is propogating with the sound-speed in zone L. And finally, from the method of characteristics, one infers that the right-edge of the rarefaction zone is propagating with speed $u_2 + c_{\rm s,2}$ in the positive direction. Hence, we have that

$$\begin{aligned} x_1 &= x_0 - c_{\rm s,L}t & (1)\\ x_2 &= x_0 + (u_2 - c_{\rm s,2})t & (2)\\ x_3 &= x_0 + u_2 t & (3)\\ x_4 &= x_0 + u_{\rm s}t & (4) \end{aligned}$$

which completes the 'analytical' solution to the Sod shock tube problem. Note that the word analytical is in single quotation marks. This is to highlight that the solution is not trully analytical, in that it involves a numerical root-finding step!

Fig. 40 shows this analytical solution at $t = 0.2$ for a Sod shock tube problem with $\gamma = 1.4$ and the following (unitless) initial conditions:

$$\begin{aligned} \rho_{\rm L} = 8.0 \qquad & \rho_{\rm R} = 1.0 \\ P_{\rm L} = 10/\gamma \qquad & P_{\rm R} = 1/\gamma \\ u_{\rm L} = 0.0 \qquad & u_{\rm R} = 0.0 \end{aligned}$$

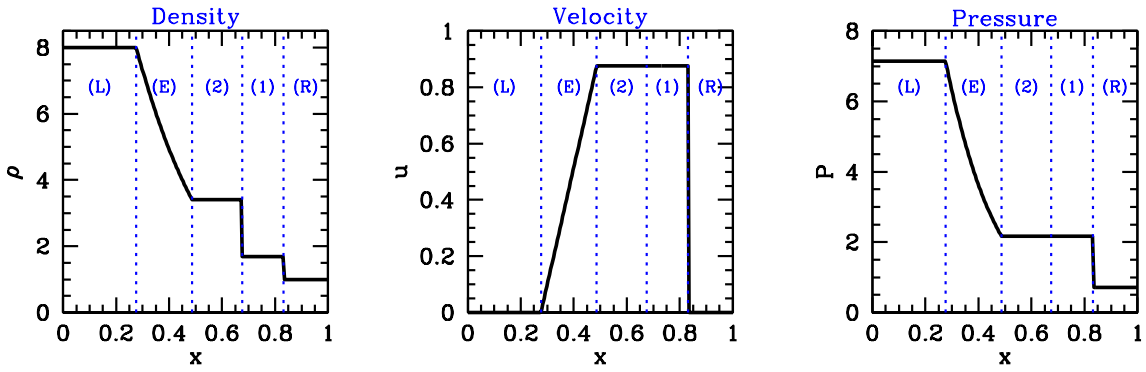

Figure 40: *Analytical solution to the SOD shock tube problem at $t = 0.2$. Note that the pressure and velocity are unchanged across the discontinuity (entropy jump) at x_3, while the density is clearly discontinuous.*

In what follows, we develop a simple 1D numerical hydro code to integrate this same Sod shock tube problem, which we can then compare with our 'analytical' solution. The code will use different Godunov schemes to do so.

As discussed above, Godunov's method, and its higher order modifications, require solving the Riemann problem at every cell boundary and for every time step. This amounts to calculating the solution in the regions between the left- and right-moving waves (i.e., zones 'E', '1', and '2' in the case of the Sod shock tube), as well as the speeds of the various waves (shock wave(s), rarefraction wave(s), and entropy jumps) involved. The solution of the general Riemann problem cannot be given in a closed analytic form, even for 1D Newtonian flows (recall, that even for the Sod shock tube a numerical root finding step is required). What can be done is to find the answer numerically, to any required accuracy, and in this sense the Riemann problem is said to have been solved exactly, even though the actual solution is not analytical.

However, mainly because of the iterations needed to solve the Riemann problem, the Godunov scheme as originally envisioned by Godunov, which involves using an exact Riemann solver at every cell-interface, is typically far too slow to be practical. For that reason, several **approximate Riemann solvers** have been developed. These can be divided in *approximate-state* Riemann solvers, which use an approximation for the Riemann states and compute the corresponding flux, and *approximate-flux* Riemann solvers, which approximate the numerical flux directly.

Here we highlight one of these approximate Riemann solvers; the **HLL(E) method**, after Harten, Lax & van Leer, who proposed this method in 1989, and which was later improved by Einfeldt (1988). The HLL(E) method is an approximate-flux Riemann solver, which assumes that the Riemann solution consists of just two waves separating three constant states; the original L and R states which border an intermediate 'HLL' state. It is assumed that, after the decay of the initial discontinuity of the local Riemann problem, the waves propagate in opposite directions with velocities $S_{\rm L}$ and $S_{\rm R}$, generating a single state (assumed constant) between them. $S_{\rm L}$ and $S_{\rm R}$ are the smallest and the largest of the signal speeds arising from the solution of the Riemann problem. The simplest choice is to take the smallest and the largest among the eigenvalues of the Jacobian matrix $\partial f_i/\partial q_j$ evaluated at some intermediate (between L and R) state. For the 1D Euler equation that we consider here, one obtains reasonable results if one simply approximates these eigenvalues as $S_{\rm L} = u_{\rm L} - c_{\rm s,L}$ and $S_{\rm R} = u_{\rm R} + c_{\rm s,R}$, where $u_{\rm L}$ and $u_{\rm R}$ are the initial fluid velocities in the L and R states, and $c_{\rm s,L}$ and $c_{\rm s,R}$ are the corresponding sound speeds. Without going into any detail, the HLL(E) flux to be used in the Godunov scheme is given by

$$\boxed{\vec{F}_{i-\frac{1}{2}}^{\,n+\frac{1}{2}} = \frac{S_{\rm R}\vec{f}_{\rm L} - S_{\rm L}\vec{f}_{\rm R} + S_{\rm L}\,S_{\rm R}\,(\vec{q}_{\rm R} - \vec{q}_{\rm L})}{S_{\rm R} - S_{\rm L}}}$$

Here we have made it explicit that the flux is a vector, where each element refers to the corresponding elements of $\vec{q}$ and $\vec{f}(\vec{q})$ of the Euler equation in conservation form. Note that the L and R states here, refer to mesh cells $i-1$ and i, respectiveley. In the case of the $F_{i+\frac{1}{2}}^{n+\frac{1}{2}}$ flux, which is needed in the Godunov scheme together with $F_{i-\frac{1}{2}}^{n+\frac{1}{2}}$, the L and R states refer to mesh cells i and $i+1$.

A simple 1D hydro-code: We are now ready to write our own simple 1D numerical hydro-code (adopting an adiabatic EoS), which we can test against the (analytical) solution of the Sod shock tube problem examined above. What follows are some of the steps that you may want to follow in writing your own code:

- Define an array $q(1:\mathrm{Nx}, 0:\mathrm{Nt}, 1:3)$ to store the discrete values of the vector $\vec{q} = (\rho, \rho u, E)^{\mathrm{t}}$ of conserved quantities on the spatial mesh x_i with $i = 1, .., \mathrm{Nx}$ and at discrete time t^n with $n = 0, 1, ..., \mathrm{Nt}$.

- Write a subroutine that computes the primary variables, $\rho(1:\mathrm{Nx})$, $u(1:\mathrm{Nx})$ and $P(1:\mathrm{Nx})$, given the conserved variables $\vec{q}$. This requires computing the pressure, which follows from $E = P/(\gamma - 1) - \frac{1}{2}\rho u^2$. Also compute the local sound speed $c_{\mathrm{s}}(1:\mathrm{Nx}) = \sqrt{\gamma P/\rho}$ (which is needed in the HLL(E) scheme).

- Write a subroutine that, given the primary variables, computes the time step $\Delta t = \alpha_{\mathrm{c}}(\Delta x/|v^n_{\mathrm{max}}|)$. Here $\alpha_{\mathrm{c}} < 1$ is the user-supplied value for the Courant parameter, and $|v^n_{\mathrm{max}}| = \mathrm{MAX}_i[|u^n_i| + c_{\mathrm{s}}(x_i)]$ denotes the maximum velocity present throughout the entire computational domain at time t^n. Since v_{max} can change with time, this means that different time steps typically adopt a different value for Δt.

- Write a subroutine that, given the array $q(1:\mathrm{Nx}, n, 1:3)$ computes the corresponding fluxes $\vec{f}(\vec{q})$ at time t^n, and store these in $f(1:\mathrm{Nx}, 1:3)$.

- Each time step (i) compute the primary variables, (ii) compute the time step, Δt, (iii) compute the fluxes $f(1:\mathrm{Nx}, 1:3)$, (iv) compute the Godunov fluxes $F^{n+\frac{1}{2}}_{i-\frac{1}{2}}$ and $F^{n+\frac{1}{2}}_{i+\frac{1}{2}}$; (this depends on the scheme used), and (v) update q using the Godunov update scheme:

$$q(i, n+1, 1:3) = q(i, n, 1:3) - \frac{\Delta t}{\Delta x}\left[F^{n+\frac{1}{2}}_{i+\frac{1}{2}}(1:3) - F^{n+\frac{1}{2}}_{i-\frac{1}{2}}(1:3)\right]$$

- Loop over time steps until the total integration time exceeds the user-defined time, and output the mesh of primary variables at the required times.

Fig. 41 shows the outcome of such a program for three different numerical schemes applied to the Sod shock tube problem. All methods start from the same ICs as discussed above (i.e., those used to make Fig. 40), and are propagated forward using time-steps that are computed using a Courant parameter $\alpha_{\mathrm{c}} = 0.8$ until $t = 0.2$. The

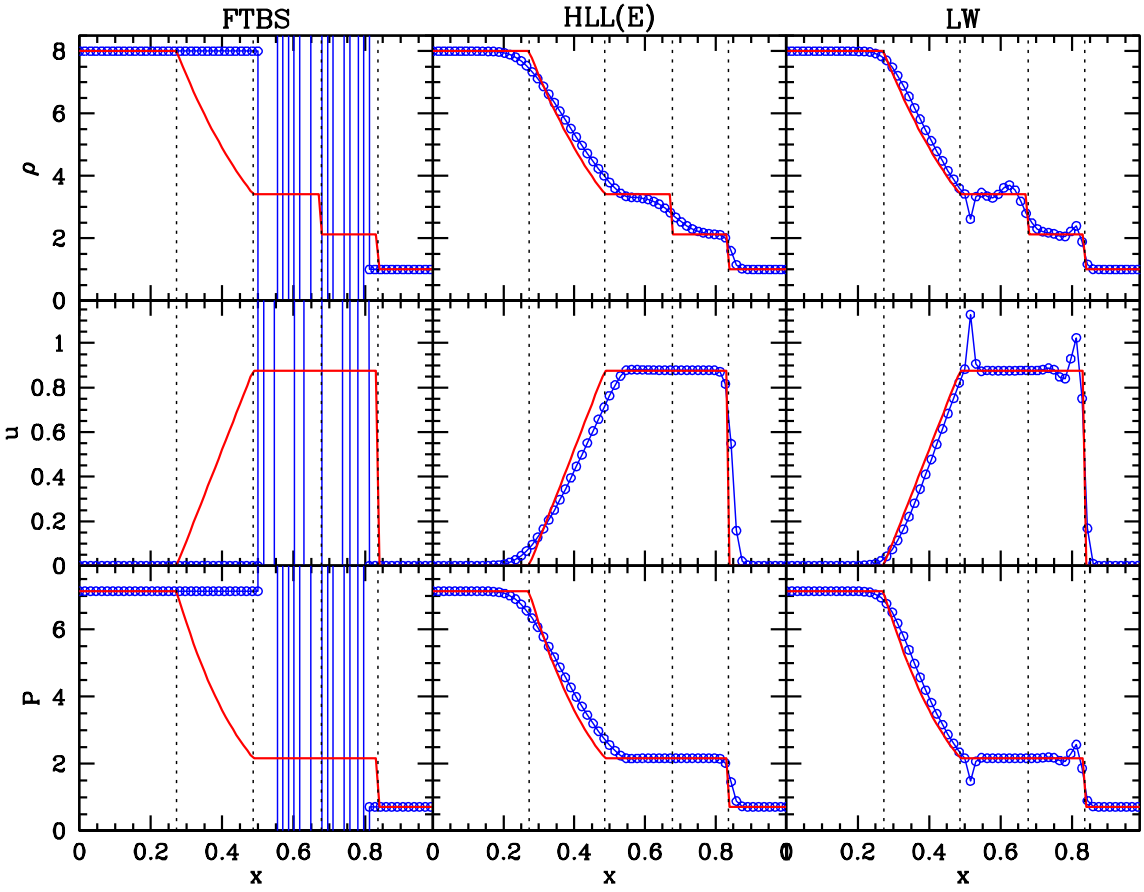

Figure 41: *Numerical integration of Sod's shock tube problem. From top to bottom the panels show the density, velocity and pressure as function of position. The 'analytical' results at* $t = 0.2$ *are indicated in red (these are identical to those shown in Fig. 40). In blue are the results from three different numerical schemes; from left to right, these are the first-order FTBS scheme, the first-order Godunov scheme with the approximate Riemann solver of HLL(E), and the second-order predictor-corrector scheme of Lax-Wendroff. All schemes adopted a spatial grid of 65 points on the domain* $x \in [0, 1]$*, and a Courant parameter* $\alpha_c = 0.8$*.*

results (in blue, open circles) are compared to the analytical solution (in red). In each column, panels from top to bottom show the density, velocity, and pressure.

The first scheme, shown in the left-hand panels, is the standard **Euler FTBS** scheme, which simply sets $F_{i-\frac{1}{2}}^{n+\frac{1}{2}} = f(q_{i-1}^n)$ (cf. Table at the end of Chapter 17). Although this scheme reduces to the stable upwind scheme in the case of the 1D linear advection equation, clearly in this more complicated case it failes miserably. The reason is easy to understand. In the Sod shock tube problem, there are multiple waves moving in different directions (forward moving shock and entropy jump, and a backward moving rarefraction wave). Hence, there is no single direction in the flow, and the FTBS scheme cannot be an upwind scheme for all these waves. For some it is a downwind scheme (equivalent to FTFS), and such a scheme is unconditionally unstable. This explains the drastic failure of this scheme. In the case of the advection equation there is only a single wave, and the FTBS (FTFS) scheme acts as an upwind scheme if $u > 0$ ($u < 0$).

What is needed, therefore, is a Godunov-scheme, which is an upwind scheme for the general, non-linear case. The middle panel shows an example, in which the fluxes are computed using the **HLL(E)** scheme discussed above. This scheme is first-order (i.e., it relies on piecewise constant reconstruction) and as such suffers from numerical diffusion, which is clearly apparent (i.e., the discontinuities in the solution are 'blurred'). Nevertheless, the scheme is stable, and captures the salient features of the analytical solution.

Finally,the right-hand panels show the results for a second-order Godunov scheme, based on the **Lax-Wendroff** fluxes. This scheme uses piecewise linear reconstruction (see Chapter 19), and is second-order in both space and time. The latter arises because this scheme uses a **predictor** and **corrector** step, according to:

$$\vec{q}_{i+\frac{1}{2}} = \frac{\vec{q}_i^n + \vec{q}_{i+1}^n}{2} - \frac{\Delta t}{2\Delta x}\left[\vec{f}(\vec{q}_{i+1}^n) - \vec{f}(\vec{q}_i^n)\right]$$

$$\vec{q}_i^{n+1} = \vec{q}_i^n - \frac{\Delta t}{\Delta x}\left[\vec{f}(\vec{q}_{i+\frac{1}{2}}) - \vec{f}(\vec{q}_{i-\frac{1}{2}})\right]$$

It uses an intermediate step, and it is apparent from combining the two steps that the final update formula is $\mathcal{Q}(\Delta t^2)$. It is left as an exersize for the student to show that this scheme reduces to the LW-scheme highlighted in Chapter 17 for the linear advection equation (i.e., when $f = vu$ with v the constant advection speed and u the

quantity that is advected). The higher-order accuracy of this scheme is better able to capture the discontinuities in the analytical solution of the Sod shock tube, but, as expected from **Godunov's theorem**, the scheme is not positivity conserving and introduces artificial over- and under-shoots.

As we have seen in Chapter 19, such over- and undershoots can be prevented by using slope (or flux) limiters. An example of such a scheme is the **MUSCL** scheme developed by van Leer, which is based on piecewise linear reconstruction combined with slope limiters. This higher-order reconstruction scheme implies that at the cell interfaces, one now has to solve so-called *generalized* Riemann problems; i.e., a discontinuity separating two linear (rather than constant) states. These are not as easy to solve as the standard Riemann problem. Hence, one typically resorts to approximate Riemann solvers.

Before closing our discussion of computational hydrodynamics, we briefly address a few loose ends. The schemes discussed in the previous four chapters are by no means exhaustive. A quick literature study will reveal many more schemes, combining higher-order reconstruction schemes with a wide variety of limiters (to assure TVD) and approximate Riemann solvers. Another topic we haven't really discussed is that of source terms. In our discussion of computational hydrodynamics we have restricted our discussion to **homogeneous** conservation laws. However, most astrophysical situations involve source and sink terms, especially in the form of gravity and radiation. Adding these terms to the hydro-equations makes the conservation laws **inhomogeneous**. How to deal with this numerically is not trivial, and an ongoing topic of investigation. The most obvious inclusion of a source term into a Godunov scheme adds extra complications to the Riemann problem and calculation of the corresponding intercell fluxes. The reader interested in learning more about these topics is referred to the excellent textbook *Riemann Solvers and Numerical Methods for Fluid Dynamics* by E.F. Toro, which presents a detailed discussion of the material covered here and much more, including alternative approximate Riemann solvers such as those by Roe and Osher, Flux Vector Splitting methods, higher-order TVD schemes, methods to include source terms, and the extension to multiple dimensions.

Finally, as already eluded to in Chapter 17, we have focussed exclusively on Eulerian schemes. Many hydro-simulations in astrophysics make use of the Lagrangian SPH method. It is left as an exersize for the interested reader to research this different methodology. Hopefully the material provided here will facilitate such a self-study.

Plasma Physics

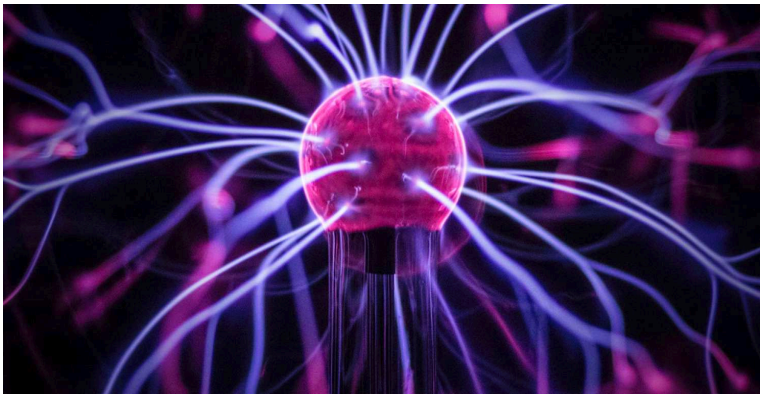

The following chapters give an elementary introduction into the rich topic of plasma physics. The main goal is to highlight how plasma physics differs from that the physics of neutral fluids. After introducing some characteristic time and length scales, we discuss plasma orbit theory and plasma kinetic theory before considering the dynamics of collisionless plasmas, described by the Vlasov equations, and that of collisional plasma, described (under certain circumstances) by the equations of magnetohydrodynamics.

Plasma is a rich topic, and one could easily devote an entire course to it. The following chapters therefore only scratch the surface of this rich topic. Readers who want to get more indepth information are referred to the following excellent textbooks
- *Introduction to Plasma Theory* by D.R. Nicholson
- *The Physics of Plasma* by T.J.M. Boyd & J.J. Sandweson
- *Plasma Physics for Astrophysics* by R.M. Kulsrud
- *The Physics of Fluids and Plasmas* by A.R. Choudhuri
- *Introduction to Modern Magnetohydrodynamics* by S. Galtier

CHAPTER 22

Plasma Characteristics

Roughly speaking a **plasma** is a fluid in which the constituent particles are charged. More specifically, a plasma is a fluid for which the **plasma parameter** (defined below) $g < 1$.

Plasma dynamics is governed by the interaction of the charged particles with the self-generated (through their charges and current densities) electromagnetic fields. This feedback loop (motion of particles generates fields, and the dynamics of the particles depends on the fields) is what makes plasma physics such a difficult topic.

NOTE: As is well known, accelerated charges emit photons. Hence, the charged particles in a plasma will lose energy. As long as the timescale of this energy loss is long compared to the processes of interest, we are justified in ignoring these **radiative losses**. Throughout we assume this to be the case.

NOTE ABOUT UNITS: in this and the following chapters on plasma physics we adopt the Gaussian system of units. This implies that the Coulomb force between two charges q_1 and q_2 is given by

$$F = \frac{q_1 q_2}{r^2}$$

By contrast, the same Coulomb law in the alternative SI unit system is given by

$$F = \frac{1}{4\pi\varepsilon_0}\frac{q_1 q_2}{r^2}$$

with ε_0 the vacuum permittivity. Using Gaussian units also implies that the electric and magnetic fields have the same dimensions, and that the **Lorentz force** on a particles of charge q is given by

$$\vec{F} = q\left[\vec{E} + \frac{\vec{v}}{c} \times \vec{B}\right]$$

See any textbook on electromagnetism for details.

In a **neutral fluid**, the interactions (also called collisions) among the particles are **well-separated**, **short-range**, and causing **large deflections**. In between the collisions, the particles travel in straight lines.

In a **plasma**, the interactions are **long-range**, not well-separated (i.e., each particle undergoes **many interactions simultanously**), and each individual collision typically causes only a **small deflection**. Consequently, the trajectories of particles in a plasma are very different from those in a neutral fluid (see Fig.1 in Chapter 1).

If the plasma is **weakly ionized**, then a charged particle is more likely to have a collision with a neutral particle. Such collisions take place when the particles are very close to each other and usually produce large deflections, similar to collisions between two neutral particles. Hence, a weakly ionized plasma can be described using the **Boltzmann equation**.

If the plasma is **highly ionized**, Coulomb interactions among the charged particles dominate. These are long-range interactions, and typically result in small deflections (seee below). In addition, a particle typically has interactions with multiple other particles simultaneously. Hence, the collisions are not instantaneous, well-separated, and localized (i.e., short-range). Consequently, the Boltzmann equation does not apply, and we need to derive an alternative dynamical model. Unfortunately, this is a formidable problem that is not completely solved for an arbitrary, inhomogeneous magnetized plasma.

In our discussion of **neutral fluids** we have seen that a system of particles can be treated like a **continuum fluid** iff frequent collisions keep the distribution function in local regions close to a **Maxwellian**. Although not easy to proof, there is ample experimental evidence that shows that the collisions in a **plasmas** also relax to a **Maxwellian**. We therefore will seek to develop some continuum fluid model to describe our plasma.

Characteristic Length and Time Scales:
We now describe a number of important length scales and time scales relevant for plasmas. Let n_{e} and n_{i} refer to the number densities of electrons and ions, respectively. Unless specified otherwise, we shall assume that ions are singly ionized. Since most of the matter in the Universe is hydrogen, this is a reasonable assumption to

make in astrophysics (i.e., $n_{\rm i}$ is then basically the number density of free protons). In astrophysics these number densities can span many orders of magnitudes. For example, the ISM has $n_{\rm e} \sim 1\,{\rm cm}^{-3}$, while stellar interiors have densities $n_{\rm e} \sim 10^{25}\,{\rm cm}^{-3}$.

The **charge density** of a plasma is defined as

$$\rho = e(n_{\rm p} - n_{\rm e})$$

with e the charge of an electron. In a plasma, the strong electrostatic interactions among positively and negatively charged particles ensure that volumes with statistically large numbers of particles are **nearly neutral** (i.e., $\rho \simeq 0$). Hence, plasmas have some characteristics in common with neutral fluids. However, on small enough scales, particles feel the strong, electromagnetic forces from individual particles. Although a charged particle in a plasma in principle produces a long-range EM field, its effect is usually screened off by particles of the opposite charge within a distance called de **Debye length**. The Debye lengths for electrons and ions are given by

$$\boxed{\lambda_{\rm e,i} = \left(\frac{k_{\rm B}\,T_{\rm e,i}}{8\pi n e^2}\right)^{1/2} \sim 740\,{\rm cm}\left(\frac{T\,[\,{\rm eV}]}{n\,[\,{\rm cm}^{-3}]}\right)^{1/2}}$$

(for a derivation, see any good textbook on Plasma Physics), while the **total Debye length**, $\lambda_{\rm D}$, is defined by

$$\lambda_{\rm D}^{-2} = \lambda_{\rm e}^{-2} + \lambda_{\rm i}^{-2}$$

Because of Debye shielding, the net electrical potential around a charge q is given by

$$\phi = \frac{q}{r}\exp(-r/\lambda_{\rm D})$$

Debye shielding is a prime example of collective behavior in a plasma; it indicates that each charged particle in a plasma, as it moves, basically carries, or better, tries to carry, a cloud of shielding electrons and ions with it.

• On scales $\lambda \gg \lambda_{\rm D}$, a plasma can be considered charge-neutral: any charge imbalance produces strong electrostatic forces which quickly restore charge-neutrality.

• On scales $\lambda \ll \lambda_{\rm D}$ particles experience strong Coulomb interactions.

The average number of particles on which a charged particle excerts an influence is roughly $n\,\lambda_{\rm D}^3$, with n the average number density of particles. Associated with this is the **Plasma Parameter**

$$\boxed{g \equiv \frac{1}{n\,\lambda_{\rm D}^3} = \frac{(8\pi)^{3/2}\,e^3\,n^{1/2}}{(k_{\rm B}\,T)^{3/2}}}$$

NOTE: some authors (unfortunately) refer to the plasma parameter as g^{-1}.

• When $g \gg 1$, the number of particles on which a charged particle exerts an influence is small, and the system behaves like a neutral fluid. Such a fluid is generally not considered a plasma!

• When $g \ll 1$, many particles undergo simultaneous interactions, and as a consequence, the fluid manifests **collective behavior**. This is known as the **plasma limit**.

NOTE: The plasma parameter $g \propto n^{1/2}$. Hence, low density plasma's are more 'plasma-like' (display more collective phenomenology). Even though the number of particles per volume is smaller, the total number of particles within a Debye volume, $\lambda_{\rm D}^3$, is larger.

The average distance between particles is of the order $n^{-1/3}$. Hence, the average potential energy of electrostatic interactions is of the order $e^2\,n^{1/3}$. We thus see that

$$\frac{\langle \text{P.E.} \rangle}{\langle \text{K.E.} \rangle} \propto \frac{e^2\,n^{1/3}}{k_{\rm B}\,T} \propto g^{2/3}$$

In other words, *the plasma parameter is a measure for the ratio between the average potential energy associated with collisions and the average kinetic energy of the particles.*

• When $g \ll 1$, interactions among the particles are weak, but a large number of particles interact simultaneously, giving rise to plasma behavior.

• When $g \gg 1$, interactions among the particles are strong, but few particles interact collectively, and the fluid behaves like a neutral fluid. In fact, if $g > 1$ then the

typical kinetic energy of the electrons is smaller then the potential energy due its nearest neighbor, and there would be a strong tendency for the electrons and ions to recombine, thus destroying the plasma. The need to keep the fluid ionized means that most plasmas have temperatures in excess of ~ 1 eV (or they are exposed to strong ionizing radiation).

The plasma parameter is a measure of the dominance of collective interactions over individual collisions. The most fundamental of these collective interactions are the **plasma oscillations** that are set up in response to a charge imbalance. The strong electrostatic fields which drive the electrons to re-establish neutrality cause oscillations about the equilibrium position at a characteristic frequency, the **plasma frequency** $\omega_{\rm p}$. Since the imbalance occurs over a characteristic distance $\lambda_{\rm D}$, and the thermal speed of the electrons is $v_{\rm e} \sim (k_{\rm B}T_{\rm e}/m_{\rm e})^{1/2}$, we have that the **electron plasma frequency**

$$\boxed{\omega_{\rm pe} = \frac{v_{\rm e}}{\lambda_{\rm e}} = \left(\frac{4\pi n_{\rm e} e^2}{m_{\rm e}}\right)^{1/2} \simeq 56.5\,{\rm kHz}\,(n_{\rm e}\,[\,{\rm cm}^{-3}])^{1/2}}$$

The corresponding frequency for ions, the **ion plasma frequency**, is defined by

$$\omega_{\rm pi} = \left(\frac{4\pi n_{\rm i}(Ze)^2}{m_{\rm i}}\right)^{1/2}$$

with Ze the charge of the ion. The **total** plasma frequency for a two-component plasma is defined as

$$\omega_{\rm p}^2 \equiv \omega_{\rm pe}^2 + \omega_{\rm pi}^2$$

Since for most plasmas in nature $\omega_{\rm pe} \gg \omega_{\rm pi}$, we have that typically $\omega_{\rm p} \approx \omega_{\rm pe}$.

Any applied field with a frequency less than the electron plasma frequency is prevented from penetrating the plasma by the more rapid response of the electrons, which neutralizes the applied field. Hence, a plasma is not transparent to electromagnetic radiation of frequency $\omega < \omega_{\rm pe}$. An example of such long-wavelength radiation that is typically inhibited from traversing a plasma is cyclotron radiation, which is the non-relativistic version of synchrotron radiation.

Collisions We now turn our attention to the collisions in a plasma. Our goal is two fold: to derive under what conditions collisions are important, and (ii) to demonstrate

that in a plasma weak collisions (causing small deflections) are more important that strong collisions (causing large angle deflections).

As we have seen above, a particle in a plasma is feeling the Coulomb force from all g^{-1} particles inside its Debye volume. Hence, unlike in a neutral gas, where particles have individual short-range interactions, moving freely in between, in a plasma the particle have many simultaneous, long-range (i.e., of order the Debye length) interactions.

From our definition of a plasma (i.e., $g \ll 1$) we know that the potential energy of the 'average' interaction of particles with their nearest neighbor is small. This means that the strongest of all its g^{-1} simultaneous interactions (i.e., that with its nearest neighbor) is, on average, weak. Thus, it is safe to conclude that a charged particle in a plasma simultaneously undergoes of order g^{-1} weak interactions (aka 'collisions'). In fact, as we shall see shortly, even the combined effect of all these g^{-1} simultanous collisions is still relatively weak.

The importance of collisions is most meaningfully expressed by the **collision frequency** (which is the inverse of the **two-particle collisional relaxation time**), which we now proceed to calculate.

Consider a charged particle of charge q and mass m having an encounter with impact parameter b with another particle with charge q' and mass m'. Let v_0 be the speed of the encounter when the charges are still widely separated. In what follows we assume that $m' = \infty$, and we treat the encounter from the rest-frame of m', which coincides with the center-of-mass. This is a reasonable approximation for an encounter between an electron and a much heavier ion. It makes the calculation somewhat easier, and is anyways accurate to a factor of two or so. Let $x = v_0 t$ describe the trajectory of m in the case where it would not be deflected by m'. If the scattering angle is small, then the final speed in the x-direction (i.e., the original direction of m) will be close to v_0 again. However, the particle will have gained a perpendicular momentum

$$mv_\perp = \int_{-\infty}^{\infty} F_\perp(t)\mathrm{d}t$$

where $F_{\rm perp}(t)$ is the perpendicular force experienced by the particle along its trajectory. As long as the deflection angle is small, we may approximate that trajectory as the unperturbed one (i.e., $x = v_0 t$). Note that this is exactly the same approximation as we make in our treatment of the impulse approximation in Chapter 16.

Next we use that

$$F_\perp = \frac{q\,q'}{r^2}\sin\theta$$

where $\sin\theta = b/r$. Using this to substitute for r in the above expression, we obtain that

$$v_\perp = \frac{q\,q'}{m\,b^2}\int_{-\infty}^{\infty}\sin\theta^3(t)\,\mathrm{d}t$$

Using that

$$x = -r\cos\theta = \frac{-b\cos\theta}{\sin\theta} = v_0 t$$

we see that

$$\mathrm{d}t = \frac{b}{v_0}\,\frac{\mathrm{d}\theta}{\sin^2\theta}$$

Substituting this in the integral expression we obtain

$$v_\perp = \frac{q\,q'}{m\,v_0\,b}\int_0^{\pi}\sin\theta\,\mathrm{d}\theta = \frac{2q\,q'}{m\,v_0\,b}$$

Our approximation that the collision must be weak (small deflection angle) breaks down when $v_{\rm perp} \simeq v_0$. In that case all the forward momentum is transformed into perpendicular momentum, and the deflection angle is 90°. This happens for an impact parameter

$$b_{90} = \frac{2q\,q'}{m\,v_0^2}$$

In some textbooks on plasma physics, this length scale is called the **Landau length**. Using this expression we have that

$$\frac{v_\perp}{v_0} = \frac{b_{90}}{b}$$

NOTE: although the above derivation is strictly only valid when $b \gg b_{90}$ (i.e., $v_\perp \ll v_0$), we shall consider b_{90} the border between weak and strong collisions, and compute the combined impact of all 'weak' collisions (i.e., those with $b > b_{90}$).

But first, let us compute the collision frequency for strong collisions. Let n be the number density of targets with which our particle of interest can have a collision. The cross section for each target for a strong interaction is πb_{90}^2. In a time t the

particle of interest traverses a distance $v_0 t$, which implies that the expectation value for the number of strong interactions during that time is given by

$$\langle N_{\rm L} \rangle = n\,\pi b_{90}^2\,v_0\,t$$

where the subscript 'L' refers to Large (deflection angle). Using that the corresponding collision frequency is the inverse of the time it takes for $\langle N_{\rm L}\rangle = 1$, we obtain that

$$\boxed{\nu_{\rm L} = n\,\pi b_{90}^2\,v_0 = \frac{4\pi n q^2 q'^2}{m^2 v_0^3} = \frac{4\pi n e^4}{m^2 v_0^3}}$$

where the last step only holds if, as assumed here, all ions have $Z = 1$.

Recall that a typical charged particle is simultaneously undergoing g^{-1} collisions. Only very few of these will be large angle deflections (strong collisions). To see this. we can use that the potential energy between the two colliding particles at a separation b_{90} is e^2/b_{90}. Substituting the expression for b_{90} we see that this is equal to $\frac{1}{2}mv_0^2$, which is the kinetic energy. Thus, when $qq' < 0$ and $b < b_{90}$ we are basically in the regime of **recombination**. Furthermore, as we have seen above $\langle$P.E.$\rangle/\langle$K.E.$\rangle \propto g^{2/3}$, which for a plasma is much smaller than unity. Hence, a particle will undergo many more small angle collisions than large angle collisions.

We now proceed to compute the combined effect of all these many small angle collisions. Since the perpendicular direction in which the particle is deflected by each individual collision is random, we have that $\langle v_{\rm perp}\rangle = 0$. However, the second moment, $\langle v_{\rm perp}^2\rangle$ will not be zero. As before, in a time t the number of collisions that our subject particle will experience with impact parameters in the range b-$b + {\rm d}b$ is given by

$$\langle N_{\rm coll}\rangle = n\,2\pi b\,{\rm d}b\,v_0\,t$$

Hence, using that each collision causes a $v_{\rm perp} = v_0(b_{90}/b)$, we can calculate the total change in $v_{\rm perp}^2$ by integrating over all impact parameters

$$\langle v_\perp^2\rangle = \int_{b_{\rm min}}^{b_{\rm max}} {\rm d}b\,n\,2\pi\,b\,v_0\,t\,\frac{v_0^2 b_{90}^2}{b^2} = 2\pi\,n\,v_0^3\,t\,b_{90}^2\,\ln\left(\frac{b_{\rm max}}{b_{\rm min}}\right)$$

Substituting the expression for b_{90} and using that $b_{\rm max} \simeq \lambda_{\rm D}$ (i.e., a charged particle only experiences collisions with particles inside the Debye length) and $b_{\rm min} = b_{90}$ (i.e., collisions with $b < b_{90}$ are *strong* collisions), we find that

$$\langle v_\perp^2\rangle = \frac{8\pi\,n\,e^4\,t}{m^2 v_0}\,\ln\left(\frac{\lambda_{\rm D}}{b_{90}}\right)$$

Next we use that the typical velocity of charges is the thermal speed, so that $v_0 \simeq k_{\rm B}T/m$, to write that

$$\frac{\lambda_{\rm D}}{b_{90}} = \frac{\lambda_{\rm D} m v_0^2}{2e^2} = 2\pi\, n\, \lambda_{\rm D}^3 = 2\pi g^{-1}$$

where in the third step we have used the definition of the Debye length. Since for a plasma $g^{-1} \gg 2\pi$ we have that $\ln(\lambda_{\rm D}/b_{90}) \simeq \ln\Lambda$, where we have introduced the inverse of the plasma parameter $\Lambda \equiv g^{-1}$. The quantity $\ln\Lambda$ is known as the **Coulomb logarithm**.

If we now define the **collision frequency** $\nu_{\rm c}$ due to small-angle collisions as the inverse of the time it takes for $\langle v_\perp^2 \rangle$ to become of the order of v_0^2, then we obtain

$$\boxed{\nu_{\rm c} = \frac{8\pi\, n\, e^4}{m^2 v_0^3}\, \ln\Lambda}$$

Upon comparing this with the collision frequency of large-angle collisions, we see that

$$\frac{\nu_{\rm c}}{\nu_{\rm L}} = 2\ln\Lambda$$

This is a substantial factor, given that $\Lambda = g^{-1}$ is typically very large: i.e., for $\Lambda = 10^6$ we have the $\nu_{\rm c} \sim 28\nu_{\rm L}$ indicating that small-angle collisions are indeed much more important than large-angle collisions.

Let us now compare this collision frequency to the plasma frequency. By once again using that v_0 is of order the thermal velocity, and ignoring the small difference between $\lambda_{\rm D}$ and $\lambda_{\rm e}$, we find that

$$\frac{\omega_{\rm c}}{\omega_{\rm p,e}} = \frac{2\pi\,\nu_{\rm c}}{\omega_{\rm p,e}} \simeq \frac{2\pi\,\ln\Lambda}{2\pi\, n\, \lambda_{\rm D}^3} = \frac{\ln\Lambda}{\Lambda} \sim \Lambda^{-1}$$

Hence, we see that the collision frequency is much, much smaller than the plasma frequency, which basically indicates that, in a plasma, particle collisions are far less important than collective effects: a plasma wave with frequency near $\omega_{\rm p,e}$ will oscillate many times before experiencing significant damping due to collisions. Put differently, **collisional relaxation** mechanisms in a plasma are far less important than **collective relaxation** mechanisms, such as, for example, **Landau damping** (to be discussed in a later chapter).

Finally, we point out that, since both the Coulomb force and the gravitational force scale as r^{-2}, the above derivation also applies to gravitational systems. All that is requires is to replace $q\,q' = e^2 \rightarrow Gm^2$, and the derivation of the collision frequencies now apply to gravitational N-body systems. This is the calculation that is famously used to derive the **relaxation time** of a gravitational system. The only non-trivial part in that case is what to use for $b_{\rm max}$; since there is no equivalent to Debye shielding for gravity, there is no Debye length. It is common practice (though contentious) to therefore adopt $b_{\rm max} \simeq R$ with R a characteristic length or maximum extent of the gravitational system under consideration. In a gravitational system, we also find that the two-body, collisional relaxation time is very long, which is why we approximate such systems as 'collisionless'. Similar to a plasma, in a gravitational system relaxation is not due to two-particle collisions, but due to collective effects (i.e., violent relaxation) and to more subtle relaxation mechanisms such as phase mixing.

Let's take a closer look at this comparison. If we define the **two-body relaxation time** as the inverse of the collision frequency, we see that for a plasma

$$\boxed{t_{\rm relax}^{\rm plasma} = \frac{\Lambda}{\ln\Lambda}\,t_{\rm p} \simeq \frac{\Lambda}{\ln\Lambda}\frac{2\pi}{\omega_{\rm p}} \simeq \frac{\Lambda}{\ln\Lambda}10^{-4}{\rm s}\,\left(\frac{n_{\rm e}}{\rm cm^{-3}}\right)^{-1/2}}$$

Here we have used the ratio between the collision frequency and plasma frequency derived above, and we have used the expression for $\omega_{\rm p} \equiv 2\pi/t_{\rm p}$ in terms of the electron density. We thus see that the two-body relaxation time for a plasma is very short. Even for a plasma with $\Lambda = n\lambda_{\rm D}^3 = 10^{10}$, the relaxation time for plasma at ISM densities ($\sim 1\ {\rm cm}^{-3}$) is only about 12 hours, which is much shorter than any hydrodynamical time scale in the plasma (but more longer than the characteristic time scale on which the plasma responds to a charge-imbalance, which is $t_{\rm p} = 2\pi/\omega_{\rm p} \simeq 0.1$ms). Hence, although a plasma can often be considered **collisionless** (in which case its dynamics are described by the **Vlasov equation**, see Chapter 24), on astrophysical time scales, plasmas are collisionally relaxed, and thus well described by a **Maxwell-Boltzmann distribution**.

In the case of a gravitational N-body system, the two-body relaxation time is given by

$$t_{\rm relax}^{\rm Nbody} \simeq \frac{\Lambda}{\ln\Lambda}\,\frac{t_{\rm cross}}{10}$$

with $t_{\rm cross} \simeq R/V \simeq (2/\pi)t_{\rm dyn}$ (for a detailed derivation, see Binney & Tremaine 2008). If, as discussed above, we set $\Lambda = b_{\rm max}/b_{90}$ with $b_{\rm max} \simeq R$ the size of the gravitational system and $b_{90} = 2Gm/\sigma^2$, with σ the characteristic velocity dispersion, then it is easy to see that $\Lambda = [NR\,\sigma^2]/[2G(Nm)] \sim N$, where we have used the **virial relation** $\sigma^2 = GM/R$ with $M = Nm$ (see Chapter 15). Hence, we obtain the well-known expression for the two-body relaxation time of a gravitational N-body system

$$\boxed{t_{\rm relax}^{\rm Nbody} \simeq \frac{N}{10\ln N}\, t_{\rm cross}}$$

And since $t_{\rm cross}$ can easily be of order a Gyr in astrophysical systems like dark matter halos or galaxies, while $N \gg 1$, we see that $t_{\rm relax}^{\rm Nbody}$ is typically much larger than the Hubble time. Hence, gravitational N-body systems are much better approximations of trully collisionless systems than plasmas, and their velocity distributions can thus *not* be assumed to be Maxwellian.

As a final discussion of our comparison of plasmas and gravitational systems, let's consider the force fields. In the latter case, the forces are gravitational forces which are gradients of the gravitational potential: $\vec{F} \propto \nabla\Phi$. Note that Φ is the sum of N point-mass potentials. When N is sufficiently large, this total Φ is sufficiently smooth that a test-particle only feels the combined (collective) force of all N particles; it only notices the coarsiness of the potential when it comes sufficiently close to an individual particle (i.e., with b_{90}) to experience a large angle deflection, which is very rare. In fact, it is more likely to feel the coarsiness in terms of the cumulative effect of many small-angle deflections. When N becomes smaller the potential becomes coarser (larger small-scale fluctuations) and the system becomes more collisional in nature.

In a plasma the forces are Lorentz forces $\vec{F} = q\left[\vec{E} + \frac{\vec{v}}{c} \times \vec{B}\right]$. The E and B fields are due to the positions and motions of the individual charges. On large scales ($\lambda > \lambda_{\rm D}$), the electromagnetic (EM) fields, and hence the resulting Lorentz forces, are always smooth (no manifestation of coarsiness). However, on sufficiently small scales ($\lambda < \lambda_{\rm D}$), the level of coarsiness of the EM fields depends on the number of particles inside the Debye volume (something we called the inverse of the plasma parameter $g^{-1} = \Lambda$). If Λ is sufficiently small, individual charged particles feel the microscopic E and B fields due to individual charges within the Debye volume, giving rise to coarsiness and thus collisionality. Only if Λ is sufficiently large, will the impact of coarsiness be negligible (that is, will the corresponding two-body relaxation time be sufficiently long).

CHAPTER 23

Plasma Orbit Theory

In describing a fluid, and plasmas are no exception, we are typically not interested in the trajectories of individual particles, but rather in the behaviour of the statistical ensemble. Nevertheless, one can obtain some valuable insight as to the behavior of a plasma if one has some understanding of the typical orbits that charged particles take. In this chapter we therefore focus on **plasma orbit theory**, which is the study of the motion of individual particles in a plasma.

A particle of mass m and charge q moving in an EM field is subject to the **Lorentz force** and therefore satisfies the following equation of motion:

$$m\frac{\mathrm{d}\vec{v}}{\mathrm{d}t} = q\left(\vec{E} + \frac{\vec{v}}{c} \times \vec{B}\right)$$

Each particle is subjected to the EM field produced by the other particles. In addition, there may be an external *magnetic* field imposed on the plasma. The interior of a plasma is usually shielded from external *electrical* fields.

A charged particle moving in a **uniform, magnetic field**, $\vec{B}$, has a motion that can be decomposed into

1. a circular motion with **gyrofrequency** $\omega_\mathrm{c} = |q|B/mc$ and **gyroradius** $r_0 = mv_\perp c/|q|B$ around a central point called the **guiding center**. Here $v_\perp$ is the component of velocity perpendicular to the magnetic field lines.
2. a translatory motion of the guiding center.

This combination gives rise to a **helical motion** along the magnetic field lines.

NOTE: The gyroradius is also known as the **Larmor radius** or the **cyclotron radius**.

What about the motion in a **non-uniform, magnetic field**, $\vec{B}(\vec{x})$? As long as the non-uniformities in $\vec{B}(\vec{x})$ are small over the scale of the gyroradius, i.e.,

$|\vec{B}/(\mathrm{d}\vec{B}/\mathrm{d}r)| < r_0$, one can still meaningfully decompose the motion into a circular motion around the guiding center and the motion of the guiding center itself. The latter can be quite complicated, though. The aim of plasma orbit theory is to find equations describing the motion of the guiding center. Unfortnately, there is no general equation of motion for the guiding center in an arbitrary EM field. Rather, plasma orbit theory provides a 'bag of tricks' to roughly describe what happens under certain circumstances. In what follows we discuss four examples: three circumstances under which the guiding center experiences a **drift**, and one in which the guiding center is **reflected**.

There are three cases in which the guiding center experiences a 'drift':

(A) drift due to the effect of a perpendicular force
(B) drift due to a gradient in the magnetic field
(C) drift due to curvature in the magnetic field

We now discuss these in turn.

(A) The effect of a perpendicular force:
Consider the case of an **external force**, $\vec{F}$ (e.g., gravity), acting on a charged particle in a direction **perpendicular** to a **uniform magnetic field**. The equation of motion then is

$$m\frac{\mathrm{d}\vec{v}}{\mathrm{d}t} = \vec{F} + \frac{q}{c}\,\vec{v}\times\vec{B}$$

In the limit where $\vec{B}$ vanishes, the particle simply moves in the direction of $\vec{F}$. In the limit where $\vec{F}$ vanishes, the particle makes a circular motion around the magnetic field line. When *both* $\vec{F}$ and $\vec{B}$ are present, the guiding center of the circular motion will drift in a direction perpendicular to both $\vec{F}$ and $\vec{B}$. To understand where this comes from, consider the ion's trajectory depicted in Fig. 42. When the ion is at the top of its trajectory, the Lorentz force is pointing in the direction opposite to $\vec{F}$, and the downward acceleration of the particle is less than in the absence of $\vec{F}$. As a consequence the trajectory at this point is less strongly bent. However, when the ion is near the bottom of its trajectory, the Lorentz force enhances $\vec{F}$, and the net acceleration upward is stronger than in the absence of $\vec{F}$, causing a stronger curvature in the trajectory. It is not difficult to show that this causes the guiding

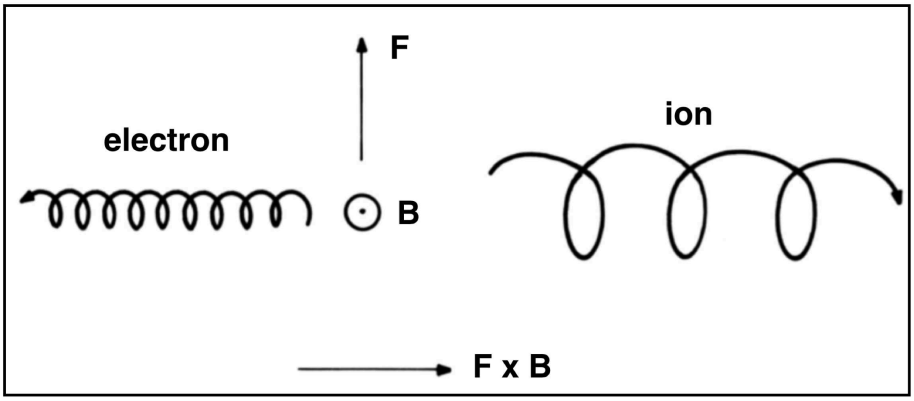

Figure 42: *Drift of a gyrating particle in crossed gravitational and magnetic fields. The magnetic field is pointing out of the page, while the gravitational force is pointing upward. Note that the positively and negatively charged particles drift in opposite directions, giving rise to a non-zero current in the plasma.*

centre to drift with a velocity

$$\vec{v}_{\rm GC} = \frac{c}{q}\frac{\vec{F}\times\vec{B}}{B^2}$$

Note that positively and negatively charged particles will drift in opposite directions, thereby giving rise to a non-zero **current** in the plasma. This will *not* be the case if the external force is the electrical force, i.e., if $\vec{F} = q\vec{E}$. In that case

$$\vec{v}_{\rm GC} = c\frac{\vec{E}\times\vec{B}}{B^2}$$

which does not depend on the charge; hence, all particles drift in the same direction and no current arises.

(B) Gradient Drift:

If the magnetic field has a gradient ∇B in the direction perpendicular to $\vec{B}$, there will also be a drift of the guiding center. The origin is very similar to that of the drift in the presence of an external force discussed above. Assume the same geometry as in Fig. 42, but now imagine there being a gradient ∇B in same direction as $\vec{F}$, but with $F = 0$. This once again causes a different acceleration in the upward and downward directions when the ion is near the top or bottom of its trajectory, causing a similar difference in curvature at the top and bottom as in Fig. 42.

It can be shown that the resulting drift of the guiding center is given by:

$$\vec{v}_{\rm GC} = \pm\frac{1}{2} v_\perp r_0 \, \frac{\vec{B} \times \nabla B}{B^2}$$

where, as throughout this chapter, $v_\perp$ is the component of velocity perpendicular to the magnetic field lines, r_0 is the Larmor radius, and the + and − signs correspond to positive and negative charges. Hence, particles of opposite charge drift in opposite directions, once again giving rise to a non-zero current in the plasma.

(C) Curvature Drift:
If the magnetic field is curved, with a radius of curvature $R_{\rm c}$, once again the guiding center experiences a drift. Physically this arises because as the charged particles gyrates around a curved field, a centrifugal force arises given by

$$\vec{F}_{\rm c} = -m v_\parallel^2 \, \frac{\vec{R}_{\rm c}}{R_{\rm c}^2}$$

where $v_\parallel$ is the velocity component parallel to $\vec{B}$, and $\vec{R}_{\rm c}$ is the curvature *vector* directed towards the curvature center. As a consequence of this centrifugal force, the guiding center drifts with a velocity

$$\vec{v}_{\rm GC} = -\frac{c\, m\, v_\parallel^2}{q R_{\rm c}^2} \, \frac{\vec{R}_{\rm c} \times \vec{B}}{B^2}$$

Like the gradient drift, the curvature drift is also in opposite directions for positively and negatively charged particles, and can thus give rise to a non-zero current.

Magnetic Mirrors:
In all three examples above the drift arises from a 'force' perpendicular to the magnetic field. There are also forces that are parallel to the magnetic field, and these can give rise to the concept of magnetic mirrors.

Let us first introduce the concept of **magnetic moment**. As you may recall from a course on electromagnetism, the current loop with area A and current I (i.e., the current flows along a closed loop that encloses an area A) has an associated magnetic moment given by

$$\mu = \frac{I\, A}{c}$$

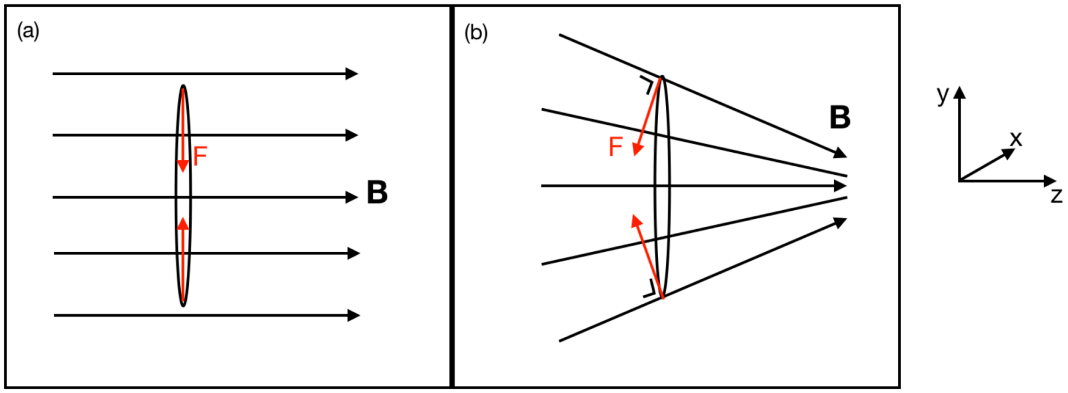

Figure 43: *Illustration of Lorentz force (red arrows) acting on a gyrating particle (indicated by ellipse) in two magnetic field configurations. In panel (a) the field lines are parallel, and the Lorentz force has no component along the z-direction. In the configuration shown in panel (b), though, the Lorentz force, which is always perpendicular to the local magnetic field, now has a component in the z-direction, pointing away from where the magnetic field is stronger.*

A charged particle moving along its Larmor radius is such a loop with $A = \pi r_0^2$ and $I = q(\Omega/2\pi)$. Using that $\Omega = v_\perp/r_0$ and substituting the definition of the Larmor radius, we find that the magnetic moment of a charge gyrating in a magnetic field B is given by

$$\mu = \frac{\pi r_0^2 q v_\perp}{2\pi c r_0} = \frac{\frac{1}{2}mv_\perp^2}{B}$$

The magnetic moment is an **adiabatic invariant**, which means that it is conserved under slow changes in an external variable. In other words, if B only changes slowly with position and time, then the magnetic momentum of a charged particle gyrating is conserved!

Now consider the magnetic field topologies shown in Fig. 43. In panel (a), on the left, the field is uniform and all field lines run parallel. The ellipse represents a gyration of a particle whose guiding center moves along the central field line. The Lorentz force is perpendicular to both $\vec{B}$ and $v_\perp$ and pointing towards the guiding center. Now consider the topology in panel (b). The field lines converge towards the right. At the top of its gyro-radius, the magnetic field now makes an angle wrt the magnetic field line corresponding to the guiding center, and as a result the Lorentz force (indicated in red), now has a non-zero component in the z-direction. Hence, the particle will be accelerated away from the direction in which the field strength increases!

To make this quantitative, let us compute the Lorentz force in the z-direction:

$$F_z = \frac{q}{c}\left(\vec{v}\times\vec{B}\right)_z = \frac{q}{c}v_\perp B_R$$

where B_R is the magnetic field component in the cylindrical R-direction, in which the z-direction is as indicated in Fig. 43. Using the Maxwell equation $\nabla\cdot\vec{B}=0$, we have that

$$\frac{1}{R}\frac{\partial}{\partial R}\left(RB_R\right)+\frac{\partial B_z}{\partial z}=0$$

which implies

$$R\,B_R = -\int_0^R R\,\frac{\partial B_z}{\partial z}(R)\mathrm{d}R$$

If we take into account that $\frac{\partial B_z}{\partial z}$ does not vary significantly over one Larmor radius, we thus find that

$$B_R = -\frac{1}{2}R\,\frac{\partial B_z}{\partial z}$$

Substituting this in our expression for the Lorentz force in the z-direction, with R equal to the Larmor radius, we find that

$$F_z = -\frac{1}{2}mv_\perp^2\frac{1}{B}\frac{\partial B_z}{\partial z} = -\mu\frac{\partial B_z}{\partial z}$$

This makes it clear that the Lorentz force has a non-zero component, proportional to the magnetic moment of the charged particle, in the direction opposite to that in which the magnetic field strength increases.

Now we are ready to address the concept of magnetic **mirror confinement**. Consider a magnetic field as depicted in Fig. 44. Close to the coils, the magnetic field is stronger than in between. Now consider a particle gyrating along one of these field lines, as shown. Suppose the particle starts out with kinetic energy $K_0=\frac{1}{2}m(v_\perp^2+v_\parallel^2)$ and magnetic moment μ. Both of these quantities will be conserved as the charged particle moves. As the particle moves in the direction along which the strength of $\vec{B}$ increases (i.e., towards one of the coils), v_{perp} must increase in order to guarantee conservation of the magnetic moment. However, the transverse kinetic energy can never exceed the total kinetic energy. Therefore, when the particle reaches a region of sufficiently strong B, where the transverse kinetic energy equals the total kinetic energy, it is not possible for the particle to penetrate further into regions of

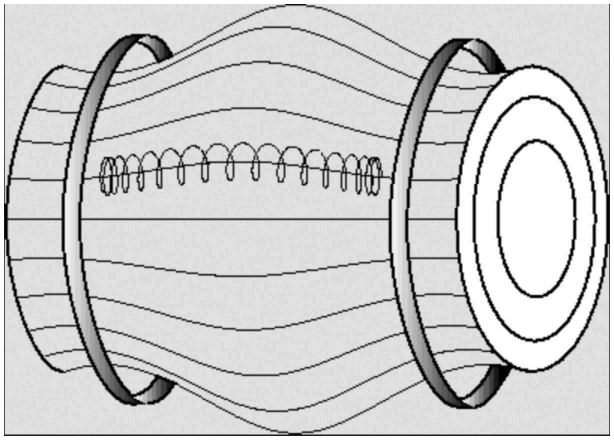

Figure 44: *Illustration of a magnetic bottle. The black horizontal curved lines depict magnetic field lines, which are 'squeezed' together at the ends by two electrical coils. As a result the magnetic field strength is larger at the ends than in the middle, creating magnetic mirrors in between charged particles can be trapped. An example of a particle trajectory is shown.*

even stronger magnetic field: the particle will be reflected back, and the region of increasing magnetic field thus acts as a reflector, known as a **magnetic mirror**.

The contraption shown in Fig. 44 is known as a **magnetic bottle** as it can be used to 'store' charged particles. Note, though, that a magnetic bottle is inherently 'leaky'. To see this, let B_0 denote the magnetic field strength in the middle of the bottle, and $B_{\rm max}$ the maximum magnetic field strength, which arises at the positions of the two coils. Let $\vec{v}_0$ be the velocity of the particle at the middle of the bottle, and let $v_{\perp,0}$ be its corresponding transverse speed: $v_{\perp,0} = v_0 \sin\alpha$. Since the transverse velocity at the time of reflection has to equal v_0, we see that only those particles will be reflected for which $\sin^2\alpha > B_0/B_{\rm max}$. Particles for which α is smaller make up a **loss cone**, as these particles will leak out of the magnetic bottle.

Magnetic bottles are not only found in laboratories; the Earth's magnetic field creates its own magnetic bottles due to its toroidal topology. The charged particles that are trapped give rise to what are called the Van Allen belts (electrons and protons have their own belts, as depicted in Fig. 45). As the trapped particles move back and forth between the North and South poles of the Earth's magnetic field, they experience **curvature drift** (in opposite directions for the electrons and protons). The resulting

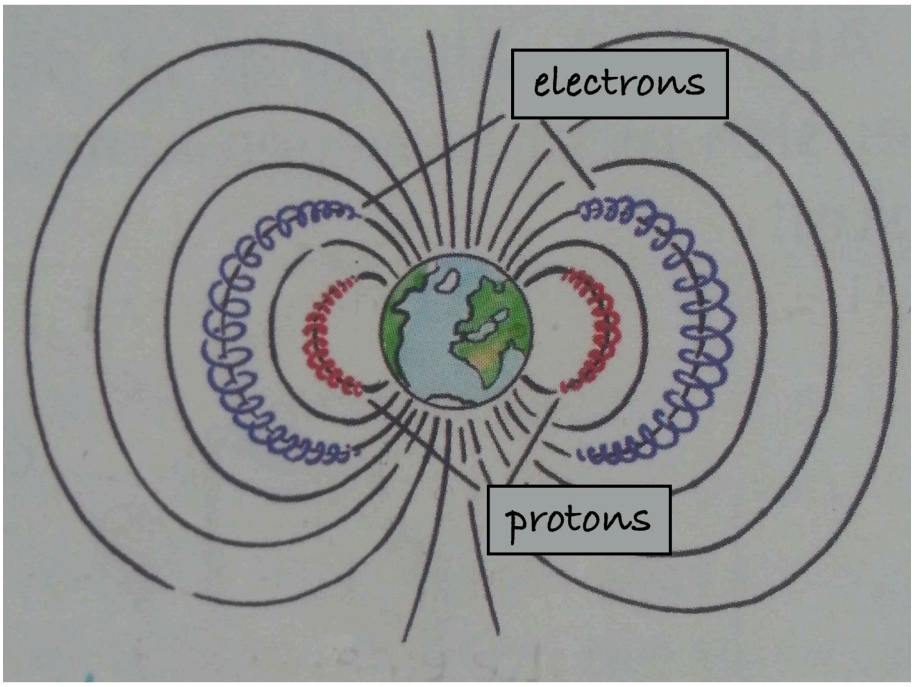

Figure 45: *Illustration of the Van Allen belts of trapped, charged particles in the toroidal magnetic field of the Earth.*

currents are called the **ring currents**.

CHAPTER 24

Plasma Kinetic Theory

In Chapter 6 we discussed the kinetic theory of fluids. Starting from the Liouville theorem we derived the BBGKY hierarchy of equations, which we repeat here for convenience:

$$\begin{aligned}
\frac{\partial f^{(1)}}{\partial t} &= \{\mathcal{H}^{(1)}, f^{(1)}\} + \int \mathrm{d}^3\vec{q}_2\,\mathrm{d}^3\vec{p}_2\,\frac{\partial U(|\vec{q}_1-\vec{q}_2|)}{\partial \vec{q}_1}\cdot\frac{\partial f^{(2)}}{\partial \vec{p}_1} \\
&\vdots \\
\frac{\partial f^{(k)}}{\partial t} &= \{\mathcal{H}^{(k)}, f^{(k)}\} + \sum_{i=1}^{k}\int \mathrm{d}^3\vec{q}_{k+1}\,\mathrm{d}^3\vec{p}_{k+1}\,\frac{\partial U(|\vec{q}_i-\vec{q}_{k+1}|)}{\partial \vec{q}_i}\cdot\frac{\partial f^{(k+1)}}{\partial \vec{p}_i}
\end{aligned}$$

Here $k = 1, 2, ..., N$, $f^{(k)}$ is the k-particle DF, which relates to the N-particle DF ($N > k$) according to

$$f^{(k)}(\vec{w}_1, \vec{w}_2, ..., \vec{w}_k, t) \equiv \frac{N!}{(N-k)!}\int \prod_{i=k+1}^{N} \mathrm{d}^6\vec{w}_i\, f^{(N)}(\vec{w}_1, \vec{w}_2, ..., \vec{w}_N, t)\,,$$

and $\mathcal{H}^{(k)}$ is the k-particle Hamiltonian given by

$$\mathcal{H}^{(k)} = \sum_{i=1}^{k}\frac{\vec{p}_i^{\,2}}{2m} + \sum_{i=1}^{k} V(\vec{q}_i) + \frac{1}{2}\sum_{i=1}^{k}\sum_{\substack{j=1\\ j\neq i}}^{k} U(|\vec{q}_i - \vec{q}_j|)$$

with $V(\vec{q})$ the potential associated with an external force, and $U(r)$ the two-body interaction potential between two (assumed equal) particles separated by a distance $r = |\vec{q}_i - \vec{q}_j|$.

All of this is completely general: it holds for any Hamiltonian system consisting of N particles, and therefore also applies to plasmas. However, we also saw that in order

to make progress, one needs to make certain assumptions that allow one to truncate the BBGKY hierarchy at some point (in order to achieve closure).

If one can ignore two-body collisions, then the phase-space coordinates of the particles will be uncorrelated, such that

$$f^{(2)}(\vec{q}_1, \vec{q}_2, \vec{p}_1, \vec{p}_2) = f^{(1)}(\vec{q}_1, \vec{p}_1)\, f^{(1)}(\vec{q}_2, \vec{p}_2)$$

which is equivalent to setting the **correlation function** $g(1,2) = 0$ (see Chapter 6 for details). The first equation in the BBGKY hierarchy is now closed, and yields the **Collisionless Boltzmann Equation** (CBE), which can be written as

$$\boxed{\frac{\mathrm{d}f}{\mathrm{d}t} = \frac{\partial f}{\partial t} + \dot{\vec{x}} \cdot \frac{\partial f}{\partial \vec{x}} + \dot{\vec{v}} \cdot \frac{\partial f}{\partial \vec{v}} = 0}$$

and is the fundamental evolution equation for collisionless systems. As we have seen in Chapter 22, collective effects are typically more important for plasmas then collisional effects. Hence, as long as one considers plasma effects for which collisions are NOT important (i.e., high frequency plasma waves), then one is justified in using the CBE. It is common, though, to refer to this as the **Vlasov equation**, when applied to a plasma, and we will follow that nomenclature.

In a gravitational N-body system the acceleration in the third term of the CBE $\dot{\vec{v}} = -\nabla\Phi$, where Φ follows from the **Poisson equation**

$$\nabla^2\Phi = 4\pi G\rho$$

with

$$\rho(\vec{x}, t) = m \int f(\vec{x}, \vec{v}, t)\mathrm{d}^3\vec{v}$$

In the case of a plasma, the acceleration is given by

$$\dot{\vec{v}} = \frac{q}{m}\left[\vec{E}(\vec{x}, t) + \frac{\vec{v}}{c} \times \vec{B}(\vec{x}, t)\right]$$

And since the effects of collisions are ignored here, the fields $\vec{E}$ and $\vec{B}$ are the *smooth*,

ensemble-averaged fields that satisfy the **Maxwell equations**

$$\begin{aligned}
\nabla\cdot\vec{E} &= 4\pi\rho \\
\nabla\cdot\vec{B} &= 0 \\
\nabla\times\vec{E} &= -\frac{1}{c}\frac{\partial\vec{B}}{\partial t} \\
\nabla\times\vec{B} &= \frac{4\pi}{c}\vec{J}+\frac{1}{c}\frac{\partial\vec{E}}{\partial t}
\end{aligned}$$

Here $\rho=\rho_{\rm i}+\rho_{\rm e}$ is the total charge density and $\vec{J}=\vec{J}_{\rm e}+\vec{J}_{\rm i}$ the total current density, which are related to the distribution function according to

$$\rho_{\rm s}(\vec{x},t) = q_{\rm s}\int {\rm d}^3\vec{v}\, f_{\rm s}(\vec{x},\vec{v},t)$$
$$\vec{J}_{\rm s}(\vec{x},t) = q_{\rm s}\int {\rm d}^3\vec{v}\,\vec{v}\, f_{\rm s}(\vec{x},\vec{v},t)$$

for species 's'. Thus we see that the Maxwell equations are for a plasma, what the Poisson equation is for a gravitational system. Note that the distribution function in the Vlasov equation is the sum of $f_{\rm i}(\vec{x},\vec{v},t)$ plus $f_{\rm e}(\vec{x},\vec{v},t)$.

As we discussed at great length in Chapter 6, if one wants to describe a dilute, neutral fluid in which the particles only have short-range interactions (such that $U(r)\simeq 0$ outside of some small distance $r_{\rm coll}$), then we can make the assumption of **molecular chaos**, which states that

$$f^{(2)}(\vec{q},\vec{q},\vec{p}_1,\vec{p}_2) = f^{(1)}(\vec{q},\vec{p}_1)\, f^{(1)}(\vec{q},\vec{p}_2)$$

(note that the collisions are assumed to be perfectly localized, such that we only need to know the 2-particle DF for $\vec{q}_1=\vec{q}_2=\vec{q}$). This assumption allows us to close the BBGKY hierarchy, yielding the **Boltzmann Equation**:

$$\boxed{\frac{{\rm d}f}{{\rm d}t} = \frac{\partial f}{\partial t}+\dot{\vec{x}}\cdot\frac{\partial f}{\partial\vec{x}}+\dot{\vec{v}}\cdot\frac{\partial f}{\partial\vec{v}} = I[f]}$$

Here $I[f]$ is the **collision integral**, which describes how the phase-space density around a particle (or fluid element) changes with time due to short-range collisions. Upon taking the moment equations of this Boltzmann equation we obtain a hierarchy of 'fluid equations', which we can close upon supplementing them with **constitutive**

equations for various **transport coefficients** (i.e., viscosity and conductivity) that can be computed using the **Chapman-Enskog expansion** (something we did not cover in these lecture notes).

In the case of a plasma, though, we cannot use the assumption of molecular chaos, as individual particles have many (of order g^{-1}) simultaneous long-range Coulomb interactions. This situation is very different from that of a neutral gas, and the Boltzmann equation can therefore NOT be used to describe a plasma.

So what assumption can we make for a plasma that allows us to truncate the BBGKY hierarchy? The standard approach is to assume that $h(1,2,3) = 0$ (i.e., assume that three-body correlation function is zero). This is a very reasonable assumption to make, as it basically asserts that two-body interactions are more important than three-body interactions. However, even with $h(1,2,3) = 0$ the BBGKY hierarchy yields a set of two equations (for $\partial f^{(1)}/\partial t$ and $\partial f^{(2)}/\partial t$) that is utterly unsolvable. Hence, additional assumptions are necessary. The two assumptions that are typically made to arrive at a manageable equation are

1. plasma is spatially homogeneous.
2. the two-point correlation function $g(1,2)$ relaxes much faster than the one-point distribution function $f(1)$.

The latter of these is known as **Bogoliubov's hypothesis**, and is a reasonable assumption under certain conditions. Consider for example injecting an electron into a plasma. The other electrons will adjust to the presence of this new electron in roughly the time it takes for them to have a collision with the new electron. Using that the typical speed of the electrons is $v_\mathrm{e} \propto k_\mathrm{B}T$ and using the Debye length as the typical length scale, the time scale for the injected electron to relax is $\lambda_\mathrm{e}/v_\mathrm{e} \sim \omega_\mathrm{p,e}^{-1}$. In contrast, the time for $f(1)$ to relax to the newly injected electron is $\sim g^{-1}\omega_\mathrm{p,e}^{-1}$, as all the g^{-1} particles within the Debye volume need to undergo mutual collisions.

Using the BBGKY hierarchy with $h(1,2,3) = 0$, assuming the plasma to be spatially homogeneous, and adopting Bogoliubov's hypothesis yields, after some tedious algebra the **Lenard-Balescu** equation. Although the student is not required to know or comprehend this equation, it is given here for the sake of completeness:

$$\frac{\partial f(\vec{v},t)}{\partial t} = -\frac{8\pi^4 n_\mathrm{e}}{m_\mathrm{e}^2}\frac{\partial}{\partial \vec{v}}\int \mathrm{d}\vec{k}\,\mathrm{d}\vec{v}'\,\vec{k}\vec{k}\cdot\frac{\phi^2(k)}{|\varepsilon(\vec{k},\vec{k}\cdot\vec{v})|^2}\,\delta[\vec{k}\cdot(\vec{v}-\vec{v}')]\,\left[f(\vec{v})\,\frac{\partial f}{\partial \vec{v}'} - f(\vec{v}')\frac{\partial f}{\partial \vec{v}}\right]$$

Here

$$\phi(k) = \frac{e^2}{2\pi^2 k^2}$$

is the Fourier transform of the Coulomb potential $\phi(x) = e^2/|x|$, and

$$\varepsilon(\vec{k},\omega) = 1 + \frac{\omega_{\rm p,e}^2}{k^2} \int {\rm d}\vec{v}\, \frac{\vec{k}\cdot(\partial f/\partial \vec{v})}{\omega - \vec{k}\cdot\vec{v}}$$

is called the **dielectric function**, which basically represents the plasma shielding of a test particle. Note that $\vec{x}$ does not appear as an argument of the distribution function, which reflects the assumption of a homogeneous plasma. And the term in square brackets has no explicit time-dependence, which reflects Bogoliubov's hypothesis. We emphasize that because of the assumptions that underly the Lenard-Balescu equation, it is NOT applicable to all plasma processes. Although it can be used to describe, say, the collisional relaxation of an electron beam in a plasma, it cannot be used to describe for example the collisional damping of *spatially inhomogeneous* wave motion.

The rhs of the Lenard-Balescu equation represents the physics of two-particle collisions. This is evident from the fact that the term $\phi(k)/\varepsilon(\vec{k},\vec{k}\cdot\vec{v})$ appears squared. This term represents the Coulomb potential of a charged particle (the $\phi(k)$-part) together with its shielding cloud (represented by the dielectric function). Hence, the fact that this term appears squared represents the collision of two shielded particles. It may be clear that this is not an easy equation to deal with. However, one can obtain a simplified but fairly accurate form of the Lenard-Balescu equation that can be recast in the form of a **Fokker-Planck equation**

$$\boxed{\frac{\partial f(\vec{v},t)}{\partial t} = -\frac{\partial}{\partial v_i}\left[A_i\, f(\vec{v})\right] + \frac{1}{2}\frac{\partial^2}{\partial v_i \partial v_j}\left[B_{ij}\, f(\vec{v})\right]}$$

Here

$$A_i = \frac{8\pi n_{\rm e} e^4 \ln\Lambda}{m_{\rm e}^2}\, \frac{\partial}{\partial v_i} \int {\rm d}\vec{v}\,'\, \frac{f(\vec{v}\,',t)}{|\vec{v}-\vec{v}\,'|}$$

is called the **coefficient of dynamical friction**, which represents the slowing down of a typical particle because of many small angle collisions, and

$$B_{ij} = \frac{4\pi n_{\rm e} e^4 \ln\Lambda}{m_{\rm e}^2}\, \frac{\partial^2}{\partial v_i \partial v_j} \int {\rm d}\vec{v}\,'\, |\vec{v}-\vec{v}\,'|\, f(\vec{v}\,',t)$$

is the **diffusion coefficient**, which represents the increase of a typical particle's velocity (in the direction perpendicular to its instantaneous velocity) due to the many small angle collisions.

If the two terms on the rhs of the Fokker-Planck equation balance each other, such that $\partial f(\vec{v},t)/\partial t = 0$, then the plasma has reached an equilibrium. It can be shown that this is only the case if $f(\vec{v})$ follows a **Maxwell-Boltzmann distribution**. This is another way of stating that two-body collisions drive the systems towards a Maxwellian.

Note that the **Fokker-Planck equation** is a very general equation in physics; it describes the evolution of a distribution function due to any phenomenon that in some approximate sense can be considered **Markovian**. A well known example is **Brownian motion**. The Fokker-Planck equation is also used for describing the collisional evolution of gravitational N-body systems (i.e., globular clusters), while the first-order diffusion coefficient A_i is used to describe the orbital decay of a massive body due to dynamical friction (cf. Chapter 16). Hence, once more we see the strong similarity between gravitational N-body systems and plasmas.

CHAPTER 25

Vlasov Equation & Two-Fluid Model

In Chapter 22 we have seen that the two-body collision frequency of a plasma is much smaller than the plasma frequency (by roughly a factor $\Lambda = g^{-1}$). Hence, there are plasma phenomena that have a characteristic time scale that is much shorter than the two-body relaxation time. For such phenomena, collisions can be ignored, and we may consider the plasma as being **collisionless**.

And as we have seen in the previous chapter, the equation that governs the dynamics of a collisionless plasma is the **Vlasov equation**.

$$\frac{\partial f}{\partial t} + \vec{v} \cdot \frac{\partial f}{\partial \vec{x}} + \frac{\vec{F}}{m} \cdot \frac{\partial f}{\partial \vec{v}} = 0$$

with

$$\vec{F} = n \int \mathrm{d}\vec{x}_2 \mathrm{d}\vec{v}_2 \vec{F}_{12} f^{(1)}(\vec{x}_2, \vec{v}_2, t)$$

the smooth force acting on particle 1 due to the long-range interactions of all other particles (within the Debye length). This equation derives from the BBGKY hierarchy upon neglectiong the two-particle correlation function, $g(1,2)$, which arises due to Coulomb interactions among particles within each others Debye volume. Hence, $\vec{F}$ assumes that the force field (for a plasma that entails $\vec{E}(\vec{x},t)$ and $\vec{B}(\vec{x},t)$) are perfectly smooth.

An important application of the Vlasov equation is the so-called **two-fluid model of plasma physics**, in which the plasma is regarded as an inter-penetrating mixture of a negatively charged fluid of electrons, and a positively charged fluid of ions. In that case,

$$f(\vec{x},\vec{v},t) = f_\mathrm{e}(\vec{x},\vec{v},t) + f_\mathrm{i}(\vec{x},\vec{v},t)$$

where the subscripts 'e' and 'i' refer to electrons and ions, respectively. Since the **Vlasov equation** is linear, both f_e and f_i obey the Vlasov equation. If the force $\vec{F}$ is purely electromagnetic (i.e., we can ignore the gravitational force), then we have

that

$$\boxed{\frac{\partial f_{\rm a}}{\partial t} + \vec{v} \cdot \frac{\partial f_{\rm a}}{\partial \vec{x}} + \frac{q_{\rm a}}{m}\left(\vec{E} + \frac{\vec{v}}{c} \times \vec{B}\right) \cdot \frac{\partial f_{\rm a}}{\partial \vec{v}} = 0}$$

where 'a' is either 'e' or 'i'.

Rather than solving the Vlasov equation, we follow the same approach as with our neutral fluids, and our collisionless fluids, and solve instead the moment equations, by multiplying the Vlasov equation with $\chi(\vec{v})$ and integrating over all of velocity (momentum) space (cf. Chapter 7).

For $\chi = 1$ this yields the **continuity equation**

$$\frac{\partial n_{\rm a}}{\partial t} + \nabla \cdot (n_{\rm a}\, \vec{u}_{\rm a}) = 0$$

while $\chi = m_{\rm a}\vec{v}_{\rm a}$ yields the **momentum equations**

$$m_{\rm a}\, n_{\rm a}\left[\frac{\partial \vec{u}_{\rm a}}{{\rm d}t} + (\vec{u}_{\rm a} \cdot \nabla)\, \vec{u}_{\rm a}\right] = -\nabla P_{\rm a} + q_{\rm a} n_{\rm a}\left(\vec{E} + \frac{\vec{u}_{\rm a}}{c} \times \vec{B}\right)$$

Note that the continuity equation is exactly the same as for a neutral fluid or a collisionless fluid, while the momentum equations are the same as the **Euler equations** for a **neutral, inviscid fluid** or the **Jeans equations** for a **collisionless fluid**, except that the force is now electromagnetic, rather than gravitational.

We emphasize that we have ignored **viscosity** here, something we will continue to do throughout our discussion of plasma physics. More accurately, the above momentum equations should be the **Navier-Stokes equations**, i.e., there should be an additional term $\mu[\nabla^2 \vec{u}_{\rm a} + \frac{1}{3}\nabla(\nabla \cdot \vec{u}_{\rm a})]$ on the rhs. As we are mainly concerned with astrophysical flows, for which the Reynolds number is large, ignoring **viscosity** when discussing astrophysical plasmas is a reasonable thing to do.

As for neutral fluids, we need to complement these moment equations with an equation of state (EoS) in order to close the equations. Without going into detail, in most cases the EoS of a plasma can be taken to have one of the following three forms:

$$\begin{array}{ll} P_{\rm a} = 0 & (\text{"cold plasma"}) \\ P_{\rm a} = n_{\rm a}\, k_{\rm B}\, T_{\rm a} & (\text{"ideal plasma"}) \\ P_{\rm a} = C n_{\rm a}^{\gamma} & (\text{"adiabatic processes"}) \end{array}$$

A 'cold plasma' is a plasma in which the random motions of the particles are not important.

NOTE: in the presence of strong magnetic fields, the thermodynamic properties of the plasma can be very different in directions parallel and perpendicular to $\vec{B}$; in those cases the pressure cannot be fully described by a scalar, but requires a stress-tensor-equivalent instead. We will not consider such situations here.

Since the momentum equations for our plasma contain the electric and magnetic fields, we need to complement the moment equations and EoS with the **Maxwell equations**

$$\begin{aligned} \nabla \cdot \vec{E} &= 4\pi(n_\mathrm{i} - n_\mathrm{e})\, e \\ \nabla \cdot \vec{B} &= 0 \\ \nabla \times \vec{E} &= -\frac{1}{c}\frac{\partial \vec{B}}{\partial t} \\ \nabla \times \vec{B} &= \frac{4\pi}{c}(n_\mathrm{i}\vec{u}_\mathrm{i} - n_\mathrm{e}\vec{u}_\mathrm{e})\, e + \frac{1}{c}\frac{\partial \vec{E}}{\partial t} \end{aligned}$$

Upon inspection, this complete set of 18 equations (8 Maxwell eqs, 2×3 momentum equations, 2 continuity equations, and 2 equations of state) describes the evolution of a total of 16 scalar quantitie: $\vec{E}$ (3), $\vec{B}$ (3), $\vec{u}_\mathrm{i}$ (3), $\vec{u}_\mathrm{e}$ (3), n_i, n_e, P_i, and P_e. This set of equations constitutes the **two-fluid model** of plasma physics. Note that this model derives from the **Vlasov equation**, and can therefore only be used to describe plasma phenomena in which collisions can be neglected.

As an example of an application of the two-fluid model, consider **electro-magnetic oscillations** in a plasma.

Let's assume the plasma to be 'cold' (i.e., $P_\mathrm{e} = P_\mathrm{i} = 0$), and consider perturbations in a uniform, homogeneous plasma. The perturbation analysis treatment is exactly analogous to that of accoustic waves in Chapter 12: First, apply small perturbations to the dynamical quantities (i.e., $n_0 \to n_0 + n_1$, $\vec{E}_0 \to \vec{E}_0 + \vec{E}_1$, etc, where subscripts '0' refer to the unperturbed equilibrium solution. Next, linearize the equations,

which implies that we ignore all higher-order terms. For the momentum equations this yields

$$m_{\rm e}\, n_0\, \frac{\partial \vec{v}_1}{\partial t} = -e\, n_0\, \vec{E}_1$$

Note that the magnetic force $\vec{v}_1 \times \vec{B}_1$ is second-order in the perturbed quantities and therefore neglected. For the Maxwell equations we obtain that

$$\nabla \times \vec{B}_1 = -\frac{4\pi}{c}\, n_0\, e\, \vec{v}_1 + \frac{1}{c}\frac{\partial \vec{E}}{\partial t}$$

and

$$\nabla \times \vec{E}_1 = -\frac{1}{c}\frac{\partial \vec{B}_1}{\partial t}.$$

Combining these equations, and assuming all perturbations to be of the form EXP$[-i(\vec{k}\cdot \vec{x} - \omega t)]$, which implies that $\partial/\partial t \to -i\omega$ and $\nabla \to -i\vec{k}$, one obtains the **dispersion relation** $\omega(\vec{k})$. In the case of our two-fluid model, this dispersion relation has the form

$$\vec{k} \times (\vec{k} \times \vec{E}_1) = -\frac{\omega^2}{c^2}\left(1 - \frac{\omega_{\rm p}^2}{\omega^2}\right)\vec{E}_1$$

Here

$$\omega_{\rm p} = \left(\frac{4\pi\, n_0\, e^2}{m_{\rm e}}\right)^{1/2}$$

is the **plasma frequency** in the undisturbed plasma. This dispersion relation corresponds to two physically distinct types of wave modes:

Plasma Oscillations:
These are oscillation modes for which

$$E_{1x} = E_{1y} = 0\,, \qquad \omega^2 = \omega_{\rm p}^2$$

where the z-direction is taken to be along $\vec{k}$. Hence, since the group velocity $v_{\rm g} = \partial\omega/\partial k = 0$ we see that these correspond to **non-propagating**, **longitudinal** oscillations with a frequency equal to the plasma frequency. These are called **plasma waves**, or **Langmuir waves**. Physically, they are waves in which perturbations in $\vec{E}$, cause a separation between electrons and ions, which results in an electrostatic restoring force. Note that the plasma frequency depends only on the density of the plasma. If the plasma is not cold (i.e., $P_{\rm a} \neq 0$), then it follows that these Langmuir oscillations become travelling waves.

Electromagnetic waves:
These are oscillation modes for which

$$E_{1z} = 0\,, \qquad \omega^2 = \omega_{\rm p}^2 + k^2 c^2$$

where as before the z-direction is taken to be along $\vec{k}$. Hence, these are **transverse** waves. In fact, these are simply electromagnetic waves, but modified by the plasma. The group velocity (i.e., the velocity with which information propagates) is given by

$$v_{\rm g} \equiv \frac{\partial \omega}{\partial k} = c\sqrt{1 - \frac{\omega_{\rm p}^2}{\omega^2}}$$

which is less than the speed of light, c. For comparison, the **phase velocity** is given by

$$v_{\rm ph} \equiv \frac{\omega}{k} = \frac{c}{\sqrt{1 - \frac{\omega_{\rm p}^2}{\omega^2}}}$$

which is larger than c. Note, though, that this does not violate special relativity, as no physical signal is travelling at this speed (i.e., it does not carry any information).

• If $\omega \gg \omega_{\rm p}$, we have that $\omega^2 = k^2 c^2$ which is the usual dispersion relation for EM waves in a vacuum, and $v_{\rm g} = c$. The frequency of these EM waves is too high for the plasma to respond, and plasma effects are negligible. When $\omega \downarrow \omega_{\rm p}$ then the EM waves slow down, and the phase velocity increases. The **refractive index** of a medium is defined as $n \equiv c/v_{\rm ph} = ck/\omega$, which for a plasma is given by $n^2 = 1 - (\omega_{\rm p}/\omega)^2$. Hence, when $\omega \downarrow \omega_{\rm p}$ we have that $n \downarrow 0$.

• If $\omega < \omega_{\rm p}$, then k and $v_{\rm g}$ become imaginary. This indicates that the EM waves simply cannot penetrate the plasma; they are reflected back. The reason is that the plasma can counteract the oscillations in the EM field at a rate that is faster, thereby shorting the fluctuations, and thus the EM wave. This explains why low-frequency radio signals can be reflected from the ionispheric plasma, and why cyclotron radiation cannot travel through the plasma that permeates the Universe (unless it derives from very strong magnetic fields, in which case the frequency can be larger than the plasma frequency). Note that in this regime, strictly speaking the Vlasov equation is no longer applicable, as the time scale for collisions becomes comparable to, or shorter than, that of the perturbation.

The above analysis is based on a perturbation analysis of the two-fluid model, which is based on moment equations of the Vlasov equation. Landau performed a more thorough analysis, by actually perturbing the **Vlasov equation** itself. He found that the Langmuir waves will damp, a process known as **Landau damping**.

This damping may come as a surprise (as it did to Landau, when he first derived this result). After all, damping is typically associated with dissipation, and hence requires either radiation, or collisions that convert wave energy into random, thermal energy. But the Vlasov equation includes neither radiation nor collisions. So where does this damping come from? Without going through a rigorous derivation, which is somewhat tedious, involving nasty complex contour integrals, we merely sketch how Landau damping arises from the energy exchange between an electromagnetic wave with phase velocity $v_{\rm ph} \equiv \omega/k$ and particles in the plasma with velocities approximately equal to $v_{\rm ph}$; these particles can interact strongly with the wave (similar to how particles that are in near-resonance with a perturber can exchange energy with it). Particles that have a velocity $v \lesssim v_{\rm ph}$ will be *accelerated* (i.e., gaining energy) by the electric field of the Langmuir wave to move with the phase velocity of the wave. Particles with $v \gtrsim v_{\rm ph}$, on the other hand, will be *decelerated* (losing energy). All in all, the particles have a tendency to synchronize with the wave. An imbalance between energy gainers and energy losers arises from the fact that the velocity distribution of a plasma is typically a Maxwell-Boltzmann distribution; hence, there will be slightly more particles with $v < v_{\rm ph}$ (energy gainers) than particles with $v > v_{\rm ph}$ (energy losers). Hence, there is a net tranfer of energy from the wave to the particles, causing the former to damp.

A famous metaphor for Landau damping involves surfing. One can view Langmuir waves as waves in the ocean, and the particles as surfers trying to catch the wave, all moving in the same direction. If the surfer is moving on the water surface at a velocity slightly less than the waves he will eventually be caught and pushed along by the wave (gaining energy). On the other hand, a surfer moving slightly faster than a wave will be pushing on the wave as he moves uphill (losing energy to the wave). Within this metaphor, it is also clear that if the surfer is not moving at all, no exchange of energy happens as the wave simply moves the surfer up and down as it goes by. Also a wind-surfer, who is moving much faster than the wave won't interact much with the wave either.

Hence, **Landau damping** arises from gradients in the distribution function at the phase velocity of the wave, which can cause a transfer of energy from the wave to

the particles; Landau damping is a prime example of a **wave-particle interaction**. As first pointed out by Lynden-Bell, it is similar to **violent relaxation** for a purely collisionless, gravitational system, in which the energy in potential fluctuations (i.e., oscillations in the gravitational system, for example due to gravitational collapse) are transferred into random motions, ultimately leading to virialization (relaxation).

CHAPTER 26

Magnetohydrodynamics

As discussed in the previous chapter, when discussing phenomena in which electrons and ions respond differently (such as the response of a plasma to electromagnetic oscillations), the two-fluid model (or Vlasov equation) has to be applied.

When we consider phenomena with length scales much larger than the **Debye length**, and time scales much longer than the inverse of the **plasma frequency**, charge separation is small, and can typically be neglected. In that case we don't need to treat electrons and ions separately. Rather, we treat the plasma as a single fluid. Note, though, that as we are considering phenomena with longer time scales, our **one-fluid model** of plasma physics will have to account for collisions (i.e., we won't be able to use the Vlasov equation as our starting point). As we will see, the main effect of these collisions is to transfer momentum between electrons and ions, which in turn manifests as an electrical current.

A formal derivation of the MHD equation is a formidable task. We instead follow a more heuristic approach in what follows. In the previous chapter we derived a two-fluid model by taking moment equations of the Vlasov equations for the electron and ion species. We follow the same approach here. However, since in MHD we cannot ignore collisions, we have to supplement the Vlasov equation with a collision term:

$$\boxed{\frac{\partial f_\mathrm{a}}{\partial t} + \vec{v}\cdot\frac{\partial f_\mathrm{a}}{\partial \vec{x}} + \frac{q_\mathrm{a}}{m}\left(\vec{E} + \frac{\vec{v}}{c}\times\vec{B}\right)\cdot\frac{\partial f_\mathrm{a}}{\partial \vec{v}} = \left(\frac{\partial f_\mathrm{a}}{\partial t}\right)_\mathrm{coll}}$$

where as before 'a' refers to a species, either 'e' or 'i'. As we will see, we can obtain the necessary insight to develop our one-fluid model, without regard of what this collision term looks like in detail.

By integrating the above 'Boltzmann-like' equation over velocity space, we obtain the **continuity equation**

$$\frac{\partial n_{\rm a}}{\partial t} + \nabla \cdot (n_{\rm a}\, \vec{u}_{\rm a}) = 0$$

where we have used that

$$\int {\rm d}\vec{v} \left(\frac{\partial f_{\rm a}}{\partial t}\right)_{\rm coll} = 0$$

This term represents the change in the number of particles of species 'a' in a small volume of configuration space due to collisions. To good approximation this is zero, which follows from the fact that while Coulomb interactions can cause large changes in momentum (when $b < b_{90}$), they do not cause much change in the positions of the particles. Hence, the collision term leaves the continuity equation unaltered.

For the momentum equation, we multiply the above 'Boltzmann-like' equation with velocity and again integrate over velocity space. If we once again ignore viscosity, this yields exactly the same equation as for the two-fluid model discussed in the previous chapter, but with one additional, *collisional term*:

$$m_{\rm a}\, n_{\rm a} \left[\frac{\partial \vec{u}_{\rm a}}{{\rm d}t} + (\vec{u}_{\rm a} \cdot \nabla)\, \vec{u}_{\rm a}\right] = -\nabla P_{\rm a} + q_{\rm a} n_{\rm a} \left(\vec{E} + \frac{\vec{u}_{\rm a}}{c} \times \vec{B}\right) + \vec{C}_{\rm a}$$

where

$$\boxed{\vec{C}_{\rm a} = m_{\rm a} \int {\rm d}\vec{v}\, \vec{v} \left(\frac{\partial f_{\rm a}}{\partial t}\right)_{\rm coll}}$$

This term represents the change in the momentum of species 'a' at position $\vec{x}$ due to Coulomb interactions. Note that a given species cannot change its momentum through collisions with members of its own species (i.e., the center of mass of two electrons is not changed after they have collided with each other). Hence, $\vec{C}_{\rm e}$ represents the change in the momentum of the electrons due to collisions with the ions, and $\vec{C}_{\rm i}$ represents the change in the momentum of the ions due to collisions with the electrons. And, since the total momentum is a conserved quantity, we have that $\vec{C}_{\rm e} = -\vec{C}_{\rm i}$.

Since in MHD we treat the plasma as a single fluid, we now define the relevant quanties:

total mass density	$\rho \equiv m_{\rm e}\, n_{\rm e} + m_{\rm i}\, n_{\rm i}$
total charge density	$\rho_{\rm c} \equiv q_{\rm e}\, n_{\rm e} + q_{\rm i}\, n_{\rm i} = e(n_{\rm i} - n_{\rm e})$
com fluid velocity	$\vec{u} \equiv \dfrac{1}{\rho}\,(m_{\rm i}\, n_{\rm i}\, \vec{u}_{\rm i} + m_{\rm e}\, n_{\rm e}\, \vec{u}_{\rm e})$
current density	$\vec{J} = q_{\rm e}\, n_{\rm e}\, \vec{u}_{\rm e} + q_{\rm i}\, n_{\rm i}\, \vec{u}_{\rm i}$
total pressure	$P = P_{\rm e} + P_{\rm i}$

By multiplying the continuity equations for the electrons with $m_{\rm e}$, and adding it to the continuity equation for the ions multiplied by $m_{\rm i}$, one obtains the **MHD continuity equation**,

$$\boxed{\frac{\partial \rho}{\partial t} + \nabla \cdot (\rho \vec{u}) = 0}$$

This equation, which expresses **mass conservation**, is identical to the continuity equation for a neutral fluid.

In addition, we also have **charge conservation** which is given by

$$\boxed{\frac{\partial \rho_{\rm c}}{\partial t} + \nabla \cdot \vec{J} = 0}$$

For the **momentum equation**, it is common to assume that $\partial n_{\rm a}/\partial t$ and $u_{\rm a}$ are small compared to other terms. This allows one to neglect terms that contain products of these small quantities, which in turn allows one to add the momentum equations for electrons and ions, yielding:

$$\boxed{\rho \frac{\partial \vec{u}}{\partial t} = -\nabla P + \rho_{\rm c}\vec{E} + \frac{1}{c}\vec{J} \times \vec{B}}$$

In general, in MHD one assumes that $n_{\rm e} \simeq n_{\rm i}$, which implies that the charge density, $\rho_{\rm c}$, is typically (very) small. We adopt that assumption here as well, which implies that the $\rho_{\rm c}\vec{E}$ term in the momentum equations vanishes and that we no longer need to consider the charge conservation equation.

In MHD, the **energy equation** is the same as for a neutral fluid, except that there is an additional term to describe **Ohmic dissipation** (aka Ohmic loss). In the absence of radiation, viscosity and conduction, we therefore have

$$\boxed{\rho \frac{{\rm d}\varepsilon}{{\rm d}t} = -P\,\nabla\cdot\vec{u} - \frac{J^2}{\sigma}}$$

Here $J^2 = \vec{J}\cdot\vec{J}$ and σ is the **electric conductivity**. The Ohmic dissipation term describes how collisions convert magnetic energy into thermal energy. Hence, it is similar in nature to the **viscous dissipation rate**, $\mathcal{V}$, which describes how collisions manifest as viscosity in converting bulk motion (shear) in thermal energy (see Chapter 5).

Since both the momentum and energy equations contain the current density, we need to complement them with an equation for the time-evolution of $\vec{J}$. This relation, called the **generalized Ohm's law**, derives from multiplying the momentum equations for the individual species by $q_{\rm a}/m_{\rm a}$, adding the versions for the electrons and ions, while once again ignoring terms that contain products of small quanties (i.e., $\partial n_{\rm a}/\partial t$ and $u_{\rm a}$). Using that $\vec{C}_{\rm e} = -\vec{C}_{\rm i}$, that $n_{\rm i} \approx n_{\rm e}$, that $P_{\rm e} \approx P_{\rm i} \approx P/2$, and that $m_{\rm i}^{-1} \ll m_{\rm e}^{-1}$, one can show that

$$\boxed{\frac{m_{\rm e}\,m_{\rm i}}{\rho e^2}\,\frac{\partial\vec{J}}{\partial t} = \frac{m_{\rm i}}{2\rho e}\nabla P + \vec{E} + \frac{1}{c}\vec{u}\times\vec{B} - \frac{m_{\rm i}}{\rho e c}\vec{J}\times\vec{B} + \frac{m_{\rm i}}{\rho e}\vec{C}_{\rm i}}$$

(for a derivation see the excellent textbook *Introduction to Plasma Theory* by D.R. Nicholson).

The above generalized Ohm's law is rather complicated. But fortunately, in most circumstances certain terms are significantly smaller than others and can thus be ignored. Before discussing which terms can be discarded, though, we first give a heuristic derivation of the **collision term** $\vec{C}_{\rm i}$.

As already mentioned above, $\vec{C}_{\rm e} = -\vec{C}_{\rm i}$ describes the transfer of momentum from the electrons to the ions (and vice-versa). Let's consider the **strong** interactions, i.e., those with an impact parameter $b \simeq b_{90}$. Since the electron basically loses all its forward momentum in such a collision, we have that the electron fluid loses an average momentum $m_{\rm e}(\vec{u}_{\rm e} - \vec{u}_{\rm i})$ to the ion fluid per strong electron-ion encounter. Hence, the *rate* of momentum transfer is approximately given by

$$\vec{C}_{\rm e} = -m_{\rm e}\, n_{\rm e}\, \nu_{\rm L}\, (\vec{u}_{\rm e} - \vec{u}_{\rm i})$$

where $\nu_{\rm L}$ is the collision frequency for strong collisions. Since the current density is $\vec{J} = q_{\rm e}\, n_{\rm e}\, \vec{u}_{\rm e} + q_{\rm i}\, n_{\rm i}\, \vec{u}_{\rm i} \simeq n_{\rm e}\, e\, (\vec{u}_{\rm i} - \vec{u}_{\rm e})$, where we have used that $n_{\rm i} \simeq n_{\rm e}$, we can write this as

$$\vec{C}_{\rm e} = +n_{\rm e}\, e\, \eta\, \vec{J}$$

where

$$\eta = \frac{m_{\rm e}\, \nu_{\rm L}}{n_{\rm e}\, e^2}$$

This parameter is called the **electric resistivity**, and is the inverse of the **electric conductivity**, σ. Substituting the expression for $\nu_{\rm L}$ derived in Chapter 22 (and using $v_0 \sim v_{\rm e} \sim (3k_{\rm B}T/m_{\rm e})^{1/2}$), we find that

$$\eta = \frac{4\pi}{3\sqrt{3}}\, \frac{m_{\rm e}^{1/2}\, e^2}{(k_{\rm B}\, T)^{3/2}} \approx 2.4\, \frac{m_{\rm e}^{1/2}\, e^2}{(k_{\rm B}\, T)^{3/2}}$$

Using a much more rigorous derivation of the electrical resistivity, accounting for the whole range of impact parameters, Spitzer & Härm (1953) obtain (assuming that all ions have $Z = 1$)

$$\eta = 1.69 \ln \Lambda\, \frac{m_{\rm e}^{1/2}\, e^2}{(k_{\rm B}\, T)^{3/2}}$$

in reasonable agreement with our crude estimate.

Using the above expression for $\vec{C}_{\rm e}$, the collision term in the generalized Ohm's law reduces to $\vec{J}/\sigma$. Typically, especially when considering low frequency phenomena, which we tend to do with MHD, the $\partial\vec{J}/\partial t$ term is small compared to this collision term and can thus be ignored. In addition, for a sufficiently 'cold' plasma the ∇P terms can also be neglected. Finally, since currents are typically small the $\vec{J} \times \vec{B}$

term, which describes the **Hall effect**, is typically small compared to $\vec{u}/c \times \vec{B}$. Hence, we can simplify the generalized Ohm's law to read

$$\boxed{\vec{J} = \sigma \left(\vec{E} + \frac{\vec{u}}{c} \times \vec{B} \right)}$$

This equation is usually referred to as **Ohm's law**.

The MHD equations derived thus far (mass continuity, charge continuity, momentum conservation and Ohm's law) need to be complemented with the **Maxwell equations**. Fortunately, these can also be simplified. Let's start with Ampère's circuital law

$$\nabla \times \vec{B} = \frac{4\pi}{c} \vec{J} + \frac{1}{c} \frac{\partial \vec{E}}{\partial t}$$

It can be shown (see §3.6 in *The Physics of Fluids and Plasma* by A.R. Choudhuri) that

$$\left[\frac{1}{c} \frac{\partial \vec{E}}{\partial t} \right] / \left[\nabla \times \vec{B} \right] \sim \frac{v^2}{c^2}$$

Hence, in the *non-relativistic* regime considered here, the **displacement current** is negligble, which implies that $\vec{J} = \frac{c}{4\pi} \nabla \times \vec{B}$. Combined with Ohm's law, we therefore have that

$$\vec{E} = \frac{c}{4\pi\sigma} (\nabla \times \vec{B}) - \frac{\vec{u}}{c} \times \vec{B}$$

Hence, we see that, in MHD, the electric field does not have to be considered an independent variable; instead, it can be obtained from $\vec{u}$ and $\vec{B}$.

Plugging the above expression for $\vec{E}$ in Faraday's law of induction

$$\nabla \times \vec{E} = -\frac{1}{c} \frac{\partial \vec{B}}{\partial t}$$

which is another Maxwell equation, yields that

$$\frac{\partial \vec{B}}{\partial t} = -\frac{c^2}{4\pi\sigma} \nabla \times (\nabla \times \vec{B}) + \nabla \times (\vec{u} \times \vec{B})$$

Using the vector identity $\nabla \times (\nabla \times \vec{B}) = \nabla(\nabla \cdot \vec{B}) - \nabla^2 \vec{B}$ (see Appendix A), and the fact that $\nabla \cdot \vec{B} = 0$ (yet another Maxwell equation), we finally obtain the **induction equation**

$$\boxed{\frac{\partial \vec{B}}{\partial t} = \nabla \times (\vec{u} \times \vec{B}) + \lambda \nabla^2 \vec{B}}$$

where

$$\lambda \equiv \frac{c^2}{4\pi\sigma}$$

is called the **magnetic diffusivity**. As is evident from the induction equation, it describes the rate at which the magnetic field diffuses due to collisions in the plasma.

Before we finally summarize our set of MHD equations, we apply one final modification by expanding the Lorentz force term, $\vec{J} \times \vec{B}$, in the moment equations. Using Ampère's circuital law without the displacement current, we have that

$$\frac{1}{c}(\vec{J} \times \vec{B}) = \frac{1}{4\pi}(\nabla \times \vec{B}) \times \vec{B} = \frac{1}{4\pi}\left[(\vec{B} \cdot \nabla)\vec{B} - \nabla\left(\frac{B^2}{2}\right)\right]$$

where the last step is based on a standard vector identity (see Appendix A).
Next, using that

$$\left(\vec{B} \cdot \nabla\right)\vec{B} = B_j \frac{\partial B_i}{\partial x_j} = \frac{\partial B_i B_j}{\partial x_j} - B_i \frac{\partial B_j}{\partial x_j} = \frac{\partial B_i B_j}{\partial x_j}$$

where the last step follows from the fact that $\nabla \cdot \vec{B} = 0$, we can now write the momentum equations in *index form* as

$$\rho \frac{\partial u_i}{\partial t} = -\frac{\partial P}{\partial x_i} - \frac{\partial}{\partial x_i}\left(\frac{B^2}{8\pi}\right) + \frac{\partial}{\partial x_j}\left(\frac{B_i B_j}{4\pi}\right) = +\frac{\partial}{\partial x_j}\left[\sigma_{ij} - M_{ij}\right]$$

Here $\sigma_{ij} = -P\delta_{ij}$ is the **stress tensor** (in the absence of viscosity) and

$$M_{ij} \equiv \frac{B^2}{8\pi}\delta_{ij} - \frac{B_i B_j}{4\pi}$$

is the **magnetic stress tensor**. Its' diagonal elements represent the **magnetic pressure**, while its off-diagonal terms arise from **magnetic tension**.

The following table summarizes the full set of **resistive MHD** equations. These are valid to describe low-frequency plasma phenomena for a relatively cold plasma in which $n_\mathrm{e} \simeq n_\mathrm{i}$, such that the charge density can be neglected. Note also that conduction, viscosity, radiation and gravity are all neglected (the corresponding terms are trivially added). A fluid that obeys these MHD equations is called a **magnetofluid**.

Continuity Eq.	$\dfrac{\mathrm{d}\rho}{\mathrm{d}t} = -\rho\,\nabla\cdot\vec{u}$
Momentum Eqs.	$\rho\,\dfrac{\mathrm{d}\vec{u}}{\mathrm{d}t} = -\nabla P + \dfrac{1}{c}\vec{J}\times\vec{B}$
Energy Eq.	$\rho\,\dfrac{\mathrm{d}\varepsilon}{\mathrm{d}t} = -P\,\nabla\cdot\vec{u} - \dfrac{J^2}{\sigma}$
Ohm's Law	$\vec{J} = \sigma\left(\vec{E} + \dfrac{\vec{u}}{c}\times\vec{B}\right)$
Induction Eq.	$\dfrac{\partial\vec{B}}{\partial t} = \nabla\times(\vec{u}\times\vec{B}) + \lambda\,\nabla^2\vec{B}$
Constitutive Eqs.	$\lambda = \dfrac{c^2}{4\pi\sigma}\,, \qquad \sigma^{-1} = \eta \propto \dfrac{m_\mathrm{e}^{1/2}e^2}{(k_\mathrm{B}T)^{3/2}}$

The equations of resistive MHD

Note that in the momentum equations we have written the Lagrangian derivative $\mathrm{d}\vec{u}/\mathrm{d}t$, rather than the Eulerian $\partial\vec{u}/\partial t$ that we obtained earlier in our derivation. This is allowed, since we had assumed that both $(\vec{u}_\mathrm{e}\cdot\nabla)\vec{u}_\mathrm{e}$ and $(\vec{u}_\mathrm{i}\cdot\nabla)\vec{u}_\mathrm{i}$ are small compared to other terms, which therefore also applies to $(\vec{u}\cdot\nabla)\vec{u}$.

Note also that although we have written the above set of MHD equations including the electric field $\vec{E}$, this is not an independent dynamical quantity. After all, as

already mentioned above, it follows from $\vec{B}$ and $\vec{u}$ according to

$$\vec{E} = \frac{c}{4\pi\sigma}\nabla \times \vec{B} - \frac{\vec{u}}{c} \times \vec{B}$$

In fact, **Ohm's law** is not required to close this set of equations as the current density $\vec{J}$ can be computed directly from the magnetic field $\vec{B}$ using Ampère's circuital law without displacement current; $\nabla \times \vec{B} = (4\pi/c)\vec{J}$.

Hence, we see that in the end MHD is actually remarkably similar to the hydrodynamics of neutral fluids. The 'only' additions are the magnetic field, which adds an additional pressure and an (anisotropic) tension, and the Coulomb collisions, which cause Ohmic dissipation and a diffusion of the magnetic fields. To further strengthen the similarities with regular fluid hydrodynamics, note that the **induction equation** is very similar to the **vorticity equation**

$$\frac{\partial \vec{w}}{\partial t} = \nabla \times (\vec{u} \times \vec{\omega}) - \nabla \times \left(\frac{\nabla P}{\rho}\right) + \nu \nabla^2 \vec{\omega}$$

(see Chapter 8). Here $\vec{w}$ is the **vorticity** and ν the **kinetic viscosity**. Except for the **baroclinic** term, which is absent in the induction equation, vorticity and magnetic field (in the MHD approximation) behave very similar (cf., magnetic field lines and vortex lines).

Motivated by this similarity, we now define the **magnetic Reynolds number**

$$\mathcal{R}_{\rm m} = \frac{U\,L}{\lambda}$$

with U and L the characteristic velocity and length scales of the plasma flow. Recall (from Chapter 11), the definition of the **Reynolds number** $\mathcal{R} = U\,L/\nu$. We thus merely replaced the **kinetic viscosity** with the **magnetic diffusivity**, which is proportional to the **electric resistivitiy** (and thus inversely proportional to the **conductivity**).

• When $\mathcal{R}_{\rm m} \ll 1$, the second term in the induction equation dominates, which therefore becomes

$$\frac{\partial B}{\partial t} \simeq \lambda\,\nabla^2 \vec{B}$$

This is the situation one typically encounters in laboratory plasmas, where U and L are small. The implication is that, the magnetic field in laboratory plasmas, when

left to itself, decays away due to magnetic diffusion. This can be understood from the fact that magnetic fields are directly related to currents, which die away due to **Ohmic dissipation** unless one applies a source of voltage.

• When $\mathcal{R}_{\rm m} \gg 1$, the first term in the induction equation dominates, which therefore becomes

$$\frac{\partial B}{\partial t} \simeq \nabla \times (\vec{u} \times \vec{B})$$

This is the situation we typically encounter in astrophysics, where U and L are large. In the limit of infinite conductivity (i.e., zero electrical resistivity, and thus zero magnetic diffusivity), the above equation is exact, and we talk of **ideal MHD**. Obviously, with infinite conductivity there is also no Ohmic dissipation, and the energy equation in ideal MHD is therefore identical to that for a neutral fluid. Hence, for ideal MHD the full, closed set of equations reduces to

Continuity Eq.	$\dfrac{\mathrm{d}\rho}{\mathrm{d}t} = -\rho\,\nabla\cdot\vec{u}$
Momentum Eqs.	$\rho\,\dfrac{\mathrm{d}\vec{u}}{\mathrm{d}t} = -\nabla P + \dfrac{1}{c}\vec{J}\times\vec{B}$
Energy Eq.	$\rho\,\dfrac{\mathrm{d}\varepsilon}{\mathrm{d}t} = -P\,\nabla\cdot\vec{u}$
Induction Eq.	$\dfrac{\partial\vec{B}}{\partial t} = \nabla\times(\vec{u}\times\vec{B})$
Ampère's law	$\nabla\times\vec{B} = \dfrac{4\pi}{c}\,\vec{J}$

The equations of ideal MHD

The reader may wonder what happens to Ohm's law in the limit where $\sigma \to \infty$; In order to assure only finite currents, we need to have that $E + \vec{u}/c \times \vec{B} = 0$, and thus $\vec{E} = \frac{1}{c}\vec{u} \times \vec{B}$. However, since $\vec{E}$ is not required (is not an independent dynamical quantity), this is of little relevance.

An important implication of ideal MHD is that

$$\frac{\mathrm{d}}{\mathrm{d}t}\int_S \vec{B}\cdot\mathrm{d}^2 s = 0$$

This expresses that the magnetic flux is conserved as it moves with the fluid. This is known as **Alfvén's theorem of flux freezing**. It is the equivalent of **Helmholtz' theorem** that $\mathrm{d}\Gamma/\mathrm{d}t = 0$ for an inviscid fluid (with Γ the circularity). An implication is that, in the case of ideal MHD, two fluid elements that are connected by a magnetic flux line, will remain connected by that same magnetic flux line.

(Ideal) MHD is used to describe many astrophysical processes, from the magnetic field topology of the Sun, to angular momentum transfer in accretion disks, and from the formation of jets in accretion disks, to the magnetic breaking during star formation. One can also apply linear perturbation theory to the ideal MHD equations, to examine what happens to a magnetofluid if it is perturbed. If one ignores viscosity, heat conduction, and electric resistivity (i.e., we are in the ideal MHD regime), then the resulting **dispersion relation** is given by

$$\omega^2\vec{u}_1 = (c_\mathrm{s}^2 + u_\mathrm{A}^2)(\vec{k}\cdot\vec{u}_1)\vec{k} + \vec{u}_\mathrm{A}\cdot\vec{k}\left[(\vec{u}_\mathrm{A}\cdot\vec{k})\vec{u}_1 - (\vec{u}_\mathrm{A}\cdot\vec{u}_1)\vec{k} - (\vec{k}\cdot\vec{u}_1)\vec{u}_\mathrm{A}\right]$$

Here $\vec{u}_\mathrm{A}$ is a characteristic velocity, called the **Alfvén velocity**, given by

$$\boxed{\vec{u}_\mathrm{A} = \frac{\vec{B}_0}{\sqrt{4\pi\rho_0}}}$$

The above dispersion relation, $\omega(\vec{k})$, for given sound speed, c_s, and Alvén velocity, $\vec{v}_\mathrm{A}$, of the magnetofluid, is the basic dispersion relation for **hydromagnetic waves**. Although it has a complicated looking form, there is one solution that is rather simple. It corresponds to a purely tranverse wave in which the displacement, and therefore the velocity perturbation $\vec{u}_1(\vec{x},t)$, is perpendicular to both the wave vector $\vec{k}$ and the magnetic field (which is in the direction of $\vec{u}_\mathrm{A}$). Under those conditions the dispersion relation reduces to

$$\omega^2 = (\vec{v}_\mathrm{A}\cdot\vec{k})^2$$

These waves, called **Alfvén waves**, have a group velocity $v_\mathrm{g} = \partial\omega/\partial\vec{k} = \vec{v}_\mathrm{A}$ and are moving, with that velocity, along the magnetic field lines.

Any wave is driven by some restoring force. In the case of accoustic waves these are pressure gradients, while the restoring force in the case of the plasma oscillations (**Langmuir waves**) discussed in the previous chapter arise from the electrical field that results from a separation of electrons and ions. In the case of perturbations to a magnetofluid, there are two restoring forces that play a role; pressure gradients and magnetic tension. In the case of Alfvèn waves the restoring force is purely the tension in the magnetic field lines (pressure plays no role). Hence, Alfvén waves are similar to the waves in a rope or string, which are also transverse waves. The group velocity of these waves is proportional to $\sqrt{\text{tension/density}}$. Since the magnetic tension is given by $B^2/4\pi$, we see that the Alfvén velocity has exactly the same form.

Note that in the case of ideal MHD the resistivity is zero, and there is thus no diffusion or dissipation of the magnetic fields, which instead are 'frozen' into the fluid. In the case of resistive MHD (i.e., if the magnetic resistivity is non-zero) the Alfvén waves will experience damping, thereby transferring the energy stored in the magnetic wave to random, thermal energy.

Alfvèn waves, though, are not the only solution to the dispersion relation given above. There are two additional solutions, corresponding to **fast mode** and **slow mode** waves. Contrary to the Alfvèn waves, the restoring force for these modes is a combination of magnetic tension *and* pressure (i.e., they are mixtures of acoustic and magnetic waves). Without going into any detail, we only mention in closing that any disturbance of a magnetofluid can be represented as a superposition of the Alfvèn, fast and slow modes.

Supplemental Material

Appendices

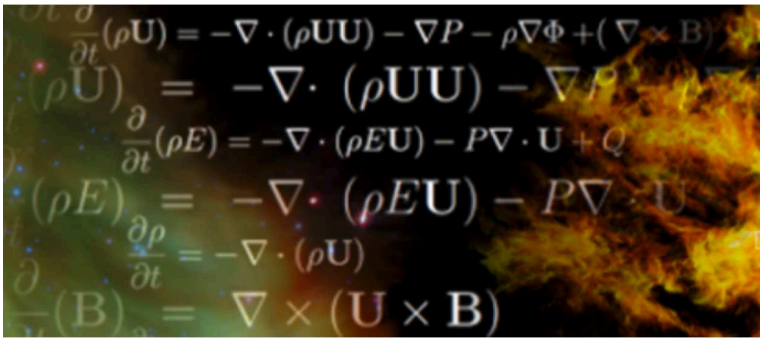

The following appendices provide supplemental material, including some calculus and radiation essentials that is relevant for this course. Students are assumed to be familiar with this. An exception are Appendices F, G, H, J and L which provide details that are NOT considered part of this course's curriculum. They are included to provide background information for those readers that want to know a bit more.

Appendix A

Vector Calculus

Vector: $\vec{A} = (a_1, a_2, a_3) = a_1\hat{i} + a_2\hat{j} + a_3\hat{k}$

Amplitude of vector: $|\vec{A}| = \sqrt{a_1^2 + a_2^2 + a_3^2}$

Unit vector: $|\vec{A}| = 1$

Basis: In the above example, the unit vectors $\hat{i}$, $\hat{j}$ and $\hat{k}$ form a vector basis.
Any 3 vectors $\vec{A}$, $\vec{B}$ and $\vec{C}$ can form a vector basis
as long as $\det(\vec{A}, \vec{B}, \vec{C}) \neq 0$.

Determinant:
$$\det(\vec{A}, \vec{B}) = \begin{vmatrix} a_1 & a_2 \\ b_1 & b_2 \end{vmatrix} = a_1 b_2 - a_2 b_1$$

$$\det(\vec{A}, \vec{B}, \vec{C}) = \begin{vmatrix} a_1 & a_2 & a_3 \\ b_1 & b_2 & b_3 \\ c_1 & c_2 & c_3 \end{vmatrix} = a_1 \begin{vmatrix} b_2 & b_3 \\ c_2 & c_3 \end{vmatrix} + a_2 \begin{vmatrix} b_3 & b_1 \\ c_3 & c_1 \end{vmatrix} + a_3 \begin{vmatrix} b_1 & b_2 \\ c_1 & c_2 \end{vmatrix}$$

Geometrically:
$\det(\vec{A}, \vec{B}) = \pm$ area of parallelogram
$\det(\vec{A}, \vec{B}, \vec{C}) = \pm$ volume of parallelepiped

Multiplication by scalar:
$\alpha\,\vec{A} = (\alpha a_1, \alpha a_2, \alpha a_3)$
$|\alpha\,\vec{A}| = |\alpha|\,|\vec{A}|$

Summation of vectors: $\vec{A} + \vec{B} = \vec{B} + \vec{A} = (a_1 + b_1, a_2 + b_2, a_3 + b_3)$

Einstein Summation Convention: $a_i\, b_i = \sum_i a_i b_i = a_1 b_1 + a_2 b_2 + a_3 b_3 = \vec{a} \cdot \vec{b}$
$\partial A_i / \partial x_i = \partial A_1/\partial x_1 + \partial A_2/\partial x_2 + \partial A_3/\partial x_3 = \nabla \cdot \vec{A}$
$A_{ii} = A_{11} + A_{22} + A_{33} = \mathrm{Tr}\, \vec{A}$ (trace of $\vec{A}$)

Dot product (aka scalar product): $\vec{A} \cdot \vec{B} = a_i\, b_i = |\vec{A}|\, |\vec{B}| \cos\theta$
$\vec{A} \cdot \vec{B} = \vec{B} \cdot \vec{A}$

Useful for:

- computing angle between two vectors: $\cos\theta = \vec{A} \cdot \vec{B} / (|\vec{A}|\, |\vec{B}|)$
- check orthogonality: two vectors are orthogonal if $\vec{A} \cdot \vec{B} = 0$
- compute projection of $\vec{B}$ in direction of $\vec{A}$, which is given by $\vec{A} \cdot \vec{B} / |\vec{A}|$

Cross Product (aka vector product): $\vec{A} \times \vec{B} = \begin{vmatrix} \hat{i} & \hat{j} & \hat{k} \\ a_1 & a_2 & a_3 \\ b_1 & b_2 & b_3 \end{vmatrix} = \varepsilon_{ijk} a_i\, b_j\, \hat{e}_k$
$|\vec{A} \times \vec{B}| = |\vec{A}|\, |\vec{B}| \sin\theta = \det(\vec{A}, \vec{B})$

NOTE: ε_{ijk} is called the **Levi-Civita tensor**, which is described in Appendix F.

In addition to the dot product and cross product, there is a third vector product that one occasionally encounters in dynamics;

Tensor product: $\vec{A} \otimes \vec{B} = \overline{\overline{\mathbf{AB}}}$ $\qquad (\overline{\overline{\mathbf{AB}}})_{ij} = a_i b_j$
$\vec{A} \otimes \vec{B} \neq \vec{B} \otimes \vec{A}$

The tensor product $\overline{\overline{\mathbf{AB}}}$ is a tensor of rank two and is called a **dyad**. It is best to define a dyad by what it *does*: it transforms a vector $\vec{C}$ into another vector with the direction of $\vec{A}$ according to the rule

$$(\vec{A} \otimes \vec{B})\, \vec{C} = \vec{A}\, (\vec{B} \cdot \vec{C})$$

A **dyadic** is a linear combination of dyads (i.e., $4(\vec{a} \odot \vec{b} + 2(\vec{c} \odot \vec{d}) - 7(\vec{e} \odot \vec{f})$). Dyadics are important because *each tensor of rank two can be written as a dyadic!*.

$\vec{A} \cdot \vec{B} = \vec{B} \cdot \vec{A}$	$\vec{A} \times \vec{B} = -\vec{B} \times \vec{A}$
$(\alpha\vec{A}) \cdot \vec{B} = \alpha(\vec{A} \cdot \vec{B}) = \vec{A} \cdot (\alpha\vec{B})$	$(\alpha\vec{A}) \times \vec{B} = \alpha(\vec{A} \times \vec{B}) = \vec{A} \times (\alpha\vec{B})$
$\vec{A} \cdot (\vec{B} + \vec{C}) = \vec{A} \cdot \vec{B} + \vec{A} \cdot \vec{C}$	$\vec{A} \times (\vec{B} + \vec{C}) = \vec{A} \times \vec{B} + \vec{A} \times \vec{C}$
$\vec{A} \cdot \vec{B} = 0 \quad \rightarrow \quad \vec{A} \perp \vec{B}$	$\vec{A} \times \vec{B} = 0 \quad \rightarrow \quad \vec{A} \parallel \vec{B}$
$\vec{A} \cdot \vec{A} = \lvert\vec{A}\rvert^2$	$\vec{A} \times \vec{A} = 0$

Triple Scalar Product: $\vec{A} \cdot (\vec{B} \times \vec{C}) = \det(\vec{A}, \vec{B}, \vec{C}) = \varepsilon_{ijk} a_i \, b_j \, c_k$
$\vec{A} \cdot (\vec{B} \times \vec{C}) = 0 \quad \rightarrow \quad \vec{A}, \vec{B}, \vec{C}$ are coplanar
$\vec{A} \cdot (\vec{B} \times \vec{C}) = \vec{B} \cdot (\vec{C} \times \vec{A}) = \vec{C} \cdot (\vec{A} \times \vec{B})$

Triple Vector Product: $\vec{A} \times (\vec{B} \times \vec{C}) = (\vec{A} \cdot \vec{C})\, \vec{B} - (\vec{A} \cdot \vec{B})\, \vec{C}$
as is clear from above, $\vec{A} \times (\vec{B} \times \vec{C})$ lies in plane of $\vec{B}$ and $\vec{C}$.

Useful to remember: $(\vec{A} \times \vec{B}) \cdot (\vec{C} \times \vec{D}) = (\vec{A} \cdot \vec{C})\, (\vec{B} \cdot \vec{D}) - (\vec{A} \cdot \vec{D})\, (\vec{B} \cdot \vec{C})$
$(\vec{A} \times \vec{B}) \times (\vec{C} \times \vec{D}) = \Big[\vec{A} \cdot (\vec{B} \times \vec{D})\Big]\, \vec{C} - \Big[\vec{A} \cdot (\vec{B} \times \vec{C})\Big]\, \vec{D}$

Gradient Operator: $\nabla = \vec{\nabla} = \left(\frac{\partial}{\partial x}, \frac{\partial}{\partial y}, \frac{\partial}{\partial z}\right)$
This **vector operator** is sometimes called the **nabla** or **del** operator.

Laplacian operator: $\nabla^2 = \nabla \cdot \nabla = \frac{\partial^2}{\partial x^2} + \frac{\partial^2}{\partial y^2} + \frac{\partial^2}{\partial z^2}$
This is a **scalar operator**.

Differential: $f = f(x, y, z) \quad \rightarrow \quad \mathrm{d}f = \frac{\partial f}{\partial x}\, \mathrm{d}x + \frac{\partial f}{\partial y}\, \mathrm{d}y + \frac{\partial f}{\partial z}\, \mathrm{d}z$

Chain Rule: If $x = x(t)$, $y = y(t)$ and $z = z(t)$ then $\frac{\mathrm{d}f}{\mathrm{d}t} = \frac{\partial f}{\partial x}\frac{\mathrm{d}x}{\mathrm{d}t} + \frac{\partial f}{\partial y}\frac{\mathrm{d}y}{\mathrm{d}t} + \frac{\partial f}{\partial z}\frac{\mathrm{d}z}{\mathrm{d}t}$
If $x = x(s, t)$, $y = y(s, t)$ and $z = z(s, t)$ then $\frac{\partial f}{\partial s} = \frac{\partial f}{\partial x}\frac{\partial x}{\partial s} + \frac{\partial f}{\partial y}\frac{\partial y}{\partial s} + \frac{\partial f}{\partial z}\frac{\partial z}{\partial s}$

Gradient Vector: $\nabla f = \text{grad} f = \left(\frac{\partial f}{\partial x}, \frac{\partial f}{\partial y}, \frac{\partial f}{\partial z}\right)$
the gradient vector at (x, y, z) is normal to the level surface through the point (x, y, z).

Directional Derivative: The derivative of $f = f(x, y, z)$ in direction of $\vec{u}$ is
$\mathrm{D}_u f = \nabla f \cdot \frac{\vec{u}}{|\vec{u}|} = |\nabla f| \cos\theta$

Vector Field: $\vec{F}(\vec{x}) = (F_x, F_y, F_z) = F_x\hat{i} + F_y\hat{j} + F_z\hat{k}$
where $F_x = F_x(x, y, z)$, $F_y = F_y(x, y, z)$, and $F_z = F_z(x, y, z)$.

Divergence of Vector Field: $\text{div}\vec{F} = \nabla \cdot \vec{F} = \frac{\partial F_x}{\partial x} + \frac{\partial F_y}{\partial y} + \frac{\partial F_z}{\partial z}$
A vector field for which $\nabla \cdot \vec{F} = 0$ is called **solenoidal** or **divergence-free**.

Curl of Vector Field: $\text{curl}\vec{F} = \nabla \times \vec{F} = \begin{vmatrix} \hat{i} & \hat{j} & \hat{k} \\ \partial/\partial x & \partial/\partial y & \partial/\partial z \\ F_x & F_y & F_z \end{vmatrix}$
A vector field for which $\nabla \times \vec{F} = 0$ is called **irrotational** or **curl-free**.

Laplacian of Vector Field: $\nabla^2\vec{F} = (\nabla \cdot \nabla)\vec{F} = \nabla(\nabla \cdot \vec{F}) - \nabla \times (\nabla \times \vec{F})$
Note that $\nabla^2\vec{F} \neq \nabla(\nabla \cdot \vec{F})$: **do not make this mistake**.

Let $S(\vec{x})$ and $T(\vec{x})$ be scalar fields, and let $\vec{A}(\vec{x})$ and $\vec{B}(\vec{x})$ be vector fields:

$\nabla S = \text{grad} S = \text{vector}$	$\nabla^2 S = \nabla \cdot (\nabla S) = \text{scalar}$
$\nabla \cdot \vec{A} = \text{div}\vec{A} = \text{scalar}$	$\nabla^2\vec{A} = (\nabla \cdot \nabla)\,\vec{A} = \text{vector}$
$\nabla \times \vec{A} = \text{curl}\vec{A} = \text{vector}$	

$$\nabla \times (\nabla S) = 0 \qquad \operatorname{curl}\operatorname{grad} S = 0$$

$$\nabla \cdot (\nabla \times \vec{A}) = 0 \qquad \operatorname{div}\operatorname{curl} \vec{A} = 0$$

$$\nabla(ST) = S\,\nabla T + T\,\nabla S$$

$$\nabla \cdot (S\vec{A}) = S(\nabla \cdot \vec{A}) + \vec{A} \cdot \nabla S$$

$$\nabla \times (S\vec{A}) = (\nabla S) \times \vec{A} + S(\nabla \times \vec{A})$$

$$\nabla \cdot (\vec{A} \times \vec{B}) = \vec{B} \cdot (\nabla \times \vec{A}) - \vec{A} \cdot (\nabla \times \vec{B})$$

$$\nabla \times (\vec{A} \times \vec{B}) = \vec{A}(\nabla \cdot \vec{B}) - \vec{B}(\nabla \cdot \vec{A}) + (\vec{B} \cdot \nabla)\vec{A} - (\vec{A} \cdot \nabla)\vec{B}$$

$$\nabla(\vec{A} \cdot \vec{B}) = (\vec{A} \cdot \nabla)\vec{B} + (\vec{B} \cdot \nabla)\vec{A} + \vec{A} \times (\nabla \times \vec{B}) + \vec{B} \times (\nabla \times \vec{A})$$

$$\vec{A} \times (\nabla \times \vec{A}) = \tfrac{1}{2}\nabla(\vec{A} \cdot \vec{A}) - (\vec{A} \cdot \nabla)\vec{A}$$

$$\nabla \times (\nabla^2 \vec{A}) = \nabla^2(\nabla \times \vec{A})$$

Appendix B

Conservative Vector Fields

Line Integral of a Conservative Vector Field: Consider a curve γ running from location $\vec{x}_0$ to $\vec{x}_1$. Let $\mathrm{d}\vec{l}$ be the directional element of length along γ (i.e., with direction equal to that of the tangent vector to γ), then, for any scalar field $\Phi(\vec{x})$,

$$\int_{\vec{x}_0}^{\vec{x}_1} \nabla\Phi \cdot \mathrm{d}\vec{l} = \int_{\vec{x}_0}^{\vec{x}_1} \mathrm{d}\Phi = \Phi(\vec{x}_1) - \Phi(\vec{x}_0)$$

This implies that the line integral is independent of γ, and hence

$$\oint_c \nabla\Phi \cdot \mathrm{d}\vec{l} = 0$$

where c is a closed curve, and the integral is to be performed in the counter-clockwise direction.

Conservative Vector Fields:
A conservative vector field $\vec{F}$ has the following properties:

- $\vec{F}(\vec{x})$ is a gradient field, which means that there is a scalar field $\Phi(\vec{x})$ so that $\vec{F} = \nabla\Phi$
- Path independence: $\oint_c \vec{F} \cdot \mathrm{d}\vec{l} = 0$
- Irrotational = curl-free: $\nabla \times \vec{F} = 0$

Appendix C

Integral Theorems

Green's Theorem: Consider a 2D vector field $\vec{F} = F_x\hat{i} + F_y\hat{j}$

$$\oint \vec{F} \cdot \mathrm{d}\vec{l} = \int\int_A \nabla \times \vec{F} \cdot \hat{n}\, \mathrm{d}A = \int\int_A |\nabla \times \vec{F}|\, \mathrm{d}A$$

$$\oint \vec{F} \cdot \hat{n}\, \mathrm{d}l = \int\int_A \nabla \cdot \vec{F}\, \mathrm{d}A$$

NOTE: in the first equation we have used that $\nabla \times \vec{F}$ is always pointing in the direction of the normal $\hat{n}$.

Gauss' Divergence Theorem: Consider a 3D vector field $\vec{F} = (F_x, F_y, F_z)$
If S is a closed surface bounding a region D with normal pointing outwards, and $\vec{F}$ is a vector field defined and differentiable over all of D, then

$$\int\int_S \vec{F} \cdot \mathrm{d}\vec{S} = \int\int\int_D \nabla \cdot \vec{F}\, \mathrm{d}V$$

Stokes' Curl Theorem: Consider a 3D vector field $\vec{F} = (F_x, F_y, F_z)$
If C is a closed curve, and S is *any* surface bounded by C, then

$$\oint_c \vec{F} \cdot \mathrm{d}\vec{l} = \int\int_S (\nabla \times \vec{F}) \cdot \hat{n}\, \mathrm{d}S$$

NOTE: The curve of the line intergral must have positive orientation, meaning that $\mathrm{d}\vec{l}$ points counterclockwise when the normal of the surface points towards the viewer.

Appendix D

Curvi-Linear Coordinate Systems

In astrophysics, one often works in **curvi-linear**, rather than **Cartesian** coordinate systems. The two most often encountered examples are the **cylindrical** (R, ϕ, z) and **spherical** (r, θ, ϕ) coordinate systems.

In this chapter we describe how to handle **vector calculus** in non-Cartesian coordinate systems (Euclidean spaces only). After giving the 'rules' for arbitrary coordinate systems, we apply them to cylindrical and spherical coordinate systems, respectively.

Vector Calculus in an Arbitrary Coordinate System:

Consider a vector $\vec{x} = (x, y, z)$ in Cartesian coordinates. This means that we can write

$$\vec{x} = x\,\vec{e}_x + y\,\vec{e}_y + z\,\vec{e}_z$$

where $\vec{e}_x$, $\vec{e}_y$ and $\vec{e}_z$ are the unit directional vectors. Now consider the same vector $\vec{x}$, but expressed in another **general** (arbitrary) coordinate system; $\vec{x} = (q_1, q_2, q_3)$. It is tempting, **but terribly wrong**, to write that

$$\vec{x} = q_1\,\vec{e}_1 + q_2\,\vec{e}_2 + q_3\,\vec{e}_3$$

where $\vec{e}_1$, $\vec{e}_2$ and $\vec{e}_3$ are the unit directional vectors in the new (q_1, q_2, q_3)-coordinate system. In what follows we show how to properly treat such generalized coordinate systems.

In general, one expresses the distance between (q_1, q_2, q_3) and $(q_1 + \mathrm{d}q_1, q_2 + \mathrm{d}q_2, q_3 + \mathrm{d}q_3)$ in an arbitrary coordinate system as

$$\mathrm{d}s = \sqrt{h_{ij}\,\mathrm{d}q_i\,\mathrm{d}q_j}$$

Here h_{ij} is called the **metric tensor**. In what follows, we will only consider **orthogonal** coordinate systems for which $h_{ij} = 0$ if $i \neq j$, so that $\mathrm{d}s^2 = h_i^2\,\mathrm{d}q_i^2$ (Einstein summation convention) with $h_i = \sqrt{h_{ii}}$.

An example of an orthogonal coordinate system are the Cartesian coordinates, for which $h_{ij} = \delta_{ij}$. After all, the distance between two points separated by the infinitesimal displacement vector $\mathrm{d}\vec{x} = (\mathrm{d}x, \mathrm{d}y, \mathrm{d}z)$ is $\mathrm{d}s^2 = |\mathrm{d}\vec{x}|^2 = \mathrm{d}x^2 + \mathrm{d}y^2 + \mathrm{d}z^2$.

The coordinates (x, y, z) and (q_1, q_2, q_3) are related to each other via the **transformation relations**

$$\begin{aligned} x &= x(q_1, q_2, q_3) \\ y &= y(q_1, q_2, q_3) \\ z &= z(q_1, q_2, q_3) \end{aligned}$$

and the corresponding inverse relations

$$\begin{aligned} q_1 &= q_1(x, y, z) \\ q_2 &= q_2(x, y, z) \\ q_3 &= q_3(x, y, z) \end{aligned}$$

Hence, we have that the **differential vector** is:

$$\mathrm{d}\vec{x} = \frac{\partial \vec{x}}{\partial q_1}\,\mathrm{d}q_1 + \frac{\partial \vec{x}}{\partial q_2}\,\mathrm{d}q_2 + \frac{\partial \vec{x}}{\partial q_3}\,\mathrm{d}q_3$$

where

$$\frac{\partial \vec{x}}{\partial q_i} = \frac{\partial}{\partial q_i}(x, y, z)$$

The **unit directional vectors** are:

$$\vec{e}_i = \frac{\partial \vec{x}/\partial q_i}{|\partial \vec{x}/\partial q_i|}$$

which allows us to rewrite the expression for the **differential vector** as

$$\mathrm{d}\vec{x} = \left|\frac{\partial \vec{x}}{\partial q_1}\right|\,\mathrm{d}q_1\,\vec{e}_1 + \left|\frac{\partial \vec{x}}{\partial q_2}\right|\,\mathrm{d}q_2\,\vec{e}_2 + \left|\frac{\partial \vec{x}}{\partial q_3}\right|\,\mathrm{d}q_3\,\vec{e}_3$$

and thus

$$|\mathrm{d}\vec{x}|^2 = \left|\frac{\partial \vec{x}}{\partial q_i}\right|^2\,\mathrm{d}q_i^2$$

(Einstein summation convention). Using the definition of the metric, according to which $|\mathrm{d}\vec{x}|^2 = h_i^2 \mathrm{d}q_i^2$ we thus infer that

$$\boxed{\boxed{h_i = \left|\frac{\partial \vec{x}}{\partial q_i}\right|}}$$

Using this expression for the metric allows us to write the **unit directional vectors** as

$$\vec{e}_i = \frac{1}{h_i}\frac{\partial \vec{x}}{\partial q_i}$$

and the **differential vector** in the compact form as

$$\mathrm{d}\vec{x} = h_i \, \mathrm{d}q_i \, \vec{e}_i$$

From the latter we also have that the **infinitesimal volume element** for a general coordinate system is given by

$$\mathrm{d}^3\vec{x} = |h_1 \, h_2 \, h_3| \, \mathrm{d}q_1 \, \mathrm{d}q_2 \, \mathrm{d}q_3$$

Note that the absolute values are needed to assure that $\mathrm{d}^3\vec{x}$ is positive.

Now consider a vector $\vec{A}$. In the Cartesian **basis** $\mathcal{C} = \{\vec{e}_x, \vec{e}_y, \vec{e}_z\}$ we have that

$$[\vec{A}]_{\mathcal{C}} = A_x\,\vec{e}_x + A_y\,\vec{e}_y + A_z\,\vec{e}_z$$

In the **basis** $\mathcal{B} = \{\vec{e}_1, \vec{e}_2, \vec{e}_3\}$, corresponding to our generalized coordinate system, we instead have that

$$[\vec{A}]_{\mathcal{B}} = A_1\,\vec{e}_1 + A_2\,\vec{e}_2 + A_3\,\vec{e}_3$$

We can rewrite the above as

$$[\vec{A}]_{\mathcal{B}} = A_1 \begin{pmatrix} e_{11} \\ e_{12} \\ e_{13} \end{pmatrix} + A_2 \begin{pmatrix} e_{21} \\ e_{22} \\ e_{23} \end{pmatrix} + A_3 \begin{pmatrix} e_{31} \\ e_{32} \\ e_{33} \end{pmatrix} = \begin{pmatrix} A_1 e_{11} + A_2 e_{21} + A_3 e_{31} \\ A_2 e_{12} + A_2 e_{22} + A_3 e_{32} \\ A_3 e_{13} + A_2 e_{23} + A_3 e_{33} \end{pmatrix}$$

and thus

$$[\vec{A}]_{\mathcal{B}} = \begin{pmatrix} e_{11} & e_{21} & e_{31} \\ e_{12} & e_{22} & e_{32} \\ e_{13} & e_{23} & e_{33} \end{pmatrix} \begin{pmatrix} A_1 \\ A_2 \\ A_3 \end{pmatrix} \equiv \mathbf{T} \begin{pmatrix} A_1 \\ A_2 \\ A_3 \end{pmatrix}$$

Using similar logic, one can write

$$[\vec{A}]_{\mathcal{C}} = \begin{pmatrix} e_{x1} & e_{y1} & e_{z1} \\ e_{x2} & e_{y2} & e_{z2} \\ e_{x3} & e_{y3} & e_{z3} \end{pmatrix} \begin{pmatrix} A_x \\ A_y \\ A_z \end{pmatrix} = \begin{pmatrix} 1 & 0 & 0 \\ 0 & 1 & 0 \\ 0 & 0 & 1 \end{pmatrix} \begin{pmatrix} A_x \\ A_y \\ A_z \end{pmatrix} = \mathbf{I} \begin{pmatrix} A_x \\ A_y \\ A_z \end{pmatrix}$$

and since $\vec{A}$ is the same object independent of its basis we have that

$$\mathbf{I} \begin{pmatrix} A_x \\ A_y \\ A_z \end{pmatrix} = \mathbf{T} \begin{pmatrix} A_1 \\ A_2 \\ A_3 \end{pmatrix}$$

and thus, we see that the relation between $[\vec{A}]_{\mathcal{B}}$ and $[\vec{A}]_{\mathcal{C}}$ is given by

$$[\vec{A}]_{\mathcal{C}} = \mathbf{T}\,[\vec{A}]_{\mathcal{B}}\,, \qquad\qquad [\vec{A}]_{\mathcal{B}} = \mathbf{T}^{-1}\,[\vec{A}]_{\mathcal{C}}$$

For this reason, $\mathbf{T}$ is called the **transformation of basis matrix**. Note that the columns of $\mathbf{T}$ are the unit-direction vectors $\vec{e}_i$, i.e., $T_{ij} = e_{ij}$. Since these are orthogonal to each other, the matric $\mathbf{T}$ is said to be **orthogonal**, which implies that $\mathbf{T}^{-1} = \mathbf{T}^{\mathrm{T}}$ (the inverse is equal to the transpose), and $\det(T) = \pm 1$.

Now we are finally ready to determine how to write our position vector $\vec{x}$ in the new basis $\mathcal{B}$ of our generalized coordinate system. Let's write $\vec{x} = a_i\,\vec{e}_i$, i.e.

$$[\vec{x}]_{\mathcal{B}} = \begin{pmatrix} a_1 \\ a_2 \\ a_3 \end{pmatrix}$$

We started this chapter by pointing out that it is tempting, but wrong, to set $a_i = q_i$ (as for the Cartesian basis). To see this, recall that $|\vec{x}| = \sqrt{(a_1)^2 + (a_2)^2 + (a_3)^2}$, from which it is immediately clear that each a_i needs to have the dimension of length. Hence, when q_i is an angle, clearly $a_i \neq q_i$. To compute the actual a_i you need to use the transformation of basis matrix as follows:

$$[\vec{x}]_{\mathcal{B}} = \mathbf{T}^{-1}\,[\vec{x}]_{\mathcal{C}} = \begin{pmatrix} e_{11} & e_{12} & e_{13} \\ e_{21} & e_{22} & e_{23} \\ e_{31} & e_{32} & e_{33} \end{pmatrix} \begin{pmatrix} x \\ y \\ z \end{pmatrix} = \begin{pmatrix} e_{11}x + e_{12}y + e_{13}z \\ e_{21}x + e_{22}y + e_{23}z \\ e_{31}x + e_{32}y + e_{33}z \end{pmatrix}$$

Hence, using our expression for the unit direction vectors, we see that

$$\boxed{\boxed{a_i = \frac{1}{h_i}\left(\frac{\partial x_j}{\partial q_i}\,x_j\right) = \frac{1}{h_i}\left(\frac{\partial \vec{x}}{\partial q_i}\cdot\vec{x}\right)}}$$

Hence, the position vector in the generalized basis $\mathcal{B}$ is given by

$$[\vec{x}]_{\mathcal{B}} = \sum_i \frac{1}{h_i}\left(\frac{\partial \vec{x}}{\partial q_i}\cdot\vec{x}\right)\vec{e}_i$$

and by operating $\mathrm{d}/\mathrm{d}t$ on $[\vec{x}]_{\mathcal{B}}$ we find that the corresponding velocity vector in the $\mathcal{B}$ basis is given by

$$[\vec{v}]_{\mathcal{B}} = \sum_i h_i\,\dot{q}_i\,\vec{e}_i$$

with $\dot{q}_i = \mathrm{d}q_i/\mathrm{d}t$. Note that the latter can also be inferred more directly by simply dividing the expression for the **differential vector** ($\mathrm{d}\vec{x} = h_i\,q_i\,\vec{e}_i$) by $\mathrm{d}t$.

Next we write out the gradient, the divergence, the curl and the Laplacian for our generalized coordinate system:

The gradient:

$$\nabla\psi = \frac{1}{h_i}\frac{\partial\psi}{\partial q_i}\vec{e}_i$$

The divergence:

$$\nabla\cdot\vec{A} = \frac{1}{h_1h_2h_3}\left[\frac{\partial}{\partial q_1}(h_2h_3A_1) + \frac{\partial}{\partial q_2}(h_3h_1A_2) + \frac{\partial}{\partial q_3}(h_1h_2A_3)\right]$$

The curl (only one component shown)**:**

$$(\nabla\times\vec{A})_3 = \frac{1}{h_1h_2}\left[\frac{\partial}{\partial q_1}(h_2A_2) - \frac{\partial}{\partial q_2}(h_1A_1)\right]$$

The Laplacian:

$$\nabla^2\psi = \frac{1}{h_1h_2h_3}\left[\frac{\partial}{\partial q_1}\left(\frac{h_2h_3}{h_1}\frac{\partial\psi}{\partial q_1}\right) + \frac{\partial}{\partial q_2}\left(\frac{h_3h_1}{h_2}\frac{\partial\psi}{\partial q_2}\right) + \frac{\partial}{\partial q_3}\left(\frac{h_1h_2}{h_3}\frac{\partial\psi}{\partial q_3}\right)\right]$$

The Convective operator:

$$(\vec{A}\cdot\nabla)\,\vec{B} = \left[\frac{A_i}{h_i}\frac{\partial B_j}{\partial q_i} + \frac{B_i}{h_i\,h_j}\left(A_j\frac{\partial h_j}{\partial q_i} - A_i\frac{\partial h_i}{\partial q_j}\right)\right]\,\vec{e}_j$$

Vector Calculus in Cylindrical Coordinates:

For cylindrical coordinates (R, ϕ, z) we have that

$$x = R\cos\phi \qquad y = R\sin\phi \qquad z = z$$

The **scale factors** of the **metric** therefore are:

$$h_R = 1 \qquad h_\phi = R \qquad h_z = 1$$

and the position vector is $\vec{x} = R\vec{e}_R + z\vec{e}_z$.

Let $\vec{A} = A_R\vec{e}_R + A_\phi\vec{e}_\phi + A_z\vec{e}_z$ an arbitrary vector, then

$$\begin{aligned} A_R &= A_x\cos\phi - A_y\sin\phi \\ A_\phi &= -A_x\sin\phi + A_y\cos\phi \\ A_z &= A_z \end{aligned}$$

In cylindrical coordinates the **velocity vector** becomes:

$$\begin{aligned} \vec{v} &= \dot{R}\,\vec{e}_R + R\,\dot{\vec{e}}_R + \dot{z}\,\vec{e}_z \\ &= \dot{R}\,\vec{e}_R + R\,\dot{\phi}\,\vec{e}_\phi + \dot{z}\,\vec{e}_z \end{aligned}$$

The Gradient:

$$\nabla\cdot\vec{A} = \frac{1}{R}\frac{\partial}{\partial R}(RA_R) + \frac{1}{R}\frac{\partial A_\phi}{\partial\phi} + \frac{\partial A_z}{\partial z}$$

The Convective Operator:

$$\begin{aligned} (\vec{A}\cdot\nabla)\,\vec{B} &= \left(A_R\frac{\partial B_R}{\partial R} + \frac{A_\phi}{R}\frac{\partial B_R}{\partial\phi} + A_z\frac{\partial B_R}{\partial z} - \frac{A_\phi B_\phi}{R}\right)\vec{e}_R \\ &+ \left(A_R\frac{\partial B_\phi}{\partial R} + \frac{A_\phi}{R}\frac{\partial B_\phi}{\partial\phi} + A_z\frac{\partial B_\phi}{\partial z} + \frac{A_\phi B_R}{R}\right)\vec{e}_\phi \\ &+ \left(A_R\frac{\partial B_z}{\partial R} + \frac{A_\phi}{R}\frac{\partial B_z}{\partial\phi} + A_z\frac{\partial B_z}{\partial z}\right)\vec{e}_z \end{aligned}$$

The Laplacian:

$$\text{scalar}: \quad \nabla^2\psi = \frac{1}{R}\frac{\partial}{\partial R}\left(R\frac{\partial\psi}{\partial R}\right) + \frac{1}{R^2}\frac{\partial^2\psi}{\partial\phi^2} + \frac{\partial^2\psi}{\partial z^2}$$

$$\begin{aligned}\text{vector}: \quad \nabla^2\vec{F} &= \left(\nabla^2 F_R - \frac{F_R}{R^2} - \frac{2}{R^2}\frac{\partial F_\theta}{\partial\theta}\right)\vec{e}_R \\ &+ \left(\nabla^2 F_\theta + \frac{2}{R^2}\frac{\partial F_R}{\partial\theta} - \frac{F_\theta}{R^2}\right)\vec{e}_\theta \\ &+ \left(\nabla^2 F_z\right)\vec{e}_z\end{aligned}$$

Vector Calculus in Spherical Coordinates:

For spherical coordinates (r, θ, ϕ) we have that

$$x = r\sin\theta\cos\phi \qquad y = r\sin\theta\sin\phi \qquad z = r\cos\theta$$

The **scale factors** of the **metric** therefore are:

$$h_r = 1 \qquad h_\theta = r \qquad h_\phi = r\sin\theta$$

and the position vector is $\vec{x} = r\vec{e}_r$.

Let $\vec{A} = A_r\vec{e}_r + A_\theta\vec{e}_\theta + A_\phi\vec{e}_\phi$ an arbitrary vector, then

$$\begin{aligned} A_r &= A_x\sin\theta\cos\phi + A_y\sin\theta\sin\phi + A_z\cos\theta \\ A_\theta &= A_x\cos\theta\cos\phi + A_y\cos\theta\sin\phi - A_z\sin\theta \\ A_\phi &= -A_x\sin\phi + A_y\cos\phi \end{aligned}$$

In spherical coordinates the **velocity vector** becomes:

$$\begin{aligned} \vec{v} &= \dot{r}\,\vec{e}_r + r\,\dot{\vec{e}}_r \\ &= \dot{r}\,\vec{e}_r + r\,\dot{\theta}\,\vec{e}_\theta + r\,\sin\theta\,\dot{\phi}\,\vec{e}_\phi \end{aligned}$$

The Gradient:

$$\nabla\cdot\vec{A} = \frac{1}{r^2}\frac{\partial}{\partial r}(r^2A_r) + \frac{1}{r\sin\theta}\frac{\partial}{\partial\theta}(\sin\theta A_\theta) + \frac{1}{r\sin\theta}\frac{\partial A_\phi}{\partial\phi}$$

The Convective Operator:

$$\begin{aligned} (\vec{A}\cdot\nabla)\,\vec{B} &= \left(A_r\frac{\partial B_r}{\partial r} + \frac{A_\theta}{r}\frac{\partial B_r}{\partial\theta} + \frac{A_\phi}{r\sin\theta}\frac{\partial B_r}{\partial\phi} - \frac{A_\theta B_\theta + A_\phi B_\phi}{r}\right)\vec{e}_r \\ &+ \left(A_r\frac{\partial B_\theta}{\partial r} + \frac{A_\theta}{r}\frac{\partial B_\theta}{\partial\theta} + \frac{A_\phi}{r\sin\theta}\frac{\partial B_\theta}{\partial\phi} + \frac{A_\theta B_r}{r} - \frac{A_\phi B_\phi\cot\theta}{r}\right)\vec{e}_\theta \\ &+ \left(A_r\frac{\partial B_\phi}{\partial r} + \frac{A_\theta}{r}\frac{\partial B_\phi}{\partial\theta} + \frac{A_\phi}{r\sin\theta}\frac{\partial B_\phi}{\partial\phi} + \frac{A_\phi B_r}{r} + \frac{A_\phi B_\theta\cot\theta}{r}\right)\vec{e}_\phi \end{aligned}$$

The Laplacian:

$$\text{scalar}: \quad \nabla^2\psi = \frac{1}{r^2}\frac{\partial}{\partial r}\left(r^2\frac{\partial\psi}{\partial r}\right) + \frac{1}{r^2\sin\theta}\frac{\partial}{\partial\theta}\left(\sin\theta\frac{\partial\phi}{\partial\theta}\right) + \frac{1}{r^2\sin^2\theta}\frac{\partial^2\psi}{\partial\psi^2}$$

$$\begin{aligned}\text{vector}: \quad \nabla^2\vec{F} &= \left(\nabla^2 F_r - \frac{2F_r}{r^2} - \frac{2}{r^2\sin\theta}\frac{\partial(F_\theta\sin\theta)}{\partial\theta} - \frac{2}{r^2\sin\theta}\frac{\partial F_\phi}{\partial\phi}\right)\vec{e}_r \\ &+ \left(\nabla^2 F_\theta + \frac{2}{r^2}\frac{\partial F_r}{\partial\theta} - \frac{F_\theta}{r^2\sin\theta} - \frac{2\cos\theta}{r^2\sin^2\theta}\frac{\partial F_\phi}{\partial\phi}\right)\vec{e}_\theta \\ &+ \left(\nabla^2 F_\phi + \frac{2}{r^2\sin\theta}\frac{\partial F_r}{\partial\phi} + \frac{2\cos\theta}{r^2\sin^2\theta}\frac{\partial F_\theta}{\partial\phi} - \frac{F_\phi}{r^2\sin^2\theta}\right)\vec{e}_\phi\end{aligned}$$

Appendix E

Differential Equations

The equations of fluid dynamics are all differential equations. In order to provide the necessary background, this appendix gives a very brief overview of the basics.

A differential equation is an **ordinary differential equation (ODE)** if the unknown function depends on only 1 independent variable.

If the unknown function depends on two or more independent variables, then the differential equation is a **partial differential equation (PDE)**.

The **order** of a differential equation is that of the highest derivative appearing in the equation.

Consider the following examples:

$$\begin{aligned} [\mathbf{a}] \quad & \tfrac{\mathrm{d}u}{\mathrm{d}x} = 2x^2 - 4 \\ [\mathbf{b}] \quad & \mathrm{e}^u \tfrac{\mathrm{d}^2u}{\mathrm{d}x^2} + 3\left(\tfrac{\mathrm{d}u}{\mathrm{d}x}\right)^4 = 2 \\ [\mathbf{c}] \quad & \tfrac{\partial^2 u}{\partial t^2} - 4\tfrac{\partial^2 u}{\partial x^2} = 0 \end{aligned}$$

Equation [**a**] is an ODE of order 1, equation [**b**] is an ODE of order 2, and equation [**c**] is a PDE of order 2.

In what follows we shall often use the following **shorthand notation:**

$$u' \equiv \frac{\mathrm{d}u}{\mathrm{d}x}\,, \qquad u'' \equiv \frac{\mathrm{d}^2u}{\mathrm{d}x^2}\,, \qquad u^{(n)} \equiv \frac{\mathrm{d}^n u}{\mathrm{d}x^n}\,.$$

When the independent variable is time, we often use a dot rather than a hyphen, i.e., $\dot{u} = \mathrm{d}u/\mathrm{d}t$, $\ddot{u} = \mathrm{d}^2u/\mathrm{d}t^2$, etc.

When dealing with PDEs, we use the following shorthand:

$$u_{,x} \equiv \frac{\partial u}{\partial x}\,, \qquad u_{,xy} \equiv \frac{\partial^2 u}{\partial x \partial y}\,, \qquad u_{,tt} \equiv \frac{\partial^2 u}{\partial^2 t}\,,$$

etc. Consider the following examples

$$\begin{aligned} \nabla^2 u = 0 \quad &\leftrightarrow \quad u_{,xx} + u_{,yy} + u_{,zz} = 0 \\ \nabla(\nabla \cdot u) + \nabla^2 u + u = 0 \quad &\leftrightarrow \quad u_{k,ki} + u_{i,jj} + u_i = 0 \end{aligned}$$

Note that in the latter we have adopted the Einstein summation convention.

A differential equation along with subsidiary conditions on the unknown function and its derivatives, all given at the same value of the independent variable, consistitute an **initial value problem**.

If the subsidiary conditions are given at more than one value of the independent variable, the problem is a **boundary value problem** and the conditions are **boundary conditions**.

There are three broad classes of boundary conditions:

- **Dirichlet boundary conditions:** The value of the dependent variable is specified on the boundary.
- **Neumann boundary conditions:** The normal derivative of the dependent variable is specified on the boundary.
- **Cauchy boundary conditions:** Both the value and the normal derivative of the dependent variable are specified on the boundary.

Cauchy boundary conditions are analogous to the initial conditions for a second-order ODE. These are given at one end of the interval only.

Linear and non-linear PDEs: A linear PDE is one that is of first degree in all of its field variables and partial derivatives.

Consider the following examples:

$$\begin{aligned}
&[\mathbf{a}] \quad \tfrac{\partial u}{\partial x} + \tfrac{\partial u}{\partial y} = 0 \\
&[\mathbf{b}] \quad \tfrac{\partial u}{\partial x} + \left(\tfrac{\partial u}{\partial y}\right)^2 = 0 \\
&[\mathbf{c}] \quad \tfrac{\partial^2 u}{\partial x^2} + \tfrac{\partial^2 u}{\partial y^2} = x + y \\
&[\mathbf{d}] \quad \tfrac{\partial u}{\partial x} + \tfrac{\partial u}{\partial y} = u^2 \\
&[\mathbf{e}] \quad \tfrac{\partial^2 u}{\partial x^2} + u\,\tfrac{\partial^2 u}{\partial y^2} = 0
\end{aligned}$$

Equations **[a]** and **[c]** are linear, while **[b]**, **[d]** and **[e]** are all non-linear.

We can write the above equations in **operator notation** as:

$$\begin{aligned}
&[\mathbf{a}] \quad L(u) = 0 \quad \text{with} \quad L := \frac{\partial}{\partial x} + \frac{\partial}{\partial y} \\
&[\mathbf{b}] \quad L(u) = 0 \quad \text{with} \quad L := \frac{\partial}{\partial x} + \left(\frac{\partial}{\partial y}\right)^2 \\
&[\mathbf{c}] \quad L(u) = x + y \quad \text{with} \quad L := \frac{\partial^2}{\partial x^2} + \frac{\partial^2}{\partial y^2} \\
&[\mathbf{d}] \quad L(u) = 0 \quad \text{with} \quad L := \frac{\partial}{\partial x} + \frac{\partial}{\partial y} - u^2 \\
&[\mathbf{e}] \quad L(u) = 0 \quad \text{with} \quad L := \frac{\partial^2}{\partial x^2} + u\,\frac{\partial^2}{\partial y^2} = 0
\end{aligned}$$

Homogeneous and non-homogeneous PDEs: Let L be a **linear** operator. Then, a linear PDE can be written in the form

$$L(u) = f(x_1, x_2, x_3, ..., x_n, t)$$

The PDE is said to be homogeneous iff $f(x_1, x_2, x_3, ..., x_n, t) = 0$. Thus, in the examples above, equation **[a]** is homogeneous, while **[c]** is non-homogeneous (aka inhomogeneous).

In (hydro-)dynamics, we typically encounter three types of second-order PDEs, classified as **elliptic**, **hyperbolic**, and **parabolic**. Each type has certain characteristics that help determine if a particular finite element approach is appropriate to the problem being described by the PDE. Interestingly, just knowing the type of PDE can give us insight into how smooth the solution is, how fast information propagates, and the effect of initial and boundary conditions.

Consider a second-order PDE for the unknown function $u(x, y)$ of the form

$$a\,u_{,xx} + b\,u_{,xy} + c\,u_{,yy} + d\,u_{,x} + e\,u_{,y} + f\,u + g = 0$$

where each of a, b,...,g are allowed to be functions of x and/or y.

Elliptic: The above PDE is called elliptic if $b^2 - 4ac < 0$.
An example is the 2D **Poisson equation** $u_{,xx} + u_{,yy} = f$ (which has $a = c = 1$ and $b = 0$). The solutions of elliptic PDEs are always smooth, and boundary data at any point affect the solution at all points in the domain. There is no temporal propagation, yet elliptic PDEs convey the effect of objects on each other. Newtonian mechanics is an example of this, which is why the Poisson equation is elliptic.

Parabolic: The above PDE is called parabolic if $b^2 - 4ac = 0$.
An example is the **heat equation** $u_{,t} = u_{,xx}$ (which has $a = 1$ and $b = c = 0$) which describes heat flow in a 1D system. Parabolic PDEs are usually time dependent and represent diffusion-like processes (i.e., dissipation, convection). Solutions are smooth in space but may possess singularities.

Hyperbolic: The above PDE is called hyperbolic if $b^2 - 4ac > 0$.
An example is the **wave equation** $u_{,xx} - \frac{1}{c_s^2}\,u_{,tt} = f$ (which has $b = 0$, $a = 1$ and $c = -1/c_s^2 < 0$). In a system modeled with a hyperbolic PDE, information travels at a finite speed referred to as the wavespeed (c_s in the example here). Information is not transmitted until the wave arrives. The smoothness of the solution to a hyperbolic PDE depends on the smoothness of the initial and boundary conditions. For instance, if there is a jump in the data at the start or at the boundaries, then the jump will propagate as a shock in the solution. If, in addition, the PDE is nonlinear, then shocks may develop even though the initial conditions and the boundary conditions are smooth.

Finally, since solving PDEs can often be reduced to solving (sets) of ODEs, a few words about solving the latter. Problems involving ODEs can always be reduced to a set of first-order ODEs! For example, the 2nd order ODE

$$\frac{\mathrm{d}^2u}{\mathrm{d}x^2} + s(x)\,\frac{\mathrm{d}u}{\mathrm{d}x} = t(x)$$

can be rewritten as two first-order ODEs

$$\frac{\mathrm{d}u}{\mathrm{d}x} = v(x)\,, \qquad \frac{\mathrm{d}v}{\mathrm{d}x} = t(x) - s(x)v(x)$$

Consider the general n^{th}-order initial value problem

$$\frac{\mathrm{d}^nu}{\mathrm{d}x^n} = a_{n-1}(x)\,\frac{\mathrm{d}^{n-1}}{\mathrm{d}x^{n-1}} + \ldots\ldots + a_1(x)\,\frac{\mathrm{d}u}{\mathrm{d}x} + a_0(x)\,u(x) + f(x)$$

with $u(0) = c_0$, $u'(0) = c_1$, $u''(0) = c_2$, ... ,$u^{(n-1)}(0) = c_{n-1}$ as the initial values. In general, this can be written in matrix form as

$$\mathbf{u}' = \mathbf{A}(x)\,\mathbf{u}(x) + \mathbf{f}(x)$$

with the initial values given by $\mathbf{u}(0) = \mathbf{c}$. Here the elements of $\mathbf{u}$ are given by $u_1 = u(x)$, $u_2 = u'(x)$, ..., $u_n = u^{(n-1)}(x)$. Theses are interrelated with the elements of $\mathbf{u}'$ by the equations $u_1' = u_2$, $u_2' = u_3$, ... ,$u_{n-1}' = u_n$, $u_n' = u^{(n)}(x)$. The matrices $\mathbf{A}(x)$ and $\mathbf{f}(x)$ are related to $a_i(x)$ and $f(x)$ according to

$$\mathbf{A}(x) = \begin{pmatrix} 0 & 1 & 0 & 0 & \cdots & 0 \\ 0 & 0 & 1 & 0 & \cdots & 0 \\ 0 & 0 & 0 & 1 & \cdots & 0 \\ \vdots & \vdots & \vdots & \vdots & & \vdots \\ 0 & 0 & 0 & 0 & \cdots & 1 \\ a_0(x) & a_1(x) & a_2(x) & a_3(x) & \cdots & a_{n-1}(x) \end{pmatrix}$$

and

$$\mathbf{f}(x) = \begin{pmatrix} 0 \\ 0 \\ \vdots \\ 0 \\ f(x) \end{pmatrix}$$

Hence, solving an ODE of order N reduces to solving a set of N coupled first-order differential equations for the functions u_i $(i = 1, 2, ..., N)$ having the general form

$$\frac{\mathrm{d}u_i}{\mathrm{d}x} = f_i(x, u_1, u_2, ..., u_n)$$

where the functions f_i on the rhs are known.

Appendix F

The Levi-Civita Symbol

The **Levi-Civita symbol**, also known as the **permutation symbol** or the **anti-symmetric symbol**,is a collection of numbers, defined from the sign of a permutation of the natural numbers $1, 2, 3, ..., n$. It is often encountered in linear algebra, vector and tensor calculus, and differential geometry.

The n-dimensional Levi-Civita symbol is indicated by $\varepsilon_{i_1 i_2 ... i_n}$, where each index $i_1, i_2, ..., i_n$ takes values $1, 2, ..., n$, ans has the defining property that the symbol is total antisymmetric in all its indices: when any two indices are interchanged, the symbol is negated:

$$\varepsilon_{...i_p...i_q...} = -\varepsilon_{...i_q...i_p...}$$

If any two indices are equal, the symbol is zero, and when all indices are unequal, we have that

$$\varepsilon_{i_1 i_2 ... i_n} = (-1)^p \varepsilon_{1,2,...n}$$

where p is called the **parity of the permutation**. It is the number of pairwise interchanges necessary to unscramble $i_1, i_2, ..., i_n$ into the order $1, 2, ..., n$. A permutation is said to be even (odd) if its parity is an even (odd) number.

Example: what is the parity of $\{3, 4, 5, 2, 1\}$?

$$\{1, 2, 3, 4, 5\}$$
$$\{\mathbf{3}, 2, \mathbf{1}, 4, 5\}$$
$$\{3, \mathbf{4}, 1, \mathbf{2}, 5\}$$
$$\{3, 4, \mathbf{5}, 2, \mathbf{1}\}$$

Answer: $p = 3$, since three pairwise interchanges are required.

In three dimensions the Levi-Civita symbol is defined by

$$\varepsilon_{ijk} = \begin{cases} +1 & \text{if } (i,j,k) \text{ is (1,2,3), (2,3,1), or (3,1,2)} \\ -1 & \text{if } (i,j,k) \text{ is (3,2,1), (1,3,2), or (2,1,3)} \\ 0 & \text{if } i = j, \text{ or } j = k, \text{ or } k = i \end{cases}$$

Appendix G

The Viscous Stress Tensor

As discussed in Chapter 4, the deviatoric stress tensor, τ_{ij}, is only non-zero in the presence of shear in the fluid flow. This suggests that

$$\tau_{ij} = T_{ijkl} \frac{\partial u_k}{\partial x_l}$$

where T_{ijkl} is a proportionality tensor of **rank** four. In what follows we derive an expression for T_{ijkl}. We start by noting that since σ_{ij} is symmetric, we also have that τ_{ij} will be symmetric. Hence, we expect that the above dependence can only involve the **symmetric** component of the deformation tensor, $\mathcal{T}_{kl} = \partial u_k / \partial x_l$. Hence, it is useful to split the deformation tensor in its **symmetric** and **anti-symmetric** components:

$$\frac{\partial u_i}{\partial x_j} = e_{ij} + \xi_{ij}$$

where

$$\begin{aligned} e_{ij} &= \frac{1}{2}\left[\frac{\partial u_i}{\partial x_j} + \frac{\partial u_j}{\partial x_i}\right] \\ \xi_{ij} &= \frac{1}{2}\left[\frac{\partial u_i}{\partial x_j} - \frac{\partial u_j}{\partial x_i}\right] \end{aligned}$$

The symmetric part of the deformation tensor, e_{ij}, is called the **rate of strain tensor**, while the anti-symmetric part, ξ_{ij}, expresses the **vorticity** $\vec{w} \equiv \nabla \times \vec{u}$ in the velocity field, i.e., $\xi_{ij} = -\frac{1}{2}\,\varepsilon_{ijk}\,w_k$. Note that one can always find a coordinate system for which e_{ij} is diagonal. The axes of that coordinate frame indicate the **eigendirections** of the strain (compression or stretching) on the fluid element.

In terms of the relation between the viscous stress tensor, τ_{ij}, and the deformation tensor, $\mathcal{T}_{kl}$, there are a number of properties that are important.

- **Locality:** the $\tau_{ij} - \mathcal{T}_{kl}$-relation is said to be **local** if the stress tensor is only a function of the deformation tensor and thermodynamic state functions like temperature.

- **Homogeneity:** the $\tau_{ij} - \mathcal{T}_{kl}$-relation is said to be **homogeneous** if it is everywhere the same. The viscous stress tensor may depend on location $\vec{x}$ only insofar as $\mathcal{T}_{ij}$ or the thermodynamic state functions depend on $\vec{x}$. This distinguishes a fluid from a solid, in which the stress tensor depends on the stress itself.

- **Isotropy:** the $\tau_{ij} - \mathcal{T}_{kl}$-relation is said to be **isotropic** if it has no preferred direction.

- **Linearity:** the $\tau_{ij} - \mathcal{T}_{kl}$-relation is said to be **linear** if the relation between the stress and rate-of-strain is linear. This is equivalent to saying that τ_{ij} does not depend on $\nabla^2\vec{u}$ or higher-order derivatives.

A fluid that is local, homogeneous and isotropic is called a **Stokesian** fluid. A Stokesian fluid that is linear is called a **Newtonian** fluid. Experiments have shown that most (astrophysical) fluids are Newtonian to good approximation. Hence, in what follows we will assume that our fluids are Newtonian, unless specifically stated otherwise. For a Newtonian fluid, it can be shown (using linear algebra) that the most general form of our proportionality tensor is given by

$$T_{ijkl} = \lambda\delta_{ij}\delta_{kl} + \mu\left(\delta_{ik}\delta_{jl} + \delta_{il}\delta_{jk}\right)$$

Hence, for a **Newtonian** fluid the **viscous stress tensor** is

$$\tau_{ij} = 2\mu e_{ij} + \lambda e_{kk}\delta_{ij}$$

where μ is the **coefficient of shear viscosity**, λ is a scalar, δ_{ij} is the Kronecker delta function, and $e_{kk} = \mathrm{Tr}(e) = \partial u_k/\partial x_k = \nabla\cdot\vec{u}$ (summation convention).

Note that (in a Newtonian fluid) the viscous stress tensor depends **only** on the symmetric component of the deformation tensor (the rate-of-strain tensor e_{ij}), but **not** on the antisymmetric component which describes **vorticity**. You can understand the fact that viscosity and vorticity are unrelated by considering a fluid disk in solid body rotation (i.e., $\nabla\cdot\vec{u} = 0$ and $\nabla\times\vec{u} = \vec{w} \neq 0$). In such a fluid there is no "slippage", hence no shear, and therefore no manifestation of viscosity.

Thus far we have derived that the stress tensor, σ_{ij}, which in principle has 6 unknowns, can be reduced to a function of three unknowns only (P, μ, λ) as long as the fluid is **Newtonian**. Note that these three scalars, in general, are functions of temperature and density. We now focus on these three scalars in more detail, starting with the pressure P. To be exact, P is the **thermodynamic equilibrium pressure**, and is normally computed thermodynamically from some equation of state, $P = P(\rho, T)$. It is related to the translational kinetic energy of the particles when the fluid, in equilibrium, has reached **equipartition** of energy among **all** its degrees of freedom, including (in the case of molecules) rotational and vibrations degrees of freedom.

In addition to the thermodynamic equilibrium pressure, P, we can also define a **mechanical pressure**, P_{m}, which is purely related to the translational motion of the particles, **independent** of whether the system has reached full equipartition of energy. The mechanical pressure is simply the average normal stress and therefore follows from the stress tensor according to

$$P_{\mathrm{m}} = -\frac{1}{3}\,\mathrm{Tr}(\sigma_{ij}) = -\frac{1}{3}\,(\sigma_{11} + \sigma_{22} + \sigma_{33})$$

Using that

$$\sigma_{ij} = -P\,\delta_{ij} + 2\,\mu\,e_{ij} + \lambda\,e_{kk}\,\delta_{ij}$$

we thus obtain the following relation between the two pressures:

$$P_{\mathrm{m}} = P - \eta\,\nabla\cdot\vec{u}$$

where

$$\eta = \frac{2}{3}\mu + \lambda = \frac{P - P_{\mathrm{m}}}{\nabla\cdot\vec{u}}$$

is the **coefficient of bulk viscosity**. We can now write the stress tensor as

$$\sigma_{ij} = -P\delta_{ij} + \mu\left[\frac{\partial u_i}{\partial x_j} + \frac{\partial u_j}{\partial x_i} - \frac{2}{3}\delta_{ij}\frac{\partial u_k}{\partial x_k}\right] + \eta\,\delta_{ij}\frac{\partial u_k}{\partial x_k}$$

This is the full expression for the stress tensor in terms of the coefficients of **shear viscosity**, μ, and **bulk viscosity**, η.

Appendix H

Equations of State

Equation of State (EoS): a thermodynamic equation describing the state of matter under a given set of physical conditions. In what follows we will always write our EoS in the form $P = P(\rho, T)$. Other commonly used forms are $P = P(\rho, \varepsilon)$ or $P = P(\rho, S)$.

Ideal Gas: a hypothetical gas that consists of identical point particles (i.e. of zero volume) that undergo perfectly elastic collisions and for which interparticle forces can be neglected.

An ideal gas obeys the **ideal gas law:** $P\,V = N\,k_{\rm B}\,T$.

Here N is the total number of particles, $k_{\rm B}$ is Boltzmann's constant, and V is the volume occupied by the fluid. Using that $\rho = N\,\mu m_{\rm p}/V$, where μ is the **mean molecular weight** in units of the proton mass $m_{\rm p}$, we have that the **EoS for an ideal gas** is given by

$$P = \frac{k_{\rm B}\,T}{\mu\,m_{\rm p}}\,\rho$$

`NOTE:` astrophysical gases are often well described by the ideal gas law. Even for a fully ionized gas, the interparticle forces (Coulomb force) can typically be neglected (i.e., the potential energies involved are typically $< 10\%$ of the kinetic energies). Ideal gas law breaks down for dense, and cool gases, such as those present in gaseous planets.

Maxwell-Boltzmann Distribution: the distribution of particle momenta, $\vec{p} = m\vec{v}$, of an ideal gas follows the Maxwell-Boltzmann distribution.

$$\mathcal{P}(\vec{p})\,\mathrm{d}^3\vec{p} = \left(\frac{1}{2\pi m k_\mathrm{B} T}\right)^{3/2} \exp\left(-\frac{p^2}{2m k_\mathrm{B} T}\right)\,\mathrm{d}^3\vec{p}$$

where $p^2 = \vec{p}\cdot\vec{p}$. This distribution follows from maximizing entropy under the following assumptions:

1. all magnitudes of velocity are *a priori* equally likely
2. all directions are equally likely (isotropy)
3. total energy is constrained at a fixed value
4. total number of particles is constrained at a fixed value

Using that $E = p^2/2m$ we thus see that $\mathcal{P}(\vec{p}) \propto e^{-E/k_\mathrm{B}T}$.

Pressure: pressure arises from (elastic) collisions of particles. A particle hitting a wall head on with momentum $p = mv$ results in a transfer of momentum to the wall of $2mv$. Using this concept, and assuming isotropy for the particle momenta, it can be shown that

$$\boxed{P = \zeta\, n\, \langle E\rangle}$$

where $\zeta = 2/3$ ($\zeta = 1/3$) in the case of a non-relativistic (relativistic) fluid, and

$$\langle E\rangle = \int_0^\infty E\,\mathcal{P}(E)\,\mathrm{d}E$$

is the average, translational energy of the particles. In the case of our ideal (non-relativistic) fluid,

$$\langle E\rangle = \left\langle \frac{p^2}{2m}\right\rangle = \int_0^\infty \frac{p^2}{2m}\,\mathcal{P}(p)\,\mathrm{d}p = \frac{3}{2}k_\mathrm{B}T$$

Hence, we find that the **EoS for an ideal gas** is indeed given by

$$\boxed{P = \frac{2}{3}\, n\, \langle E \rangle = n\, k_{\rm B}\, T = \frac{k_{\rm B} T}{\mu m_{\rm p}}\, \rho}$$

Specific Internal Energy: the internal energy per unit mass for an ideal gas is

$$\varepsilon = \frac{\langle E \rangle}{\mu m_{\rm p}} = \frac{3}{2} \frac{k_{\rm B} T}{\mu m_{\rm p}}$$

Actually, the above derivation is only valid for a true 'ideal gas', in which the particles are point particles. More generally,

$$\boxed{\varepsilon = \frac{1}{\gamma - 1} \frac{k_{\rm B} T}{\mu m_{\rm p}}}$$

where γ is the **adiabatic index**, which for an ideal gas is equal to $\gamma = (q+5)/(q+3)$, with q the internal degrees of freedom of the fluid particles: $q = 0$ for point particles (resulting in $\gamma = 5/3$), while diatomic particles have $q = 2$ (at sufficiently low temperatures, such that they only have rotational, and no vibrational degrees of freedom). The fact that $q = 2$ in that case arises from the fact that a diatomic molecule only has two relevant rotation axes; the third axis is the symmetry axis of the molecule, along which the molecule has negligible (zero in case of point particles) moment of inertia. Consequently, rotation around this symmetry axis carries no energy.

Photon gas: Having discussed the EoS of an ideal gas, we now focus on a gas of photons. Photons have energy $E = h\nu$ and momentum $p = E/c = h\nu/c$, with h the Planck constant.

Black Body: an idealized physical body that absorbs all incident radiation. A black body (BB) in thermal equilibrium emits electro-magnetic radiation called **black body radiation**.

The **spectral number density distribution** of BB photons is given by

$$n_\gamma(\nu, T) = \frac{8\pi\nu^2}{c^3} \frac{1}{e^{h\nu/k_{\rm B}T} - 1}$$

which implies a **spectral energy distribution**

$$u(\nu, T) = n_\gamma(\nu, T)\, h\nu = \frac{8\pi h\nu^3}{c^3}\, \frac{1}{e^{h\nu/k_{\rm B}T} - 1}$$

and thus an **energy density** of

$$u(T) = \int_0^\infty u(\nu, T)\, {\rm d}\nu = \frac{4\sigma_{\rm SB}}{c}\, T^4 \equiv a_{\rm r}\, T^4$$

where

$$\sigma_{\rm SB} = \frac{2\pi^5 k_{\rm B}^4}{15 h^3 c^2}$$

is the **Stefan-Boltzmann constant** and $a_{\rm r} \simeq 7.6 \times 10^{-15} {\rm erg\, cm^{-3}\, K^{-4}}$ is called the **radiation constant**.

Radiation Pressure: when the photons are reflected off a wall, or when they are absorbed and subsequently re-emitted by that wall, they transfer twice their momentum in the normal direction to that wall. Since photons are relativistic, we have that **the EoS for a photon gas** is given by

$$\boxed{P = \frac{1}{3}\, n\, \langle E \rangle = \frac{1}{3}\, n_\gamma\, \langle h\nu \rangle = \frac{1}{3} u(T) = \frac{aT^4}{3}}$$

where we have used that $u(T) = n_\gamma \langle E \rangle$.

Quantum Statistics: according to quantum statistics, a collection of many indistinguishable elementary particles in **thermal equilibrium** has a momentum distribution given by

$$f(\vec{p})\, {\rm d}^3\vec{p} = \frac{g}{h^3} \left[\exp\left(\frac{E(p) - \mu}{k_{\rm B}T} \right) \pm 1 \right]^{-1} {\rm d}^3\vec{p}$$

where the signature $\pm$ takes the positive sign for fermions (which have half-integer spin), in which case the distribution is called the **Fermi-Dirac distribution**, and the negative sign for bosons (particles with zero or integer spin), in which case the distribution is called the **Bose-Einstein distribution**. The factor g is the **spin degeneracy factor**, which expresses the number of spin states the particles can have ($g = 1$ for neutrinos, $g = 2$ for photons and charged leptons, and $g = 6$

for quarks). Finally, μ is called the **chemical potential**, and is a form of potential energy that is related (in a complicated way) to the number density and temperature of the particles (see Appendix I).

Classical limit: In the limit where the mean interparticle separation is much larger than the de Broglie wavelength of the particles, so that quantum effects (e.g., Heisenberg's uncertainty principle) can be ignored, the above distribution function of momenta can be accurately approximated by the **Maxwell-Boltzmann distribution**.

Heisenberg's Uncertainty Principle: $\Delta x\ \Delta p_x > h$ (where $h = 6.63{\times}10^{-27}\mathrm{g\,cm^2\,s^{-1}}$ is Planck's constant). One interpretation of this quantum principle is that phase-space is quantized; no particle can be localized in a phase-space element smaller than the fundamental element

$$\Delta x\ \Delta y\ \Delta z\ \Delta p_x\ \Delta p_y\ \Delta p_z = h^3$$

Pauli Exclusion Principle: no more than one fermion of a given spin state can occupy a given phase-space element h^3. Hence, for electrons, which have $g = 2$, the maximum phase-space density is $2/h^3$.

Degeneracy: When compressing and/or cooling a fermionic gas, at some point all possible low momentum states are occupied. Any further compression therefore results in particles occupying high (but the lowest available) momentum states. Since particle momentum is ultimately responsible for pressure, this degeneracy manifests itself as an extremely high pressure, known as **degeneracy pressure**.

Fermi Momentum: Consider a **fully degenerate** gas of electrons of electron density n_e. It will have fully occupied the part of phase-space with momenta $p \leq p_{\rm F}$. Here $p_{\rm F}$ is the maximum momentum of the particles, and is called the **Fermi momentum**. The energy corresponding to the Fermi momentum is called the **Fermi energy**, $E_{\rm F}$ and is equal to $p_{\rm F}^2/2m$ in the case of a non-relativistic gas, and $p_{\rm F}c$ in the case of a relativistic gas.

Let V_x be the volume occupied in configuration space, and $V_p = \frac{4}{3}\pi p_{\rm F}^3$ the volume occupied in momentum space. If the total number of particles is N, and the gas is

fully degenerate, then

$$V_x\, V_p = \frac{N}{2} h^3$$

Using that $n_e = N/V_x$, we find that

$$p_{\rm F} = \left(\frac{3}{8\pi} n_e\right)^{1/3} h$$

EoS of Non-Relativistic, Degenerate Gas: Using the information above, it is relatively straightforward (see Problem Set 4) to compute the EoS for a fully degenerate gas. Using that for a non-relativistic fluid $E = p^2/2m$ and $P = \frac{2}{3}\, n\, \langle E \rangle$, while degeneracy implies that

$$\langle E \rangle = \frac{1}{N} \int_0^{E_{\rm f}} E\, N(E)\, {\rm d}E = \frac{1}{N} \int_0^{p_{\rm F}} \frac{p^2}{2m}\, \frac{2}{h^3}\, V_x\, 4\pi p^2\, {\rm d}p = \frac{3}{5}\, \frac{p_{\rm F}^2}{2m}$$

we obtain that

$$P = \frac{1}{20} \left(\frac{3}{\pi}\right)^{2/3} \frac{h^2}{m^{8/3}}\, \rho^{5/3}$$

EoS of Relativistic, Degenerate Gas: In the case of a relativistic, degenerate gas, we use the same procedure as above. However, this time we have that $P = \frac{1}{3}\, n\, \langle E \rangle$ while $E = p\, c$, which results in

$$P = \frac{1}{8} \left(\frac{3}{\pi}\right)^{1/3} \frac{c\, h}{m^{4/3}}\, \rho^{4/3}$$

White Dwarfs and the Chandrasekhar limit: White dwarfs are the end-states of stars with mass low enough that they don't form a neutron star. When the pressure support from nuclear fusion in a star comes to a halt, the core will start to contract until degeneracy pressure kicks in. The star consists of a fully ionized plasma. Assume for simplicity that the plasma consists purely of hydrogen, so that the number density of protons is equal to that of electrons: $n_{\rm p} = n_{\rm e}$. Because of **equipartition**

$$\frac{p_{\rm p}^2}{2m_{\rm p}} = \frac{p_{\rm e}^2}{2m_{\rm e}}$$

Since $m_{\rm p} >> m_{\rm e}$ we have also that $p_{\rm p} >> p_{\rm e}$ (in fact $p_{\rm p}/p_{\rm e} = \sqrt{m_{\rm p}/m_{\rm e}} \simeq 43$). Consequently, when cooling or compressing the core of a star, the electrons will become degenerate well before the protons do. Hence, white dwarfs are held up against collapse by the **degeneracy pressure from electrons**. Since the electrons are typically non-relativistic, the EoS of the white dwarf is: $P \propto \rho^{5/3}$. If the white dwarf becomes more and more massive (i.e., because it is accreting mass from a companion star), the Pauli-exclusion principle causes the Fermi momentum, $p_{\rm F}$, to increase to relativistic values. This **softens** the EoS towards $P \propto \rho^{4/3}$. Such an equation of state is too soft to stabilize the white dwarf against gravitational collapse; the white dwarf collapses until it becomes a **neutron star**, at which stage it is supported against further collapse by the degeneracy pressure from neutrons. This happens when the mass of the white dwarf reaches $M_{\rm lim} \simeq 1.44 M_\odot$, the so-called **Chandrasekhar limit**.

	Non-Relativistic	**Relativistic**
non-degenerate	$P \propto \rho T$	$P \propto T^4$
degenerate	$P \propto \rho^{5/3}$	$P \propto \rho^{4/3}$

Summary of equations of state for different kind of fluids

Appendix I

Poisson Brackets

Given two functions $A(q_i, p_i)$ and $B(q_i, p_i)$ of the **canonical** phase-space coordinates q_i and p_i, the **Poisson bracket** of A and B is defined as

$$\{A, B\} = \sum_{i=1}^{3N} \left(\frac{\partial A}{\partial q_i} \frac{\partial B}{\partial p_i} - \frac{\partial A}{\partial p_i} \frac{\partial B}{\partial q_i} \right)$$

In vector notation,

$$\{A, B\} = \sum_{i=1}^{N} \left(\frac{\partial A}{\partial \vec{q}_i} \cdot \frac{\partial B}{\partial \vec{p}_i} - \frac{\partial A}{\partial \vec{p}_i} \cdot \frac{\partial B}{\partial \vec{q}_i} \right)$$

where $\vec{q}_i = (q_{i1}, q_{i2}, q_{i3})$ and $\vec{p}_i = (p_{i1}, p_{i2}, p_{i3})$ and i now indicates a particular particle ($i = 1, 2, ..., N$).

Note that Poisson brackets are anti-symmetric, i.e., $\{A, B\} = -\{B, A\}$, and that $\{A, A\} = 0$.

Poisson brackets are an extremely powerful construct in classical mechanics (they are the equivalent of commutators in quantum mechanics). To see this, consider a function $A(q_i, p_i, t)$. If the system is Hamiltonian (i.e., q_i and p_i obey the Hamiltonian equations of motion), then we have the following correspondance:

$$\boxed{\mathrm{d}A/\mathrm{d}t = 0 \qquad \Leftrightarrow \qquad \partial A/\partial t + \{A, \mathcal{H}\} = 0}$$

To see this, use multi-variable calculus to write out the differential $\mathrm{d}A$, write out the Poisson brackets, and substitute the Hamiltonian equations of motion:

$$\begin{aligned}\{A,\mathcal{H}\} &= \sum_{i=1}^{N}\left(\frac{\partial A}{\partial \vec{q}_i}\cdot\frac{\partial \mathcal{H}}{\partial \vec{p}_i}-\frac{\partial A}{\partial \vec{p}_i}\cdot\frac{\partial \mathcal{H}}{\partial \vec{q}_i}\right)\\ &= \sum_{i=1}^{N}\left(\frac{\partial A}{\partial \vec{q}_i}\cdot\dot{\vec{q}}_i+\frac{\partial A}{\partial \vec{p}_i}\cdot\dot{\vec{p}}_i\right)\end{aligned}$$

Hence, a function of the phase-space coordinates whose Poisson bracket with the Hamiltonian vanishes is conserved along its orbit/path in a static system (static means that all partial time derivates are equal to zero). Such a quantity is called an **integral of motion**.

As we have seen in Chapter 6, the **Liouville equation** states that the Lagrangian time-derivative of the N-point DF vanishes, i.e., $\mathrm{d}f^{(N)}/\mathrm{d}t = 0$. Using the above, we can write this as

$$\partial f^{(N)}/\partial t + \{f^{(N)},\mathcal{H}\} = 0$$

which is yet another way of writing the Liouville equation. We can also use the Poisson brackets to rewrite the **Collisionless Boltzmann equation** as

$$\partial f^{(1)}/\partial t + \{f^{(1)},\mathcal{H}\} = 0$$

Note that in the latter the Hamiltonian is a function of 6 phase-space coordinates $(\vec{q},\vec{p})$, whereas in the former the Hamiltonian depends on the 6N phase-space coordinates of all N particles, i.e., on $(\vec{q}_1,\vec{q}_2,...,\vec{q}_N,\vec{p}_1,\vec{p}_2,...,\vec{p}_N)$.

The Poisson brackets are useful for writing equations in more compact form. For example, using the 6D vector $\vec{w} = (\vec{q},\vec{p})$, the **Hamiltonian equations of motion** are simply given by

$$\boxed{\dot{\vec{w}} = \{\vec{w},\mathcal{H}\}}$$

Appendix J

The BBGKY Hierarchy

In this Appendix we derive the BBGKY hierarchy of evolution equations for the k-particle distribution function $f^{(k)}(\vec{w}_1, \vec{w}_2, ...\vec{w}_k)$ starting from the **Liouville equation** for the N-particle distribution function $f^{(N)}(\vec{w}_1, \vec{w}_2, ...\vec{w}_N)$, where $N > k$. Here $\vec{w}_i \equiv (\vec{q}_i, \vec{p}_i)$ is the 6D phase-space vector of particle i,

As we have seen in Chapter 6, the Liouville equation, which is given by

$$\frac{\mathrm{d}f^{(N)}}{\mathrm{d}t} = \frac{\partial f^{(N)}}{\partial t} + \{f^{(N)}, \mathcal{H}^{(N)}\} = 0$$

expresses the incompressibilty of Hamiltonian flow in Γ-space. Here we have adopted the notation based on **Poisson brackets** (see Appendix I), and we have used the index '(N)' on the Hamiltonian to emphasize that this is the N-particle Hamiltonian

$$\mathcal{H}^{(N)}(\vec{q}_i, \vec{p}_i) = \sum_{i=1}^{N} \frac{\vec{p}_i^{\,2}}{2m} + \sum_{i=1}^{N} V(\vec{q}_i) + \frac{1}{2}\sum_{i=1}^{N}\sum_{\substack{j=1 \\ j\neq i}}^{N} U_{ij}$$

Here $V(\vec{q})$ is the potential corresponding to an **external force**, and we have used U_{ij} as shorthand notation for

$$U_{ij} \equiv U(|\vec{q}_i - \vec{q}_j|)$$

the potential energy associated with the two-body interaction between particles i and j. Note that $U_{ij} = U_{ji}$. The factor $1/2$ in the above expression for the Hamiltonian is to correct for double-counting of the particle pairs.

We can relate the N-particle Hamiltonian, $\mathcal{H}^{(N)}$ to the k-particle Hamiltonian, $\mathcal{H}^{(k)}$, which is defined in the same way as $\mathcal{H}^{(N)}$ but with N replaced by $k < N$, according to

$$\mathcal{H}^{(N)} = \mathcal{H}^{(k)} + \mathcal{H}^{(k,N)} + \sum_{i=1}^{k}\sum_{j=k+1}^{N} U_{ij}$$

Here

$$\mathcal{H}^{(k)} = \sum_{i=1}^{k} \frac{\vec{p}_i^{\,2}}{2m} + \sum_{i=1}^{k} V(\vec{q}_i) + \frac{1}{2} \sum_{i=1}^{k} \sum_{\substack{j=1 \\ j\neq i}}^{k} U_{ij}$$

and

$$\mathcal{H}^{(k,N)} = \sum_{i=k+1}^{N} \frac{\vec{p}_i^{\,2}}{2m} + \sum_{i=k+1}^{N} V(\vec{q}_i) + \frac{1}{2} \sum_{i=k+1}^{N} \sum_{\substack{j=k+1 \\ j\neq i}}^{N} U_{ij}$$

To see this, consider the U_{ij} term, for which we can write

$$\begin{aligned} \sum_{i=1}^{N} \sum_{\substack{j=i \\ j\neq i}}^{N} U_{ij} &= \sum_{i=1}^{k} \sum_{\substack{j=1 \\ j\neq i}}^{N} U_{ij} + \sum_{i=k+1}^{N} \sum_{\substack{j=1 \\ j\neq i}}^{N} U_{ij} \\ &= \sum_{i=1}^{k} \sum_{\substack{j=1 \\ j\neq i}}^{k} U_{ij} + \sum_{i=1}^{k} \sum_{j=k+1}^{N} U_{ij} + \sum_{i=k+1}^{N} \sum_{j=1}^{k} U_{ij} + \sum_{i=k+1}^{N} \sum_{\substack{j=k+1 \\ j\neq i}}^{N} U_{ij} \end{aligned}$$

The second and third terms are identical (since $U_{ij} = U_{ji}$) so that upon substitution we obtain the above relation between $\mathcal{H}^{(N)}$ and $\mathcal{H}^{(k)}$.

Now let's take the **Liouville equation** and integrate it over the entire phase-space of particles $k+1$ to N:

$$\int \prod_{n=k+1}^{N} \mathrm{d}^3\vec{q}_n \, \mathrm{d}^3\vec{p}_n \, \frac{\partial f^{(N)}}{\partial t} = \int \prod_{n=k+1}^{N} \mathrm{d}^3\vec{q}_n \, \mathrm{d}^3\vec{p}_n \, \{\mathcal{H}^{(N)}, f^{(N)}\}$$

First the LHS: using that the integration is independent of time, we take the time derivative outside of the integral, yielding

$$\frac{\partial}{\partial t} \int \prod_{n=k+1}^{N} \mathrm{d}^3\vec{q}_n \, \mathrm{d}^3\vec{p}_n \, f^{(N)} = \frac{(N-k)!}{N!} \, \frac{\partial f^{(k)}}{\partial t}$$

where we have made use of the definition of the **reduced k-particle distribution function** (see Chapter 6). Writing out the Poisson brackets in the RHS, and splitting

the summation over i in two parts, we can write the RHS as the sum of two integrals, $\mathcal{I}_1$ plus $\mathcal{I}_2$, where

$$\mathcal{I}_1 = \int \prod_{n=k+1}^{N} \mathrm{d}^3\vec{q}_n \, \mathrm{d}^3\vec{p}_n \sum_{i=1}^{k} \left(\frac{\partial \mathcal{H}^{(N)}}{\partial \vec{q}_i} \cdot \frac{\partial f^{(N)}}{\partial \vec{p}_i} - \frac{\partial \mathcal{H}^{(N)}}{\partial \vec{p}_i} \cdot \frac{\partial f^{(N)}}{\partial \vec{q}_i} \right)$$

and

$$\mathcal{I}_2 = \int \prod_{n=k+1}^{N} \mathrm{d}^3\vec{q}_n \, \mathrm{d}^3\vec{p}_n \sum_{i=k+1}^{N} \left(\frac{\partial \mathcal{H}^{(N)}}{\partial \vec{q}_i} \cdot \frac{\partial f^{(N)}}{\partial \vec{p}_i} - \frac{\partial \mathcal{H}^{(N)}}{\partial \vec{p}_i} \cdot \frac{\partial f^{(N)}}{\partial \vec{q}_i} \right)$$

Integral $\mathcal{I}_2$ vanishes. To see this, realize that $\partial \mathcal{H}^{(N)}/\partial \vec{q}_i$ is independent of $\vec{p}_i$ and $\partial \mathcal{H}^{(N)}/\partial \vec{p}_i$ is independent of $\vec{q}_i$ (this follows from the definition of the Hamiltonian). Because of this, each terms in $\mathcal{I}_2$ can be cast in the form

$$\int_{-\infty}^{+\infty} \mathrm{d}x \int_{-\infty}^{+\infty} \mathrm{d}y \, g(x) \, \frac{\partial f(x,y)}{\partial y} = \int_{-\infty}^{+\infty} \mathrm{d}x \, g(x) \, \left[f(x,y) \right]_{y=-\infty}^{y=+\infty}$$

i.e., these turn into surface integrals, and since $f^{(N)}(\vec{q}_i, \vec{p}_i) = 0$ in the limits $|\vec{q}_i| \to \infty$ (systems are of finite extent) and $|\vec{p}_i| \to \infty$ (particles have finite speed), we see that $\mathcal{I}_2$ must vanish.

In order to compute $\mathcal{I}_1$, we first write $\mathcal{H}^{(N)}$ in terms of $\mathcal{H}^{(k)}$ and $\mathcal{H}^{(k,N)}$ as indicated above. This allows us split the result in three terms, $\mathcal{I}_{1a}$, $\mathcal{I}_{1b}$ and $\mathcal{I}_{1c}$ given by

$$\mathcal{I}_{1a} = \int \prod_{n=k+1}^{N} \mathrm{d}^3\vec{q}_n \, \mathrm{d}^3\vec{p}_n \sum_{i=1}^{k} \left(\frac{\partial \mathcal{H}^{(k)}}{\partial \vec{q}_i} \cdot \frac{\partial f^{(N)}}{\partial \vec{p}_i} - \frac{\partial \mathcal{H}^{(k)}}{\partial \vec{p}_i} \cdot \frac{\partial f^{(N)}}{\partial \vec{q}_i} \right),$$

$$\mathcal{I}_{1b} = \int \prod_{n=k+1}^{N} \mathrm{d}^3\vec{q}_n \, \mathrm{d}^3\vec{p}_n \sum_{i=1}^{k} \left(\frac{\partial \mathcal{H}^{(k,N)}}{\partial \vec{q}_i} \cdot \frac{\partial f^{(N)}}{\partial \vec{p}_i} - \frac{\partial \mathcal{H}^{(k,N)}}{\partial \vec{p}_i} \cdot \frac{\partial f^{(N)}}{\partial \vec{q}_i} \right),$$

and

$$\mathcal{I}_{1c} = \int \prod_{n=k+1}^{N} \mathrm{d}^3\vec{q}_n \, \mathrm{d}^3\vec{p}_n \sum_{i=1}^{k} \left(\frac{\partial}{\partial \vec{q}_i} \left[\sum_{l=1}^{k} \sum_{j=k+1}^{N} U_{kl} \right] \cdot \frac{\partial f^{(N)}}{\partial \vec{p}_i} - \frac{\partial}{\partial \vec{p}_i} \left[\sum_{l=1}^{k} \sum_{j=k+1}^{N} U_{kl} \right] \cdot \frac{\partial f^{(N)}}{\partial \vec{q}_i} \right)$$

We now examine each of these in turn. Starting with $\mathcal{I}_{1a}$, for which we realize that the operator for $f^{(N)}$ is independent of the integration variables, such that we can take it outside of the integral. Hence, we have that

$$\mathcal{I}_{1a} = \sum_{i=1}^{k} \left(\frac{\partial \mathcal{H}^{(k)}}{\partial \vec{q}_i} \cdot \frac{\partial}{\partial \vec{p}_i} - \frac{\partial \mathcal{H}^{(k)}}{\partial \vec{p}_i} \cdot \frac{\partial}{\partial \vec{q}_i} \right) \int \prod_{n=k+1}^{N} \mathrm{d}^3 \vec{q}_n \, \mathrm{d}^3 \vec{p}_n \, f^{(N)}$$

Using the definition of the reduced k-particle distribution function, this can be written as

$$\mathcal{I}_{1a} = \frac{(N-k)!}{N!} \sum_{i=1}^{k} \left(\frac{\partial \mathcal{H}^{(k)}}{\vec{q}_i} \cdot \frac{\partial f^{(k)}}{\partial \vec{p}_i} - \frac{\partial \mathcal{H}^{(k)}}{\vec{p}_i} \cdot \frac{\partial f^{(k)}}{\partial \vec{q}_i} \right) = \frac{(N-k)!}{N!} \, \{\mathcal{H}^{(k)}, f^{(k)}\}$$

where we have made use of the definition of the Poisson brackets (see Appendix I).

Next up is $\mathcal{I}_{1b}$. It is clear that this integral must vanish, since both $\partial \mathcal{H}^{(k,N)}/\partial \vec{q}_i$ and $\partial \mathcal{H}^{(k,N)}/\partial \vec{p}_i$ are equal to zero. After all, the index i runs from 1 to k, and the phase-space coordinates of those particles do not appear in $\mathcal{H}^{(k,N)}$. This leaves $\mathcal{I}_{1c}$; since U_{kl} is independent of momentum, the second term within the brackets vanishes, leaving only

$$\mathcal{I}_{1c} = \int \prod_{n=k+1}^{N} \mathrm{d}^3 \vec{q}_n \, \mathrm{d}^3 \vec{p}_n \sum_{i=1}^{k} \left(\sum_{j=k+1}^{N} \frac{\partial U_{ij}}{\partial \vec{q}_i} \cdot \frac{\partial f^{(N)}}{\partial \vec{p}_i} \right)$$

Upon inspection, you can see that each term of the j-summation is equal (this follows from the fact that we integrate over all of $\vec{q}_j$ for each $j = k+1, ..., N$). Hence, since there are $N-k$ such terms we have that

$$
\begin{aligned}
\mathcal{I}_{1c} &= (N-k)\sum_{i=1}^{k}\int\prod_{n=k+1}^{N}\mathrm{d}^3\vec{q}_n\,\mathrm{d}^3\vec{p}_n\left(\frac{\partial U_{i,k+1}}{\partial\vec{q}_i}\cdot\frac{\partial f^{(N)}}{\partial\vec{p}_i}\right)\\
&= (N-k)\sum_{i=1}^{k}\int\mathrm{d}^3\vec{q}_{k+1}\,\mathrm{d}^3\vec{p}_{k+1}\left(\frac{\partial U_{i,k+1}}{\partial\vec{q}_i}\cdot\frac{\partial}{\partial\vec{p}_i}\right)\int\prod_{n=k+2}^{N}\mathrm{d}^3\vec{q}_n\,\mathrm{d}^3\vec{p}_n\,f^{(N)}\\
&= (N-k)\,\frac{(N-k-1)!}{N!}\sum_{i=1}^{k}\int\mathrm{d}^3\vec{q}_{k+1}\,\mathrm{d}^3\vec{p}_{k+1}\left(\frac{\partial U_{i,k+1}}{\partial\vec{q}_i}\cdot\frac{\partial f^{(k+1)}}{\partial\vec{p}_i}\right)\\
&= \frac{(N-k)!}{N!}\sum_{i=1}^{k}\int\mathrm{d}^3\vec{q}_{k+1}\,\mathrm{d}^3\vec{p}_{k+1}\left(\frac{\partial U_{i,k+1}}{\partial\vec{q}_i}\cdot\frac{\partial f^{(k+1)}}{\partial\vec{p}_i}\right)
\end{aligned}
$$

where as before we have taken the operator outside of the integral, and we have used the definition of the reduced distribution functions.

Combining everything, we obtain our final expression for the evolution of the reduced k-particle distribution function

$$
\boxed{\frac{\partial f^{(k)}}{\partial t} = \{\mathcal{H}^{(k)}, f^{(k)}\} + \sum_{i=1}^{k}\int\mathrm{d}^3\vec{q}_{k+1}\,\mathrm{d}^3\vec{p}_{k+1}\left(\frac{\partial U_{i,k+1}}{\partial\vec{q}_i}\cdot\frac{\partial f^{(k+1)}}{\partial\vec{p}_i}\right)}
$$

Note that the evolution of $f^{(k)}$ thus depends on $f^{(k+1)}$, such that the above expression represents a set of N coupled equations, known as the **BBGKY hierarchy**. Note also that this derivation is completely general; the ONLY assumption we have made along the way is that the dynamics are Hamiltonian!

For the **1-particle distribution function** the above expression reduces to

$$
\frac{\partial f^{(1)}}{\partial t} = \{\mathcal{H}^{(1)}, f^{(1)}\} + \int\mathrm{d}^3\vec{q}_2\,\mathrm{d}^3\vec{p}_2\left(\frac{\partial U_{12}}{\partial\vec{q}_1}\cdot\frac{\partial f^{(2)}}{\partial\vec{p}_1}\right)
$$

with $\mathcal{H}^{(1)} = \frac{p^2}{2m} + V(\vec{q})$ the 1-particle Hamiltonian and $f^{(2)} = f^{(2)}(\vec{q}_1, \vec{q}_2, \vec{p}_1, \vec{p}_2, t)$ the **2-particle distribution function**. This equation forms the basis for the **Boltzmann equation**, as discussed in Chapters 6 and 7.

Appendix K

Derivation of the Energy Equation

The energy equation can be obtained from the **master moment equation**

$$\boxed{\frac{\partial}{\partial t} n\langle Q\rangle + \frac{\partial}{\partial x_i}\Big[n\langle Q v_i\rangle\Big] + \frac{\partial \Phi}{\partial x_i} n\left\langle \frac{\partial Q}{\partial v_i}\right\rangle = 0}$$

by substituting

$$Q = \frac{1}{2}mv^2 = \frac{m}{2}v_i v_i = \frac{m}{2}(u_i + w_i)(u_i + w_i) = \frac{m}{2}(u^2 + 2u_i w_i + w^2)$$

Hence, we have that $\langle Q\rangle = \frac{1}{2}mu^2 + \frac{1}{2}m\langle w^2\rangle$ where we have used that $\langle u\rangle = u$ and $\langle w\rangle = 0$. Using that $\rho = m\,n$, the first term in the master moment equation thus becomes

$$\frac{\partial}{\partial t}\left[n\langle Q\rangle\right] = \frac{\partial}{\partial t}\left[\rho\frac{u^2}{2} + \rho\varepsilon\right]$$

where we have used that the specific internal energy $\varepsilon = \frac{1}{2}\langle w^2\rangle$. For the second term, we use that

$$\begin{aligned}
n\langle v_k Q\rangle &= \frac{\rho}{2}\langle (u_k + w_k)(u^2 + 2u_i w_i + w^2)\rangle \\
&= \frac{\rho}{2}\langle u^2 u_k + 2u_i u_k w_i + w^2 u_k + u^2 w_k + 2u_i w_i w_k + w^2 w_k\rangle \\
&= \frac{\rho}{2}\left[u^2 u_k + u_k\langle w^2\rangle + 2u_i\langle w_i w_k\rangle + \langle w^2 w_k\rangle\right] \\
&= \rho\frac{u^2}{2}u_k + \rho\varepsilon u_k + \rho u_i\langle w_i w_k\rangle + F_{\text{cond},k}
\end{aligned}$$

Here we use that the **conductivity** can be written as

$$F_{\text{cond},k} \equiv \rho\langle w_k\frac{1}{2}w^2\rangle = \langle \rho\varepsilon w_k\rangle$$

(see Chapter 5). Recall that conduction describes how internal energy is dispersed due to the random motion of the fluid particles. Using that $\rho\langle w_i w_k\rangle = -\sigma_{ik} = P\delta_{ik} - \tau_{ik}$, the second term of the master moment equation becomes

$$\frac{\partial}{\partial x_k}\left[n\langle v_k Q\rangle\right] = \frac{\partial}{\partial x_k}\left[\rho\frac{u^2}{2}u_k + \rho\varepsilon u_k + (P\delta_{ik} - \tau_{ik})u_i + F_{\mathrm{cond},k}\right]$$

Finally, for the third term we use that

$$\frac{\partial Q}{\partial v_k} = \frac{m}{2}\frac{\partial v^2}{\partial v_k} = m v_k$$

To understand the last step, note that in Cartesian coordinates $v^2 = v_x^2 + v_y^2 + v_z^2$. Hence, we have that

$$n\frac{\partial \Phi}{\partial x_k}\left\langle\frac{\partial Q}{\partial v_k}\right\rangle = \rho\frac{\partial \Phi}{\partial x_k}\langle v_k\rangle = \rho\frac{\partial \Phi}{\partial x_k}u_k$$

Combining the three terms in the master moment equation, we finally obtain the following form of the **energy equation**:

$$\begin{aligned}\frac{\partial}{\partial t}\left[\rho\left(\frac{u^2}{2}+\varepsilon\right)\right] = \\ -\frac{\partial}{\partial x_k}\left[\rho\left(\frac{u^2}{2}+\varepsilon\right)u_k + (P\,\delta_{jk} - \tau_{jk})\,u_j + F_{\mathrm{cond},k}\right] - \rho\,u_k\,\frac{\partial \Phi}{\partial x_k}\end{aligned}$$

Note that there is no $-\mathcal{L}$ term, which is absent from the derivation based on the Boltzmann equation, since the later does not include the effects of radiation.

Finally, we want to recast the above energy equation in a form that describes the evolution of the **internal energy**, ε. This is obtained by subtracting u_i times the **Navier-Stokes equation** in conservative, Eulerian form from the energy equation derived above.

The Navier-Stokes equation in Eulerian index form is

$$\frac{\partial u_i}{\partial t} + u_k\frac{\partial u_i}{\partial x_k} = \frac{1}{\rho}\frac{\partial \sigma_{ik}}{\partial x_k} - \frac{\partial \Phi}{\partial x_i}$$

Using the **continuity equation**, this can be rewritten in the so-called **conservation form** as

$$\frac{\partial \rho u_i}{\partial t} + \frac{\partial}{\partial x_k}\left[\rho u_i u_k - \sigma_{ik}\right] = -\rho\frac{\partial \Phi}{\partial x_i}$$

Next we multiply this equation with u_i. Using that

$$\begin{aligned} u_i \frac{\partial \rho u_i}{\partial t} &= \frac{\partial \rho u^2}{\partial t} - \rho u_i \frac{\partial u_i}{\partial t} = \frac{\partial}{\partial t}\left[\rho \frac{u^2}{2}\right] + \frac{\partial}{\partial t}\left[\rho \frac{u^2}{2}\right] - \rho u_i \frac{\partial u_i}{\partial t} \\ &= \frac{\partial}{\partial t}\left[\rho \frac{u^2}{2}\right] + \frac{\rho}{2}\frac{\partial u^2}{\partial t} + \frac{u^2}{2}\frac{\partial \rho}{\partial t} - \rho u_i \frac{\partial u_i}{\partial t} \\ &= \frac{\partial}{\partial t}\left[\rho \frac{u^2}{2}\right] + \frac{u^2}{2}\frac{\partial \rho}{\partial t} \end{aligned}$$

where we have used that $\partial u^2/\partial t = 2u_i \partial u_i/\partial t$. Similarly, we have that

$$\begin{aligned} u_i \frac{\partial}{\partial x_k}\left[\rho u_i u_k\right] &= \frac{\partial}{\partial x_k}\left[\rho \frac{u^2}{2} u_k\right] + \frac{\partial}{\partial x_k}\left[\rho \frac{u^2}{2} u_k\right] - \rho u_i u_k \frac{\partial u_i}{\partial x_k} \\ &= \frac{\partial}{\partial x_k}\left[\rho \frac{u^2}{2} u_k\right] + \frac{\rho}{2} u_k \frac{\partial u^2}{\partial x_k} + \frac{u^2}{2}\frac{\partial \rho u_k}{\partial x_k} - \rho u_i u_k \frac{\partial u_i}{\partial x_k} \\ &= \frac{\partial}{\partial x_k}\left[\rho \frac{u^2}{2} u_k\right] + \frac{u^2}{2}\frac{\partial \rho u_k}{\partial x_k} \end{aligned}$$

Combining the above two terms, and using the **continuity equation** to dispose of the two terms containing the factor $u^2/2$, the Navier-Stokes equation in conservation form multiplied by u_i becomes

$$\frac{\partial}{\partial t}\left[\rho \frac{u^2}{2}\right] + \frac{\partial}{\partial x_k}\left[\rho \frac{u^2}{2} u_k\right] = u_i \frac{\partial \sigma_{ik}}{\partial x_k} - \rho u_i \frac{\partial \Phi}{\partial x_i}$$

Subtracting this from the form of the energy equation on the previous page ultimately yields

$$\frac{\partial}{\partial t}\left(\rho \varepsilon\right) + \frac{\partial}{\partial x_k}\left(\rho \varepsilon u_k\right) = -P \frac{\partial u_k}{\partial x_k} + \mathcal{V} - \frac{\partial F_{\mathrm{cond},k}}{\partial x_k}$$

where

$$\mathcal{V} \equiv \tau_{ik} \frac{\partial u_i}{\partial x_k}$$

is the **rate of viscous dissipation**, describing the rate at which heat is added to the internal energy budget via viscous conversion of ordered motion ($\vec{u}$) to disordered energy in random particle motions ($\vec{w}$).

Next we split the first term in $\rho(\partial\varepsilon/\partial t)+\varepsilon(\partial\rho/\partial t)$ and the second term in $\rho u_k(\partial\varepsilon/\partial x_k)+\varepsilon(\partial\rho u_k/\partial x_k)$, and use the continuity equation to obtain the (internal) **energy equation** in Lagrangian index form:

$$\boxed{\rho\frac{\mathrm{d}\varepsilon}{\mathrm{d}t} = -P\frac{\partial u_k}{\partial x_k} + \mathcal{V} - \frac{\partial F_{\mathrm{cond},k}}{\partial x_k}}$$

which is identical to the equation at the end of Chapter 5, but again without the $-\mathcal{L}$ term describing radiation.

Appendix L

The Chemical Potential

Consider a system which can exchange energy **and particles** with a reservoir, and the volume of which can change. There are three ways for this system to increase its internal energy; heating, changing the system's volume (i.e., doing work on the system), or adding particles. Hence,

$$\mathrm{d}U = T\,\mathrm{d}S - P\,\mathrm{d}V + \mu\,\mathrm{d}N$$

Note that this is the first law of thermodynamics, but now with the added possibility of changing the number of particles of the system. The scalar quantity μ is called the **chemical potential**, and is defined by

$$\mu = \left(\frac{\partial U}{\partial N}\right)_{S,V}$$

This is not to be confused with the μ used to denote the mean weight per particle, which ALWAYS appears in combination with the proton mass, m_{p}. As is evident from the above expression, the chemical potential quantifies how the internal energy of the system changes if particles are added or removed, while keeping the entropy and volume of the system fixed. The chemical potential appears in the Fermi-Dirac distribution describing the momentum distribution of a gas of fermions or bosons.

Consider an ideal gas, of volume V, entropy S and with internal energy U. Now imagine adding a particle of zero energy ($\epsilon = 0$), while keeping the volume fixed. Since $\epsilon = 0$, we also have that $\mathrm{d}U = 0$. But what about the entropy? Well, we have increased the number of ways in which we can redistribute the energy U (a macrostate quantity) over the different particles (different microstates). Hence, by adding this particle we have increased the system's entropy. If we want to add a particle while keeping S fixed, we need to decrease U to offset the increase in the number of 'degrees of freedom' over which to distribute this energy. Hence, keeping S (and V) fixed, requires that the particle has negative energy, and we thus see that $\mu < 0$.

For a fully degenerate Fermi gas, we have that $T = 0$, and thus $S = 0$ (i.e., there is only one micro-state associated with this macrostate, and that is the fully degenerate one). If we now add a particle, and demand that we keep $S = 0$, then that particle must have the Fermi energy (see Chapter 13); $\epsilon = E_{\rm f}$. Hence, for a fully degenerate gas, $\mu = E_{\rm f}$.

Finally, consider a photon gas in thermal equilibrium inside a container. Contrary to an ideal gas, in a photon gas the number of particles (photons) cannot be arbitrary. The number of photons at given temperature, T, and thus at given U, is given by the Planck distribution and is constantly adjusted (through absorption and emission against the wall of the container) so that the photon gas remains in thermal equilibrium. In other words, N_γ is not a degree of freedom for the system, but it set by the volume and the temperature of the gas. Since we can't change N while maintaining S (or T) and V, we have that $\mu = 0$ for photons.

To end this discussion of the chemical potential, we address the origin of its name, which may, at first, seem weird. Let's start with the 'potential' part. The origin of this name is clear from the following. According to its definition (see above), the chemical potential is the 'internal energy' per unit amount (moles). Now consider the following correspondences:

Gravitational potential is the gravitational energy per unit mass:

$$W = \frac{G\,m_1\,m_2}{r} \qquad \Rightarrow \qquad \phi = \frac{G\,m}{r} \qquad \Rightarrow \qquad \phi = \frac{\partial W}{\partial m}$$

Similarly, electrical potential is the electrical energy per unit charge

$$V = \frac{1}{4\pi\varepsilon_0}\frac{q_1\,q_2}{r} \qquad \Rightarrow \qquad \phi = \frac{1}{4\pi\varepsilon_0}\frac{q}{r} \qquad \Rightarrow \qquad \phi = \frac{\partial V}{\partial q}$$

These examples make it clear why μ is considered a 'potential'. Finally, the word chemical arises from the fact that the μ plays an important role in chemistry (i.e., when considering systems in which chemical reactions take place, which change the particles). In this respect, it is important to be aware of the fact that μ is an additive quantity that is conserved in a chemical reaction. Hence, for a chemical

reaction $i + j \rightarrow k + l$ one has that $\mu_i + \mu_j = \mu_k + \mu_l$. As an example, consider the annihilation of an electron and a positron into two photons. Using that $\mu = 0$ for photons, we see that the chemical potential of elementary particles (i.e., electrons) must be opposite to that of their anti-particles (i.e., positrons).

Because of the additive nature of the chemical potential, we also have that the above equation for $\mathrm{d}U$ changes slightly whenever the gas consists of different particle species; it becomes

$$\mathrm{d}U = T\,\mathrm{d}S - P\,\mathrm{d}V + \sum_i \mu_i\,\mathrm{d}N_i$$

where the summation is over all species i. If the gas consists of equal numbers of elementary particles and anti-particles, then the total chemical potential of the system will be equal to zero. In fact, in many treatments of fluid dynamics it may be assumed that $\sum_i \mu_i\,\mathrm{d}N_i = 0$; in particular when the relevant reactions are 'frozen' (i.e., occur on a timescales τ_{react} that are much longer than the dynamical timescales τ_{dyn} of interest), so that $\mathrm{d}N_i = 0$, or if the reactions go so fast ($\tau_{\mathrm{react}} \ll \tau_{\mathrm{dyn}}$) that each reaction and its inverse are in local thermodynamic equilibrium, in which case $\sum_i \mu_i\,\mathrm{d}N_i = 0$ for those species involved in the reaction. Only in the rare, intermediate case when $\tau_{\mathrm{react}} \sim \tau_{\mathrm{dyn}}$ is it important to keep track of the relative abundances of the various chemical and/or nuclear species.